Imperial College London

Neutrophil Extracellular Vesicles as Mediators of Acute Pulmonary Vascular Inflammation During Sepsis

Diianeira Maria Tsiridou

Supervisors:
Dr Kieran O'Dea (Senior Lecturer)
Prof Masao Takata (Magill Chair in Anaesthetics)

Section of Anaesthetics, Pain Medicine, and Intensive Care
Department of Surgery & Cancer, Faculty of Medicine
Imperial College London

Submitted in partial fulfilment of the requirements for the award of Doctor of Philosophy (PhD) in Clinical Medicine Research

Date of submission: 13th January 2023

Funded by the British Journal of Anaesthesia/ Royal College of Anaesthetists and the Chelsea and Westminster Health Charity

Abstract

Circulating neutrophil-derived extracellular vesicles (EVs) are acutely increased during sepsis and systemic inflammatory response syndrome. Although *in vitro* studies have shown that neutrophil-EVs have pro-inflammatory activities, little is known about their roles in the propagation of systemic inflammation. Recent studies indicate that the uptake of circulating EVs by the lungs increases dramatically during systemic inflammation, primarily through their interactions with pulmonary intravascular monocytes. In this study, we hypothesised that circulating neutrophil-EVs are potent long-range mediators of pulmonary vascular inflammation, contributing to the development of indirect acute lung injury.

Using human cell culture-based models, my main aims were to: 1) characterise neutrophil-EV uptake by pulmonary vascular cells under resting and inflammatory conditions, 2) develop a whole blood model of lipopolysaccharide (LPS)-induced neutrophil-EV subtype production, 3) isolate and characterise the pro-inflammatory activity of these neutrophil-EVs. For the assessment of neutrophil-EV function, I developed a co-culture model of pulmonary vascular inflammation, consisting of peripheral blood mononuclear cells (PMBCs) or monocytes, co-cultured with human lung microvascular endothelial cells (HLMECs).

Neutrophil-EVs were taken up by both HLMECs and monocytes and subject to dynamic changes under physiological flow and inflammatory conditions. LPS stimulation of whole blood revealed acute increases in neutrophil- and platelet-EVs. Using immunoaffinity isolation for EV subpopulations, neutrophil- but not platelet-EVs were found to be pro-inflammatory, inducing TNF-α-dependent activation of HLMECs in the presence of PBMCs or monocytes. Further investigations revealed that neutrophil-EVs activate monocytes via Toll-like receptor 4 (TLR4) signalling, in an EV surface protein-dependent manner.

These findings indicate that neutrophil-EVs released under septic-like conditions *in vitro* are potent mediators of inflammation, with the potential to generate localised inflammation within

the monocyte-enriched environment of the pulmonary vasculature. Furthermore, the neutrophil-EV protein-dependent TLR4 signalling activity suggests a novel mechanism for propagation of inflammation within the circulation from local sites of infection.

Dedications

This PhD thesis is dedicated to my family. I would like to thank my parents: Antigoni and Moysis, sisters: Thei and Athina, and grandparents: Diianeira, Stavros, Evangelia, and Theodosis for their unconditional love, support, and guidance all these years that made me the person I am today. They have constantly been my motivation and inspiration and without them, I would not have been able to accomplish my dreams.

Acknowledgements

This work would not have been possible without the valuable guidance, help, and advice of my main supervisor Dr Kieran O'Dea. I would like to thank him for trusting and supporting me, with understanding and patience every day over the last four years. I would not have been the scientist I am today without his mentorship. His knowledge and passion for science have been an inspiration for me and I will always be grateful to him, wishing nothing but the best for his future. I would also like to thank my co-supervisor Professor Masao Takata for giving me the opportunity to carry out my research in his lab and providing his support, guidance, and directions over the course of my PhD.

A big thank you goes to all the current and past members of the Critical Care team for putting up with me all these years even on difficult and bad lab days. Virginia, Marissa, Rhianna, Teresa, Yoichi, Chubicka, Diane, Sanooj, Mike, and Brij, thank you for your help with experiments and scientific support. This PhD would not have been equally enjoyable without you. Special thanks to Eirini for being the best friend and colleague and Ying Ying for being a great colleague, and friend. My appreciation goes to Dr Padmini Sarathchandra for her assistance in the electron microscopy and Claudia Peinador Marin for her collaboration in the project.

I would also like to acknowledge the British Journal of Anaesthesia/Royal College of Anaesthetists for funding my PhD.

Finally, a final big thank you goes to Miltos for supporting, loving, and keeping me sane over these years.

Statement of originality

I declare that the work submitted within this thesis is a result of my own work and that those that have assisted or advised me, have been duly recognised within the Acknowledgements.

Declaration of copyright

The copyright of this thesis rests with the author. Unless otherwise indicated, its contents are licensed under a Creative Commons Attribution-Non Commercial 4.0 International Licence (CC BY-NC).

Under this licence, researchers may copy and redistribute the material in any medium or format. They may also create and distribute modified versions of the work. This is on the condition that: they credit the author and do not use it, or any derivative works, for a commercial purpose.

When reusing or sharing this work, researchers should ensure that they make the licence terms clear to others by naming the licence and linking to the licence text. Where a work has been adapted, they should indicate that the work has been changed and describe those changes.

Please seek permission from the copyright holder for uses of this work that are not included in this licence or permitted under UK Copyright Law.

Table of contents

Index of figures

Index of tables

Abbreviations

ALI	Acute lung injury
ARDS	Acute respiratory distress syndrome
BALF	Bronchoalveolar lavage fluid
BSA	Bovine serum albumin
CAMs	Cell adhesion molecules
CARDS	COVID-19 associated ARDS
CARS	Compensatory anti-inflammatory response syndrome
COX	Cyclooxygenase
DAD	Diffuse alveolar damage
DAMPs	Damage-associated molecular patterns
DPI	Diphenyleneiodonium
EBM	Endothelial basal medium
EDTA	Ethylenediaminetetraacetic acid
EGM	Endothelial growth medium
ELISA	Enzyme-linked immunosorbent assay
ERK	Extracellular signal-regulated kinase
ESCRT	Endosomal sorting complex responsible for transport
EVs	Extracellular vesicles
FACS	Fluorescence-activated cell sorting
FBS	Foetal bovine serum
fMLP	N-Formylmethionyl-leucyl-phenylalanine
FSc	Forward scatter
FU	Fluorescence unit
FWB	FACS wash buffer
GM-CSF	Granulocyte-macrophage colony-stimulating factor
GPCRs	G-protein-coupled receptors
HAS	Human albumin solution
HCAEC	Human coronary artery endothelial cells
HLMEC	Human lung microvascular endothelial cells
HMGB-1	High mobility group box 1
HUVEC	Human umbilical vein endothelial cells
HV	Healthy volunteers
HSP	Heat shock protein
ICAM-1	Intercellular adhesion molecule 1
ICU	Intensive care unit
IFN	Interferon
IL	Interleukin
JNK	c-Jun N-terminal Kinase
LBP	LPS binding protein
LPS	Lipopolysaccharide

LT	Leukotriene
MAPK	Mitogen-activated protein kinase
MCP-1	Monocyte chemoattractant protein-1
MFI	Mean fluorescence intensity
MHC	Major histocompatibility complex
MODS	Multiple organ dysfunction syndrome
MOF	Multiple organ failure
MPO	Myeloperoxidase
MRP8/14	Myeloid-related protein 8/14
MVs	Microvesicles
MVBs	Multivesicular bodies
NAC	N-acetyl-l-cysteine
NETs	Neutrophil extracellular traps
NF-κB	Nuclear factor-κB
PAF	Platelet activating factor
PAMPs	Pathogen-associated molecular patterns
PBMCs	Peripheral blood mononuclear cells
PBS	Phosphate buffered saline
PFA	Paraformaldehyde
PFC	Parallel flow chamber
PI	Propidium iodide
PI3K	Phosphoinositide 3-kinase
PMA	Phorbol 12-myristate 13-acetate
PRRs	Pattern recognition receptors
PS	Phosphatidylserine
PSGL-1	P-selectin glycoprotein ligand-1
RBCs	Red blood cells
RES	Reticuloendothelial system
ROS	Reactive oxygen species
RPMI 1640	Roswell Park Memorial Institute Medium 1640
SD	Standard deviation
SIRS	Systemic inflammatory response syndrome
SOD	Superoxide dismutase
SOFA	Sequential Organ Failure Assessment
SSc	Side scatter
TEM	Transmission electron microscopy
TGF-β	Transforming growth factor beta
TLRs	Toll-like receptors
TNF-α	Tumour necrosis factor alpha
TNFR	TNF receptor
VCAM-1	Vascular adhesion molecule 1

1. Introduction

1.1. Acute Lung Injury (ALI) and Acute Respiratory Distress Syndrome (ARDS)

1.1.1. Definition, diagnosis, epidemiology

Acute lung injury (ALI) and its more severe clinical manifestation, acute respiratory distress syndrome (ARDS), are acute inflammatory conditions with devastating consequences in the intensive care unit (ICU) worldwide due to high mortality rates, exceeding 40 % in some instances (1-3). ARDS was first described by Ashbaugh et al., in 1967 based on twelve ICU patients with severe respiratory failure (4, 5). These patients had an acute onset of tachypnoea, hypoxaemia, and loss of compliance with a variety of causes (4). Over the next decades, several attempts have been made to define ARDS and provide uniform diagnostic criteria for this clinical syndrome that develops in response to multiple aetiologies of pulmonary and extrapulmonary origins. In 1994 the American European Consensus Conference (AECC) published a uniform definition of ARDS (**Table 1.1**) for patients presenting with acute onset of hypoxaemia (arterial oxygen tension/fraction of inspired oxygen ratio (PaO_2/FiO_2)≤200 mmHg) with diffuse bilateral pulmonary infiltrates on chest radiograph and absence of left atrial hypertension. ALI was also described in this definition as a less severe form of ARDS with similar criteria but less severe hypoxaemia (PaO_2/FiO_2≤300 mmHg) (6).

	Chest imaging (radiograph)	**Oxygen levels**	**Pulmonary artery wedge pressure**	**Timing**
ARDS	Diffuse bilateral pulmonary infiltrates	PaO_2/FiO_2≤200 mmHg	≤18 mmHg No left atrial hypertension	Acute onset
ALI	Diffuse bilateral pulmonary infiltrates	PaO_2/FiO_2≤300 mmHg	≤18 mmHg No left atrial hypertension	Acute onset

Table 1.1. Definition of ARDS and ALI according to the American European Consensus Conference.

Subsequently, the Berlin definition (**Table 1.2**) removed the term ALI and highlighted the existence of three exclusive ARDS forms depending on the level of hypoxaemia: severe ($PaO_2/FiO_2 \leq 100$ mmHg), moderate (100 mmHg$< PaO_2/FiO_2 \leq 200$ mmHg), and mild ($PaO_2/FiO_2 \leq 300$ mmHg) (7). Severe ARDS is identified by four criteria: severe findings in chest radiographs (bilateral opacities), respiratory system compliance (≤40 mL/cm H_2O), positive end-expiratory pressure (PEEP≥10 cmH_2O) and corrected expired volume per minute (≥10 L/min). In contrast to the AECC definition, it provided an explicit timeframe to define acute onset of disease and specified the onset within one week of a known clinical insult or new or worsening respiratory symptoms (7).

The 2012 Berlin Definition	
Timing	Within 1 week of a known clinical insult or new or worsening respiratory symptoms
Chest imaging	Bilateral opacities – not fully explained by effusions, lobar/lung collapse, or nodules
Oedema origin	Respiratory failure not fully explained by cardiac failure or fluid overload. Need objective assessment (e.g., echocardiography) to exclude hydrostatic oedema if no risk factors are present
Oxygenation	Severe: $PaO_2/FiO_2 \leq 100$ mmHg; with PEEP≥5 cm H_2O
	Moderate: 100 mmHg$< PaO_2/FiO_2 \leq 200$mm Hg; with PEEP≥5 cm H_2O
	Mild: $PaO_2/FiO_2 \leq 300$ mmHg; with PEEP≥5 cm H_2O

Table 1.2. Definition of ARDS according to the Berlin Definition.

When these criteria were applied to existing clinical studies, it was found that disease severity positively correlated with mortality, decreasing from 45 % in severe ARDS patients to 32 % in moderate ARDS and 27 % in patients with the mild form of the disease (3). Despite extensive

literature (more than 58,000 entries in PubMed) progress has mainly been made to understand the pathogenesis of ARDS. Due to its high complexity and broad clinical phenotype, numerous studies up to now have failed to provide efficient universal pharmacological therapies.

Epidemiology studies have been challenging mainly because ARDS and ALI do not have simple diagnostic tests. Although most studies have focused on ICU settings where patients need support with mechanical ventilation, other studies have shown that ARDS can also be observed in a non-ICU environment, hinting that ARDS incidence is highly underestimated (8). It has also been observed that numbers of ARDS and ALI cases vary considerably among countries, which could possibly reflect differences in reporting rates, population demographics and prevalence of potential risk factors correlated to ARDS (3, 9, 10).

Published in 2016, the LUNG-SAFE (Large Observational Study to Understand the Global Impact of Severe Acute Respiratory Failure) is the most updated and accurate international cohort study analysing epidemiological data on ARDS to date (11). According to LUNG-SAFE, 10.4 % of all ICU patients admitted in 50 countries (29,144 total patients) fulfilled the ARDS criteria. Similar findings resulted from a similar UK-based study, where ARDS incidence was reported as 12.5 % of all ICU admissions in a period of 6 months (12). Interestingly, both studies highlighted the low clinical recognition rates of ARDS. In the LUNG-SAFE study, ARDS was recognised on average only in 60.2 % of all ARDS cases, while Summers et al., reported that only 2 out of 43 patients with ARDS were recognised as such by the relevant hospital department (11, 12).

1.1.2. Pathogenesis

ARDS is mainly characterised by the loss of alveolar-capillary integrity leading to formation of protein-rich oedema fluid within the alveolar space, influx of neutrophils, and release of pro-inflammatory mediators (13-15). The pathophysiology of ARDS has been described as a sequence of three phases. It starts with the acute or exudative phase, proceeds with a subacute or proliferative phase, and progresses with a chronic or fibrotic phase (10, 16, 17). These three stages have distinct characteristics based on histopathological observations (18, 19).

The acute phase typically lasts for the first 7 to 10 days after the onset of ARDS (16). During this stage, the innate immune system is activated to remove the cause of inflammation, producing an excess release of pro-inflammatory cytokines (16). Neutrophils migrate from the vasculature into the air space towards pro-inflammatory cytokine and chemokine gradients (20). These recruited leukocytes can then promote further cell death and dysfunction through the release of cytotoxic mediators like reactive oxygen species (ROS), proteolytic enzymes (myeloperoxidase (MPO), neutrophil elastase) and other intracellular contents, e.g., neutrophil extracellular traps (NETs). This phase is characterised by interstitial and alveolar oedema formation and accumulation of inflammatory neutrophils and monocytes, as well as red blood cells and platelets within the alveoli. The alveolar space is thus flooded by inflammatory cells, cellular debris, fluid, and proteins, producing the histological appearance of ‘diffuse alveolar damage’, the main hallmark of ARDS (21). As a consequence, patients experience difficulty in breathing, referred to as decreased lung compliance, arterial hypoxaemia and in severe cases respiratory failure (22).

The second phase, referred to as the subacute or proliferative phase, spans over the next 2 weeks in survivors. During this period, repair mechanisms are activated to resolve the pulmonary oedema and restore the fluid balance within the pulmonary vasculature. Type II alveolar epithelial cells start to proliferate and differentiate into type I alveolar epithelial cells,

which repair the damaged epithelium. Fibroblasts and myofibroblasts appear in the interstitial space and mediate fibrin and collagen deposition to restore the alveolar vasculature (13).

In some cases, after the proliferative phase, the lung progresses to the fibrotic stage, a more chronic condition, which is characterised by significant distortion of the lung architecture and increased collagen and fibrin deposition. The degree of fibrotic damage varies from mild to severe, depending on any secondary complications such as sepsis, that can lead to lung fibrosis and collagen deposition and have been linked to poor outcomes with reduced lung compliance and respiratory function (23-25).

1.1.3. Aetiology

ALI and ARDS develop in response to a variety of insults, either as direct insults through the airways or indirect insults via the circulation (14). Although the end state requiring support with mechanical ventilation is common in all ARDS cases, the underlying pathophysiology can be quite different. Broadly AECC has categorised ALI into two subgroups based on the initial insult: direct (pulmonary) and indirect (extrapulmonary) ALI (7). In cases of direct ALI, damage is caused mainly in the alveolar epithelial cells with capillary endothelium remaining relatively intact, while indirect ALI mainly develops in the settings of systemic inflammation and results in injury of intravascular pulmonary endothelial cells. Crucial pathophysiological differences exist between the two forms of ALI (7, 26-29). In direct ALI features such as alveolar oedema formation accompanied by fibrin and collagen deposition, and neutrophil aggregation and apoptosis are commonly observed with increased levels of inflammatory mediators observed mainly in bronchoalveolar lavage fluid (BALF) (30). On the other hand, indirect ALI presents with increased vascular congestion, permeability, and interstitial oedema with a tendency for monocyte/macrophage margination (as opposed to neutrophils in direct ALI) (31) and increased serum rather than BALF levels of inflammatory mediators (32). The most common

causes of ARDS are pneumonia (bacterial or viral), non-pulmonary sepsis, aspiration of gastric contents, and severe trauma or burn injury and these account for more than 85 % of all ARDS cases (10). **Table 1.3** summarises known clinical disorders that have been linked to the development of ALI (6, 14, 26, 33, 34).

Clinical disorders linked with the development of ALI	
Direct (pulmonary) lung injury	**Indirect (extrapulmonary) lung injury**
Pneumonia (bacterial or viral more common, fungal les common)	Sepsis/Systemic inflammatory response syndrome (SIRS)
Gastric content aspiration	Severe trauma
Near drowning	Blood transfusion (fresh frozen plasma, platelets, red blood cells)
Fat embolism	Cardiopulmonary bypass
Inhalation injury	Severe burn injury
Reperfusion injury (lung transplant/pulmonary embolism)	Acute kidney injury/ renal dysfunction
Mechanical ventilation	Acute pancreatitis
Pulmonary contusion	Drug overdose

Table 1.3. Underlying pathologies linked with the development of direct and indirect ALI/ARDS. Adapted from Ware et al. (14).

It is important to note that although these two forms of ALI present with distinct differences, it is challenging to accurately discriminate them in a clinical setting as they might co-exist occasionally in the same patient, making it difficult to specify the origin of the initial insult. Previous clinical evidence suggests that patients with indirect ALI are more prone to develop severe disease, multiple organ failure (MOF), and have increased plasma levels of biomarkers for endothelial and epithelial injury (35, 36). An interesting intersection of the pathophysiology of direct and indirect types of ALI is the recent coronavirus disease 2019 (COVID-19).

The recent COVID-19 pandemic has drawn considerable attention towards ARDS and ALI to better understand their pathophysiology and associated inflammatory propagation among various organs. The severe acute respiratory syndrome coronavirus-2 (SARS-CoV-2) was first identified in December 2019 in Wuhan, Hubei, China and is the virus that causes the coronavirus disease COVID-19 (37). As of January 2023, there have been reported over 665 million cases of SARS-CoV-2 infection worldwide, and 6.71 million associated deaths (38). This has resulted in a massive increase of patients presenting with ARDS in clinical centres around the world. Whilst SARS-CoV-2 frequently presents with mild symptoms such as fever, dry cough, anosmia, and ageusia and patients do not require hospitalisation (39), in severe cases COVID-19 can result in pneumonia and eventually a form of ARDS described as COVID-19 associated ARDS (CARDS) (40-42). Data from individual studies indicated that 1 in 3 (33 %) of hospitalised patients with COVID-19 infection develops ARDS while 3 out of 4 (75 %) of COVID-19 patients in ICU have ARDS (40, 43, 44).

Since the beginning of the COVID-19 pandemic, reports highlighted that CARDS is different from the typical ARDS (39). However, later with better understanding of the CARDS pathophysiology, evidence suggested that COVID-19 associated pneumonia shares common characteristics with ARDS with patients presenting with profound diffuse alveolar damage in the lung and similar respiratory mechanics (44, 45). CARDS is generally linked to a form of direct ALI as SARS-CoV-2 directly affects the lung (26). However, CARDS presents with profound hypoxaemia despite very compliant lungs, significant pulmonary interstitial oedema, a dysregulated inflammatory response, and thrombosis, which is suggestive of endothelial injury and therefore has a component of indirect ALI (26, 46-48).

1.1.4. Management

Despite extensive efforts to fully understand and characterise ALI and ARDS, there is still no effective treatment to prevent their development or a 'gold-standard' therapy to date. The heterogeneity of the syndrome combined with diagnostic challenges, complicate the management of this disease.

The current management strategy mainly focuses on the identification and treatment of the underlying cause(s) (see **Table 1.3**). In parallel, supportive therapy is used to limit further lung injury, prevent lung oedema formation, promote oedema absorption, and in general help the body recover (49). Supportive therapy strategies include fluid management techniques (50, 51), respiratory support via lung-protective mechanical ventilation in the ICU (10), and pharmacological or adjunct therapies. Conservative fluid management has been established after the Fluids and Catheters Treatment Trial (FACTT) clinical trial, where net fluid balance was reduced, oxygen levels were improved, and eventually, ventilator-free days were promoted (51). Mechanical ventilation has been the main improvement in the field of ARDS research over the last decades but although it could rescue some patients, in cases of severe hypoxaemia, it can cause ventilator-induced lung injury and haemorrhagic pulmonary oedema (52). Evidence up to now suggests that the use of low tidal volumes and plateau airway pressure can significantly reduce mortality (10). Numerous studies over the years have identified potential targets in preclinical models. Clinical trials including statins (53, 54), anti-platelet therapies (55), nitric oxide (56), corticosteroids (57, 58), antiproteases and ketoconazole (59, 60), aspirin (61), macrolide antibiotics (62, 63), neutrophil elastase inhibitors (64), β-adrenergic agonists (65, 66), and surfactant replacement (67) have failed to improve clinical outcomes and reduce mortality in ARDS and ALI patients. Similarly, other pharmacologic interventions that are known to promote lung repair, such as keratinocyte growth factor (68), granulocyte-monocyte colony stimulating factor (GM-CSF) (69), and mesenchymal stem cells (70, 71) have also failed to provide conclusive evidence for improved

clinical outcomes in ARDS patients. Recently cell therapy and targeted nanoparticle-mediated drug-delivery have gained increasing interest. Using nanoparticles as a delivery technique is much more advantageous as drugs can travel in inflammatory lung sites through passive, active, or physicochemical transfer, thereby significantly increasing drug potency and reducing side effects (72).

1.2. Systemic inflammatory response syndrome (SIRS) and sepsis

Systemic inflammatory response syndrome or 'SIRS' is a clinical diagnosis of a non-specific syndrome that can be caused by ischaemia, inflammation, trauma, infection or any of the aforementioned combined (73) in an infectious (e.g., sepsis) or a non-infectious (e.g., polytrauma, surgery, pancreatitis, major burns) setup (74). It is estimated that SIRS affects more than 50 % of ICU patients during their hospitalisation, and presents with fever, tachypnoea, tachycardia, and leucocytosis (75-77). SIRS is diagnosed in the presence of two or more of the following clinical symptoms: (1) fever of more than 38 °C or less than 36 °C, (2) heart rate over 90 beats per minute, (3) respiratory rate greater than 20 breaths per minute or a partial pressure of arterial carbon dioxide less than 32 mm Hg, (4) and abnormal white blood cell count (>12,000/ µL or <4,000/ µL) or immature neutrophil bands of >10 % (78).

1.2.1. Sepsis and septic shock: definition, diagnosis, epidemiology

Sepsis describes a clinical syndrome which develops in response to systemic infection or local infection with spill-over of inflammatory factors into the general circulation producing systemic inflammation (79). The definition of sepsis was originally established in a conference held in 1991 by the American College of Chest Physicians (ACCP) and the Society of Critical Care Medicine (SCCM) (Sepsis-1). According to that, sepsis represents the host's response to

microbial infection if more than one of the aforementioned SIRS criteria are met (73). When sepsis is accompanied by organ dysfunction, hypoperfusion or hypotension, it is termed ‘severe sepsis’. If the hypotension persists despite adequate fluid resuscitation, it is described by the term ‘septic shock’ (73). In 2001, a second conference was carried out by the SCCM, the European Society of Intensive Care Medicine (ESICM), the ACCP, the American Thoracic Society (ATS) and the Surgical Infection Society (SIS), in which the sepsis definition was revisited and modified to expand the diagnostic criteria (Sepsis-2) (80). In 2016, during a third consensus, it was decided that the use of SIRS criteria to diagnose sepsis was not appropriate, because a group of patients that developed organ dysfunction without fulfilling the SIRS criteria was omitted from the diagnosis (78). Therefore, the clinical definition of sepsis was changed to: ‘a life-threatening dysregulated immune response to proven or suspected infection (bacterial, viral, or fungal), which if unresolved may progress to its severest form, septic shock’ (Sepsis-3). Since multiple organ dysfunction was incorporated within the main definition, ‘severe sepsis’ stopped to exist as a term, while ‘septic shock’ was defined as a subset of sepsis, with profound circulatory and cellular/metabolic abnormalities linked with enhanced mortality (78). SIRS on the other hand was redefined as a normal host response to infection that may be adaptive in some cases.

It has been shown that improved clinical outcomes require early diagnosis and treatment with intravenous fluids and antibiotics (81, 82). Therefore, during the third consensus, the Sequential (sepsis-related) Organ Failure Assessment (SOFA) scoring system (83) was incorporated, to replace the use of SIRS criteria and improve the diagnostic rates (78, 79) The SOFA scoring system was established during a consensus meeting in 1994 and includes markers of the pulmonary, haematological, hepatic, central neurological, renal, and cardiovascular systems, to describe quantitively the degree of organ dysfunction in critically ill patients (83).

Sepsis is the infectious form of SIRS and one of the main causes of death worldwide with an estimated mortality rate around 38 % (77, 84, 85). According to the UK Sepsis Trust

organisation, the number of people who develop sepsis is continuously increasing, with around 245,000 cases each year in the UK. Death rates are estimated at 48,000 per annum, representing a cost of £ 1.5 to £2 billion annually to the NHS (86, 87).

Sepsis is one of the most common risk factors to cause indirect ARDS/ALI (88) with mortality rates as high as 53 % (89). It is estimated that 75-80 % of ARDS/ALI patients have had severe sepsis with accompanying SIRS from pulmonary infection or indirect extrapulmonary sources (11, 90) (91). Direct ALI frequently develops after primary infection within the respiratory system with secondary sepsis and is mechanistically well-characterised. However, indirect ALI produced by infectious and non-infectious SIRS is considerably more complex, involving multiple dynamic extra-pulmonary systems and circulating factors that converge on the pulmonary vasculature and its unique leukocyte-enriched microenvironment (92).

1.2.2. Pathogenesis of sepsis

Roger Bone described the excessive pro-inflammatory response in sepsis as being accompanied by a counteractive anti-inflammatory response (93). He observed that if these two processes are in balance, homeostasis is maintained or restored. However, during sepsis, or non-infectious SIRS, the interaction between pro- and anti-inflammatory mediators is unbalanced and either a pro-inflammatory reaction (termed SIRS) or an anti-inflammatory reaction, termed ‘compensatory anti-inflammatory response syndrome’ (CARS) may prevail. This concept has been widely adopted since 1996 and further developed and characterised (94, 95). Subsequent studies have linked SIRS with the presence of pro-inflammatory cytokines in the systemic circulation such as tumour necrosis factor alpha (TNF-α), interleukin 6 (IL-6), interleukin 8 (IL-8), interleukin 1β (IL-1β) (96), while CARS have been associated with anti-inflammatory mediators such as transforming growth factor beta (TGF-β), soluble tumour necrosis factor receptors (sTNFR) and interleukin 10 (IL-10) (97). CARS is characterised by increased lymphocyte dysfunction because of reduced proliferation and apoptosis, decreased

pro-inflammatory cytokine response after monocyte stimulation, increased levels of anti-inflammatory cytokines (e.g., TGF-β, IL-4, and IL-10) and other hormones and immunomodulatory eicosanoids like prostaglandins (97), and decreased numbers of human leukocyte antigen (HLA) antigen-presenting receptors on monocytes (98). It clinically presents with cutaneous anergy, hypothermia, leukopenia, susceptibility to infection and failure to clear infection. It is widely considered that patients succumbing to protracted sepsis do so because of a secondary CARS-related infection (98).

Although the SIRS/CARS model had been studied extensively, the timing between the two stages remains unclear. Initially, it had been suggested that SIRS precedes CARS, but recent studies question this strict time frame and suggest that septic patients could be hyper-inflammatory or immunocompromised at any given time with both pro- and anti-inflammatory mediators upregulated (99, 100). Other studies propose a compartmentalisation model between SIRS and CARS, with pro-inflammatory conditions predominating in inflamed tissues and immunosuppressed leukocytes being present in the blood circulation (101, 102).

1.2.3. Inflammation in sepsis

The body's response to infection involves the activation of the innate immune system, which triggers downstream signalling pathways to eliminate or limit the spread of the pathogen. However, when the host's response to a given infection is dysregulated or not controlled, it can lead to excessive levels of systemic inflammation that results in dysregulation of the normal inflammatory processes and host injury mediated to tissues (103).

An overview of the local inflammatory response

The inflammatory cascade is initiated locally where in response to tissue invasion or injury, immune sentinels (i.e., macrophages and mast cells) recognise antigenic material and

respond instantly by releasing several inflammatory mediators such as cytokines and chemokines acting as chemical signals to relay the inflammatory information and recruit effector cells including neutrophils and monocytes to further enhance the local inflammatory response (104). Among the released mediators, vasoactive molecules such as histamine, produce post-capillary venule dilatation and increased vessel permeability resulting in plasma leak into the tissue. During this process the endothelium becomes activated, upregulates selectins, and displays chemoattractants which increase neutrophil recruitment, adherence, and migration towards vascular beds (105). Neutrophils within the tissue are further activated by surrounding cytokines and release chemotactic signals such as cathepsin G and azurocidin which act as chemotactic factors for the recruitment of inflammatory monocyte subsets (106, 107). Moreover, cytokines in the tissue microenvironment induce the release of neutrophil-derived toxic anti-microbial mediators such as elastase, MPO, and metalloproteinases to destroy pathogens and phagocytose microbes (108, 109).

Pathogen-associated molecular patterns (PAMPs)

PAMPs as a term was established to describe structures or motifs that are highly conserved amongst microbial pathogens and therefore suitable for host recognition as ‘foreign’ by the innate arm of immune response. PAMPs are recognised through pattern recognition receptors (PRRs). PRRs could be either surface receptors like the Toll-like receptors (TLRs), cytosolic like the nucleotide-binding oligomerisation domain (NOD)-like receptors, or soluble (humoral) factors such as complement and lectins (110). Monocytes, macrophages, neutrophils, endothelial cells, and platelets carry PRRs, which in the presence of PAMPs trigger signalling cascades that amplify the inflammatory signals, resulting in cytokine and chemokine release as well as coagulation processes and even cell death (111). Host responses to PAMPs are directly responsible for sepsis pathogenesis (112), of which lipopolysaccharide (LPS) is the most well-characterised and can be considered a prototypic PAMP.

LPS

LPS, also termed ‘endotoxin’, forms the major structural component of the outer membrane of gram-negative bacteria. Although infection with both gram-positive and gram-negative bacterial components are major causes of sepsis, it has been found that gram-negative sepsis accounts for the majority of sepsis-induced ALI cases (113). LPS is a large glycolipid consisting of three different domains, the O-antigen, the main core region, and the lipid A (114). In mammalian cells, LPS is mainly recognised by the Toll-like receptor 4 (TLR4). In humans, there have been identified 10 TLR molecules (TLR1-10) localised either to the cell surface or to intracellular compartments. TLRs present on the cell surface are the TLR1, TLR2, TLR4, TLR5, TLR6, and TLR10 and recognise microbe membrane components such as lipids and lipoproteins. Intracellular TLRs present on the endoplasmic reticulum, endosomes, or lysosomes, are the TLR3, TLR7, TLR8, and TLR9 and interact with bacterial or viral nucleic acids (115, 116).

In addition to TLR4, LPS signalling is dependent upon a group of proteins termed the ‘LPS receptor complex’. This consists of the LPS binding protein (LBP), the molecule CD14, and the extracellular adapter protein myeloid differentiation factor 2 (MD-2). LBP has the role of catalyst in transferring LPS molecules to the CD14 receptor in the host’s cells. CD14 is expressed on the cell membrane of myeloid lineage cells, mainly monocytes and macrophages, with lower levels on neutrophils. In addition to the membrane-anchored form, CD14 also exists as a soluble molecule (sCD14), which performs the same role on cells lacking the membrane CD14, such as endothelial cells. MD-2 enhances LPS binding to TLR4 to allow its downstream signal (117).

LPS causes the dimerization of two TLR4 molecules, initiating two separate signalling pathways: the early myeloid differentiation factor 88 (MyD88)-dependent pathway and the delayed MyD88-independent pathway (118). Each pathway involves specific adaptor proteins such as MyD88, Toll/IL-1 receptor homology domain-containing adapter protein (TIRAP), TIR

domain-containing adaptor-inducing interferon-β (TRIF) or TRIF-related adaptor molecule (TRAM) (119). In the MyD88-dependent response, TIRAP and MyD88 are recruited and bound to the dimerized TLR4 cytoplasmic tails, promoting a scaffold formation with the interleukin 1 receptor (IL-1R) associated kinases (IRAK)-1 and -4 and the TNFR-associated factor 6 (TRAF6) (120). The nuclear factor κB (NF-κB) and mitogen-activated protein kinase (MAPK) pathways are involved in the MyD88-dependent complex and activated through several phosphorylation events. The MAPK family consists of several kinases such as the p38 kinase, the extracellular signal-regulated kinase (ERK1/2) and the c-Jun N-terminal kinase (JNK) (121). Prior to activation, NF-κB is a cytoplasmic protein bound to the inhibitory κ-B (Iκ-B) protein. Phosphorylation of the MAPK proteins alongside Iκ-B, results in the release of NF-κB, which gets translocated to the nucleus, triggering the transcription of downstream genes, responsible for various pro-inflammatory cytokine and chemokine release, and upregulation of surface cell adhesion molecules (CAMs) and selectins (122).

Danger-associated molecular patterns (DAMPs)

Similar responses to PAMPs, have been observed in the presence of other endogenous sterile inflammatory signals which are released as danger signals from dying cells during inflammation or injury in the presence of an infection and have been described as DAMPs (123, 124). Some well-characterised DAMPs are the high morbidity group box 1 (HMGB-1) (125), and the heat shock proteins (HSPs) (126). Nuclear or mitochondrial DNA and histones released from necrotic tissue also have properties of DAMPs (127). Alike PAMPs, DAMPs are also recognised by PRRs by the innate immune cells and activate the pro-inflammatory immune response (128).

Although PAMPs and DAMPs have different origins (infectious vs. non-infectious), they serve a similar purpose in alerting the body to harm or danger. As such both have the potential to induce multiple organ dysfunction syndrome (MODS) (123), which can explain the development of SIRS following major trauma as well as the exacerbation and protraction of

inflammation in sepsis due to tissue damage despite infection control. Thus, increased levels of histones, cell-free DNA, and HMGB-1 have been found in sepsis patients and were positively correlated with MODS and overall disease severity (129, 130).

1.2.4. Soluble inflammatory mediators

In response to tissue injury and infection, cells of the innate immune system rapidly release multiple soluble mediators including cytokines, chemokines, and eicosanoids to generate an inflammatory response and eliminate the invading organism. Although their primary role is as paracrine factors acting at the local site in injection or injury, elevated levels of these soluble mediators have been found in the plasma of sepsis patients (131, 132), and therefore they have been implicated as key effector molecules involved in systemic inflammation and sepsis pathogenesis (133-135).

Lipid mediators

Lipid-derived mediators include eicosanoids and the platelet-activating factor (PAF). Eicosanoids are mainly derived from arachidonic acid cleaved from membrane phospholipids by phospholipase A_2 upon cell activation, which are then converted by cyclooxygenase (COX), and lipoxygenase into prostaglandins (PGD_2, PGE_2, PGF_2, PGI_2) or thromboxane A2 and leukotrienes (LTA_4, LTB_4, LTC_4, LTD_4, LTE_4), respectively. There are two COX isoforms, COX-1 which is constitutively expressed in most tissues and COX-2 which is activated in immune effector cells such as monocytes, upon inflammation. COX-2 inhibition has been found to reverse inflammation (136), whereas COX-2 deficient mice were protected from sepsis-induced inflammation and had a better outcome (137). Most prostaglandins have vasodilatory functions apart from PGF_2 and thromboxane A2, which have been identified as potent vasoconstrictive molecules (138). Leukotrienes, mainly LTB_4, have pro-inflammatory activity towards neutrophils and monocytes, causing inflammatory cytokine and chemokine release

and increasing their recruitment in local inflammatory vascular beds. Similarly, PAF has been found to promote leukocyte adhesion to endothelium (139).

In a randomised cohort trial, elevated levels of LTB_4 and PGF_2 were observed in sepsis non-survivors and correlated with ARDS development (140). In a second study, increased PAF concentration was correlated with sepsis-induced acute renal failure (141). However, clinical trials using non-steroidal anti-inflammatory drugs for COX inhibition or PAF receptor antagonist did not reduce disease severity or mortality (142-145).

Chemokines

Chemokines are a family of small proteins, that signal through G-protein-coupled receptors (GPCRs) and are secreted by a variety of immune cells. Chemokine secretion leads to the recruitment of immune effector cells, such as monocytes and neutrophils, from the circulation in local sites of inflammation and/or tissue injury (146). During homeostasis, chemokines control the release of neutrophils and monocytes from the bone marrow and orchestrate the host defence against microbes. However, excessive chemokine secretion has been linked to sepsis pathophysiology as high systemic levels will interfere with local chemokine gradients (147). Once secreted, chemokines are bound to components of the extracellular matrix and form a gradient to attract cells in target areas. In humans, IL-8 (CXCL8) is the chemokine responsible for neutrophil recruitment, while in mice keratinocyte chemoattractant (KC) (CXCL1) is the respective homologue (148). Monocyte chemoattractant protein-1 (MCP-1) (CCL2) is involved in monocyte recruitment (149) and enhances monocyte adhesion in inflamed endothelial cells (150).

Cytokines

Cytokines are small proteins, whose main function during the onset of infection or tissue injury is to coordinate and enhance the inflammatory response. They serve as signalling and communication mediators among cells and have autocrine, paracrine, and endocrine effects.

Although cytokines are released as part of the innate immune response, both lymphoid and myeloid immune cell populations can produce them during infection. There are five main cytokine families: the tumour necrosis factor (TNF) family, interleukin (IL) family, colony stimulating factors (CSFs), interferon (IFN) family, and the TGF-β family. Depending on their functions, these cytokines are categorised into pro- and anti-inflammatory. They might have pleiotropic effects (the same cytokine can have different functions upon different target cells), can function antagonistically (opposing functions) or synergistically (multiple cytokines acting collaboratively), and can be redundant (similar endpoint effects can arise from different cytokines) (151).

The main pro-inflammatory cytokines observed in sepsis are TNF-α, IL-1β, IL-6, and IFN-γ. Following PAMP or DAMP binding to host PRRs such as complement, TLRs and scavenger receptors activate multiple signalling pathways leading to the expression of common gene classes that are involved in inflammation, adaptive immunity, and cellular metabolism (78). These include MAPKs, Janus kinases (JAKs), signal transducers and activators of transcription (STATs), and the NF-κB. These intermediates trigger the expression of early activation genes for pro-inflammatory cytokines like TNF-α, several interleukins (IL-1β, IL-12, IL-18), and type I IFNs. Their secretion results in vasodilation and upregulation of adhesion molecules, which enhance the sequestration and adhesion of leukocytes in inflamed areas. Monocytes and macrophages are the main cells that produce TNF-α and IL-1β. Upon their release, TNF-α and IL-1β bind to their respective TNF receptors (TNFR1/TNFR2), or IL-1R and activate downstream signalling pathways such as the MAPK and NF-κB (151).

These cytokines initiate the cascade of other pro-inflammatory cytokines including IL-6, and INF-γ. The systemic release of all these pro-inflammatory mediators can trigger an auto-amplifying effect termed ‘cytokine storm’ (152). IL-6 is not only released by monocytes, but endothelial cells, lymphocytes, and fibroblasts as well and is involved in the coagulation process, promoting the release of tissue factor. It also induces the proliferation and maturation

of T and B cells. In the context of sepsis, circulating levels of IL-6 have been correlated with the severity of sepsis and pancreatitis-induced ARDS (153).

The above events result in an increased expression of endothelial cell adhesion molecules transforming the endothelium into a pro-adhesive surface for circulating leukocytes and platelets. Similarly, changes in endothelial regulators of coagulation switch the endothelium from a healthy (anticoagulant) state to a septic (procoagulant) state (154).

Although high levels of pro-inflammatory cytokines are observed in local sites of infection, anti-inflammatory cytokines have been found in sepsis patients' plasma, and are associated with poor outcome (155, 156). Their main role is to antagonise the activity of pro-inflammatory cytokines regulating the intensity of the inflammatory response and to assist in its resolution. Macrophages and T cells are the main cell types secreting anti-inflammatory cytokines such as IL-10, IL-4, and IL-13. TGF-β released by macrophages and B and T lymphocytes, inhibits lymphocyte proliferation, suppresses secretion of TNF-α and IL-1β, and promotes wound healing (157).

Although the processes involved in the regulation of local inflammatory responses are well established, it is still unclear how cytokines lead to systemic inflammation and remote organ failures.

1.2.5. Coagulation and microcirculatory dysfunction in sepsis

Coagulation in sepsis

Systemic induction of a pro-coagulant state has a central role in the pathogenesis of sepsis, affecting the microcirculation (154). Briefly, the clotting cascade activated by endothelial injury consists of a series of linked reactions, in which thrombin, a serine protease, once activated is free to activate its downstream substrates. These reactions can be accelerated by the

presence of other cofactors (factors VIIa and Va). Thrombin converts fibrinogen into soluble strands of fibrin, which act together with platelets providing the structural integrity needed for clot formation. Fibrin formation is the result of the intrinsic and the extrinsic pathway. The extrinsic pathway is regulated by tissue factor and is the primary pathway for the initiation of blood coagulation. Regulators of the clotting pathway are mechanisms that keep platelets and the coagulation cascade in balance to prevent abnormalities that can lead to an increased tendency towards thrombosis. Namely, these are the protein C which is activated by thrombin and together bind to thrombomodulin, a cell surface protein; antithrombin, a serine protease inhibitor that degrades thrombin and other blood clotting factors; tissue factor pathway inhibitor (TFPI) that limits the action of tissue factor; plasmin, a plasma protein that catalyses the degradation of fibrin; and lastly, prostacyclin (PGI2) and nitric oxide that promote synthesis of cAMP which inhibit platelet activation. Eventually, blood clots are reorganised and absorbed by a process termed fibrinolysis. Once activated the inflammatory and coagulation pathways interact with one another to further amplify the host response, which may subsequently lead to thrombotic diseases (78, 154, 158, 159).

A major pathogenic factor in early-stage sepsis is microcirculatory dysfunction. Patients commonly present with increased blood flow heterogeneity and decreases in functional capillary density (160). These changes appear to have a role in sepsis prognosis as their severity and persistence over time have been correlated with worse outcome and decreased survival rates (161, 162). Under physiological conditions, endothelial cells regulate the microvascular flow by releasing vasodilators, mainly nitric oxide. During sepsis, the nitric oxide system gets highly dysregulated. Subsequently, the functions of resident cell types within the microvasculature, such as endothelial, smooth muscle, red blood cells, platelets and leukocytes become impaired resulting in hypoperfusion of blood capillaries (163). If this reduced perfusion is not managed, blood flow and tissue oxygenation become compromised, and circulatory shock and tissue hypoxia follow. Systemic inflammation promotes a pro-coagulant state further compounding microcirculatory dysfunction (154). Tissue hypoxia

produces cellular injury that exacerbates inflammation and coagulation, producing a vicious cycle that ultimately results in MOF and eventually death (160).

1.2.6. Biomarkers in sepsis

Early diagnosis is of paramount importance for sepsis and can highly decrease morbidity and mortality in patients (81). A key element for early diagnosis is the existence of accurate biomarkers. The term biomarker refers to an indicator of a patient's condition that can be quantified accurately (164). Several studies over the years have focused on identifying inflammatory biomarkers for sepsis, such as markers of cellular activation, soluble pro-inflammatory mediators, and similarly the soluble and cellular indicators of immune suppression (165).

Under inflammatory or infectious conditions, abnormal blood cell counts can be a valuable biomarker. Both lymphocyte and neutrophil counts have been used clinically as one of the criteria to identify SIRS (73). However, apart from increases in number, expression of leukocyte surface molecules is altered during sepsis and these changes have been useful prognostic sepsis biomarkers. CD64 is the high-affinity Fc-gamma receptor 1 of the immunoglobulin molecule, with very low expression on resting neutrophils. Several studies have investigated CD64 expression on neutrophils in septic patients and correlated elevated CD64 expression with disease progression (166-169). CD11b is an integrin β2 subunit present on neutrophils and monocytes, which promotes their adhesion to the endothelium in sites of inflammation. Its expression is increased on neutrophils upon bacterial infection and has also been proposed as a useful diagnostic marker (169). Depression of monocyte function has also been investigated as a clinical indicator of severity or prognosis of critical illness with downregulation of the Class II major histocompatibility complex (MHC) protein HLA-DR on septic patients, being the main example (170-172). Other soluble monocyte-derived mediators include the soluble form of the receptor for advanced glycation end-products (RAGE) and the

soluble form of CD14, both of which have been found elevated in septic patients over several studies and correlated with severity and increased mortality (173-175). Their release is essential for the development of SIRS and therefore could be valuable biomarkers for sepsis.

Apart from surface activation markers, systemic levels of pro-inflammatory cytokines such as TNF-α, IL-1β, and IL-6 serve as soluble markers of the inflammatory response and pathophysiology it produces (165). IL-10 is the main anti-inflammatory cytokine released during the immunosuppressive phase in sepsis. Elevated serum IL-10 levels have been associated with lower survival rates and correlated with decreased HLA-DR monocyte expression (172). Soluble tumour necrosis factor receptors (TNFRs) have also been suggested as potential sepsis biomarkers and proved successful tools to identify sepsis from other inflammatory conditions and highlight patients with higher risk (176). TGF-β has been a less useful biomarker to identify high-risk septic patients, but in a study, it was suggestive of sepsis-induced ARDS development (177).

Lactate is the most widely used prognostic biomarker for sepsis because elevated serum levels indicate organ dysfunction, a common sepsis complication (178). Lactate is a product of anaerobic glycolysis occurring under hypoxic conditions. It has been found that in sepsis patients, microcirculatory dysfunction leads to decreased tissue perfusion and eventually organs resort to anaerobic glycolysis, producing lactate (165). Several studies have associated increased lactate levels with mortality and worse outcomes (179-181).

Procalcitonin (PCT) and C-reactive protein (CRP) are the most common protein biomarkers of infection and/or inflammation (182). Normally PCT is produced by cells within the thyroid and is converted in calcitonin, without being released in the circulation. During inflammation, PCT is produced directly by stimulating bacterial components or is induced by inflammatory cytokines like TNF-α and IL-6 (164). CRP is a pentameric acute-phase protein that triggers complement activation and activates endothelial cells, monocytes, and platelets (183). PCT

and CRP levels are routinely checked to diagnose and monitor sepsis in clinical settings. PCT has been found to be more accurate and specific for bacterial infections than CRP (184).

1.2.7. Current management

Even though the pathogenesis of sepsis has been well studied and there is now a clear understanding of the basic mechanisms, the mortality to date remains unacceptably high (77, 84, 85). The current management strategy for sepsis patients involves mainly supportive therapies (185). Early detection and administration of antibiotics can be very beneficial (82). The hypotension (systolic blood pressure <90 mm Hg, or a drop in systolic blood pressure of >40 mm Hg) caused by the microcirculatory dysfunction observed in sepsis is managed by intravenous administration of resuscitative electrolyte or glucose-containing fluids (186). Blood or plasma transfusion and the administration of vasopressors such as norepinephrine have also been found useful in patients with renal, cardiac, and respiratory failure (187). Corticosteroids, anti-inflammatory and anti-oxidant pharmacologic agents aiming to reduce inflammation, improve tissue perfusion via increased vasoconstriction, and insulin therapy has been proposed and used to manage blood hyperglycaemia (188). In cases of sepsis-induced ALI, as mentioned earlier, interventions such as oxygen administration via endotracheal intubation (mechanical ventilation) are currently used, but further research is required for new treatments.

However, the major focus in the field of sepsis treatment over the last decades has been on anti-cytokine and other inflammatory mediator-based clinical trials. More than 100 clinical trials have attempted to modulate the sepsis immunological response by selectively or non-selectively targeting endogenous inflammatory mediators, without any overall success in improving survival rates (185). TNF-α neutralising antibodies or anti-TNFR and anti-IL-1 receptor agonists have undergone several clinical trials but failed to increase the survival rate

in septic shock and severe sepsis patients (189, 190). Administration of proteins that stimulate specific immune functions such as GM-CSF, interferon γ (IFN-γ) (191), and anticoagulant molecules (anticoagulant protein C, TFPI, anti-tissue factor antibody, anti-thrombin, thrombomodulin, heparin) (192-194) did not effectively decrease mortality. Targeting of activated protein C produced initially encouraging results with increased overall survival and was used effectively in the clinic (195), however, it was withdrawn later from the market as the PROWESS-SHOCK clinical trial failed to identify any beneficial effect in patients with sepsis (196). Apart from targeting these main inflammatory mediators, other studies tried to suppress the inflammatory response more broadly by using corticosteroids (197) or non-steroidal anti-inflammatories (145), again without significant outcome. Upstream of the inflammatory and pro-coagulant response, endotoxin neutralisation attempts including monoclonal antibodies (198), polymyxin B (199), and recombinant bactericidal permeability increasing (BPI) protein (200) also did not prove to be effective. More recently, treatments with TLR4 antagonists were also investigated but did not effectively reduce mortality (201).

This lack of efficacy in targeting single mediators or specific inflammatory cascades underlines the need for the development of new alternative strategies to treat sepsis and SIRS. Given the enormous heterogeneity observed in sepsis as a disease, with multiple sites of infection, a variety of pathogens present in the patient population, coupled with patient variables such as comorbidities and genetic factors, it is very unlikely that targeting mediators individually in a non-patient specific manner will improve outcome (202).

1.3. Extracellular vesicles

Extracellular vesicles (EVs) are heterogenous lipid-membrane secreted sub-cellular particles released from virtually all cell types under basal or stress conditions. They originate from the cell plasma or endosome membrane with their molecular contents, including surface composition, dependent on the cellular source, status, and environment (203). EVs were first identified in 1967 by Peter Wolf, who described them as 'platelet dust' (204). For several years, their biological function remained unclear, and they were thought of as insignificant cell debris responsible for the disposal of cellular waste. However, further research over the years with improved techniques for the isolation, detection, and imaging of EVs, revealed their role in intercellular communication and their involvement in health and disease (203, 205, 206). Based on their size, content, and sub-cellular origin, EVs are categorised into three main sub-groups: 1) apoptotic bodies; 2) microvesicles (MVs) or microparticles (also referred as ectosomes or shedding vesicles); and 3) exosomes (207) (**Figure 1.1**). A fourth category of EVs, termed 'oncosomes', has been recently described to account for large EVs (1-10 μm) that are produced only by malignant cells (208). For this categorisation, size has been used as an absolute indicator of EV subgroups. However, considerable size overlap exists between the different EV subtypes that can result in the co-isolation of each subgroup using standard separation techniques (209). Hence, differences in the biogenesis and biochemical composition are now required as crucial additional information for accurate EV identification and description (210).

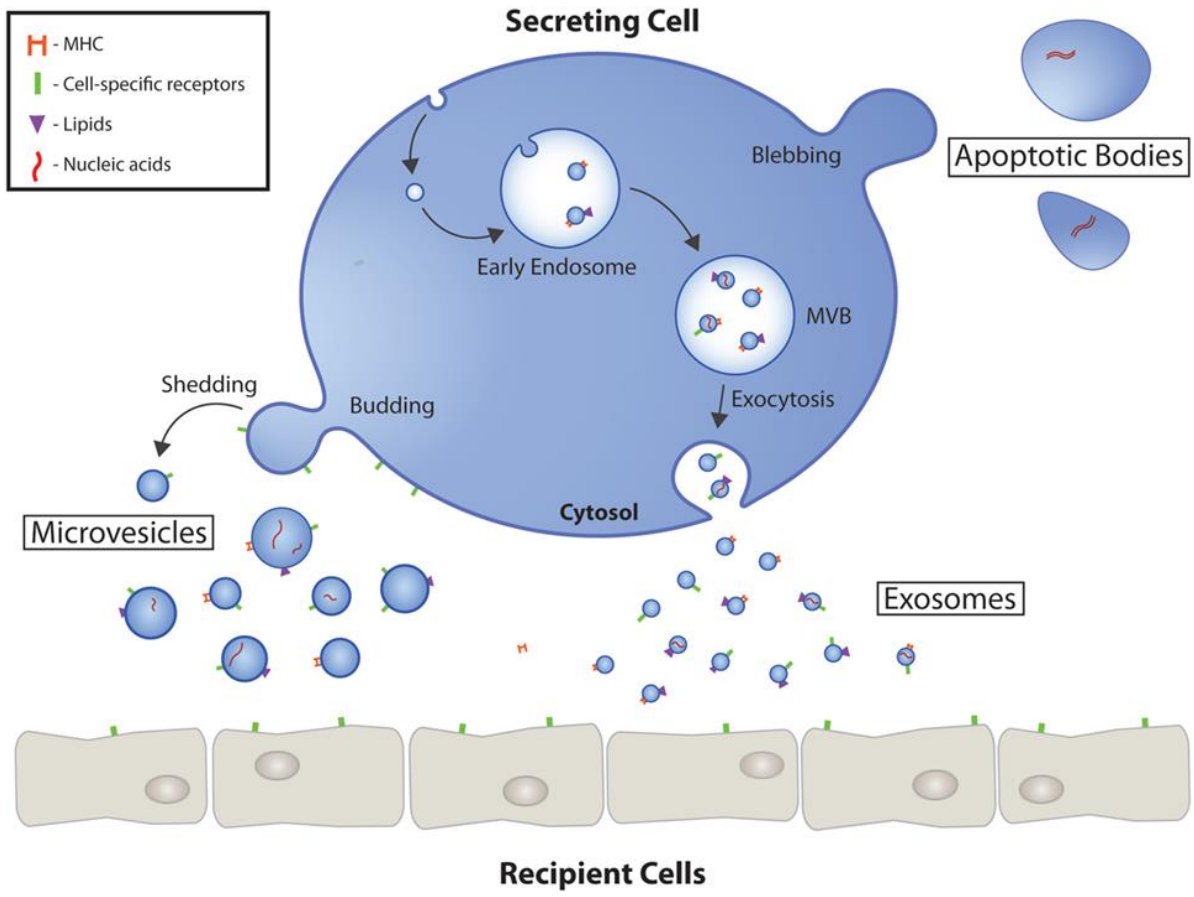

Figure 1.1. Biogenesis of the three EV types: apoptotic bodies, microvesicles, exosomes. Adapted from Gustafson et al. (211).

1.3.1. Main characteristics, biogenesis, and markers of EV subgroups

Apoptotic bodies

Apoptotic bodies are the largest EVs (1-5 μm) and are generated specifically during programmed cell death in the late stages of apoptosis. They are produced during three phases of apoptosis: concentration of nuclear chromatin, followed by cell membrane 'blistering' and eventually blebbing for the final vesicle formation (212, 213). Apoptotic bodies are rich in DNA and histones as part of the cell death process (214). They interact with target cells, through endocytosis, surface interaction or membrane fusion similarly to MVs (discussed below in detail) (215).

Exosomes

Exosomes and MVs can be released by living cells both in resting conditions and upon activation, inflammation, and apoptosis. Exosomes are the smallest EVs (30-150 nm) and are formed intracellularly by an active process, which involves inward bulging and pinching off forming early endosomes. This process results in the formation of small membranous vesicles organised in internal complexes called multivesicular bodies (MVBs). Upon formation, the MVBs are either fused with lysosomes and degraded, or fused with the plasma membrane and exocytose their contents into the extracellular environment as exosomes (216). Exosome cargo includes endosomal, cytosolic, and plasma membrane proteins and highly depends on the status of the precursor cell (207). Increasing interest over the last 40 years in exosome biology resulted in advances in understanding exosomes' role in the progression of cancer metastasis and their potential utilisation as target for immunotherapy treatments (217, 218). Exosomes serve as mediators for antigen presentation by carrying functional MHC molecules, able to activate T cells (219). Moreover, they have been involved in cancer metastasis as potent mediators contributing to the formation of a pre-metastatic niche (through fibronectin accumulation and recruitment of bone marrow-derived macrophages) (220) and influencing the tumour microenvironment. Other studies have proposed exosomes as a promising disease biomarker and indicated their potential use as vehicles for targeted therapies (221, 222).

Traditionally exosomes were characterised by exosomal marker proteins, which are main components of the endosomal sorting complex responsible for transport (ESCRT) complex such as tetraspanins (CD9, CD63, CD81), Alix, tumour susceptibility gene 101 (TSG101), heat shock protein 90β (HSP90β), and heat shock cognate 71 (HSC70) (223). However, later tetraspanins were also observed on the surface of apoptotic bodies and MVs (224). Moreover, although exosomes are generated following inward bulging of the cell membrane, occasionally, parental cell surface markers have been found on the exosome surface. This is a result of a process termed 'endosomal budding', where proteins from the inner membrane flip inside out and end up in the outer membrane (225).

Microvesicles

MVs are produced by almost all eukaryotic cell types, including circulating and vascular cells by budding from the extracellular membrane, yielding particles sized from 0.1 to 1 μm. Their lipid encapsulation makes them strong candidates for carrying mixed cargoes such as pro-inflammatory cytokines, bioactive lipids, and microRNAs (miRNAs), to their target cells within the circulation in a manner protected from dilution, neutralisation, and degradation (226).

MV biogenesis is characterised by three crucial steps: trafficking of the molecular cargo to the plasma membrane, rearrangement of the phospholipid bilayer of the plasma membrane and the cytoskeleton, and contraction-like machinery for the final vesicle pinching and release (227). Although MVs carry surface markers and proteins from their parental cells (228), differences in the cargo and surface lipid composition exist between the precursor cell and daughter MVs (229). In general, the outward blebbing of MVs upon their production results in a right-side-out membrane orientation, which explains the presence of parental surface markers on MV surface (230).

The plasma membrane is comprised of asymmetrically distributed phospholipids namely phosphatidylcholine, sphingomyelin, phosphatidylserine (PS), and phosphatidylethanolamine. The first two are positively charged and face the outer leaflet, whereas negatively charged PS and the neutral phosphatidylethanolamine are aligned on the inner surface (231). Under resting conditions, specific enzymes, the aminophospholipid translocases, maintain this asymmetric phospholipid distribution. However, upon cell activation, calcium levels are increased intracellularly, causing calpain activation, cytoskeletal contraction, and dysregulation of the aminophospholipid translocases, which consequently results in PS translocation from the inner to the outer membrane, followed by membrane budding and MV generation (232-234). As a result of these lipid rearrangements, PS is assumed to be present on the MV surface and therefore has been utilised as a generic marker of MVs for their identification and affinity-based isolation methods (230, 231, 233, 234). PS can be quantified

by annexin V binding, a calcium-dependent protein with a high affinity for the negatively charged PS. PS expression on MV surface has been correlated with several factors such as cell type, status, and stimuli that triggered their release (235, 236). Traditionally it was associated with pro-coagulant functions of MVs (237-239) after anionic phospholipid presence on platelets and platelet-EVs was correlated with binding to factor Va (240). More recently PS expression was shown to elicit anti-inflammatory effects from neutrophil EVs, following interactions with the MerTK receptor on macrophages (241, 242). Although it was initially believed that exosomes lack PS expression, Zakharova et al., reported that exosomes produced during necroptosis expressed surface PS, suggesting a distinct PS expression under specific conditions (243).

The significant overlap of size or surface marker expression among the different EV sub-categories resulted in the release of a statement from the International Society for Extracellular Vesicles (ISEV) in order to normalise the terminology used to name EVs, suggesting the use of terms such as ‘small EVs’ (rather than exosomes) for EVs<200 nm or ‘large EVs’ (instead of MVs) for EVs>200 nm to divide EV subgroups and avoid further nomenclature confusion (210). As most studies in the field rely on centrifugation steps for EV isolation and flow cytometry for EV detection and therefore cannot rule out the existence of multiple EV categories in the preparations, we decided to follow this recent nomenclature proposed by ISEV and use the term ‘EVs’ throughout to describe previous studies in the field and the current study, except in instances where the previous terminology is required for the purpose of clarity.

Main characteristics of EV subtypes			
Feature	**Apoptotic bodies**	**Microvesicles**	**Exosomes**
Shape	Heterogenous	Irregular	Cup shaped
Size	1 – 5 μm	0.1 – 1 μm	30 – 150 nm
Density (g/mL)	1.16 – 1.28	unknown	1.13 – 1.19
Origin; release mechanism	Cell surface; membrane blebbing	Cell surface; membrane budding	Endosomal pathway; MVBs fusing with cell membrane
Contents	Cell organelles, nuclear fractions	mRNA, miRNA, noncoding RNA, proteins	mRNA, miRNA, noncoding RNA, proteins
Lipids	Phosphatidylserine	Phosphatidylserine, ceramide, sphingomyelin	Cholesterol, sphingomyelin, ceramide, lipid rafts, phosphatidylserine
Surface composition: Generic markers	Annexin V, histones	Annexin V, integrins, selectins, CD40	Tetraspanins (CD9, CD63, CD81, CD151), heat shock proteins, flotillin, TSG101,

Table 1.4. Main features of EV categories.

1.3.2. EV isolation and detection methods

EVs are being produced constantly within the body and have been detected and isolated from a variety of human body fluids (244, 245) such as blood (246, 247), urine (248), semen (249), saliva (250), breast milk (251), cerebrospinal fluid (252), and BALF (253, 254) or conditioned media and cell culture supernatants in *in vitro* assays. Several techniques are used for the isolation and detection of EVs.

Isolation

EV isolation from body fluids and cell culture supernatants is based primarily on their size and density, while the separation of EV subpopulations from each other relies on these physical properties as well as specific surface markers (210). Commonly used techniques include differential centrifugation, filtration, density gradient precipitation, and immunoaffinity separation (255-257). Traditionally for MV isolation centrifugation speeds of 10-20,000 x g for up to 30 min have been used (258), whereas exosomes require >100,000 x g centrifugation for 1-48 h (259, 260). However, there is always the potential for co-isolation of smaller particles or protein aggregates even at lower centrifugation speeds. Therefore, there is no single isolation technique today available that can provide high purity or yield. Instead, combination of the existing techniques has been found to be effective for obtaining high-quality and pure EV subpopulations.

Detection

Detection and characterisation of EVs are challenging due to their small and heterogeneous sizes. However, there is no single technology to date able to delineate the full spectrum of EV characteristics in complex sample preparations (261). Overall, the EV detection assays can be categorised into two main groups based on those providing biochemical information, and those providing physical information. Once isolated, standard biochemical analyses can be conducted using immunoblotting, enzyme-linked immunosorbent assay (ELISA), nucleic acid

extraction and PCR amplification, and the whole spectrum of omics technologies (proteomics, lipidomics, genomics). For accurate physical characterisation, subcellular resolution tools are required such as electron microscopy (EM), atomic force microscopy, dynamic light scattering, nanoparticle tracking analysis, and tunable resisting pulse sensing. Although less capable of accurate size determination, flow cytometry is the most commonly used technique for the analysis of mixed EVs and routine quantification (261).

In MV ('large EV') research flow cytometry has been the most common detection technique because it allows the identification of specific MV subpopulations within a heterogenous sample based on parent cell surface lineage markers, (262). However, its capabilities are limited by its resolution of size and sensitivity, particularly as conventional flow cytometers are designed for cell rather than subcellular particle analysis. Although, higher-resolution flow cytometers have become available for general use, with the violet 405nm laser detection (263) as well as specialist flow cytometers designed specifically for subcellular particle analysis (264, 265), exosome ('small EV') detection with flow cytometry can be achieved by their attachment to beads and assessment of their properties as a population (266, 267).

1.3.3. EVs as mediators of intercellular communication

Release of soluble mediators as well as interactions via cell-to-cell contact are the two main mechanisms of intercellular communication that lead to the exchange of biological information among cells. It is now established that EVs represent a third distinct way of intercellular communication (268). In contrast to soluble mediators, which function mainly as autocrine, and paracrine mediators of intercellular communication, EVs represent a distinct pathway that is particularly suited to endocrine communication because their encapsulation and membrane-bound molecular cargoes are resistant to degradation, neutralisation and dilution (226, 228, 234). EVs are therefore effective in local communication acting on nearby target cells, but

equally so over long distances, particularly within circulating blood travelling over long distances carrying their cargo to remote tissues.

EVs contain bioactive molecular cargoes of protein mediators (cytokines and chemokines), eicosanoids, biosynthetic enzymes, membrane ligands/receptors, and nucleic acids (DNA, RNA, miRNA) (229, 269, 270). However, delivery of EVs to target cells does not guarantee the biological effects of the cargo as they will need to interact with the appropriate cellular recognition or response systems. Several types of EV-target cell interactions have been described: 1) via binding of EV membrane-associated molecules to cell surface receptors (268, 271-273); 2) release of EV content in close proximity to target cells, which then interact with cell surface receptors; 3) active internalisation of EVs by target cells and downstream intracellular signalling (274); 4) passive fusion of EVs with cell membranes of target cells and transfer of their cargo (232). There are several pathways of EV internalisation, including caveolin-mediated uptake, clathrin-dependent or independent endocytosis, micropinocytosis, and phagocytosis (275, 276).

The long-range endocrine effects of EVs within the vasculature will depend on circulation time (i.e., availability) and formation of stable associations with specific target cell populations. *In vivo* trafficking studies in small animal models usually involve the injection of labelled EVs and measurement of regional uptake by whole body imaging or excision of tissue/organs and quantification of the total label or cell-associated label. Under normal conditions, exogenously administered EVs are rapidly cleared (within minutes) from the circulation in the liver or spleen, effectively limiting their interactions with other potential target cells within the vasculature (277, 278). Organ-resident macrophages are the primary cell population responsible for EV uptake (277, 279). Although the lungs were not found to be a major site of EV uptake under normal conditions in rodents (273, 277, 280), our group recently demonstrated that during subclinical endotoxaemia in mice, EV uptake was redistributed from the liver to the lung vasculature (281). The dramatic (>20-fold) increase in the lungs was entirely due to EV uptake by intravascular lung-marginated monocytes through a combination of their increased numbers

and increased uptake capacity. Therefore, EV-cell/tissue-specific interactions within the vasculature appear to be dynamic, with switching of their target organ and cell type specificity even under relatively mild conditions of systemic inflammation.

1.3.4. EVs in sepsis and SIRS

Increased levels of circulating EVs in sepsis and SIRS patients under septic conditions suggest potential roles as biomarkers and mediators of the disease process (282-284).

Although the majority of circulating EVs under normal conditions are of platelet origin (285), increased levels of endothelial-, erythrocyte-, and leukocyte-EVs (monocyte- and neutrophil-derived) have been described in sepsis. Increased levels of platelet-, granulocyte-, and endothelial-derived EVs were first described in meningococcal sepsis (286) and since then a large number of studies reported elevated levels of circulating EVs derived from endothelial cells (287-291), leukocytes (246, 288, 291-297), and platelets (289, 291, 294, 298-300) in sepsis patients. Additional information has been obtained from studies administering LPS to produce endotoxaemia in healthy volunteers, however, these were focussed on coagulation effects related to platelet- and monocyte-EVs expressing tissue factor (301, 302).

Other studies have used levels of circulating EVs as biomarkers to assess patients' predisposition to develop ARDS or MOF and found a direct correlation between circulating EVs and ARDS or MOF susceptibility (286, 300, 303). Interestingly, Shaver et al., observed that higher levels of circulating leukocyte-derived EVs correlated with better outcome in ARDS patients, suggesting that EVs might have a protective role (303). This inconsistency between studies may in part be explained by patient heterogeneity but could also imply protective effects on EVs in some situations.

Pro-coagulant activities

The contribution of several EV subtypes towards the immunothrombotic process has been well-established. Within the vascular compartment, platelet-derived EVs represent the most abundant EV subtype under normal steady-state conditions (304). They have been largely investigated in a variety of physiological and pathological conditions and found to be significantly increased upon platelet activation by several stimuli under inflammatory conditions (e.g., thrombin, collagen, ADP) (305). Platelet-EVs bearing PS (306) and tissue factor (307) on their surface, have a vital role in the initiation of the coagulation pathway. In mice tissue factor- and P-selectin glycoprotein ligand-1 (PSGL-1) containing EVs were found to preferentially localise on injured vascular walls within developing thrombus sites, binding to activated platelets via P-selectin/PSGL-1 axis and having a role in blood coagulation (308). In a comparative assessment, platelet-EVs were found to be 50-100x more pro-coagulant compared to their parental cells (309).

Endothelial cell-derived EVs carry markers of endothelial activation, such as adhesion molecules (intercellular adhesion molecule 1 (ICAM-1), vascular adhesion molecule 1 (VCAM-1), E-selectin) and von Willebrand factor and were also associated with the coagulation process (286, 287, 310). In addition, increased endothelial cell-derived EV levels in septic shock patients have been correlated with disseminated intravascular coagulopathy (311). Similarly, erythrocyte-derived EVs have been linked with coagulation and observed to carry high levels of PS on their surface (291, 294, 312, 313).

Inflammatory activities

Contrasting with their direct relationship to coagulopathy in sepsis, the contributions of EVs to inflammation in sepsis and SIRS are likely to be more complex (282, 314). EVs from different vascular cell populations are capable of carrying inflammatory soluble mediators (cytokines, chemokines, growth factors) (315, 316) and DAMPs (histones, heat shock proteins (HSPs), HMGB-1) (317, 318).

Neutrophil-EVs show acute increases in sepsis and have been associated with mortality in critically ill patients admitted to ICU (293). They have been found to carry a number of cytotoxic mediators such as NADPH oxidase (responsible for ROS release) (319), LTB_4 (320), matrix metalloproteases (321), and neutrophil proteolytic enzymes like MPO (322, 323) and neutrophil elastase (292). Neutrophil-EVs have been found capable of activating target cells such as monocytes (293, 324) and endothelial cells (322, 325-327). However, they may also produce anti-inflammatory responses (328) *in vitro* in other cell types such as macrophages (241, 242, 329, 330) and neutrophils (331).

Monocyte-EVs have been characterised as potent inflammatory vesicles, carrying pro-inflammatory cytokines such as TNF-α and IL-1β (332, 333) and they have been found to induce increased IL-8 and MCP-1 release from airway epithelial cells (334), IL-6 and MCP-1 from podocytes (335), and TNF-α and IL-6 in monocytes and macrophages (336).

Endothelial cell-derived EVs apart from roles in coagulation, have also been described as promoters of inflammation and found to induce pulmonary vascular leakage and eventually lung injury in a rat septic model (337) and endothelial dysfunction and ALI in rat, mice, and human lungs (338).

Lastly, platelet-EVs are also involved in inflammation by directly recruiting lymphocytes and leukocytes, via chemokine release and enhancing the interaction between monocytes and endothelial cells by binding P-selectin and PSGL-1 (339).

Although there is now a body of evidence indicating acute increases of different circulating EV subtypes and linking them to the severity of different sepsis and SIRS conditions, it remains unclear how they specifically contribute to the development and resolution of acute organ inflammation and injury. Increasing our understanding of the inflammatory and injurious effects of EVs during sepsis/SIRS will require a more in-depth knowledge of their specific activities and cellular interaction in the different vascular bed microenvironments of major organs.

1.4. Importance of blood flow on EV uptake studies

Blood vessels are lined by endothelial cells, a highly dynamic and metabolically active cell type that regulates several physiological processes including tissue homeostasis, blood cell trafficking, coagulation, solute exchange, and innate and adaptive immunity. Endothelial cells constantly experience blood flow forces which affect their phenotype (e.g., polarisation (340)) and migration (341). EV binding and internalisation by endothelial cells might also be governed by blood flow forces or affected by their changes during pathological conditions, especially if mechanotransduction genes (regulated by flow forces) are involved.

Several studies have linked sepsis with alterations in microvascular blood flow (161, 162, 342-346). In septic patients, there is huge heterogeneity between hypo- and hyper-perfused areas of the body, followed by parallel decreased vascular density. The severity of these alterations has been associated with increased mortality (161, 162, 342). Most *in vitro* studies aiming to address EV functions following uptake by vascular cells under sepsis, have been carried out in static cultures. The primary limitation of these is that they ignore the effect of blood flow that is present *in vivo*. Therefore, it is perhaps unsurprising that *in vitro* and *in vivo* studies often yield contradictory results. To ensure a better understanding of basic EV biology, it is of paramount importance that studies take into consideration the dynamics of blood flow (haemodynamics). Some fundamental terms in the field of haemodynamics that need to be defined are depicted in **Table 1.5**.

Definitions of main haemodynamic terms	
Viscosity (η)	a fluid's resistance to flow (Pa*s or dyn*s/cm^2)
Shear stress (τ)	The resulting force per unit area of contact between laminae (dyn/cm^2)
Shear rate (γ)	The differential in flow velocity as a function of distance from the wall (s^{-1})

Table 1.5. Definitions of basic haemodynamic terms.

Viscosity, shear stress and shear rate are some basic terms that are used to describe the rheologic character of blood flow. The relationship between the three of them is given by the equation:

$$Shear\ stress\ (\tau) = viscosity\ (\eta) \cdot Shear\ rate\ (\gamma)$$

Due to differences in shear rate/stress among the several types of blood vessels present in the human body, we hypothesised that EV uptake dynamics are different in different parts of the body where blood flow and vessel size differ. **Table 1.6** shows the estimated physiological shear rate and shear stress values that are present in the human body (347-349). Indeed, previous studies have reported that flow forces can influence the uptake or adhesion levels of synthetic nanoparticles (350, 351), neutrophil-EVs (352), bacteria (353), macromolecules and low-density lipoprotein molecules (354) on endothelial cells.

Estimated values of shear forces in human vessels		
Blood vessel type	**Mean wall shear rate (s^{-1})**	**Mean wall shear stress (dyn/cm^2)**
Large arteries	300 – 800	11.34 – 30.4
Arterioles	500 – 1,600	19 – 60.8
Veins	20 – 200	0.76 – 7.6
Stenotic vessels	800 – 10,000	30.4 – 380

Table 1.6. Estimated shear rate and shear stress values in human body.

1.5. Hypothesis

The aims of this research investigation build on previous studies by the Critical Care Research Group based in Chelsea Westminster Hospital Imperial College London campus addressing the contribution of circulating EVs to inflammation during sepsis/SIRS.

A common phenomenon related to blood flow within the capillaries is termed 'margination' and refers to the situation where monocytes and other leukocytes reside within the lung microvasculature in contact with the vessel wall and separated from the circulating blood. During systemic inflammation, including LPS-induced endotoxaemia in animal models, the magnitude of this margination is enhanced particularly in the narrow capillaries of the lungs. Previous research from the group revealed that these marginated monocytes increased in number during subclinical endotoxaemia and linked them with increased pulmonary microvascular injury (355, 356). A follow-up study demonstrated that in healthy mice, circulating EVs are taken up mainly by Kupffer cells within the liver and to a much lesser extent by pulmonary intravascular marginated Ly6C^{high} monocytes. However, LPS-induced endotoxaemia dramatically decreased EV uptake by liver resident Kupffer cells and increased EV uptake by marginated Ly6C^{high} monocytes within the lung vasculature by several-fold, resulting in the lungs becoming a major site for intravascular EV uptake (281). More recently, we observed that EVs derived from mouse myeloid cells, mainly neutrophils, released under subclinical endotoxaemia, were potent inducers of pulmonary oedema in an isolated perfused lung model, suggesting a key role in the pathogenesis of sepsis-related indirect ALI (357).

Based on the aforementioned work, we hypothesised that circulating EVs are long-range pro-inflammatory mediators of indirect ALI during sepsis/SIRS and that their activity is dependent upon lung marginated monocytes and their crosstalk with pulmonary microvascular endothelial cells. To address this hypothesis, I first focused on studying the EV uptake and interactions with target cells within the lung microvasculature under both resting and inflammatory conditions, taking into consideration the effect of blood flow. For this part of the

project, I used neutrophil-EVs produced from isolated human primary neutrophils based on preliminary results that neutrophil-EVs have a key role in the propagation of inflammation during sepsis and SIRS. Following this, I investigated the EV production in LPS-stimulated whole blood as an *ex vivo* model of sepsis that allowed the direct comparison of different EV subtype activities produced under the same inflammatory conditions. Once the model was established, I used the main EV subpopulations produced during this stimulation, to study their functional effects and signalling mechanisms upon target cells in an *in vitro* model of pulmonary vascular inflammation.

1.6. Aims and objectives

The primary aim of this study was to define the role of neutrophil-EVs in the propagation of remote inflammation to the lungs by addressing their interactions and effects on target cells within the pulmonary vasculature.

I had four main objectives:

1. To determine neutrophil-EV uptake by target cells within the lung microvasculature *in vitro* under static and flow conditions in resting and inflammatory environments.
2. To determine EV production in an *ex vivo* whole blood model of sepsis.
3. To compare the different pro-inflammatory activities of whole blood derived-EV subtypes in a co-culture model of pulmonary vascular inflammation.
4. To investigate the signalling mechanism of pro-inflammatory EVs, leading to target cell activation.

2. Materials and methods

2.1. Introduction

This chapter describes the materials (reagents and equipment), and core methodologies used throughout this thesis. All procedures were carried out at room temperature and cell incubations/cultures at 37 °C unless otherwise stated. Additional details of materials and methods pertaining to specific chapters can be found in the methods section of its respective chapter.

2.2. Materials

2.2.1. Equipment and software

Equipment	Supplier	Application
BioTek ELx800	BioTek Instruments	ELISA (colourimetric plate reader)
BioTek FLx800	BioTek Instruments	Fluorescent plate reader (EV DiD fluorescence quantification)
Cyan ADP analyser	Beckman-Coulter	Flow cytometry
Cytek Northern Lights-3000	Cytek Biosciences	Flow cytometry
Gatan Bio Scan camera	Gatan	Transmission electron microscopy
ibidi® Pump System Quad	ibidi®	Cell culture under flow
MidiMACS™ Separator	Miltenyi Biotech	Cell and EV immunoaffinity based separation
MiniMACS™ Separator	Miltenyi Biotech	Cell and EV immunoaffinity based separation
MRW Microplate washer	Dynex Technologies	ELISA (automated plate washer)
Olympus BX60 Microscope Upright Polarising	Olympus	Immunofluorescent microscopy
Olympus CK2 microscope	Zeiss	Phase contrast microscopy
Stuart Rotator Variable Speed SB3	Stuart Science Equipment	Rotating wheel for cell mixing
Transmission Electronic Microscope JEOL 1200 EX II	JEOL	Transmission electron microscopy
Ultrawave U50 water bath sonicator	Ultrawave	EV lysis via sonication

Zeiss Axiocam microscope camera	Zeiss	Immunofluorescent microscopy

Table 2.1. Equipment.

Software	Supplier	Application
DigitalMicrograph®	Gatan	Transmission electron microscopy image acquisition
FlowJo v10.8	FlowJo LLC	Flow cytometric analysis
KS-300 software	Zeiss	Immunofluorescent microscopy image acquisition
Prism v9.3.0	GraphPad software LLC	Statistical analysis
PumpControl	ibidi®	ibidi® pump operation
SpectroFlo	Cytek Biosciences	Flow cytometry sample acquisition
Summit v4	Beckman-Coulter	Flow cytometry sample acquisition

Table 2.2. Software.

2.2.2. Reagents and consumables

In-house buffers	Constituents	Application
ELISA reagent diluent	• 1x Phosphate buffer saline (PBS) • 1 % Bovine Serum Albumin (BSA) (w/v)	ELISA
ELISA wash buffer	• 1x PBS • 0.05 % Tween-20 (v/v)	ELISA
EV lysis buffer	• 1x PBS • 1 % Triton-X100 (v/v)	Flow cytometric analysis
EV/cell sorting buffer	• 1x PBS • 0.5 % Human albumin solution (HAS) • 2 mM Ethylenediaminetetraacetic acid (EDTA) • 1x penicillin-streptomycin	EV and cell separation
FACS wash buffer	• 1x PBS • 2 % Foetal bovine serum (FBS) • 0.1 % sodium azide • 5 mM EDTA	Flow cytometry

Table 2.3. In house made buffers.

Reagent	Supplier	Application
4 % PFA	Thermo Fischer Scientific™	Immunofluorescence
7-AAD	BD Biosciences	Live/dead staining
AccuCheck counting beads	Invitrogen	Cell and EV quantification
Accutase	Sigma-Aldrich	Cell detachment
Annexin V binding buffer	Biolegend	EV labelling
anti-HSP70 monoclonal antibody (clone 4G4)	Invitrogen	HSP70 neutralisation
BD Phosflow Lyse/Fix buffer	BD Biosciences	RBC lysis
BSA (heat shock fraction)	Sigma-Aldrich	Blocking (ELISA and immunofluorescence)
Cacodylate buffer	Sigma-Aldrich	Transmission electron microscopy
Calcium ionophore A23187	Tocris Bioscience	EV production
CD11b MicroBeads, human	Miltenyi Biotec	Myeloid-EV isolation
CD61 MicroBeads, human	Miltenyi Biotec	Platelet-EV isolation
Cell dissociation buffer	Sigma-Aldrich	Cell detachment
Cytochalasin D	Sigma-Aldrich	EV uptake inhibition
DAPI mounting medium	ibidi®	Immunofluorescence
Dextran	Acros Organics	Neutrophil isolation
DiD dye	Invitrogen	EV labelling
Diluent C	Sigma-Aldrich	EV labelling
Diphenyleneiodonium	Sigma-Aldrich	ROS inhibition
DMSO	Sigma-Aldrich	Vehicle control
DNase I	New England biolabs	DNA degradation
Dynasore	Sigma-Aldrich	EV uptake inhibition
EBM™-2 Basal medium	Lonza	Cell culture

EDTA	Invitrogen	Flow cytometry
EGM™-2 MV Microvascular endothelial cell growth medium SingleQuots™	Lonza	Cell culture supplement
fMLP	Tocris Bioscience	EV production
FBS (heat inactivated)	Sigma-Aldrich	Cell culture
Gelatin solution (2 % in H_2O, tissue culture grade)	Sigma-Aldrich	Cell culture
Glutaraldehyde	Sigma-Aldrich	Transmission electron microscopy
Heat-labile proteinase K	New England biolabs	protein degradation
Histopaque-1077	Sigma-Aldrich	Neutrophil & PBMC isolation
HAS	Sera Laboratories International Ltd	Cell culture supplement
Lipopolysaccharide, Ultrapure (from *E. coli* 0111:B4)	InvivoGen	EV production & functional assays
Lipopolysaccharide From *E. coli* 055:B5, Alexa Fluor™ 488 Conjugate	Invitrogen	LPS binding assays
LY294002	Peprotech	PI3K inhibition
MACSxpress® Whole Blood Neutrophil Isolation Kit, human	Miltenyi Biotec	Neutrophil-EV isolation
N-acetyl-l-cysteine	Sigma-Aldrich	ROS inhibition
Pan Monocyte Isolation Kit, human	Miltenyi Biotec	Monocyte isolation
Paquinimod	Sigma-Aldrich	MRP14 inhibition
Penicillin-streptomycin solution (100x)	Sigma-Aldrich	Cell culture
PBS	Sigma-Aldrich	Cell culture
Polymyxin B	Sigma-Aldrich	LPS neutralisation
Propidium Iodide	Immunochemistry technologies	Live/dead staining
RPMI-1640	Sigma-Aldrich	Cell culture
SB203580	Tocris Bioscience	p38 inhibition
Sodium azide (NaN_3)	Sigma-Aldrich	Flow cytometry
StraightFrom® Whole Blood CD66b MicroBeads, human	Miltenyi Biotec	Neutrophil-EV isolation

Sulphuric acid	Sigma-Aldrich	ELISA
Superoxide dismutase	Sigma-Aldrich	ROS inhibition
TAK-242	Calbiochem	TLR4 inhibition
Tumor Necrosis Factor α (TNF-α)	Peprotech	EV production & EV uptake assays
Triton X-100	Sigma-Aldrich	EV lysis
Tween-20	Sigma-Aldrich	ELISA wash buffer
U0126	Sigma-Aldrich	MEK1/2 inhibition
Ultra-LEAF™ Purified anti-human S100A8/A9 Heterodimer Antibody (clone A15105B)	Biolegend	MRP8/14 neutralisation
Ultra-LEAF™ Purified anti-human TNF-α Antibody (clone Mab1)	Biolegend	TNF-α neutralisation
Ultra-LEAF™ Purified anti-mouse IgG1, κ isotype (clone MOPC-21)	Biolegend	Isotype control
Ultra-LEAF™ Purified anti-mouse IgG2a, κ isotype (clone MOPC-173)	Biolegend	Isotype control
Ultra-LEAF™ Purified anti-mouse IgG2b, κ isotype (clone MG2b-57)	Biolegend	Isotype control
Ultra-LEAF™ Purified anti-TLR4 antibody (CD284) (clone HTA125)	Biolegend	TLR4 neutralisation

Table 2.4. Reagents, buffers, and pharmacological agents.

Consumable	Supplier	Application
EDTA vacutainer	BD Biosciences	Blood collection
Leucosep tube	Greiner Bio-One	Neutrophil & PBMC isolation
Lithium heparin vacutainer	BD Biosciences	Blood collection
LS columns	Miltenyi Biotec	Cell & EV isolation
MS columns	Miltenyi Biotec	Cell & EV isolation
Perfusion sets for ibidi pump system	ibidi®	Cell culture under flow
µ-Slide I Luer channel slides	ibidi®	Cell culture under flow

Table 2.5. Consumables.

ELISA kit	Detection range	Constituents	Supplier
TNF-α Duoset (human)	15.6 – 1000 (pg/mL)	Capture antibody Biotinylated detection antibody Recombinant standard Streptavidin HRP	R&D systems
IL-8/CXCL8 Duoset (human)	31.2 – 2000 (pg/mL)		
IL-6 Duoset (human)	9.4 – 600 (pg/mL)		
IL-1β/IL-1F2 Duoset (human)	3.2 – 250 (pg/mL)		
CCL2/MCP-1 Duoset (human)	15.6 – 1000 (pg/mL)		
LPS ELISA (human)	0.78 – 50 ng/mL	Pre-coated 96-well plate Standard Standard diluent buffer Wash buffer Detection reagent A Detection reagent B Diluent A Diluent B TMB substrate Stop solution Plate sealer	Aviva systems biology

Table 2.6. Commercial ELISA kits.

2.3. Primary cell culture

2.3.1. Culture and maintenance of primary human lung microvascular endothelial cells (HLMECs)

The primary human lung microvascular endothelial cells (HLMECs) were supplied by Sigma-Aldrich and handled according to the manufacturer's instructions. Cells were cultured in tissue culture-treated flasks coated with tissue culture grade 0.2 % gelatin for 10 min, followed by two washes with sterile phosphate buffered saline (PBS) and then incubated at 37 °C, in 5 % CO_2. For experimental assays, HLMECs were seeded in tissue culture well plates or channel slides (µ-Slide I Luer, ibidi®). HLMECs were grown in microvascular endothelial cell growth medium (EBM™-2 Basal Medium, Lonza) supplemented with 15 % filtered (with 0.22 µm syringe filter) FBS and growth factors (EGM™-2 MV Microvascular Endothelial Cell Growth Medium SingleQuots™, Lonza) (complete media) according to the manufacturer's guidelines. **Table 2.7** summarises the growth factors included in EGM-2MV complete media. For detachment, media was removed, and cells were rinsed twice with sterile PBS and incubated with Accutase for 3 min at 37 °C. Accutase was neutralised with PBS supplemented with 5 % FBS and cells were collected and centrifuged at 300 x g, for 5 min. Supernatants were discarded and cell pellets were resuspended in fresh complete medium and seeded into new flasks, tissue culture wells, or channel slides. HLMECs were split every three to five days or whenever they reached 80-90 % monolayer confluency and seeded into new flasks (see **Table 2.8** for cell seeding conditions). The cell passage number was recorded. Throughout this thesis, HLMECs were used between passages 3-8 for experimental procedures.

Growth factors/ antibiotics
Ascorbic acid
Gentamicin
Human epidermal growth factor
Human fibroblast growth factor-B
Hydrocortisone
R3-insulin growth factor-1
Vascular endothelial growth factor

Table 2.7. Grown factors contained in the complete endothelial growth medium (EGM-2MV).

Tissue culture well/ channel slide size	HLMEC concentration (cells/mL)	HLMEC number (cells/well or slide)	Final well/slide volume (µL)
24-well plate	1.2×10^6	1.2×10^5	500
48-well plate	6×10^5	6×10^4	500
96-well plate	3×10^5	3×10^4	250
channel slides (0.4 mm)	1.2×10^6	1.2×10^5	100
channel slides (0.6 mm)	8×10^5	1.2×10^5	150
channel slides (0.8 mm)	6×10^5	1.2×10^5	200

Table 2.8. Cell seeding conditions for HLMECs in tissue culture well plates or channel slides.

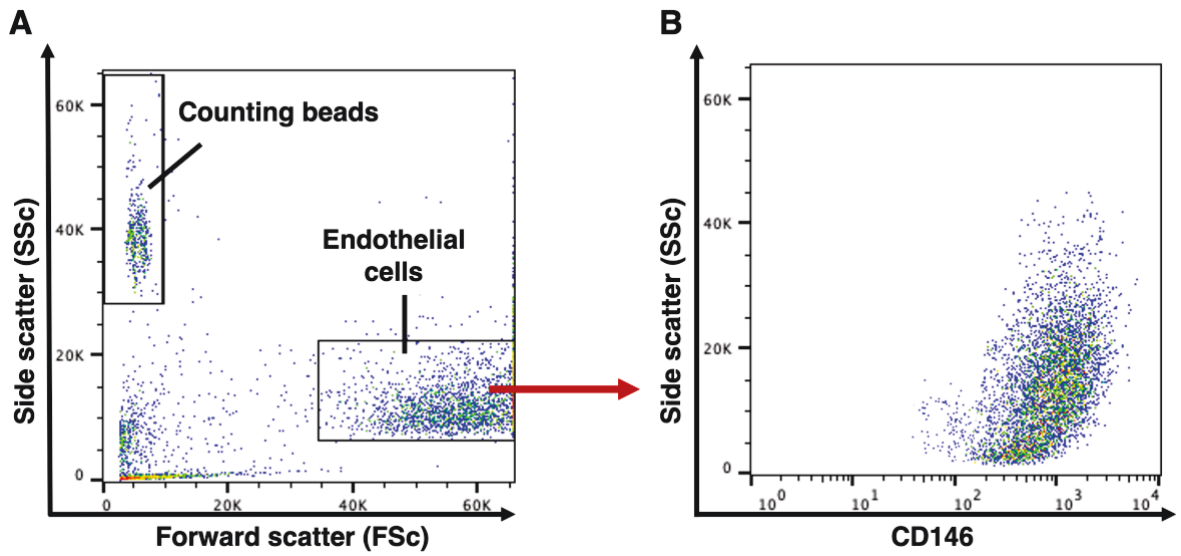

Figure 2.1. Endothelial cell analysis by flow cytometry.
HLMEC numbers and surface expression of surface molecules were determined by flow cytometry. Cells were first gated based on side (SSc) and forward scatter (FSc) (**A**) and then the endothelial cell marker, CD146 (**B**). Absolute counts were obtained with the use of AccuCheck counting beads.

2.3.2. Determination of cell or EV counts

Absolute numbers of cell or EV subpopulations were determined by flow cytometry. For cells, a volume of 10 µL of sample was transferred to a FACS tube containing 400 µL of FACS wash buffer (FWB) while for EVs 10 µL of sample was transferred to a FACS tube containing 1 mL of filtered PBS, and 10 µL AccuCheck counting beads. Absolute cell/EV counts were calculated based on the following equations.

$$\textbf{(A)}\ \text{Cells or EVs/mL} = \frac{\text{number of cell or EV events}}{\text{number of bead events}} \times \frac{\text{volume of beads}}{\text{volume of cells or EVs}} \times 10^6$$

(B) Absolute cell or EV count = cell or EV count (cells or EVs/mL) × total volume (mL)

2.3.3. Assessment of cell viability

Cell viability was assessed in experimental procedures requiring treatment of cells with chemical or pharmacological inhibitors (e.g., reactive oxygen species (ROS), kinase, and other inhibitors) to determine any induced cytotoxicity.

7-AAD staining

To determine the cell viability the 7-amino-actinomycin D (7-AAD) a fluorescent membrane impermeant dye that has a strong affinity for DNA, was used. In brief, 5 µL of 7-AAD were added to each FACS tube and incubated for 5 min with minimal light exposure before flow cytometry acquisition. 7-AAD requires permeabilisation or disruption of the cell membrane to enter and bind to double-stranded DNA by intercalating between base pairs in G-C rich regions. 7-AAD excitation and emission wavelengths are at 488 nm and at 645 nm respectively.

PI staining

Propidium iodide (PI) staining was also used to assess cellular cytotoxicity. Once the cells were processed and stained with target antibodies, 0.5 µL of PI were added to each FACS tube. Cells were acquired within 5-10 min of PI addition. PI is a membrane impermeant fluorescent nuclear and chromosome dye with excitation and emission wavelength at 493 nm and 636 nm respectively.

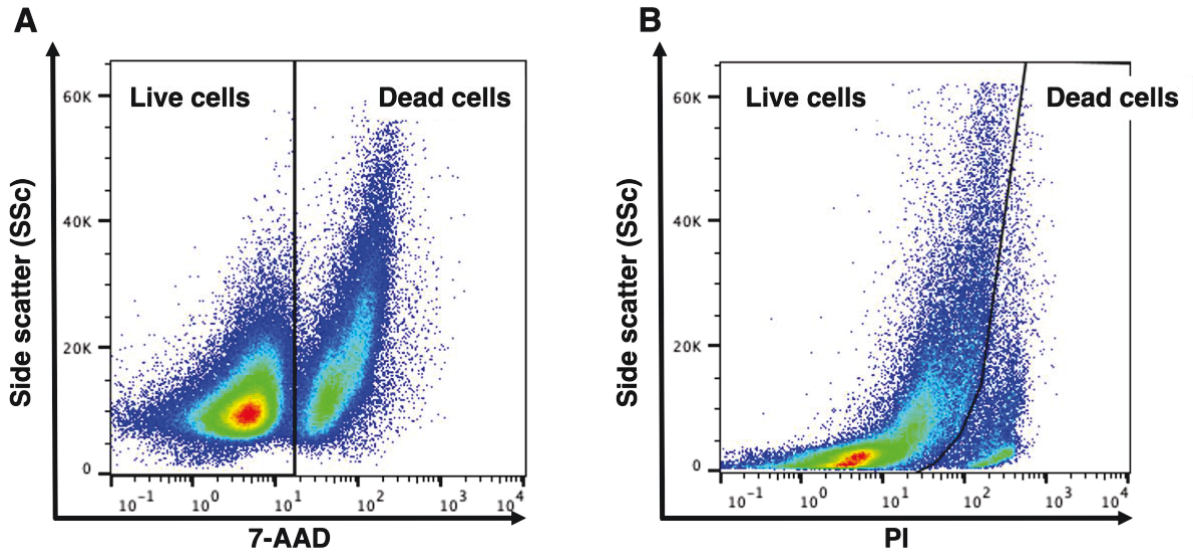

Figure 2.2. Representative flow cytometry plots showing the live/dead gating with 7-AAD and PI staining.

Following experimental procedures with treatment of cells with chemical or pharmacological inhibitors, cell viability was assessed by 7-AAD in neutrophils (**A**) or PI staining in co-cultures of PBMCs and HLMECs (**B**). Cells were stained with relevant antibodies and live/dead dyes 7-AAD or PI. The 7-AAD or PI negative cells are the live, whereas the 7-AAD or PI positive cells are the dead cell populations. Following a short incubation, cells were analysed with flow cytometry to determine the percentage of live and dead cells in each condition.

2.4. Human blood processing and collection

Ethical permission was granted by the local ethics committee (REC references 15/LO/1764 & 19/LO/1606) for obtaining peripheral venous blood from healthy, non-medicated volunteers. Signed informed consent was obtained from all participants. For neutrophil and peripheral blood mononuclear cell (PBMC) isolation, venous blood was collected in EDTA vacutainers using a 21-gauge butterfly needle and processed immediately. For whole blood stimulation, venous blood was collected in lithium-heparin vacutainers using a 21-gauge needle and processed within 30 min of collection.

2.4.1. Peripheral blood mononuclear cell (PBMC) and leukocyte isolation

PBMCs and leukocytes were isolated from whole blood by density gradient centrifugation using Histopaque-1077 and Leucosep tubes according to the manufacturer's instructions. To each Leucosep tube, a maximum volume of 20 mL EDTA-treated blood was added and centrifuged at 1,000 x g for 15 min. Following the centrifugation, blood was separated into distinct layers of plasma, PBMCs, and red blood cells (RBCs) with granulocytes (**Figure 2.3**).

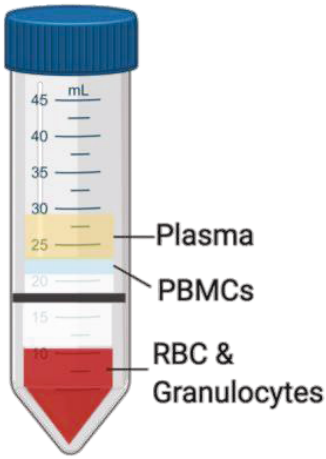

Figure 2.3. Schematic of whole blood separation after density gradient centrifugation. Granulocytes and PBMCs were isolated from whole blood by density gradient centrifugation using Histopaque-1077. Following initial separation, the resulting material contained distinct layers for different cell groups (PBMCs, RBCs-granulocytes). Figure designed with Biorender.

PBMC isolation

The top plasma layer was discarded using a Pasteur pipette or stored at -20 °C for subsequent analysis. The middle PBMC layer was gently aspirated and transferred into a new 50 mL falcon tube. PBMCs were washed by addition of cold, sterile PBS (without Ca^{2+}/Mg^{2+}) to a final volume of 50 mL and centrifuged at 400 x g for 7 min at 4 °C. The supernatant was discarded, and the wash step was repeated three times. PBMCs were then resuspended in 1 mL of cell medium (EBM supplemented with 0.5 % human albumin solution (HAS) (EBM-HAS)) or immunomagnetic bead cell sorting buffer (PBS, 0.5 % HAS, 2 mM EDTA, 1x penicillin-streptomycin) depending on the subsequent use.

Neutrophil isolation

Neutrophils were isolated using the dextran sedimentation and the hypo-osmotic lysis method. The Histopaque bottom layer containing RBCs and granulocytes was mixed with 3 % dextran (diluted in PBS) at a 1:3 (cells: dextran) ratio and left to sediment for 25 min. Then, the granulocyte-rich supernatant was centrifuged at 400 x g for 7 min at 4 °C. After centrifugation,

the cell pellet was resuspended in cold, sterile distilled H_2O and mixed using a serological pipette for 20 sec to lyse the remaining RBCs. Isotonicity was restored with 10x concentrated PBS and cells were centrifuged at 400 x g for 7 min at 4 °C and the supernatant was discarded. The cell pellet was resuspended in cold, sterile PBS and the washing step was repeated two times. The final cell pellet was resuspended in RPMI-1640 medium supplemented with 0.5 % HAS.

Different cell populations were determined in whole blood prior to neutrophil isolation by flow cytometry and identified based on their characteristic shape on FSc and SSc (**Figure 2.4, A**). Neutrophil purity was determined in the isolated cell populations with the use of specific markers present on naïve neutrophil surface, CD66b and CD11b, indicating consistent levels of purity (≥90 %) and yield using the density-gradient and dextran-based separation method (**Figure 2.4, B-C**).

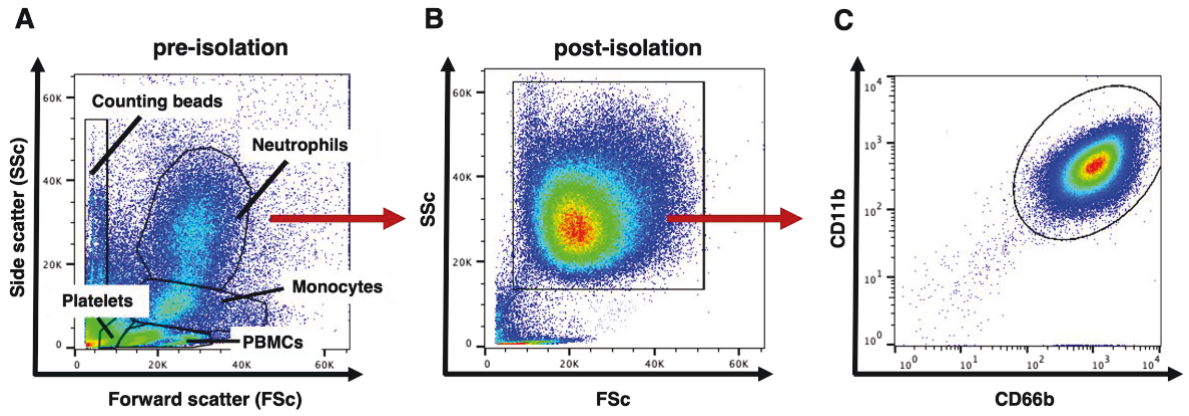

Figure 2.4. Human neutrophil gating strategy.
Human neutrophils were isolated from healthy volunteer blood. Flow cytometric analysis was used to assess the cell purity and cell counts after the isolation process. FSc versus SSc dot plot of whole blood prior to neutrophil isolation (**A**). FSc vs. SSc dot plots of post-isolation neutrophil preparation (**B**) and CD11b vs. CD66b staining of the high SSc gated population (**C**).

2.4.2. Immunoaffinity isolation of human primary monocytes by negative selection

The Miltenyi Biotec pan monocyte isolation kit was used to isolate monocyte populations from PBMCs according to the manufacturer's instructions. Following PBMC isolation by density gradient centrifugation, cell pellets were resuspended in cell sorting buffer (PBS, 0.5 % HAS, 2 mM EDTA, 1x penicillin-streptomycin). The FcR Blocking Reagent and Pan Monocyte Biotin-Antibody Cocktail (containing a cocktail of biotin-conjugated monoclonal antibodies against antigens that are not expressed on human monocytes such as CD3, CD7, CD19, CD56, CD123 and CD235a) were added to the cells and incubated for 5 min at 4 °C, before a 10 min secondary incubation with Anti-Biotin MicroBeads (10 µL FcR Blocking Reagent, 10 µL Biotin-Antibody Cocktail, and 20 µL Anti-Biotin Microbeads per 10^7 total cells). Magnetic cell separation was then performed using appropriately sized MACS® Separator and MACS® Columns, based on the number of labelled and total cells (MiniMACS® separator and medium-size (MS) column for up to 10^7 labelled cells and 2 x 10^8 total cells, MidiMACS® separator and large-size (LS) column for up to 10^8 labelled cells and 2 x 10^9 total cells). The cell suspension was applied to the column and the flow-through fraction containing the unlabelled enriched monocytes was collected. Monocytes were then centrifuged at 300 x g, 10 min, 4 °C and resuspended in assay buffer (EBM-HAS). Monocyte purity (≥90 %) was confirmed by staining for CD14, CD16 and flow cytometry.

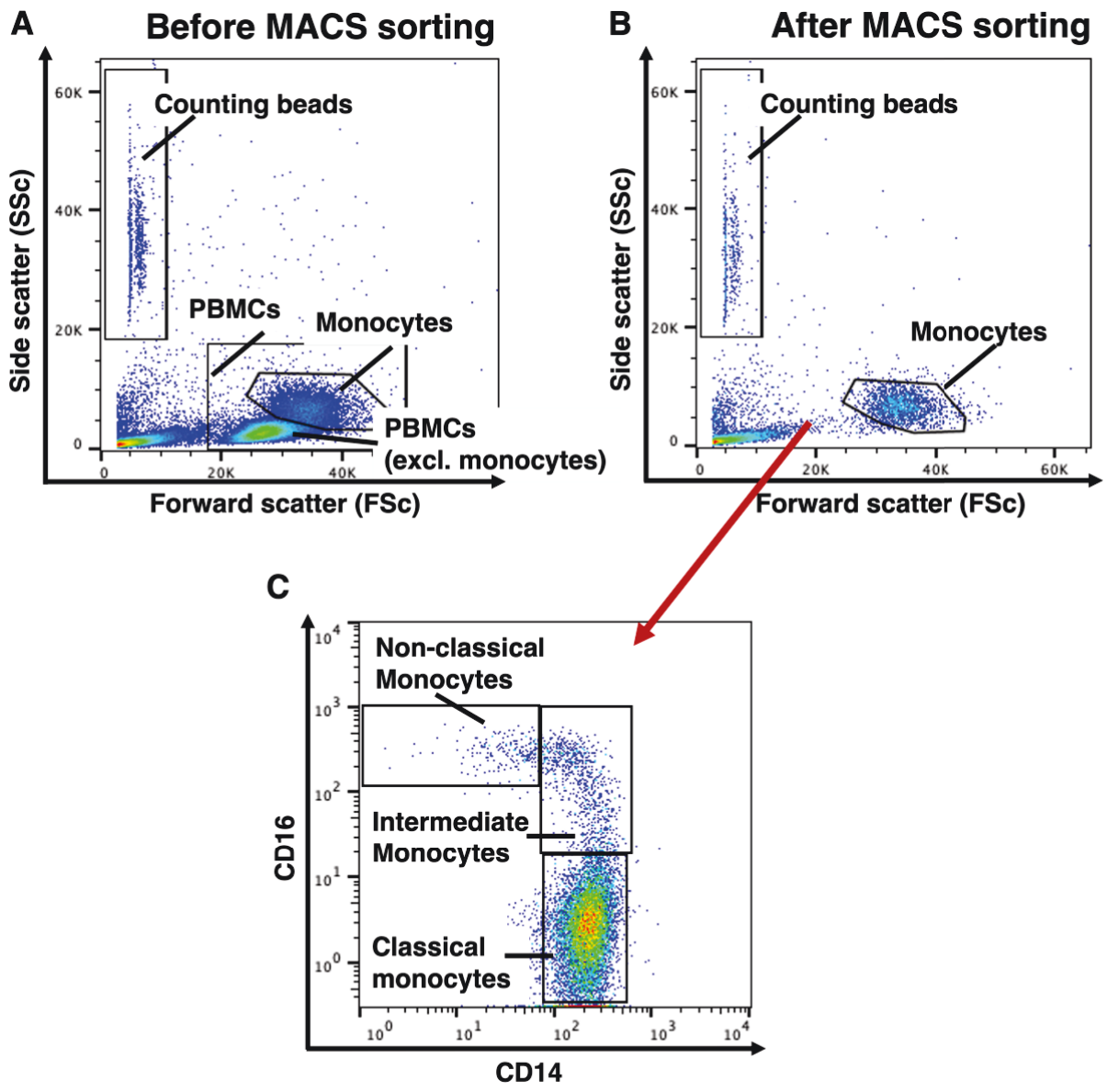

Figure 2.5. Monocyte isolation by negative selection.
Human monocytes were isolated from PBMCs using the Miltenyi Pan Monocyte immunomagnetic bead isolation method. Monocyte and PBMC numbers were determined in the initial sample and used for the calculation of separation reagents required (**A**). Following the negative selection, monocyte purity was assessed, followed by staining for the identification of classical ($CD14^{high}CD16^{low}$), intermediate ($CD14^{high}CD16^{high/low}$), and non-classical ($CD14^{low}CD16^{high}$) monocyte populations via CD14 (PE-Cy5) and CD16 (FITC) staining (**B, C**).

2.5. EVs

2.5.1. EV production and isolation by differential centrifugation

Ex vivo EV production in whole blood

For *ex vivo* EV production in whole blood, heparinised blood from healthy volunteers was stimulated with lipopolysaccharide (LPS, 100 ng/mL) (ultrapure Escherichia coli O111:B4) in 15 mL falcon tubes (5 mL/tube), at 37 °C with continuous mixing for up to 4 h. After stimulation whole blood was centrifuged at 400 x g for 10 min at 4 °C to obtain cell-free, platelet-rich plasma, which was then centrifugated at 1,000 x g for 5 min at 4 °C followed by 1,500 x g for 20 min at 4 °C to produce platelet-poor plasma. EVs were obtained by centrifugation of platelet-poor plasma at 20,800 x g for 30 min at 4 °C, with careful removal of supernatants and resuspension of the pellet in EV sorting buffer (PBS, 0.5 % HAS, 2 mM EDTA, 1x penicillin-streptomycin) or a physiological medium (e.g., EBM-HAS) for further processing.

In vitro EV production by stimulation of isolated neutrophils

Freshly isolated neutrophils were collected and incubated at 37 °C for up to 3 h in polypropylene Eppendorf tubes (2 x 10^7 neutrophils/mL) at 500 µL RPMI-HAS with continuous mixing in the presence of different stimuli. The stimuli used in the present study for *in vitro* EV production were: N-formylmethionyl-leucyl-phenylalanine (fMLP) (1 µM), LPS (100 ng/mL), calcium ionophore A23187 (1 µM), tumour necrosis factor α (TNF-α) (100 ng/mL). Samples were then cooled rapidly on ice for ~3 min and centrifuged at 400 x g for 5 min at 4 °C. The cell-free supernatants were transferred in new Eppendorf tubes and centrifuged at 20,800 x g for 30 min at 4 °C. Pellets were resuspended in EV sorting buffer or relevant medium (EBM-HAS) for further processing.

2.5.2. Immunoaffinity isolation of specific EV subtypes

Enriched populations of EV subtypes derived from different parent cell populations were obtained via immunomagnetic bead separation. Mixed EVs resuspended in EV sorting buffer were stained for cell surface markers and counted by flow cytometry. EVs were then incubated with titrated volumes of bead-conjugated antibodies (based on the EV number of the targeted subtype) for 15 min at 4 °C. **Table 2.9** summarises the EV subtypes alongside the Miltenyi MicroBead products used in this study.

EV subtype	Isolation method	Microbead product
Human myeloid-EVs ($CD11b^+$)	positive selection	CD11b MicroBeads (mouse/human)
Human neutrophil-EVs ($CD66b^+$)	positive selection	StraightFrom® Whole Blood CD66b MicroBeads (human)
Human neutrophil-EVs ($CD66b^+$)	negative selection	MACSxpress® Whole Blood Isolation kit (human)
Human platelet-EVs ($CD61^+$)	positive selection	CD61 MicroBeads (human)

Table 2.9. Immunoaffinity isolation methods of different EV subtypes.

Labelled EVs were passed through a pre-equilibrated magnetised column placed on MACS® Separator. MS columns and the miniMACS® separator magnet were used for up to 10^7 target EVs while LS columns and the midiMACS® separator magnet were used for more than 10^7 target EVs. The unbound EV suspension was collected for 'negatively-selected' EV preparations. The column was then washed three times with EV sorting buffer (MS column: 3 x 500 µL; LS column 3 x 3 mL). The 'positively-selected' column-bound EVs were eluted by removing the column from the magnet and flushed through with appropriate volume of EV sorting buffer (MS column: 1 mL; LS column: 5 mL). Positively or negatively selected EVs were then pelleted at 20,800 x g for 30 min at 4 °C and washed by centrifugation with EV

sorting buffer. Final EV samples were resuspended in media (EBM-HAS), or PBS supplemented with 0.5 % HAS (PBS-HAS) depending on the subsequent use.

2.5.3. EV labelling for uptake studies

EV labelling with fluorescent dye

To determine the EV uptake by target cells, neutrophil-EVs produced with fMLP stimulation of isolated neutrophils were used. EVs were labelled using the membrane-binding lipophilic dye DiD (1,1'-Dioctadecyl-3,3,3',3'-Tetramethylindodicarbocyanine, 4-Chlorobenzenesulfonate Salt). DiD solid was dissolved in ethanol to form a 1 mM stock, from which an intermediate stock of 30 µM was prepared in Diluent C (Sigma). EV pellets were resuspended in 0.22 µm filtered PBS (without Ca^{2+}/Mg^{2+}) and incubated with a final concentration of 5 µM DiD for 7 min in dark. DiD-labelled EVs were then washed by addition of 500 µL PBS-HAS, centrifuged at 20,800 x g for 30 min at 4 °C and resuspended in PBS-HAS. A second wash was repeated to remove any dye residues and the labelled EVs were resuspended in appropriate volume of media (EBM-HAS). Labelled EVs (10 µL) were stained with fluorophore-conjugated antibodies for 30 min at 4 °C in dark, diluted in PBS and analysed by flow cytometry.

To standardise the EV concentration used for uptake assays, total DiD fluorescence was measured using a fluorescent plate reader (Biotech FLx800) at 635 nm and 689 nm absorption and emission wavelengths respectively. DiD-labelled EVs were resuspended in PBS with 0.5 % Triton X-100 in PBS to solubilise DiD. Total EV-DiD concentrations (fluorescence units/mL) were then adjusted based on a pilot EV dose-response curve and linear calibration of EV fluorescence against number of EVs.

2.5.4. EV assays

HLMEC-only culture or PBMC-HLMEC co-culture models were developed to determine EV uptake by target cells (HLMECs or monocytes) under static and flow conditions or assess the functional properties of EV subtypes. For flow culture, a parallel flow chamber (PFC) system was used (see **Section 2.6**). In both models HLMECs were seeded in confluence in tissue culture wells (static), or channel slides (µ-Slide I Luer, ibidi®) (flow) as described in **Section 2.3.1**, using complete EBM (EGM-2MV), and left to adhere overnight. In the co-culture model of PBMCs and HLMECs, PBMCs were added to HLMECs monolayers in the ratio of monocytes (in PBMCs): HLMECs of 2: 1 in EBM-HAS. Experimental procedures (both in EV uptake and functional assays) were carried out in serum-free conditions by replacing the culture medium with EBM-HAS prior to EV addition.

EV uptake

EV uptake was determined by using the fMLP-generated EVs from isolated neutrophils. If EV uptake was determined under flow conditions, HLMECs were adapted to experimental shear stress conditions for 24 h. For EV uptake under static conditions, all cell incubations were carried out in tissue culture wells, without adaptation. To determine EV uptake by HLMECs and monocytes in a co-culture model of PBMCs and HLMECs, I developed protocols for adherence of monocyte the HLMECs, which is discussed in detail in Chapter 3. In brief, monocytes were allowed to adhere to TNF-α stimulated HLMECs and then washed prior to incubation with DiD-labelled EVs. In all assays, neutrophil-EVs and cells were co-incubated for 1 h at 37 °C. Upon completion of the cell-EV co-incubation, cells were washed three times with PBS to remove any unbound EV residues and detached using Accutase (3 min, 37 °C). Neutrophil-EV uptake by target cells was quantified by flow cytometric analysis as cell-associated DiD fluorescence.

EV functional assays

To investigate the biological functions and phenotypes of different EV subtypes, functional assays were conducted. Most of these were conducted in static conditions, however for some the PFC system was used, following the same procedures described above. Pre-determined concentrations of immunoaffinity-isolated EV subtypes were incubated in monocultures of HLMECs, or co-cultures of PBMCs or purified monocytes with HLMECs for 4 h. This assay was first established in 48-well tissue culture well plates and later optimised for high throughput analysis in 96-well tissue culture plate set-up. LPS stimulation was routinely used in HLMEC and PBMC-HLMEC as a positive control with addition of FBS to the assay medium to ensure optimal LPS signalling activity (358).

After stimulation, cell supernatants were collected and stored at -80 °C for subsequent cytokine analysis. Treated cells were washed three times with PBS and appropriate volume of pre-warmed cell dissociation buffer was applied to cells and incubated for 15 min at 37 °C. When the majority of cells acquired a rounded shape, the detachment process was stopped by addition of equal volume of ice-cold FWB. The cells were mechanically dissociated for 1 min by pipetting, placed in FACS tubes containing 3 mL of FWB, and immediately placed in ice.

2.6. Experimentation under flow conditions

2.6.1. The ibidi® Parallel Flow Chamber system

All experiments under flow conditions were performed using a PFC system manufactured by ibidi®, made up of the following components: the PumpControl software; the ibidi® Pump; and four Fluidic Units, all of which are controlled by a single air pump. Each fluidic unit consists of a channel slide (µ-Slide I Luer) connected with a perfusion set and two reservoirs sealed with air filters. The fluidic unit's active components include two switching valves. There are two connectors in the rear of the fluidic unit, one electrical connection for the valve control and a second one for the pressurised air, both of which connected the fluidic unit to the pump. The setup of the PFC system is depicted in **Figure 2.6.**

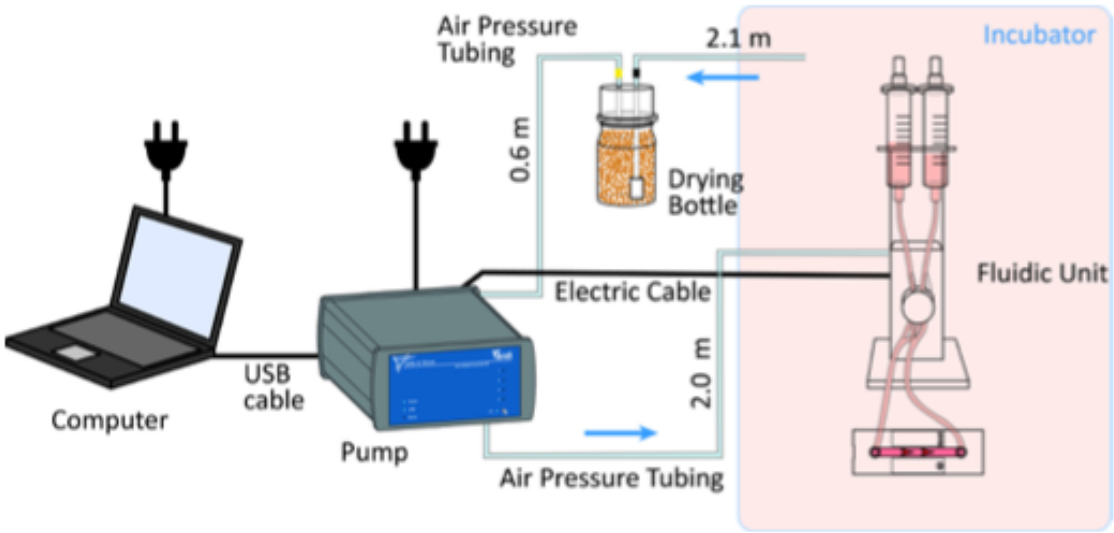

Figure 2.6. Schematic of the ibidi® parallel flow chamber system setup.
The pump is connected to a computer with a specifically designed software (PumpControl, ibidi®). Air tubing connects the pump to the fluidic unit. The blue arrows indicate the direction of air flow. Each fluidic unit consists of a channel slide on which cells are seeded, a perfusion set (tubing) and two reservoirs that contain the perfused medium. Two filters seal the reservoirs and are linked with the pump through the air tubing. Figure adapted from ibidi® website.

The ibidi® Pump system uses constant air pressure to produce a unidirectional laminar flow to cells grown in a monolayer on tissue culture-treated polymer channel slides, simulating the *in vivo* flow-induced forces. Of note, as an air pressure-induced flow system, it avoids the physical compression and potential activation of cells produced by a standard peristaltic flow system. The software allows users to customise the flow parameters to design a regimen that best simulates the *in vivo* blood flow conditions in an *in vitro* setting. However, since all four fluidic units are controlled by a single pump, the air pressure given at each time is constant for all four units. Different flow rates can be induced even from a single air pressure by combinations of different perfusion sets (tubing and channel slides).

To succeed a unidirectional flow within the channel slides, a computer-controlled two-way valve system operates. The pump supplies a constant air pressure (mbar) to the reservoirs of each fluidic unit and generates a constant flow of medium within the channel slides, measured by the flow rate (mL/min), which depends on three parameters, the pressure input, the medium viscosity, and the perfusion system's flow resistance (determined by tubing diameter and slide height). The specific flow rate (mL/min) produces a wall shear stress (dyn/cm^2) to which the cells are exposed. Before each reservoir empties, a two-way valve system reverses the flow direction. Two valves labelled V1 and V2 are switched simultaneously between two positions, as shown in the schematic below (**Figure 2.7**).

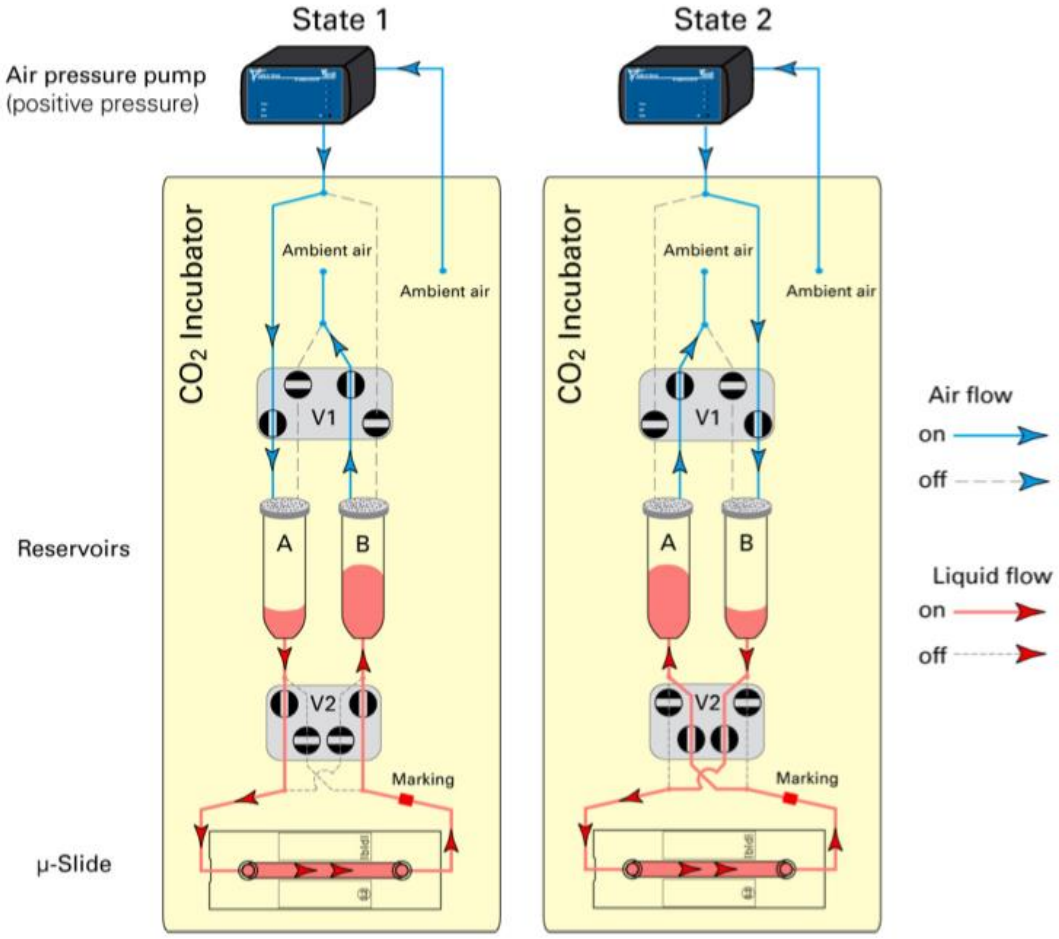

Figure 2.7. Working principle of the two-way valve system, creating a unidirectional flow within channel slides.
To obtain a unidirectional flow within the channel slides where HLMECs are seeded, a two-way valve system operates, opening and closing the valves (V1 and V2) in a controlled way to avoid emptying the reservoirs, while media is running from one to the other. The simultaneous opening of one valve and closing of the other at each state ensures that the media is running towards one direction only. Figure adapted from ibidi® website.

2.6.2. Shear stress/shear rate calculation

The selection of perfusion sets, and channel slides, enables the user to control the shear stress level generated by the ibidi® Pump System. Two perfusion sets, a blue and a red, made up of 0.8 mm and 1.6 mm diameter tubing respectively, are commercially available from ibidi® and can be used with ibidi® Pump System. Similarly, channel slides are available at heights of 0.4 mm, 0.6 mm, and 0.8 mm. The ibidi® Pump can generate air pressure up to 100 mbar. For

more precise experimentation a minimum pressure of 5 mbar and a maximum of 95 mbar is recommended. The combination of perfusion set diameter and height of channel slide determines the shear stress level in any given pressure. **Table 2.10** outlines the maximum and minimum shear stress levels generated by using each perfusion set and channel combination.

Perfusion set diameter (mm)	Channel slide height (mm)	Air pressure (mbar)	Shear stress (dyn/cm^2)	Shear rate (s^{-1})	Flow rate (mL/min)
Blue (0.8)	0.8	5	0.22	31	0.90
		95	2.60	371	10.7
	0.6	5	0.37	53	0.88
		95	4.50	643	10.7
	0.4	5	0.80	115	0.87
		95	9.40	1,342	10.2
Red (1.6)	0.8	5	1.30	187	5.4
		95	12.00	1,721	49.6
	0.6	5	2.30	325	5.4
		95	20.80	2,969	49.4
	0.4	5	4.80	684	5.2
		95	43.20	6,172	46.9

Table 2.10. Minimum and maximum shear stress and flow rates level that can be generated by the combination of each perfusion set and channel slide.
These given shear stress, shear rates and flow rates refer to medium viscosity 0.0072 dyn·s/cm^2 and temperature 37 °C.

2.6.3. Cell culture and experimentation with the ibidi® parallel flow chamber system

For cell culture and experimentation under flow conditions, HLMECs were seeded in channel slides as described above. Based on the surface area measurements, the channel slides

require a similar number of cells as the ones used in 24-well tissue culture plates. All the flow accessories (channel slides, perfusion sets, reservoirs) and the perfusate medium were prepared and left in an incubator (37 °C, 5 % CO_2) overnight, to restore the pH and reach temperature equilibrium to avoid air bubble formation. The following day, the medium in each slide was replaced with fresh and slides were introduced to the PFC system. HLMECs were adapted to the experimental flow rate for a period of 24 h before subsequent experimentation. In co-culture assays, HLMECs were adapted overnight, as with the monoculture protocol, and after the PBMC adhesion, which was performed under static conditions, co-culture slides were introduced to the experimental flow rate for a subsequent 1 h flow adaptation, before proceeding with EV uptake or functional assays under flow. During EV uptake assays with the PFC system, EV distribution in the circuit was allowed to stabilise for 5 min at a constant flow rate prior to the start of EV-cell co-incubation for 1 h. Upon completion of the experimental procedures, cells within channel slides were detached with Accutase treatment and collected by using two 1 mL syringes connected to the slides' luer port to gently rinse back and forth three times.

2.6.4. Maintenance and sterility of perfusion sets and channel slides

Using the PFC system under sterile and endotoxin-free conditions was essential for the experimental procedures carried out throughout the project. I developed a stringent cleaning routine for the perfusion sets (tubing), and channel slides. Following each experiment, all perfusate media and cells were removed and tubing and slides were drained and filled with sterile tissue culture grade water to rinse out all remaining residues. After this washing step, water was drained, and tubing and slides were filled with high quality detergent (consisting of 20 % Mucasol™ resuspended in sterile water) and incubated overnight. The following day, tubing and slides were drained and rinsed with 70 % ethanol, followed by rinsing multiple times

with sterile grade deionised water. After every three consecutive experimental uses, slides were discarded and tubing sets were autoclaved.

2.7. Flow cytometry

Flow cytometric analysis allows the identification of specific subpopulations of cells or EVs based on the cell size (detected as FSc), granularity (detected as SSc), and expression of various combinations of cell surface markers.

2.7.1. Flow cytometric staining for cells

Supernatants were discarded and cell pellets were re-suspended in 4 mL FWB before centrifugation. Supernatants were discarded and the final cell pellets were resuspended in 40 µL of FWB and kept on ice until further processing. Cell suspensions were incubated with various panels of fluorochrome-conjugated antibodies in FACS tubes for 30 min at 4 °C in dark. Antibodies were prepared in FWB in 2x of the final concentrations and 40 µL of antibody cocktails were mixed with 40 µL of cells. After staining, FACS tubes were topped up to 4 mL with FWB and centrifuged at 400 x g at 4 °C for 5 min. Supernatants were discarded and cell pellets were resuspended in 400 µL of FWB and acquired with the flow cytometer. Following sample acquisition on the flow cytometer, data were analysed with FlowJo software. The expression of surface molecules is presented as mean fluorescence intensity (MFI) throughout this thesis.

2.7.2. Flow cytometry staining and analysis of whole blood

For analysis and staining of whole blood, 100 µL of blood were transferred to FACS tubes and incubated with 100 µL of appropriate antibody cocktails for 30 min at 4 °C in dark. Following staining, 4 mL of cold FWB was added to each FACS tube, and samples were centrifuged at 400 x g at 4 °C for 5 min. Supernatants were discarded, cell pellets were vortexed vigorously, resuspended in 1 mL of 1-step Lyse/Fix Solution (1x) and incubated for 10 min in dark for fixation and red blood cell lysis. Samples were then washed once with 3 mL of FWB. Cells were pelleted by centrifugation at 400 x g at 4 °C for 5 min and resuspended in 400 µL of FWB prior to sample acquisition on the flow cytometer.

2.7.3. Flow cytometry staining and analysis of EVs

EVs were identified by flow cytometry based on three separate criteria: 1) size smaller than 1 µm; 2) positive for specific surface antigen markers, present on the surface of parental cell type; 3) detergent lysis sensitivity. The side scatter threshold was adjusted based on fluorescent sizing calibration beads (**Figure 2.8**). The gating strategy for EVs is shown in **Figure 2.9**, where neutrophil-EVs are shown as an example. A similar strategy was followed for the identification of other EV subtypes.

For antibody staining, EVs were resuspended in 0.22 µm filtered PBS (without Ca^{2+}/Mg^{2+}). 10 µL of EV suspensions were transferred in FACS tubes and incubated with 10 µL of fluorophore-conjugated antibody cocktails, which were also prepared in filtered PBS in 2x of the final concentration, for 30 min, at 4 °C. In cases of annexin V staining, antibody mixtures were prepared in annexin V binding buffer (Biolegend). Following staining 1 mL of filtered PBS (or annexin V binding buffer) and 10 µL AccuCheck counting beads were added to each sample. Upon acquisition of each sample, detergent sensitivity was confirmed by addition of 10 µL of 1 % Triton X-100 (prepared in filtered PBS) and samples were re-acquired.

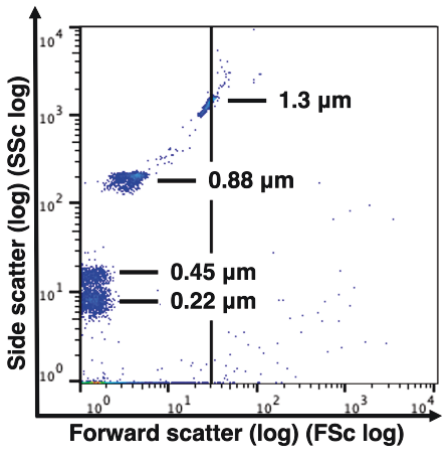

Figure 2.8. Fluorescent sizing calibration beads.
Flow cytometry gating for EVs was determined by fluorescent sizing calibration beads. A gate below 1 µm was drawn and EVs within this gate were assessed by specific surface markers.

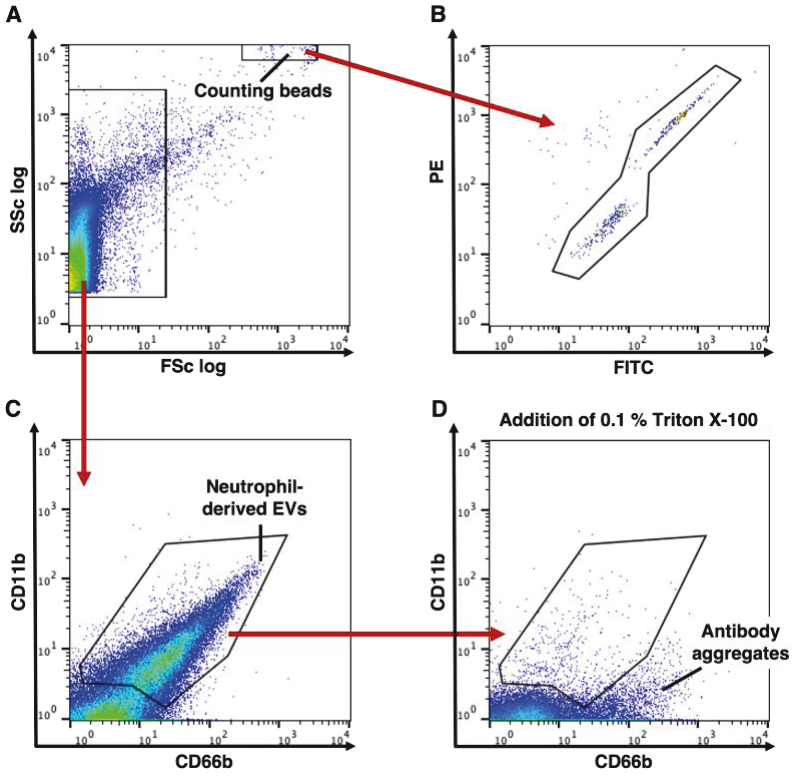

Figure 2.9. Gating strategy for neutrophil-EVs
Neutrophil-EVs within the 1 µm gate (**A**) were identified by the expression of neutrophil markers CD11b and CD66b (**C**). Absolute numbers were determined based on AccuCheck counting beads (**B**). Detergent lysis confirmed the membrane nature of the detected events (**D**).

2.7.4. Antibodies

The antibody panels used throughout this study for the identification of different EV and cell populations and the assessment of their activation following several inflammatory treatments are described in the tables of this section. All antibodies were obtained by Biolegend as fluorophore-conjugated unless otherwise stated.

Conjugate dye abbreviations:

FITC: Fluorescein isothiocyanate

PE: Phycoerythrin

PerCP: Peridinin-Chlorophyll-Protein

APC: Allophycocyanin

Cy: Cyanine

EV subtype antibody panel					
Panel	**Antigen**	**Clone**	**Fluorochrome**	**Concentration**	**Expression**
Panel A	**CD61**	VI-PL2	PECy-7	1:100	Platelets
	CD41	HIP8	APC	1:100	Platelets
	CD31	WM59	PE	1:100	Platelets
Panel B	**CD66b**	G10F5	PE-Cy7	1:80	Neutrophils
	CD11b	M1/70	PE	1:100	Neutrophils
	CD15	SSEA-1	APC	1:100	Neutrophils
Panel C	**CD14**	HCD14	PE	1:20	Monocytes
	CD11b	M1/70	PE-Cy7	1:100	Monocytes
	HLA-DR	L243	APC	1:20	Monocytes
Panel D	**Annexin V**	N/A	FITC	1:20	All EVs
	CD45	2D1	APC	1:100	Leukocytes, lymphocytes
	CD235α	HI264	PE	1:100	Red blood cells

Table 2.11. Fluorophore-conjugated antibody panels for the identification of EV subtypes produced in the LPS whole blood model.

PBMC-HLMEC co-culture antibody panel (Endothelial cell and monocyte activation)					
Panel	**Antigen**	**Clone**	**Fluorochrome**	**Concentration**	**Isotype**
Endothelial cell panel	**CD146**	P1H12	FITC	1:200	Mouse IgG1, κ
	CD62E (E selectin)	HAE-1f	PE	1:100	Mouse IgG1, κ
	CD54 (ICAM-1)	HA58	PerCP-5.5	1:300	Mouse IgG1, κ
	CD106 (VCAM-1)	STA	PE-Cy7	1:100	Mouse IgG1, κ
	CD142 (Tissue factor)	NY2	APC	1:100	Mouse IgG1, κ
Monocyte panel	**CD16**	3G8	FITC	1:200	Mouse IgG1, κ
	CD142 (Tissue factor)	NY2	PE	1:100	Mouse IgG1, κ
	CD11b	M1/70	PE-DAZZLE^{594}	1:300	Rat IgG2b, κ
	CD54 (ICAM-1)	HA58	PerCP-5.5	1:300	Mouse IgG1, κ
	CD14	HCD14	PE-Cy7	1:200	Mouse IgG1, κ
	CD86	IT2.2	APC	1:200	Mouse IgG2b, κ
	HLA-DR	L243	APC-Cy7	1:200	Mouse IgG2a, κ

Table 2.12. Fluorophore-conjugated antibody panels for the identification and activation assessment of HLMECs and monocytes present in the co-culture model.

Whole blood antibody panel					
Panel	**Antigen**	**Clone**	**Fluorochrome**	**Concentration**	**Expression**
Panel A	**CD61**	VI-PL2	PECy-7	1:200	Platelets
	CD41	HIP8	APC	1:200	Platelets
Panel B	**CD66b**	G10F5	PE-Cy7	1:200	Neutrophils
	CD11b	M1/70	APC	1:400	Neutrophils
Panel C	**CD14**	HCD14	PE-Cy7	1:200	Monocytes
	CD11b	M1/70	PE-Cy5	1:100	Monocytes
	HLA-DR	L243	APC-Cy7	1:200	Monocytes

Table 2.13. Fluorophore-conjugated antibody panels for the identification of platelets, neutrophils, and monocytes stained in whole blood.

Isolated neutrophil antibody panel				
Antigen	**Clone**	**Fluorochrome**	**Concentration**	**Isotype**
CD62L (L-selectin)	DREG-56	FITC	1:200	Mouse IgG1, κ
CD63	H5C6	PE	1:100	Mouse IgG1, κ
CD11b	M1/70	PE-DAZZLE^{594}	1:400	Rat IgG2b, κ
CD66b	G10F5	PE-Cy7	1:200	Mouse IgM, κ
CD45	2D1	APC-Cy7	1:200	Mouse IgG1, κ

Table 2.14. Fluorophore-conjugated antibody panel for the activation assessment of isolated neutrophils, after treatment with different inflammatory stimuli.

HLMEC surface phenotype antibody panels					
Panel	**Antigen**	**Clone**	**Fluorochrome**	**Concentration**	**Isotype**
Panel A	**CD146**	P1H12	FITC	1:100	Mouse IgG1, κ
	CD31	WM59	PE-DAZZLE^{594}	1:200	Mouse IgG1, κ
	CD62E (E-selectin)	HAE-1f	PE	1:50	Mouse IgG1, κ
	CD54 (ICAM-1)	HA58	PerCP-5.5	1:300	Mouse IgG1, κ
	CD106 (VCAM-1)	STA	APC	1:100	Mouse IgG1, κ
Panel B	**CD146**	P1H12	FITC	1:100	Mouse IgG1, κ
	CD31	WM59	PE-DAZZLE^{594}	1:200	Mouse IgG1, κ
	CD61	VI-PL2	APC	1:200	Mouse IgG1, κ
	CD204 (Scavenger receptor A)	7C9C20	PE	1:100	Mouse IgG2a, κ
	CD36 (Scavenger receptor B)	5-271	PE-Cy7	1:100	Mouse IgG2a, κ
Panel C	**CD146**	P1H12	FITC	1:100	Mouse IgG1, κ
	CD31	WM59	PE-DAZZLE^{594}	1:200	Mouse IgG1, κ
	CD144 (VE-cadherin)	BV9	APC	1:100	Mouse IgG2a, κ

Table 2.15. Fluorophore-conjugated antibody panel for the assessment of HLMEC phenotype following adaptation to flow.

The majority of the analysis was performed using a Cyan™ ADP flow cytometer fitted with blue (488nm) and red (638nm) laser. In the final stages of the work, a small set of assays was conducted by using the Cytek® Northern Lights™ full spectrum flow cytometer fitted with an additional violet (405nm) laser increasing EV detection and resolution. To avoid inconsistencies, I have presented the data acquired with the Cytek® Northern Lights™ in separate graphs. Untreated as well as LPS-treated cells were used as negative and positive controls in each assay for the relative comparison between previous data.

2.8. Enzyme Linked Immunosorbent Assay (ELISA)

Levels of soluble mediators in cell culture supernatants were determined using appropriate sandwich ELISA kits (R&D systems – DuoSet ELISA). The assays were conducted according to the manufacturer's instructions. In brief, Maxisorp™ 96-well microplates were coated overnight at 4 °C with 50 µL of the recommended working concentration of appropriate capture antibodies diluted in filtered PBS. The following morning, each well was washed 3 times with the recommended ELISA wash buffer (0.05 % Tween-20 in PBS), residual fluid was aspirated, and the plates were blotted dry. Plates were blocked with 1 % BSA for 1 h. The washing and aspiration procedure described above was repeated, before addition of 50 µL samples and standards in duplicate wells. Samples were incubated for 2 h. Washing and aspiration steps were repeated, followed by addition of 50 µL of the respective biotinylated detection antibodies at recommended working concentrations for 2 h. Washing and aspiration steps were repeated and 50 µL of streptavidin-conjugated horseradish peroxidase (HRP) was added and incubated for 20 min in dark. After the final wash cycle, 50 µL of a liquid substrate (3,3',5,5' Tetramethylbenzidine Liquid Substrate Super Sensitive Form) was added to each well for colour development over 10-20 min. Once standards were suitably developed, the substrate reaction was stopped by addition of 50 µL of a stop solution (2 M sulphuric acid). The plates were gently swirled to ensure thorough solution mixing and the optical density of each well was read at a wavelength of 450 nm using an absorbance colorimetric microplate reader (Biotek ELx800).

2.9. Immunofluorescent microscopy

To assess the effect of cell adaptation to flow conditions on the morphology and alignment of HLMECs, immunofluorescent staining and wide-field microscopy were used. HLMECs were seeded in channel slides and adapted to the experimental flow rate for 24 h. Cells were washed three times *in situ* with PBS, fixed using 4 % paraformaldehyde (PFA) in PBS for 10 min and washed twice with PBS. Following fixation, the cells were permeabilised with 0.5 % Triton X-100 in PBS for 5 min and washed again twice. After permeabilization, the cells were blocked in 1 % BSA in PBS for 30 min, washed, and stained with appropriate antibodies. Upon staining, cells were washed twice and mounted with the ibidi® Mounting Medium with DAPI. A minimum of 10 fields of x 200 X magnification views were observed and photographed using a Zeiss AxioCam camera on an Olympus BX60 upright immunofluorescent microscope with Zeiss KS-300 software. Images were analysed using the ImageJ software.

2.10. Electron Microscopy

Purified neutrophil-EVs were imaged by transmission electron microscopy (TEM) after positive MicroBead selection. Once purified, EVs were pelleted by 20,800 x g, 30 min centrifugation and resuspended in fixation buffer consisting of 2.5 % glutaraldehyde in 0.1 M sodium cacodylate buffer and incubated for 1 h in ice. Upon fixation, EVs were washed twice with 0.1 M sodium cacodylate buffer and resuspended in 50 µL of the same buffer for overnight storage at 4 °C. The next day, 10 µL EVs were incubated on top of copper TEM grids for 15 min and washed twice with ultrapure distilled water. Grids were stained with 50 µL of 2 % uranyl acetate and lead citrate for 10 min and washed again with distilled water. Excess liquid was removed by blotting with filter paper before image acquisition using the Transmission Electronic Microscope JEOL 1200 EX II. Digital images were captured using a Gatan Bio Scan camera model at 150,000 X magnification. Digital Micrograph software was used to analyse images.

2.11. Statistical Analysis

All data throughout this thesis are shown as individual values in scatter dot plots with mean ± standard deviation (SD) (if parametric) or scatter dot plots with median ± interquartile range (if non-parametric). The model assumption of normality of residuals was assessed by the Shapiro-Wilk test. Parametric (normally distributed) data were analysed by two-tailed Student's t-test, one-way ANOVA with Bonferroni's or Dunnet's multiple comparisons test or two-way ANOVA with Sidak's multiple comparison test. For non-parametric data, Mann-Whitney U-test or Kruskal-Wallis with Dunn's multiple comparisons test was used. Time course data were analysed using a two-way ANOVA or a t-test of endpoint values. In cases where normality tests were underpowered due to small n numbers, scatter plots were used to allow graphical inspection of data distribution and analysed by parametric tests where appropriate. All data analyses were performed using GraphPad Prism software (version 9.5.0). A p-value of less than 0.05 was defined as the minimum threshold for statistical significance.

3. Neutrophil-EV uptake by target cells within the pulmonary microvasculature in an *in vitro* model of flow

Parts of the data produced for this chapter have been published as a conference abstract

Tsiridou DM, O'Dea KP, Tan YY, Takata M. Neutrophil-Derived Microvesicle Uptake under Flow Conditions in an In Vitro Model of Pulmonary Vascular Inflammation. The FASEB Journal. 2020 Apr;34(S1):1-. (359)

3.1. Background

Clinical studies have demonstrated that levels of circulating EVs are acutely elevated in sepsis and non-infectious SIRS patients (246, 286, 293, 300). *In vitro*, vascular cell-derived EVs have been shown to promote pro-coagulant, pro-inflammatory, and anti-inflammatory responses, all of which are relevant to sepsis pathogenesis (325, 326, 329, 330). Although the *in vitro* findings may be extrapolated to disease conditions, there is little direct *in vivo* evidence showing how intravascular EVs contribute to tissue inflammation or organ dysfunction.

EVs can interact with humoral factors in the blood (360), but for them to have direct effects on vascular cells, requires direct physical contact (361). The intravascular biodistribution and cellular interactions of circulating EVs have been studied by injecting *in vitro* labelled EVs into animal models and by evaluating their uptake by target cells *in vitro* (271, 273). It has been found that under resting conditions, the liver and spleen are the major sites of systemically administered-EV clearance via their uptake by organ-resident macrophages and to a lesser degree, liver endothelial cells (273, 277, 279). Although several studies evaluated EV biodistribution and trafficking as a means of targeted drug delivery during disease conditions such as cancer and kidney injury (362-366), the effect of acute systemic inflammation on EV biodistribution has received little attention, despite their increased output under these conditions. Considering that changes in EV target cell type or vascular distribution could affect the responses they produce, our group decided to investigate EV uptake under inflammatory conditions, finding substantive changes in the biodistribution of EVs from a mouse macrophage line (J774A.1) injected into mice pre-treated with a low-dose of LPS. The normal uptake of EVs within the liver (observed in resting conditions) was reduced with a partial redirection to the lungs via increased uptake by monocytes marginated within the pulmonary vasculature (under endotoxaemic conditions) (281).

In parallel to this *in vivo* study, our group investigated monocyte- and neutrophil-EV uptake and cell activation in *in vitro* models, using human primary cells. A discrepancy was noted

between substantial EV uptake by HLMECs *in vitro* and the absence of detectable uptake by lung endothelial cells in the mouse model, despite detectable uptake by liver endothelial cells in the same experiments (281).

Endothelial cells line the inside surface of blood vessels in direct contact with blood flow and are subjected to mechanical shear stress forces. It is known that such forces have an important role in endothelial cell phenotype (367, 368) and this may have an impact on EV uptake by endothelial cells. Although species differences could explain our contradicting observations in *in vivo* and *in vitro* EV uptake by endothelial cells, we speculated that standard static cell culture conditions promoted EV-cell binding and uptake *in vitro*, whereas shear stress under flow conditions prevented EV binding and uptake by lung endothelial cells *in vivo*. We, therefore, hypothesised that such flow-dependent effects could lead to increased neutrophil-EV interactions during cessation of pulmonary microvascular flow *in vivo*, such as occurs during hypoxic vasoconstriction in lungs or reduced perfusion of vessels during septic shock, and that this phenomenon would promote neutrophil-EV interactions that result in endothelial activation and/or injury.

3.2. Aims

To extend the current understanding of EV-target cell interactions during systemic inflammation I aimed to:

1. Evaluate *in vitro* methods for EV production from human primary neutrophils and labelling for uptake studies.
2. Develop an *in vitro* model of EV uptake by pulmonary endothelial cells and monocytes under flow conditions.
3. Evaluate the effect of shear stress and inflammation on neutrophil-EV uptake by target cells.

3.3. Protocols

3.3.1. Leukocyte isolation from healthy volunteer blood

PBMCs were separated from whole blood by density gradient centrifugation using Leucosep tubes and Histopaque-1077. Neutrophils were isolated from the Histopaque-1077 pellet by 3 % dextran sedimentation and osmotic lysis to remove red blood cells (see **Section 2.4.1** for more details). In both PBMC and neutrophil isolation assays, cells were washed three times in PBS (without Ca^{2+}/Mg^{2+}) and resuspended in assay buffer (RPMI-1640 or EBM, supplemented with 0.5 % HAS according to the subsequent protocols) for further use in EV production or functional assays. PBMC and neutrophil absolute counts and purity were determined by flow cytometry, based on forward (FSc) and side scatter (SSc) profiles and AccuCheck counting beads.

3.3.2. Neutrophil stimulation for cell activation and EV release

Neutrophil activation and EV production were investigated under 'one-hit' inflammatory stimulation conditions. Isolated human neutrophils were stimulated at a density of 1 x 10^7 cells per tube in 500 µL (2 x 10^7 cells/mL) in microfuge tubes at 37 °C for a period of 30 min to 3 h, in static or rotating conditions. During stimulation, neutrophils were maintained in suspension by continuous mixing on a rotating wheel in the vertical plane at 150 rpm. The different stimuli conditions are summarised in **Table 3.1**.

EV type	Stimuli	Concentration	Time
spontaneous	untreated	N/A	30 min to 20 h
1-hit	fMLP	1 μM	30 min
1-hit	LPS	100 ng/mL	3 h
1-hit	A23187	1 μM	30 min
1-hit	TNF-α	100 ng/mL	30 min

Table 3.1. Stimulation conditions for neutrophil-EV production.

3.3.3. EV isolation, fluorescent labelling, and quantification

To determine EV uptake by target cells, EVs were isolated from parental cells by differential centrifugation (**Section 2.5.1**) and washed twice. EVs were labelled with the lipophilic fluorescent dye DiD (5 μM, 7 min, dark) and then stained with conjugated antibodies for the neutrophil markers CD11b and CD66b and analysed by flow cytometry (CyAn ADP analyser). EV concentrations for uptake assays were standardised based on total incorporated DiD fluorescence, measured using a fluorescence plate reader (Biotek FLx800) (**Section 2.5.3**).

3.3.4. EV uptake by target cells *in vitro*

EV uptake by HLMECs was evaluated under standard static tissue culture conditions and physiological flow conditions using a parallel flow chamber system (PFC) manufactured by ibidi®. This system produces constant unidirectional laminar flow within a channel slide where HLMECs are seeded. By selection of the different bore size perfusion tubing and the prefabricated channel slides (μ-Slide I Luer, ibidi®) with different internal heights, a range of shear stress values could be generated with up to 4 slides running in parallel using the ibidi® Fluidic Unit Quad system. In **Section 2.6.1** of the materials and methods chapter, the working principle and setup of the PFC system are described in detail. **Table 3.2** summarises the shear

stress values used for the experimental procedures carried out in this thesis, alongside the combination of perfusion set and ibidi® channel slide type used to achieve these.

Perfusion set diameter (mm)	Channel slide height (mm)	Shear stress (dyn/cm^2)	Shear rate (s^{-1})
Blue (0.8)	0.8	0.56	78.0
	0.4	2.07	287.5
Red (1.6)	0.6	5.00	695.0
	0.4	10.95	1521.0

Table 3.2. Shear stress range using the same air pressure and different combinations of perfusion set and channel slide.

All cell culture or cell-EV co-incubation assays were carried out at 37 °C unless otherwise stated. HLMECs (1.2 x 10^5/well or slide) were seeded into 24-well culture plates (for static conditions) or ibidi® channel slides (for flow conditions) at confluence prior to EV uptake and left to adhere overnight. The following day, medium in each well or channel slide was replaced, before the slides were introduced to the PFC system for a 24-hour adaptation period, where cells were exposed to experimental flow rate and shear stress conditions. The cell media in the PFC system circuit was replaced from complete EGM-2MV media to EBM-HAS and DiD-labelled neutrophil-EVs were added to the reservoirs of the PFC system (50,000 FU/mL). EV distribution in the circuit was allowed to stabilise for 5 min at a constant flow rate prior to the start of the experiment. EV uptake was carried out for 1 h. For mechanistic studies, pharmacological inhibitors were added to cells for a period of 30 min prior to addition of DiD-labelled EVs. To harvest cells, the conditioned media was discarded, and slides were gently rinsed back and forth three times with PBS via two 1 mL syringes connected to the slide's luer ports. Cells were then detached with Accutase enzymatic treatment for 3-5 min or until cell detachment was visualised with an inverted microscope. Cells were centrifuged and stained

with an endothelial cell marker (CD146) and cell-associated DiD fluorescence was measured by flow cytometry (**Figure 3.1, A**).

To more closely model EV uptake in the pulmonary vasculature, a co-culture model of PBMCs and HLMECs was developed. HLMECs were seeded in tissue culture wells (for static conditions) or ibidi® channel slides (for flow conditions) and the flow-treated cells were adapted to the experimental flow rate for 24 h as described above. The following day, HLMECs in both static and flow conditions were stimulated with TNF-α (100 ng/mL, 2 h) to induce upregulation of cell adhesion molecules and promote monocyte adherence. Following TNF-α treatment, PBMCs were added to HLMEC monolayers at a ratio of monocytes: HLMECs 2: 1 (2.4×10^5 monocytes/well or slide) and left to adhere under static conditions for 2 h. Flow-treated co-cultures were adapted to flow for 1 h at the experimental shear stress conditions for each sample. The PFC circuit medium was replaced to remove non-adherent cells and DiD-labelled neutrophil-EVs were added and incubated with cells for 1 h prior to flow cytometric analysis. Non-adherent cells were removed from static cultures as well prior to EV addition (**Figure 3.1, B**).

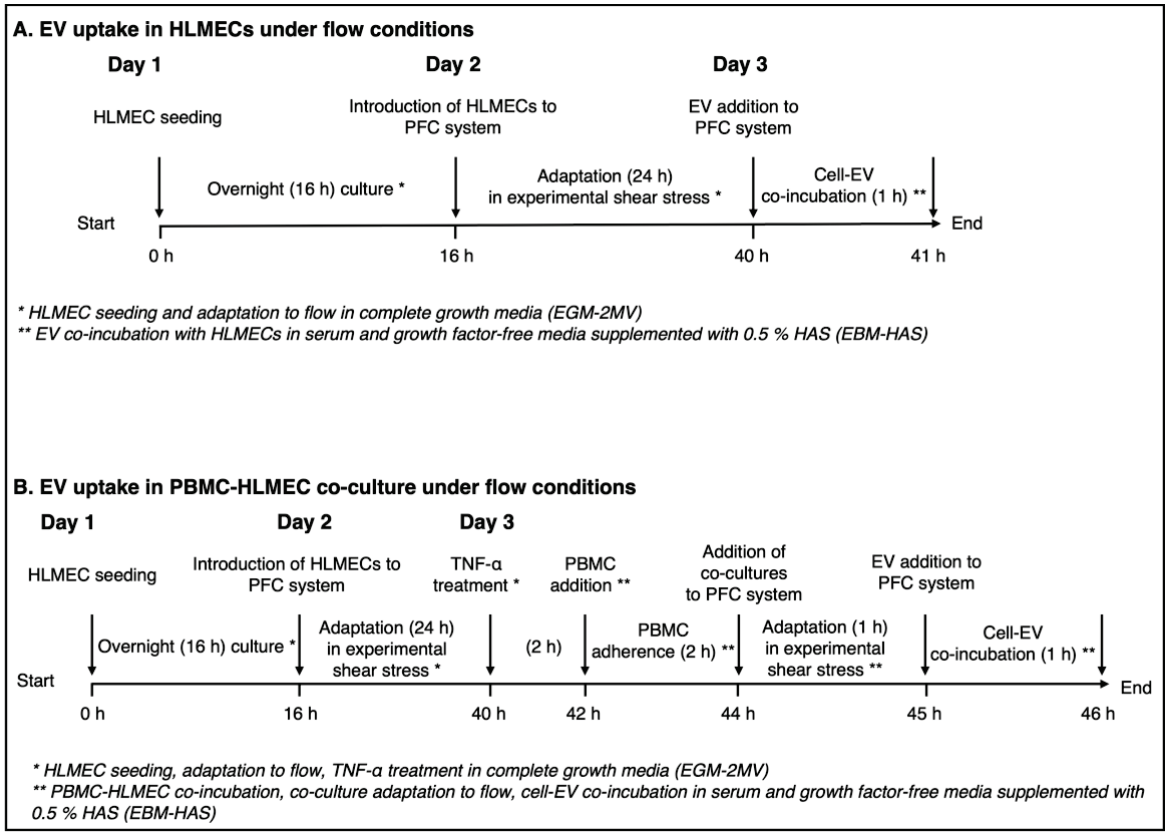

Figure 3.1. *In vitro* models of neutrophil-EV uptake under flow conditions.
Schematic representation of the protocols developed for the assessment of neutrophil-EV uptake under flow conditions in HLMECs only (**A**) and PBMC-HLMEC co-cultures (**B**).

3.3.5. Immunofluorescent staining of HLMECs in PFC slides

The effect of flow on the morphology and alignment of HLMECs was investigated by using immunofluorescent staining. Upon completion of the 24 h adaptation experiments, cells were washed *in situ* and fixed in 4 % PFA in PBS for 10 min, permeabilised with 0.5 % Triton X-100 in PBS for 5 min, and blocked in 1 % BSA in PBS for 30 min. Cells were stained with 5 µg/mL mouse anti-human monoclonal anti-VE-cadherin (CD144, clone: BV9, Biolegend) antibody at 37 °C for 1 h. Washed cells were incubated with 5 µg/mL goat anti-mouse polyclonal IgG (Alexa Fluor™ 488, Biolegend) fluorescent secondary antibody for 45 min at 37 °C in dark. Cells were mounted with the ibidi® Mounting Medium with DAPI and analysed with an immunofluorescent microscope with Zeiss KS-300 software.

3.4. Results

3.4.1. Development of methodology to assess human neutrophil activation and EV production *in vitro*

To investigate neutrophil-EV uptake using *in vitro* models of pulmonary endothelial cells, I first evaluated existing neutrophil stimulation protocols commonly used for neutrophil-EV generation. Human primary neutrophils were isolated from healthy volunteer blood and analysed by flow cytometry. As the standard method for neutrophil-EV production, I investigated the use of a single stimulus and compared neutrophil activation and EV release in response to fMLP, LPS, TNF-α, and the calcium ionophore A23187. Cells were stimulated with relevant concentrations of the agonists summarised in **Table 3.1** in a rotating wheel to ensure constant mixing. Control cells were kept on ice or incubated without any stimuli at 37 °C. Neutrophil activation was determined by the expression of the surface markers CD11b, CD66b, and L-selectin (**Figure 3.2, A-C**). fMLP, TNF-α, and calcium ionophore A23187, effectively activated neutrophils indicated by the complete loss of surface L-selectin. However, LPS treatment did not cause any L-selectin cleavage although it significantly upregulated CD66b expression. It is important to note here that these experiments were carried out in serum-free conditions, which might explain the lack of responses with LPS treatment. Comparing responses to all three markers, calcium ionophore A23187 appeared to be the most potent stimulus of neutrophil activation.

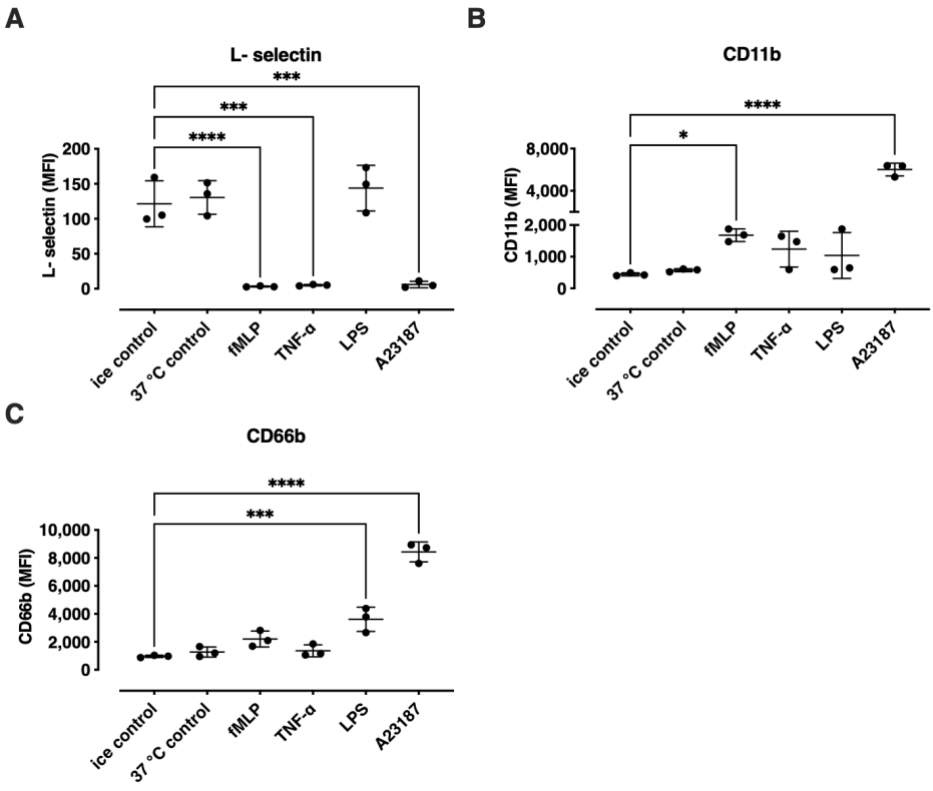

Figure 3.2. Neutrophil activation after stimulation with inflammatory agonists.
Freshly isolated neutrophils from healthy volunteer blood were incubated in the presence of fMLP (1 µM, 30 min), TNF-α (100 ng/mL, 30 min), LPS (100 ng/mL, 3 h), calcium ionophore A23187 (1 µM, 30 min), or without any stimuli at 37 °C in rotating conditions at a concentration of 1 x 10^7 cells/tube in 500 µL. Neutrophil activation markers were measured by flow cytometry: L-selectin (**A**), CD11b (**B**), and CD66b (**C**). Calcium ionophore A23187 was the most potent and consistent stimulus based on the markers assessed. Data are analysed by one-way ANOVA with Bonferroni's multiple comparisons test (A-C; mean ± SD). n=3, *p<0.05, ***p<0.001, ****p<0.0001.

Neutrophil-EV production was quantified as EV numbers per cell to allow comparison between experiments if neutrophil densities were modified (**Figure 3.3**). Neutrophil-EVs were identified based on their size (<1 µm) and surface markers CD11b and CD66b and were distinguished from background noise and antibody aggregates based on their sensitivity to lipid solubilising detergent (0.1 % Triton X-100) (369). The neutrophil-EV gating strategy can be found in **Figure 2.8**. By using fluorescent sizing calibration beads (**Figure 2.7**), a 1 µm upper size gate was determined and a threshold for smaller particles was set in the CyAn ADP analyser. As observed with cell activation**,** fMLP, TNF-α, and calcium ionophore A23187 generated significant numbers of neutrophil-EVs compared to untreated or 'sham'-treated neutrophils.

LPS did not lead to significant EV release, despite a longer 3 h incubation, which as with neutrophils' partial activation response, might be ascribed to lack of serum.

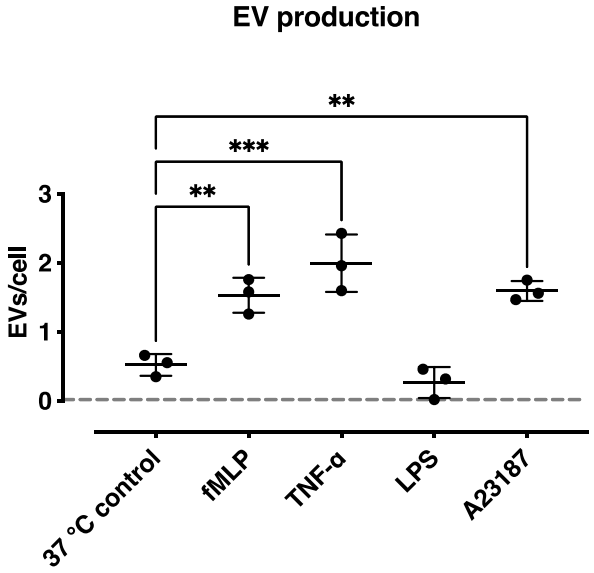

Figure 3.3. Neutrophil-EV production by human neutrophils after stimulation with inflammatory agonists.
Freshly isolated neutrophils from healthy volunteer blood were incubated in the presence of fMLP (1 µM, 30 min), TNF-α (100 ng/mL, 30 min), LPS (100 ng/mL, 3 h), calcium ionophore A23187 (1 µM, 30 min), or without any stimuli as a control (30 min), at 1 x10^7 cells/ml in 500 µL of RPMI-HAS in microfuge tubes at 37 °C under rotating conditions. Neutrophils stored on ice were used for baseline measurement of EV release (dotted line). EV numbers were determined in cell-free supernatants by flow cytometry. fMLP, TNF-α, and calcium ionophore A23187 induced significant neutrophil-EV release as compared to the untreated control. LPS treatment did not result in neutrophil-EV production. Data are analysed by one-way ANOVA with Bonferroni's multiple comparisons test (mean ± SD). n=3, **p<0.01, ***p<0.001.

Mature circulating neutrophils are short-lived and readily undergo rapid apoptosis under *in vitro* conditions (370) and this phenomenon has been linked to EV release in neutrophils and other cells (371-374). Therefore, spontaneous EV release was assessed in this experimental setup. Extended incubation periods at 37 °C for up to 20 h were used under rotating or static serum-free culture conditions. Neutrophil incubation in static culture did not lead to significant EV release, even with prolonged incubation (**Figure 3.4, A**). By contrast, rotating culture resulted in substantial neutrophil-EV release at late time points (20 h) (**Figure 3.4, B**).

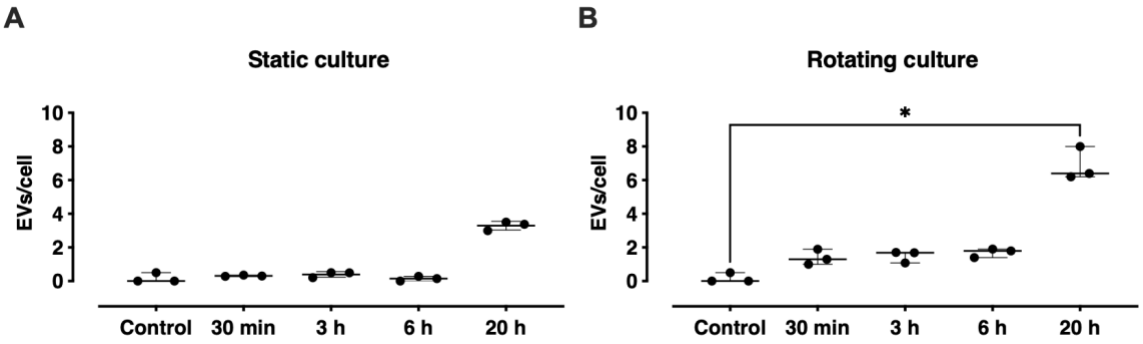

Figure 3.4. Spontaneous neutrophil-EV release from non-stimulated neutrophils in static and rotating culture.
Freshly isolated neutrophils were incubated for 30 min, 3, 6, and 20 h in static or rotating culture at 37 °C. Neutrophils stored on ice were used for baseline measurement of EV release (control). EV numbers were determined in cell-free supernatants by flow cytometry. No spontaneous EV release was observed in static culture (**A**). Rotating culture resulted in significant EV release after 20 h incubation (**B**). Data are analysed by Kruskal-Wallis with Dunn's multiple comparisons test (A-B; median ± interquartile range). n=3, *p<0.05.

As a chemotactic factor, fMLP has been commonly used to generate EVs from neutrophils, via G-protein-coupled receptor (GPCR) signalling through the N-formyl peptide receptors (375, 376). In our assays, fMLP generated a significant amount of neutrophil-EVs and as a physiologically relevant and relatively specific neutrophil stimulus, we decided to use it as the main method of EV generation for uptake experiments.

3.4.2. Fluorescent labelling of neutrophil-EVs

To investigate EV uptake by target cells *in vitro*, fMLP-generated neutrophil-EVs were labelled with the far-red lipophilic dye DiD. To assess DiD incorporation, labelled neutrophil-EVs were gated as $CD11b^{+}CD66b^{+}$ events (**Figure 3.5, A**) and levels of DiD fluorescence were determined by flow cytometry. DiD has an excitation peak at 646 nm and an emission peak at 663 nm, similar to the APC fluorophore, and therefore it was measured using the red laser and the CyAn ADP channel 8 emission filter 660/20. Neutrophil-EVs were successfully

labelled with DiD, as the majority of DiD$^+$ events were also positive for CD66b and sensitive to detergent lysis (**Figure 3.5, B**).

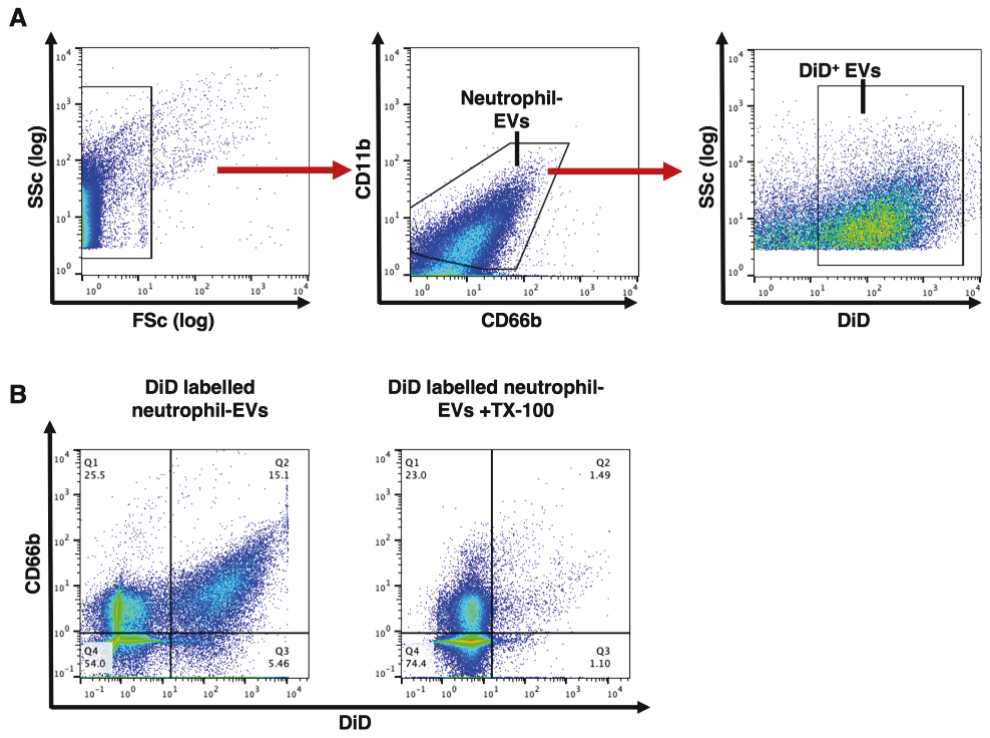

Figure 3.5. Gating strategy of neutrophil-EVs labelled with the DiD fluorescent dye.
Neutrophil-EVs were produced from fMLP-stimulated human neutrophils (1 µM, 30 min, 37 °C), isolated by differential centrifugation and labelled with DiD (5 µM, 7 min). After two washes, EVs were stained with anti-CD11b (PE) and anti-CD66b (PE-Cy7) antibodies. Gating strategy for the quantification of DiD positive neutrophil-EVs (**A**). The majority of DiD$^+$ events appeared to be positive for neutrophil-EV markers and were sensitive to non-ionic detergent lysis (Triton X-100, 0.1 %), confirming their vesicular nature (**B**).

The DiD fluorescence of labelled EVs was determined in a fluorescent plate reader as fluorescence units (FU)/mL. Based on pilot uptake experiments (data not shown), a concentration of 50,000 FU/mL (~8 x 10^5 neutrophil-EVs/mL) was chosen for the standardisation of subsequent EV uptake experiments. Initially, preliminary tests of DiD-labelled neutrophil-EV uptake by HLMECs under standard static culture (24-well plates) were performed. As a lipophilic molecule, DiD precipitates may form in aqueous buffers and be sedimented during the EV centrifugation steps. Therefore, mock incubation of DiD in buffer only (PBS-HAS) without EVs was conducted as a control. Indeed, the PBS-DiD preparations

without EVs produced a detectable fluorescent signal in the fluorescent plate reader, even though of lower magnitude than the DiD-EV samples (data not shown). HLMECs were co-incubated for 1 h, with either standardised numbers of DiD-labelled neutrophil-EVs (50,000 FU/mL) or an equal volume of the sham PBS-DiD and cell-associated DiD fluorescence was measured by flow cytometry.

Significant increases in cell-associated DiD fluorescence indicated that HLMECs were capable of neutrophil-EV uptake under static *in vitro* culture conditions (**Figure 3.6**). However, the uptake appeared heterogeneous between cells with a significant proportion of cells remaining negative for DiD fluorescence. Incubation of HLMECs with the mock PBS-DiD preparations did not produce any fluorescent signal and therefore uptake of insoluble DiD was excluded as a significant contributor to the signal produced by DiD-labelled EV preparations.

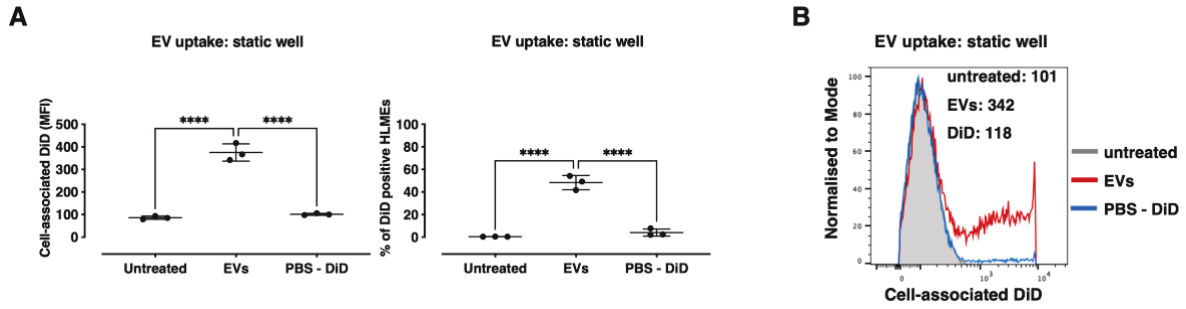

Figure 3.6. Evaluation of DiD-labelled neutrophil-EV uptake by HLMECs under static conditions. HLMECs were co-incubated with neutrophil-EVs (50,000 FU/mL) for 1 h and EV uptake was quantified by flow cytometry, as cell-associated DiD fluorescence (MFI) and percentage of positive HLMECs for DiD signal. 'Sham' control of DiD incubation in PBS (PBS-DiD) without any EVs was used to assess any non-specific signal resulting from the dye. DiD-labelled neutrophil-EVs were taken up by HLMECs whereas the sham PBS-DiD control did not produce detectable fluorescence in HLMECs (**A**). Data are analysed by one-way ANOVA with Bonferroni's multiple comparisons test (A; mean ± SD). n=3, ****p<0.0001. Histogram representative of 3 separate uptake experiments (**B**).

3.4.3. Development of an *in vitro* model of EV uptake under pulmonary microvasculature flow conditions

First, the adaptation of HLMECs to flow conditions was investigated, as vascular shear stress affects not only the endothelial function (e.g., release of vasodilators in arterioles) but surface

phenotype and morphology as well (367, 368, 377, 378) and therefore could have an impact on processes related to EV uptake. To evaluate the changes in HLMEC phenotype in response to flow adaptation, the expression of surface molecules related to cell adhesion, binding of particles (scavenger receptors), and morphology (alignment with the direction of flow) was measured. For these pilot experiments, a single shear stress of 5 dyn/cm^2 was used based on vein wall shear stress as an upper estimate for lung capillaries (which cannot be measured) (347-349). HLMECs were seeded in ibidi® channel slides and exposed to a constant flow of 5 dyn/cm^2 for 1, 24, or 48 h. Non-flow adapted cells in ibidi® channel slides were used as control. After flow treatment, cells were detached enzymatically and stained for surface marker expression for flow cytometric analysis or fixed *in situ* for phase contrast and immunofluorescence microscopy.

HLMECs were gated based on CD146 expression and SSc (**Chapter 2, Figure 2.1**) to ensure uniform analysis of the main cell population between experiments. Of the cell surface molecules assessed, there were no significant changes in ICAM-1 (CD54), VCAM-1 (CD106), integrin $\alpha_v\beta_3$ (CD61), VE-cadherin (CD144), scavenger receptor A (CD204), or scavenger receptor B (CD36) compared to non-flow adapted HLMECs (**Figure 3.7, A-B, E-G**). However, PECAM-1 (CD31) expression was found to be significantly reduced at 24 and 48 h of flow culture (**Figure 3.7, C**) and MCAM (CD146) showed a reduction, but this did not reach statistical significance (n=3) (**Figure 3.7, D**).

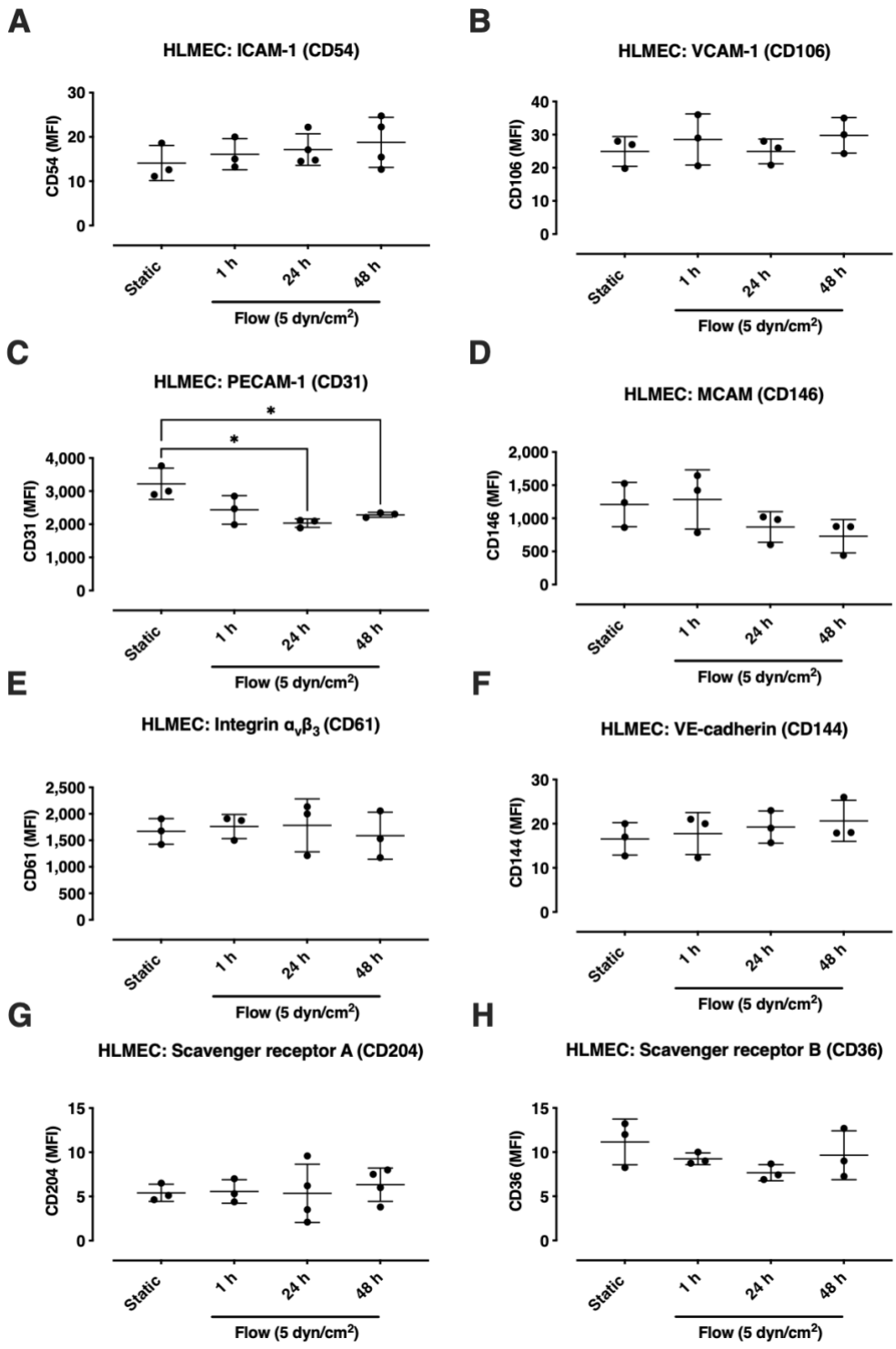

Figure 3.7. Effect of adaptation to flow on HLMEC surface markers.

HLMECs were seeded in ibidi® channel slides and adapted to flow (5 dyn/cm^2) for 1, 24, or 48 h. Non-flow treated HLMECs were cultured in channel slides under static conditions. Flow adaptation did not produce any substantial effect on the surface expression of the HLMEC adhesion molecules ICAM-1 (**A**), VCAM-1 (**B**), and receptors integrin $\alpha_v\beta_3$ (**E**), VE-cadherin (**F**), and scavenger receptors A (**G**) and B (**H**) regardless of the exposure time. PECAM (CD31) (**C**) and MCAM (CD146) (**D**) expression was reduced by 24 and 48 h adaptation period to the physiological flow of 5 dyn/cm^2, with only PECAM (CD31) reduction reaching statistical significance. Data are analysed by one-way ANOVA with Dunnett's multiple comparisons test (A-H; mean ± SD). n=3-4, *p<0.05.

The effect of flow on cell morphology was assessed with non-fluorescent phase contrast microscopy and immunofluorescent staining of VE-cadherin, a protein present on cellular junctions. Cells acquired a partial but not completely uniform alignment with the direction of flow after 24 h or 48 h flow treatment (**Figure 3.8**).

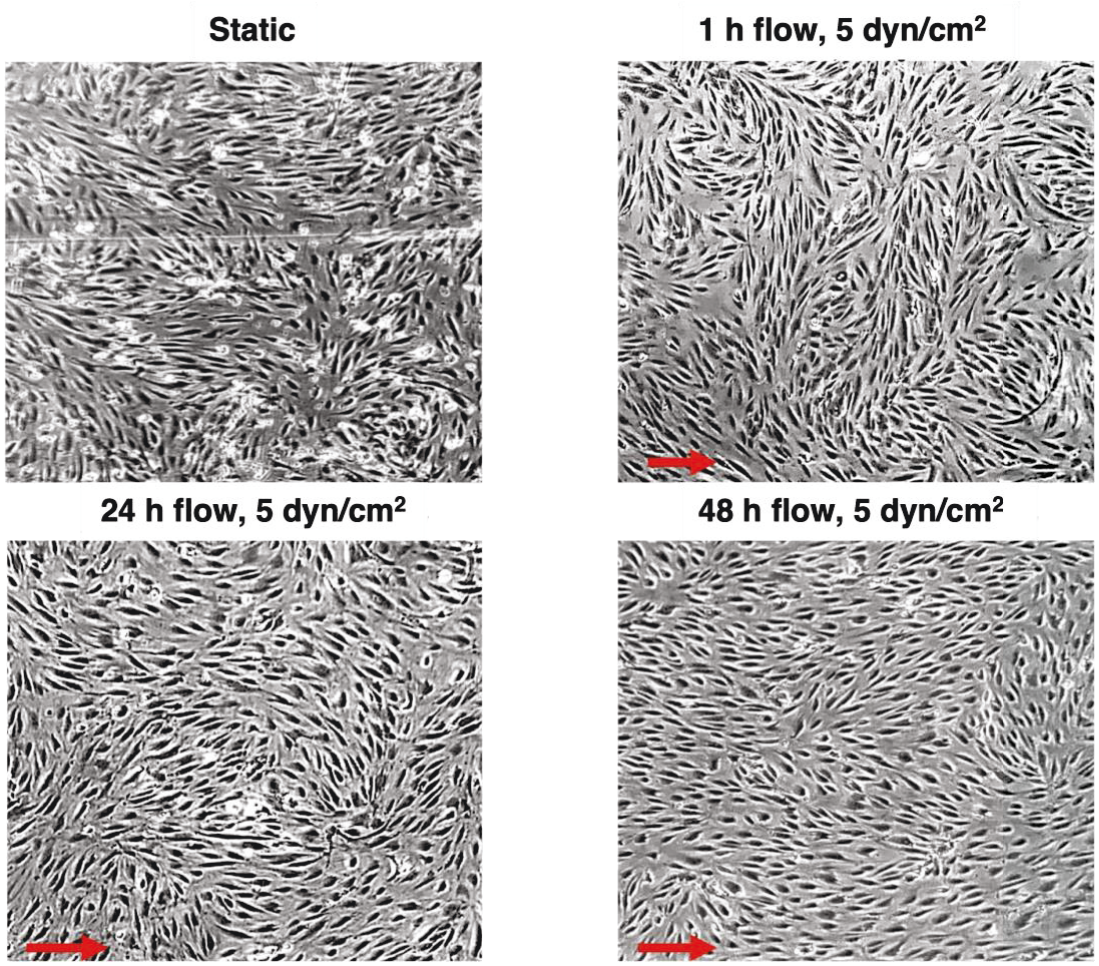

Figure 3.8. Effect of adaptation to flow on morphology and alignment of HLMECs.
HLMECs were seeded in channel slides and adapted to flow (5 dyn/cm^2) for 1, 24, or 48 h, while non-flow treated HLMECs cultured in channel slides under static conditions were used as control. Cells were observed and imaged with an inverted phase contrast microscope (40 X magnification), after the completion of the respective adaptation periods. Red arrows indicate the direction of flow. HLMECs developed an elongated shape after adaptation (24, 48 h) to flow and polarised partially towards the direction of flow.

Immunofluorescent staining for VE-cadherin provided clearer evidence that the flow conditions used resulted in cell alignment in the direction of flow (**Figure 3.9**).

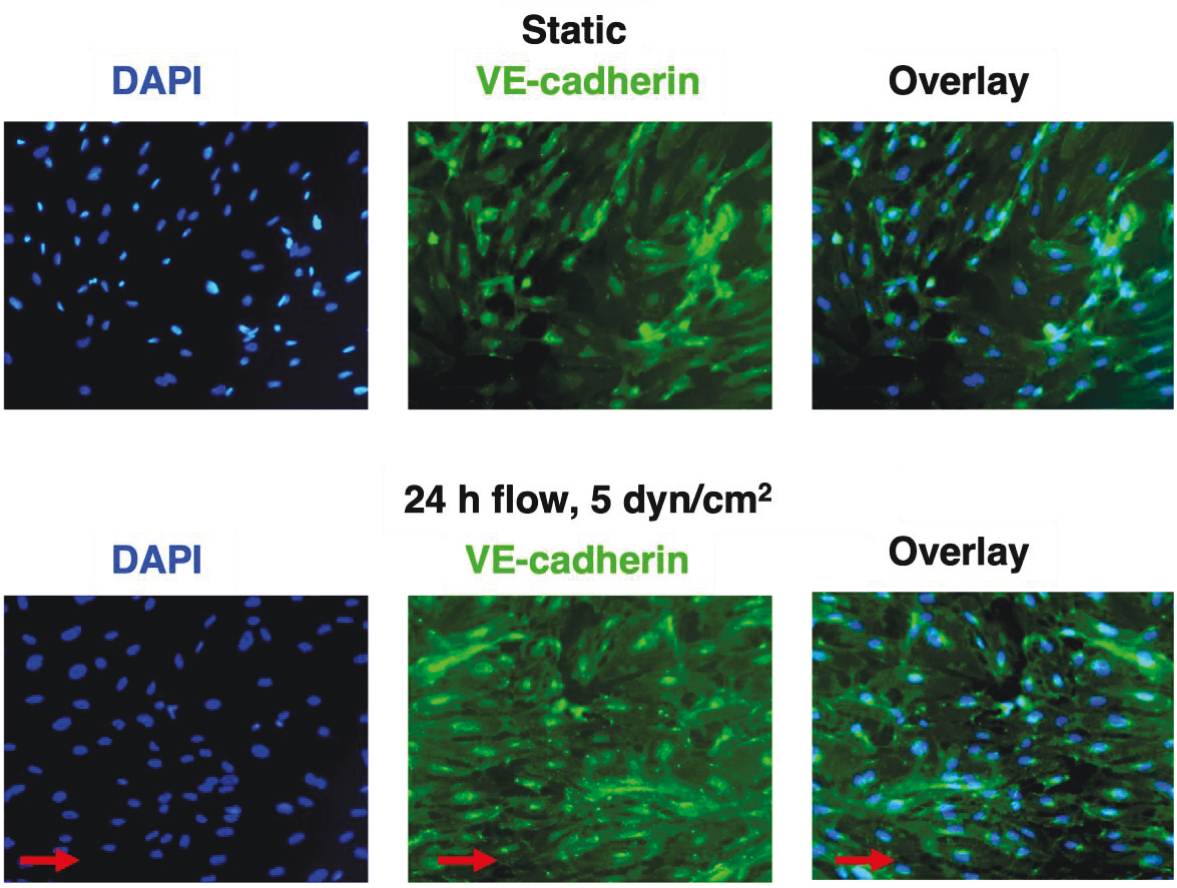

Figure 3.9. Visualisation of the effect of adaptation to flow on HLMEC alignment with immunofluorescent staining for VE-cadherin.
HLMECs were seeded in channel slides and adapted to flow (5 dyn/cm^2) for 24 h. Non-flow treated HLMECs were cultured in ibidi® channel slides under static conditions. After the completion of the flow adaptation period, cells were fixed and stained with DAPI (blue, cell nuclei) and anti-VE-cadherin (green, cell junctions). Cells were observed with a fluorescent microscope at 200 X magnification. Red arrows indicate the direction of flow. Under flow conditions, HLMECs appeared to align in the direction of flow.

3.4.4. Characterisation of neutrophil-EV uptake by HLMECs under flow conditions

Once the protocols for neutrophil-EV production, labelling and cell experimentation under flow were established, the next goal was to investigate neutrophil-EV uptake by HLMECs *in vitro* under flow conditions.

As a continuation of experiments evaluating the effects of adaptation to flow, the impact of HLMEC pre-adaptation to flow for periods of 0, 1, 24, or 48 h (5 dyn/cm^2) to the subsequent uptake of neutrophil-EV uptake under flow conditions (5 dyn/cm^2) was investigated. As before,

the non-flow adapted HLMECs were seeded in ibidi® channel slides and cultured in static conditions up until neutrophil-EV addition. DiD-labelled neutrophil-EVs were incubated with pre-adapted or non-adapted to flow HLMECs for 1 h (5 dyn/cm^2) and uptake was assessed by quantification of cell-associated DiD MFI by flow cytometry.

A substantial reduction in neutrophil-EV uptake was observed in flow-adapted (1, 24, 48 h) HLMECs compared to non-adapted cells under flow conditions. However, the adaptation period *per se* (comparison between 1, 24, and 48 h), did not produce significant differences in neutrophil-EV uptake by HLMECs (**Figure 3.10**).

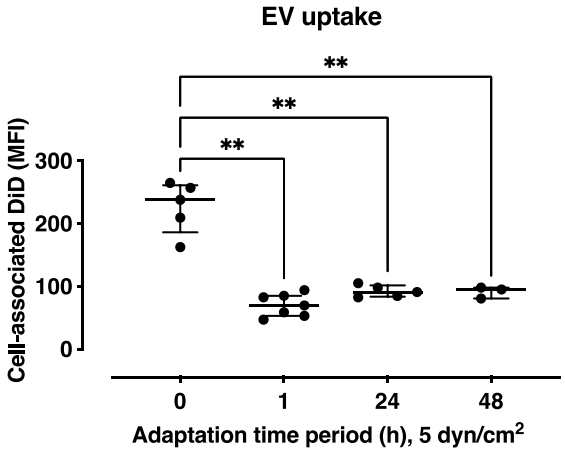

Figure 3.10. Effect of flow adaptation on EV uptake by HLMECs under flow conditions.
HLMECs were seeded in channel slides and adapted to flow (5 dyn/cm^2) for 1, 24, or 48 h. Non-flow adapted HLMECs were seeded in ibidi® channel slides. DiD-labelled neutrophil-EVs (50,000 FU/mL) were incubated with HLMECs under flow conditions (5 dyn/cm^2) for 1 h. EV uptake was quantified by flow cytometric analysis as cell-associated DiD fluorescence. Flow adaptation significantly reduced EV uptake by HLMECs. However, the adaptation period *per se* did not have any effect. Data are analysed by one-way ANOVA with Dunnett's multiple comparisons test (mean ± SD). n=3-7, **p<0.01.

Although EV uptake after adaptation for 24 h was not different from 1 h, we decided to employ the 24 h adaptation period for all uptake experiments based in part on the evidence of adaptation to flow via realignment at 24 h but not 1 h suggesting significant phenotypic

changes (e.g., rearrangement of the endothelial cytoskeleton) that would require several hours.

Next, the uptake of DiD-labelled neutrophil-EVs and PBS-DiD 'sham' control without EVs was compared. As with the static culture results (**Figure 3.6**), uptake of PBS-DiD label without EVs was negligible while incubation with DiD-labelled neutrophil-EVs resulted in a significant DiD signal on HLMECs (**Figure 3.11**).

Contrary to our predictions, these findings, and the adaptation to flow data suggested that flow at relatively low shear stresses did not appear to have a dramatic inhibitory effect on uptake. We are aware that EV-uptake in these later experiments appeared slightly higher compared to our previous runs, even though the same neutrophil-EV concentrations of 50,000 FU/mL were used (**Figure 3.10**). As some of the older experiments were part of assay development, our techniques were further improved over the course of the study which could explain these minor differences.

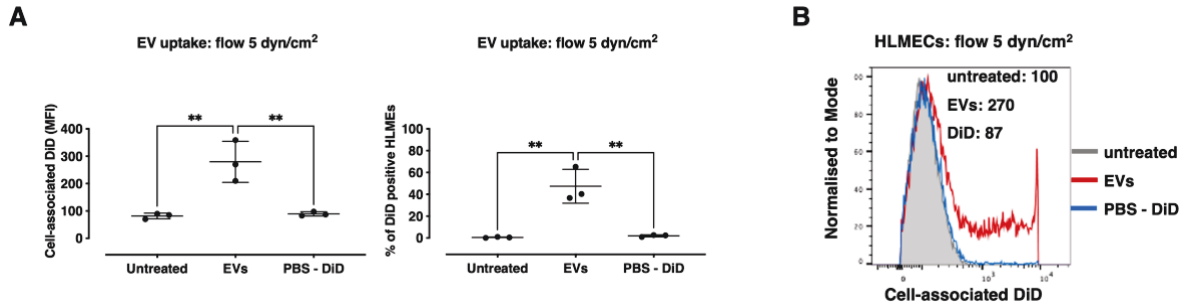

Figure 3.11. Evaluation of DiD-labelled neutrophil-EV uptake by HLMECs under flow conditions. HLMECs were seeded in channel slides and adapted to flow (5 dyn/cm^2) for 24 h. HLMECs were co-incubated with DiD-labelled neutrophil-EVs (50,000 FU/mL) or PBS-DiD without EVs for 1 h under flow conditions (5 dyn/cm^2). EV uptake was measured by flow cytometry and quantified as cell-associated DiD fluorescence (MFI) and percentage of positive HLMECs for DiD signal. HLMECs took up neutrophil-EVs under flow conditions, while incubation of HLMECs with the PBS-DiD control did not produce detectable cell-associated DiD fluorescence (**A**). Data are analysed by one-way ANOVA with Bonferroni's multiple comparisons test (A; mean ± SD). n=3, **p<0.01. Histogram representative of 3 separate uptake experiments (**B**).

3.4.5. Comparison of neutrophil-EV uptake by HLMECs under static and flow conditions

I then performed a direct side-by-side comparison of DiD-labelled neutrophil-EV uptake by HLMECs under standard static tissue culture versus flow conditions (5 dyn/cm^2) and observed that uptake was significantly higher in static compared to flow conditions (**Figure 3.12**). Interestingly, despite the use of the same neutrophil-EV preparations and HLMECs, levels of uptake under static culture conditions showed considerable variability compared to flow conditions.

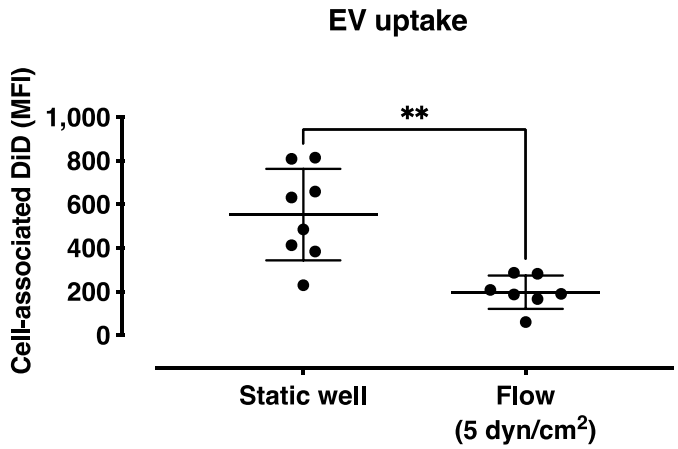

Figure 3.12. Physiological flow reduces neutrophil-EV uptake by HLMECs.
HLMECs were seeded in tissue culture wells (static) or ibidi® channel slides (flow, 5 dyn/cm^2). Flow-treated cells were pre-adapted to flow for 24 h (5 dyn/cm^2). DiD-labelled neutrophil-EVs (50,000 FU/mL) were incubated with HLMECs for 1 h and EV uptake was quantified by flow cytometric analysis as cell-associated DiD fluorescence. Uptake was significantly lower under flow compared to static conditions. Data are analysed by two-tailed unpaired t-test (mean ± SD). n=7-8, **p<0.01.

Next, neutrophil-EV uptake was evaluated over a range of physiological shear stress conditions. By combining channel slides of different heights and perfusion sets of different diameters, I was able to compare four different shear stress conditions in parallel using the ibidi® Quad system (see **Table 3.2** for details). With increasing shear stress from the lowest value of 0.56 dyn/cm^2 up to 10.95 dyn/cm^2, a ~3-fold decrease in uptake was observed (0.56

dyn/cm^2: 318.9±170.2 vs. 10.95 dyn/cm^2: 109.2±46.5 MFI) (**Figure 3.13**). Furthermore, uptake was more variable at the lower shear stress and decreased with increasing shear stress. This change suggested that variability was not exclusive to static culture conditions and that increasing shear stress forces may reduce experimental variables determining EV binding and uptake by HLMECs.

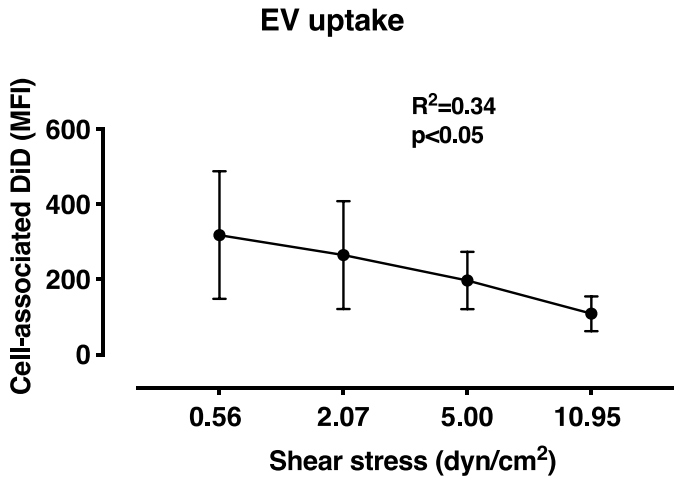

Figure 3.13. Increasing shear stress reduces neutrophil-EV uptake by HLMECs.
HLMECs were seeded in ibidi® channel slides of appropriate height (0.4, 0.6, 0.8 mm), which combined with the appropriate diameter perfusion sets (0.8 or 1.6 mm) produced the four different shear stresses 0.56, 2.07, 5, 10.95 dyn/cm^2, and adapted for 24 h. The uptake of DiD-labelled neutrophil-EVs (50,000 FU/mL) by HLMECs was then determined by flow cytometry after 1 h perfusion at the same shear stresses as the ones used for the adaptation period. Increasing shear stress within the range of 0.56 to 10.95 dyn/cm^2 resulted in decreased EV uptake. Data are analysed by one-way ANOVA test for linear trend (mean ± SD). n=4-7, *p<0.05.

To investigate the effect of acute pulmonary vascular inflammation on neutrophil-EV uptake, pre-adapted to flow HLMECs were treated with TNF-α (100 ng/mL, 2 h, 5 dyn/cm^2) prior to incubation with DiD-labelled EVs. For practicality, this TNF-α stimulation protocol was chosen based on significant adhesion molecule upregulation on HLMEC surface, similar to the standard 4 h (TNF-α 100 ng/mL) or overnight treatment with lower TNF-α concentration (10 ng/mL) observed in pilot experiments (**Figure 3.14**). Neutrophil-EV uptake by HLMECs under flow conditions was increased by almost 2-fold as a result of TNF-α pre-treatment (**Figure 3.15**).

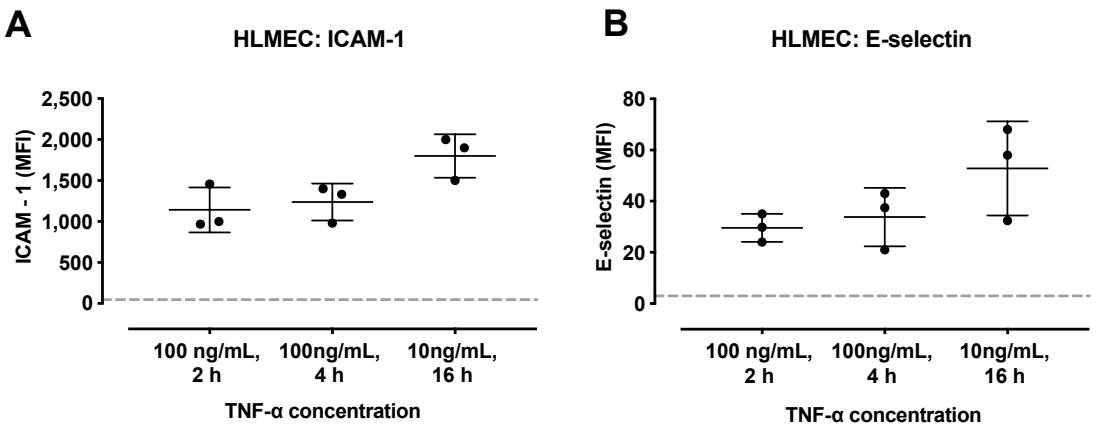

Figure 3.14. Upregulation of cell adhesion molecule expression on HLMECs after TNF-α treatment.
HLMECs were seeded in tissue culture well plates and treated with TNF-α (100 ng/mL) for 2 or 4 h or TNF-α (10 ng/mL) overnight (16 h). Cell activation was assessed by adhesion molecule expression, measured by flow cytometry. TNF-α treatment induced the upregulation of ICAM-1 (**A**) and E-selectin (**B**) on HLMECs, compared to untreated cells (dotted line) at similar levels, regardless of concentration or incubation period, without significant differences observed with the different TNF-α treatment protocols. Data are analysed by one-way ANOVA with Bonferroni's multiple comparisons test (A-B; mean ± SD). n=3.

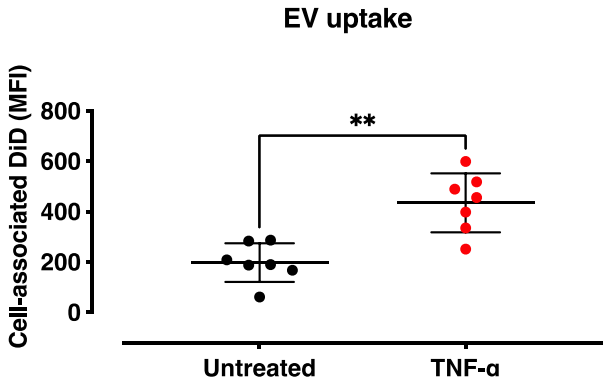

Figure 3.15. Inflammation enhances neutrophil-EV uptake by HLMECs under flow conditions. HLMECs were seeded in ibidi® channel slides and adapted to flow (5 dyn/cm^2) for 24 h. The following day, they were treated with TNF-α 100 ng/mL for 2 h under flow conditions prior to EV addition. After replacement of the TNF-α containing medium with EBM-HAS, DiD-labelled neutrophil-EVs (50,000 FU/mL) were incubated with HLMECs for 1 h with flow (5 dyn/cm^2). EV uptake was quantified by flow cytometric analysis of cell-associated DiD fluorescence. TNF-α pre-treatment significantly increased neutrophil-EV uptake by HLMECs compared to resting conditions. Data are analysed by two-tailed unpaired t-test (mean ± SD). n=7, **p<0.01.

Next, the effect of HLMEC pre-activation with TNF-α (100 ng/mL, 2 h) on neutrophil-EV uptake over a range of different shear stress conditions was evaluated. In contrast to resting HLMECs, where EV uptake was significantly decreased with increasing shear stress, increasing shear stress resulted in increased EV uptake by TNF-α pre-activated HLMECs (resting HLMECs 5 dyn/cm^2: 198±77, 10.95 dyn/cm^2: 109±47 vs. TNF-α pre-activated HLMECs 5 dyn/cm^2: 435±117, 10.95 dyn/cm^2: 886±95 MFI) (**Figure 3.16**).

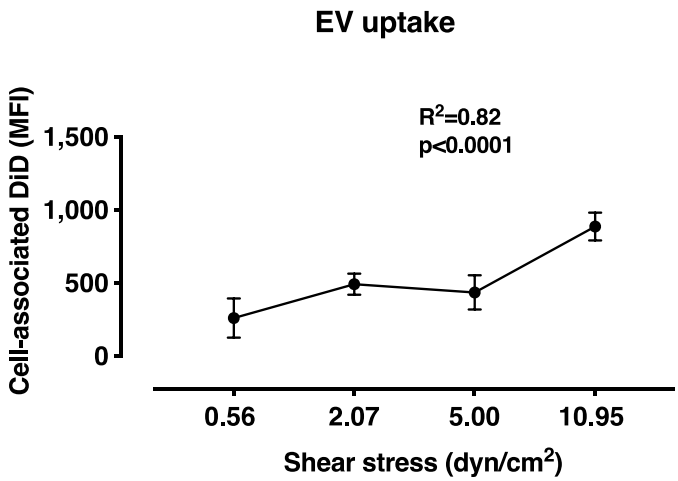

Figure 3.16. Increasing shear stress increases neutrophil-EV uptake by HLMECs under inflammatory conditions.
HLMECs were seeded in ibidi® channel slides of appropriate height (0.4, 0.6, 0.8 mm), which combined with the appropriate diameter perfusion sets (0.8 or 1.6 mm) produced the four different shear stresses 0.56, 2.07, 5, 10.95 dyn/cm^2, and adapted for 24 h. The following day, HLMECs were treated with TNF-α (100 ng/mL, 2 h) under the same flow conditions. After replacement of the TNF-α containing medium with EBM-HAS, DiD-labelled neutrophil-EVs (50,000 FU/mL) were incubated with HLMECs for 1 h with flow (at each shear stress value) and uptake was determined by flow cytometry. Increasing shear stress within the range of 0.56 to 10.95 dyn/cm^2 resulted in increased EV uptake. Data are analysed by one-way ANOVA test for linear trend (mean ± SD). n=4-7, ****p<0.0001.

3.4.6. Neutrophil-EV uptake by HLMECs involves endocytosis pathways

Next, the basic mechanisms of neutrophil-EV uptake by HLMECs under static culture conditions were investigated. To determine active uptake versus passive surface binding, low temperature (4 °C) incubations were used, as well as endocytosis inhibitors, cytochalasin D and dynasore. Neutrophil-EV uptake was significantly reduced at 4 °C compared to 37 °C, indicating an active internalisation process (**Figure 3.17**). Both cytochalasin D, which blocks the cytoskeletal function via actin microfilament disruption and is involved in macropinocytosis, and dynasore, a dynamin GTPase inhibitor acting as a clathrin-mediated endocytosis inhibitor, significantly decreased EV uptake (**Figure 3.17**). Taken together these findings, neutrophil-EV uptake is clearly an active process, involving both macropinocytosis and clathrin-mediated endocytosis pathways.

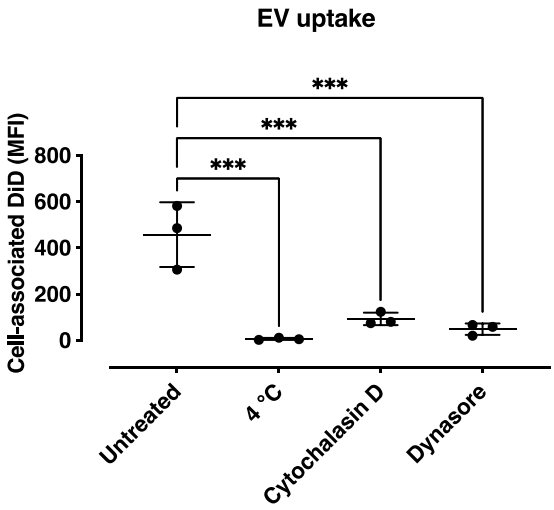

Figure 3.17. HLMECs internalise neutrophil-EVs via active endocytosis.
HLMECs were seeded in tissue culture well plates and pre-incubated with cytochalasin D (2 mM) or dynasore (250 µM) for 30 min prior to EV addition. DiD-labelled neutrophil-EVs (50,000 FU/mL) were incubated with HLMECs for 1 h at 37 °C. EV uptake was quantified by flow cytometric analysis as cell-associated DiD fluorescence. The untreated group represents HLMEC-EV treatment without any inhibitors, at 37 °C, while in the 4 °C treated group HLMEC-EV co-incubation was performed at 4 °C. EV incubation with HLMECs at 4 °C resulted in complete uptake inhibition, indicating an active process. Pre-treatment of HLMECs with both endocytosis inhibitors significantly reduced EV uptake. Data are analysed by one-way ANOVA with Bonferroni's multiple comparisons test (mean ± SD). n=3, ***p<0.001.

3.4.7. Characterisation of neutrophil-EV uptake in a co-culture model of PBMCs and HLMECs

As the main target cell population of circulating EVs in mouse lungs *in vivo (281)*, our next aim was to model neutrophil-EV uptake by lung-marginated monocytes *in vitro* under static and flow conditions. To better simulate the human pulmonary vascular environment, a co-culture model of human primary monocytes and HLMECs was developed under physiological flow conditions. HLMECs were seeded in tissue culture wells or ibidi® channel slides and adapted to flow (5 dyn/cm^2) for 24 h, as previously described. Fresh PBMCs were isolated from healthy volunteer blood and standardised based on monocyte numbers. To enable firm adhesion of monocytes to HLMEC monolayers, HLMECs were pre-activated with TNF-α (100 ng/mL, 2 h) under the same flow conditions. Following a static PBMC adherence step for 2 h, the co-culture slides were inserted to the PFC system and adapted to flow (5 dyn/cm^2) for a

subsequent 1 h. Loosely and non-adherent PBMCs were removed prior to EV addition. For static culture, since HLMECs were seeded in tissue culture wells, no flow adaptation was performed and TNF-α activation as well as PBMC adherence and neutrophil-EV co-incubation were all conducted in static conditions. Non-adherent PBMCs were removed in this protocol as well, prior to EV addition.

HLMECs (TNF-α pre-treated) and monocytes were found to take up similar amounts of neutrophil-EVs under static conditions (HLMECs: 196±71 vs. monocytes: 173±77 MFI) (**Figure 3.18**). However, under flow (5 dyn/cm^2), neutrophil-EV uptake by monocytes became significantly higher than HLMECs and increased more than 9-fold compared to static conditions (monocyte uptake static: 173±77 vs. flow: 1622±286 MFI).

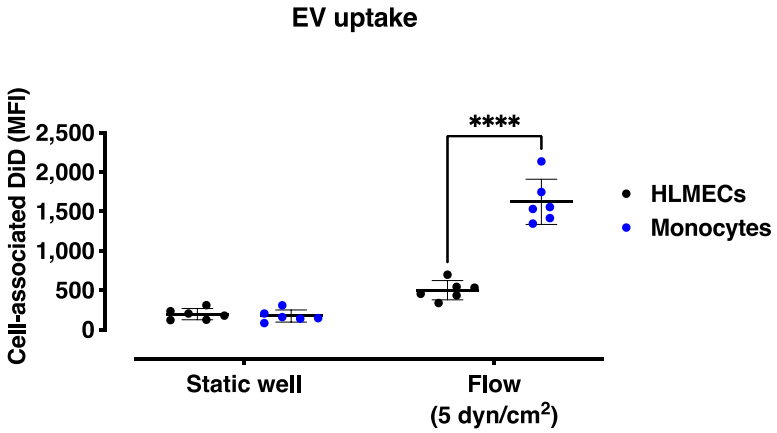

Figure 3.18. Neutrophil-EV uptake by HLMECs and monocytes under static and physiological flow conditions.
HLMECs were seeded in tissue culture well plates (static) or ibidi® channel slides (flow) and activated with TNF-α (100 ng/mL) for 2 h. For flow conditions, HLMECs were adapted to flow (5 dyn/cm^2) for 24 h prior to TNF-α activation. PBMCs were added to HLMECs (monocyte: HLMEC ratio 2: 1) and left to adhere in static, for 2 h. For flow conditions, after static PBMC adherence, co-cultures were adapted to flow (5 dyn/cm^2) for 1 h and loosely/non-adherent PBMCs were removed. DiD-labelled neutrophil-EVs (50,000 FU/mL) were added to co-cultures for 1 h and EV uptake was measured by flow cytometry as cell-associated DiD fluorescence for HLMECs (CD146$^+$) and monocytes (CD45$^+$CD14$^+$). Under static conditions, HLMECs and monocytes took up neutrophil-EVs at a similar level, while flow markedly increased EV uptake by monocytes (3.5-fold higher than HLMECs; 9-fold higher than monocyte uptake in static). Data are analysed by two-way ANOVA with Sidak's multiple comparisons test (mean ± SD). n=6, ****p<0.0001.

By using a range of shear stress conditions (0.56-10.95 dyn/cm^2) as described before, we observed that with low shear stress (0.56 dyn/cm^2) EV uptake by monocytes is decreased compared to higher shear stress (ranging from 2.07 to 10.95 dyn/cm^2). However, EV uptake by monocytes reached a maximum level at shear values above 2.07 dyn/cm^2, presumably due to no further shear-dependent effects or saturation of monocyte uptake capacity (**Figure 3.19**).

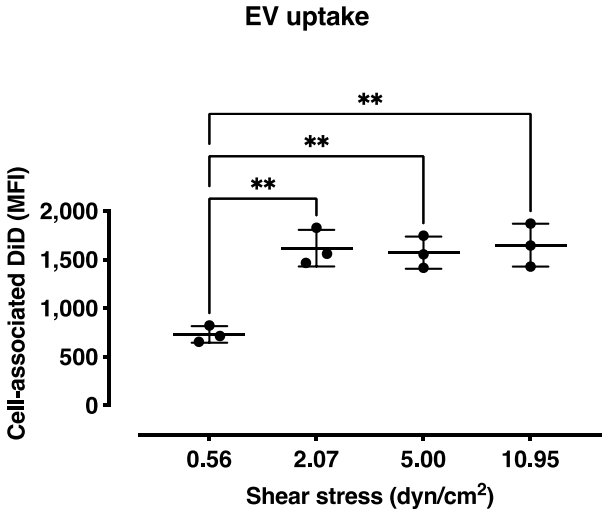

Figure 3.19. Neutrophil-EV uptake by monocytes is enhanced by flow but not affected by increasing shear stress.
Neutrophil-EV uptake by monocytes under increasing shear stress conditions was measured by using the co-culture model of PBMCs and HLMECs and the previously described shear stress range of 0.56-10.95 dyn/cm^2. DiD-labelled neutrophil-EVs (50,000 FU/mL) were added to co-cultures for 1 h and EV uptake was quantified by flow cytometry as cell-associated DiD fluorescence. Increasing shear stress enhanced EV uptake by monocytes, reaching a plateau at 2.07 dyn/cm^2. Further increases in shear stress did not enhance EV uptake by monocytes. Data are analysed by one-way ANOVA with Bonferroni's multiple comparisons tests (mean ± SD). n=3, **p<0.01.

3.5. Discussion

Our group and others have demonstrated that neutrophil-EVs are acutely elevated in burns and sepsis patients (246, 286, 324, 327, 379). These results were replicated in a mouse model of endotoxaemia, where neutrophils showed the most acute increases in numbers compared to other vascular EV subtypes (357). Neutrophil-EV uptake has been shown in a variety of cell types including human umbilical vein endothelial cells (HUVECs) (319, 352, 380), neutrophils (381), monocytes (293, 324, 380), macrophages (242, 330, 382), and natural killer (NK) cells (383) under *in vitro* conditions. We hypothesised that flow may be an important determinant for EV interactions with target cells within the pulmonary microvasculature. After establishing protocols for neutrophil-EV production, we found that HLMECs take up neutrophil-EVs *in vitro* and that uptake is reduced with flow compared to static cell culture conditions. Increasing shear stress decreased neutrophil-EV uptake under resting conditions, but stimulation of HLMECs with TNF-α had the opposite effect, with EV uptake increasing with increased shear stress. This effect of flow had more pronounced effects on monocytes, with several-fold increases in neutrophil-EV uptake at physiological shear stress. Overall, these results suggest that flow is likely to be an important regulator of neutrophil-EV uptake by target cells within the pulmonary vasculature and distinct uptake mechanisms may exist during different inflammatory and pathophysiological conditions.

I started my investigations into human neutrophil-EV biology by assessing different methods for their production *in vitro*. Primary neutrophils were treated with four inflammatory stimuli that have been previously used for neutrophil-EV release, fMLP (292, 296, 325, 352, 384), LPS (385-387), TNF-α (241, 319, 321), and calcium ionophore A23187 (322) and their potency on neutrophil activation and EV release was compared. Apart from LPS, the other three agonists resulted in substantial cell activation indicated by the upregulation of CD66b (388, 389), downregulation of L-selectin (390) and EV release. It should be noted that the lack of effect with LPS treatment could relate to the absence of serum during stimulation, a requirement for

its optimal signalling. As fMLP is a potent physiological chemoattractant for neutrophils and a more specific stimulus than TNF-α and calcium ionophore A23187, it was considered the most appropriate stimulus for routine neutrophil-EV production in the subsequent assays.

Confirming a previous observation by the group, I found that HLMECs do take up DiD-labelled neutrophil-EVs under standard *in vitro* culture conditions. This result contrasts with the lack of EV (macrophage-derived) uptake by pulmonary vascular endothelial cells in mice *in vivo* (281). The use of lipophilic dyes, such as DiD, for EV uptake studies has been questioned because of precipitation, aggregation, and increased dye half-life compared to EV-half life, which in longer studies may be an issue as the dye fluorescence might be sustained and detectable for periods exceeding that of EVs' persistence itself (391, 392). However, I explored the nature of the cell-associated DiD fluorescence and found that incubation with insoluble dye alone did not lead to any detectable signal in HLMECs.

To establish the model of EV uptake under flow conditions, I first investigated the pre-adaptation of HLMECs by culturing them with flow for different periods. Flow adaptation was proven important by others as sudden exposure to flow *in vitro*, caused morphological changes (cell polarisation and elongation) in endothelial cells (340, 368, 393). However, these studies were carried out with arterial or vein endothelial cells, which may not be relevant to capillary endothelial cells that are exposed to lower shear stresses and as single cells can envelop the entire vessel wall. I did not find any obvious changes in the surface protein marker expression of HLMECs, apart from reductions in expression of junctional proteins CD31 and CD146; although further repeats would be necessary to confirm this observation and extrapolate its functional implication. However, the partial alignment of cells did indicate that flow produced a measurable adaptation response. Of note, it has been previously observed that endothelial cells in culture behave differently from endothelial cells *in situ* (394) including having increased sensitivity to permeability *in vitro* (395), absence of glycocalyx (396), and detectable alterations in membrane protein expression (397). This most likely reflects the loss

of environmental cues and a default adaptation to *in vitro* conditions and highlights the need to perform experiments with minimal passage number of primary endothelial cell cultures.

A more striking impact of flow pre-adaptation was observed with neutrophil-EV uptake, as pre-adapted HLMECs had 2-3-fold higher neutrophil-EV uptake compared to non-adapted HLMECs. Signalling in endothelial cells has been demonstrated upon re-introduction of flow by Chatterjee and colleagues studying mechano-sensing in non-hypoxic ischaemic reperfusion injury in the lungs (398, 399). Whether this process relates to changes in uptake of nano- and microparticles (including EVs) by endothelial cells would require measurement of functional endpoints related to endocytosis. Although preliminary data, this finding may support our hypothesis that hypoxic vasoconstriction and transient cessation of pulmonary vascular flow have significant effects on interactions of resident cells with circulating EVs, which may subsequently lead to functional implications.

As a next step to understand neutrophil-EV uptake by HLMECs, I investigated whether the static conditions of standard cell culture acted as a factor in promoting *in vitro* uptake of EVs. Comparing EV uptake under flow in the ibidi® PFC system and under static conditions in a multi-well plate, EV uptake was still evident under flow but of a significantly lower magnitude. Shear stress plays a crucial role in determining capture and internalisation of nanoparticles by human endothelial cells. Lin et al., found that in human coronary arterial endothelial cells (HCAECs) uptake of polystyrene nanoparticles (of 100 nm size) was markedly decreased with physiological shear stresses of 1 or 5 dyn/cm^2 compared to static culture (350). Moreover, Dickerson et al., observed that nanoparticle adhesion to HUVECs was negatively correlated with increased shear stress (351), while Gomez and colleagues showed a clear (more than 2-fold) reduction in neutrophil-EV adherence to HUVECs with high shear stress (13 dyn/cm^2) compared to static incubations (352). Apart from nano- and microparticles adhesion of *Neisseria meningitidis* bacteria (0.6 – 1 µm size) in both HUVECs and a brain endothelial cancer cell line, was also negatively affected by increased shear stress conditions with a substantial reduction from static to flow conditions of uptake (353). This phenomenon of

decreased uptake with flow compared to static conditions has also been observed with the uptake of macromolecules such as heparan sulfate, and low-density lipoprotein in HCAECs (354).

Diffusion is a term used to describe a net, (random) type of molecule movement that generally occurs locally at low speeds, because of concentration gradient differences and does not require bulk motion. Convection, on the other hand, refers to a fluid motion that is driven by body forces (including gravity). In static culture, diffusion is therefore likely to be the dominant mechanism for generating cell-EV contact, albeit with some convection produced during the initial set-up of plates and warming within the incubator. Conversely, in the PFC system EV movement occurs mostly via continuous flow of media and therefore is probably a convection-driven process. The lower uptake during flow with moderate shear stress (5 dyn/cm^2) suggests that despite convection-generated cell-EV interactions, capture and uptake is more limited under physiological flow conditions than in static cell culture. This interpretation and modulation of EV uptake by shear stress was confirmed by the trend for reduced uptake over a range of increasing physiologically relevant shear stresses observed by us and others (350, 351).

Interestingly, TNF-α pre-treatment of HLMECs increased their neutrophil-EV uptake under flow, and in contrast to the EV uptake pattern in resting HLMECs, higher shear stresses increased rather than reduced the EV uptake. An obvious explanation for increased uptake is the increased cell adhesion molecule expression on TNF-α treated HLMECs, promoting neutrophil-EV binding to HLMECs similar to their parent cells. The uptake-promoting effects of shear stress could be derived from certain receptor-ligand interactions that require a threshold shear force to support the leukocyte rolling. For example, low shear stress forces decrease the L-selectin and PSGL-1 bond formation, whereas higher shear forces enhance it (400-402). Although PSGL-1 is constitutively expressed on endothelial cells, inflammatory stimulation significantly enhances the functional binding capacity of monocytes or P-selectin-bearing particles to endothelial cells (403). A similar type of bond might be responsible for the

neutrophil-EV-HLMEC capture under higher shear stress rates that could be hidden upon the resting status of endothelial cells.

To further examine EV uptake within the pulmonary vascular environment, I developed a PBMC-HLMEC co-culture system to assess EV uptake under flow conditions and enable the direct comparison between HLMECs and adherent monocytes. In static cultures, EV uptake was similar between each cell type, whereas uptake by monocytes under flow conditions was almost 3-fold higher than in HLMECs and increased by ~9-fold compared to monocytes under static conditions. This could be attributed to the existence of scavenger receptors on monocytes, that enable them to capture particles as the main effector cells of phagocytosis processes. Convective forces under physiological flow conditions might enhance the interactions between EVs and monocytes, effectively increasing EV uptake compared to static cultures.

Using a pharmacological inhibitor-based approach, I demonstrated that HLMECs internalise EVs via macropinocytosis and clathrin- and dynamin-dependent endocytosis. EV co-incubation with HLMECs at 4 °C abolished EV uptake, while cytochalasin D, an actin polymerisation inhibitor effective against macropinocytosis (276), and dynasore, a dynamin inhibitor, specific for clathrin- and dynamin-dependent endocytosis (404) inhibited neutrophil-EV uptake by HLMECs. Of note, these experiments were only performed in static cultures due to difficulties in using low temperature and large volumes of the inhibitors required to perform the assays in the PFC system. In future studies, it would be interesting to assess if the same endocytic pathways are involved in EV uptake under flow conditions and whether EV uptake by monocytes follows similar mechanisms.

Lastly, it has been previously reported that incubation of synthetic polystyrene or silica nanoparticles in the presence of serum, leads to modifications on EV surface by serum proteins, a phenomenon described as ‘corona formation’ (405-407). The presence of this corona layer decreased nanoparticle uptake by epithelial (breast, lung, cervical) or brain

endothelial cells (405, 406) and modified the internalisation mechanisms switching between clathrin- and dynamin-dependent endocytosis (in the absence of serum) and phagocytosis (in serum presence) in monocyte-like THP-1 cells and macrophages (407). Although the corona formation in the biological EVs used in this study might differ from the synthetic ones, it was decided to conduct our assays in serum free conditions, to avoid any unknown off-target effects mediated by humoral responses. We acknowledge though that the effect of serum on neutrophil-EV uptake and its physiological relevance should be studied in the future to fully explain any biological effects this might have. In fact, the discrepancies observed in EV uptake between human and mouse endothelial cells in this and a previous study in the group (281), could be attributed to serum presence in the *in vivo* mouse model. Similar differences were observed by Kamps and colleagues before, in the uptake of phosphatidylserine-bearing liposomes by rat liver endothelial cells *in vivo* and in serum-free *ex vivo* (isolated perfused rat system), and *in vitro* models, that were assigned to serum-induced protein shielding of scavenger receptors (that were found responsible for uptake) (408, 409).

4. Characterisation of EV subtype production and activity in LPS-stimulated whole blood

Parts of the data produced for this chapter have been published as a conference abstract and a journal publication:

Tsiridou DM, O'Dea KO, Tan YYT, Takata M. Late Breaking Abstract-Myeloid-derived microvesicles as acute mediators of sepsis-induced lung vascular inflammation. European Respiratory Journal 2020; 56: Suppl. 64,4468 (410)

Tan YY, O'Dea KP, Tsiridou DM, Pac Soo A, Koh MW, Beckett F, et al. Circulating Myeloid Cell-derived Extracellular Vesicles as Mediators of Indirect Acute Lung Injury. Am J Respir Cell Mol Biol. 2023;68(2):140-9 (357)

4.1. Background

Elevated levels of circulating EVs in sepsis and non-infectious SIRS suggest that they have important roles as biomarkers and/or mediators of the systemic inflammatory and injury response (282). Furthermore, as increases in levels of blood cell-derived EV subtypes are often observed (291), there is potential for a diverse range of EV-mediated physiological and pathophysiological effects. Defining the respective roles of different EV subtypes in sepsis/SIRS is challenging, with previous functional analyses of patient-derived material usually carried out with total (unfractionated) EV preparations isolated by differential centrifugation (286, 289, 291, 411). Consequently, most *in vitro* and *in vivo* studies into EV subtype function are centred around isolated cell populations, *in vitro* stimulated with a single agonist that is often specific to the parent cell population and not always relevant to sepsis/SIRS. Unfortunately, such reductionist *in vitro* approaches do not model the complex responses and conditions that would contribute to EV generation in sepsis/SIRS and therefore more physiologically and clinically relevant modelling is needed. Although plasma samples from septic patients or LPS-challenged human volunteers represent the most clinically relevant source for EVs, they may not be the most representative of EV functions due to the rapid production and clearance of circulating EVs mainly by cells of the reticuloendothelial system (277, 278). Therefore, as with circulating cytokines (412), circulating EV levels or phenotypes reported in critically ill patients do not necessarily provide an accurate picture of EV production and functional properties.

LPS from Gram-negative bacteria is widely used experimentally as a non-infectious septic stimulus based on its high potency and ability to reproduce sepsis symptoms and pathophysiology when administrated to healthy volunteers and animal models (413-417). LPS administered to healthy volunteers has also been shown to induce the release of circulating EVs, derived mainly from platelets and monocytes, with pro-coagulant activity (299, 301, 302, 418-421). *In vitro*, LPS induces direct activation of cells, including monocytes, platelets,

endothelial cells, and neutrophils, alongside potent pro-inflammatory cytokine responses. When used to stimulate whole blood, LPS is a convenient model to simulate at least some of the *in vivo* inflammatory cell responses and crosstalk produced during sepsis. However, studies on EV production in LPS-stimulated whole blood appear to be quite limited, concerned mainly with coagulation activities. Evaluating the inflammatory activities of EVs generated in an LPS whole blood model would have the advantage of incorporating at least some of the multiple responses contributing to circulating EV generation in sepsis/SIRS. However, isolating EV subtypes from mixed populations after their production is more technically challenging than generation of EV subtypes from their isolated parent cell populations.

As part of an ongoing investigation into EV subtype function in a mouse model of endotoxaemia, our group recently characterised early EV kinetics in response to intravenous LPS administration. Finding acute release of EVs (1-4 h), my colleague (Dr Ying Ying Tan) developed an immunomagnetic bead-based method of EV subtype isolation and administration to an isolated perfused lung model of ALI (357). This chapter describes my investigation into the generation of human EV subtypes in LPS-stimulated whole blood, and the development of methods to isolate EV subtypes using immunoaffinity separation followed by an evaluation of their activity, in an *in vitro* mixed cell culture model of human pulmonary vascular inflammation.

4.2. Aims

To obtain insights into the pro-inflammatory activity of EVs produced during endotoxaemia, I aimed to:

1. Characterise the EV subtype production kinetics in LPS-stimulated whole blood.
2. Develop methods for immunoaffinity-based isolation of individual EV subtypes from mixed EV populations produced in whole blood.
3. Evaluate the activity of different EV subtypes in an *in vitro* cell culture model of pulmonary vascular inflammation.

4.3. Protocols

4.3.1. EV production in an *ex vivo* whole blood model

Blood was collected from healthy volunteers into heparinised vacutainers and transferred to 15 mL conical polypropylene falcon tubes at 5 mL per tube. LPS (100 ng/mL) was added, and tubes were maintained under continuous mixing on a rotating wheel for 1 - 4 h at 37 °C. Blood was sequentially centrifuged at 400 × g (10 min), 1000 × g (5 min), and 1500 × g (20 min) to produce platelet poor plasma, which was then centrifuged at 20,800 × g for 30 min. The pelleted EV fraction was resuspended in EV sorting buffer (PBS, 0.5 % HAS, 2 mM EDTA, 1 % penicillin-streptomycin) for analysis and subtype isolation.

4.3.2. EV subtype quantification by flow cytometry

EVs were quantified by flow cytometry (for more details see **Chapter 2**, **Section 2.7.3**). EVs were stained for two or three markers conjugated to phycoerythrin (PE), allophycocyanin (APC or Alexa-fluor 647), or PE-Cyanine7 (PE-Cy7). The following cell-derived populations were examined: platelet-, neutrophil-, monocyte-, erythrocyte-, and CD11b-lymphoid cell-derived EVs (see **Chapter 2**, **Table 2.11**). EV numbers were determined using fluorescent counting beads during sample acquisition.

4.3.3. Immunoaffinity isolation of EV subtypes

Myeloid-EVs ($CD11b^+$), were isolated from platelet poor plasma using anti-CD11b MicroBeads (Miltenyi Biotec). As the manufacturer's protocol was designed for cell isolation, I performed a titration of anti-CD11b beads and identified a bead-to-myeloid-EV ratio of 1 µL beads to 1 x 10^6 $CD11b^+$ cells in 10 x the volume of sorting buffer (e.g., 10 µL buffer per 1 µL bead

suspension) for optimal EV recovery. After vortexing, the EV-bead mixture was incubated for 15 min at 4 °C, with re-mixing every ~5 min. Labelled EVs were then loaded onto magnetised MS or LS columns (Miltenyi Biotec) depending on the number of beads, according to the manufacturer's instructions. EVs were eluted from columns by removal from the magnetic field and flushed through with appropriate volume of EV sorting buffer. Platelet-EVs were isolated with anti-CD61 MicroBeads (Miltenyi Biotec) following the same protocol, including the same bead volume to EV count ratio. Flow cytometry was used to quantify EVs before and after selection. Percentage recovery and depletion were calculated based on **Equations A and B** below:

Percentage recovery (%) =

(A)

$$\frac{\text{Targeted EVs eluted}}{\text{Targeted EVs before fractionation}} \text{ x } 100\ \%$$

Percentage depletion (%) =

(B)

$$1 - \frac{\text{Non targeted EVs eluted}}{\text{Non targeted EVs before fractionation}} \text{ x } 100\ \%$$

4.3.4. EV functional assays

An *in vitro* co-culture model was established to assess the inflammatory activity of EV subtypes. HLMECs were seeded in 48-well plates at a density of 6 x 10^4 cells/well in complete EBM-2MV media and left to adhere overnight. PBMCs were isolated from healthy volunteer blood (see **Chapter 2**, **Section 2.4.1**) and added to HLMEC monocultures at a density of 1.2 x 10^5 monocytes/well with replacement of culture media with EBM-HAS. After 2 h, 6 x 10^6 $CD11b^+$ or $CD61^+$ EVs were added per well to co-cultures to a final volume of 500 µL and co-incubated for 4 h. Non-adherent cells were removed, and wells were treated with cell dissociation solution for 15 min at 37 °C to recover the adherent cells. Total cells recovered were separated by centrifugation, and analysed directly by flow cytometry. EV-free supernatants were stored at -80 °C for subsequent analysis of cytokine concentrations by ELISA. A schematic of the EV isolation and co-culture timeline is shown in **Figure 4.1.**

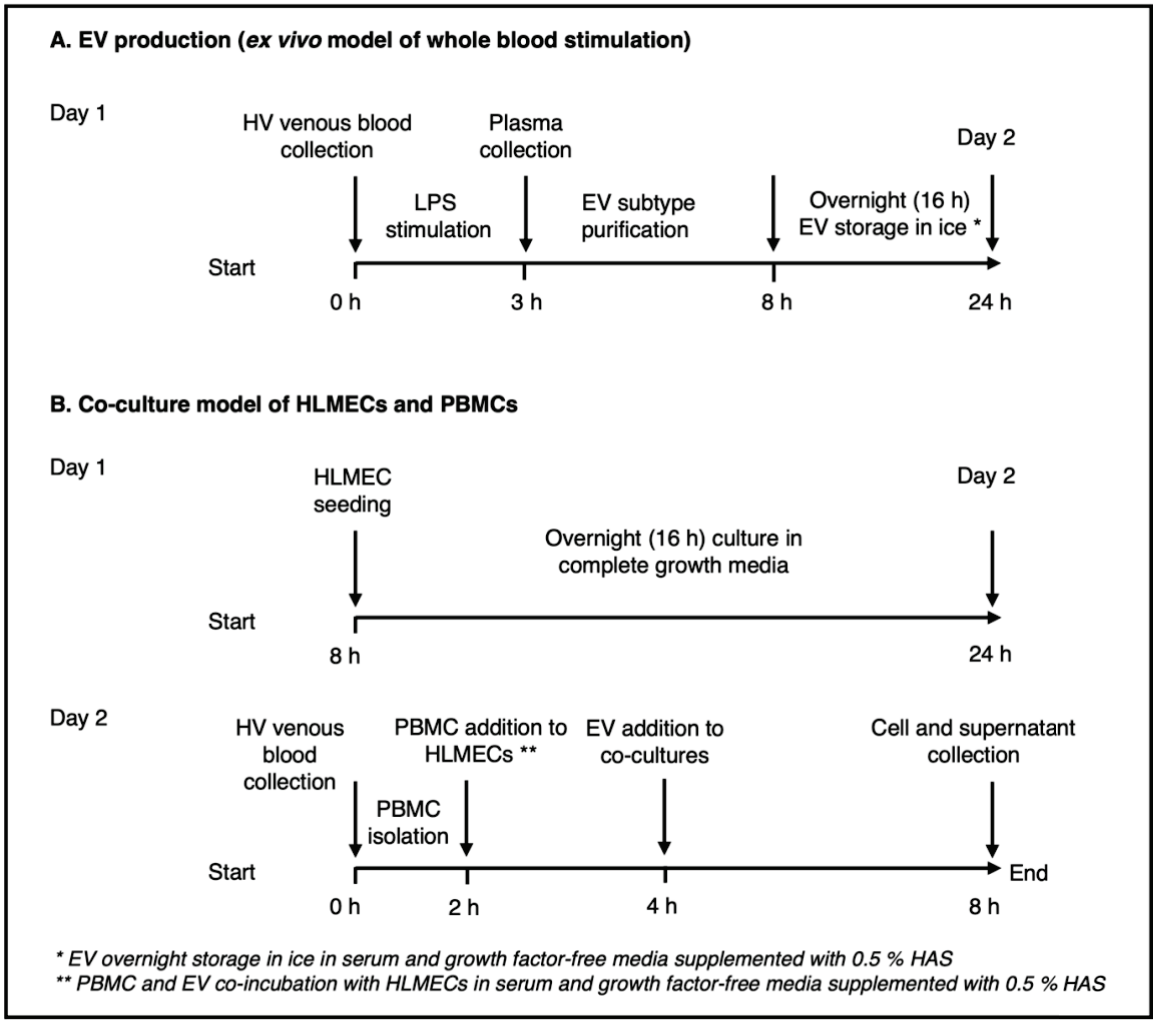

HV: healthy volunteer

Figure 4.1. Schematic of EV production and their evaluation in an *in vitro* co-culture assay.
EVs were produced in healthy volunteer whole blood model by stimulation with LPS (100 ng/mL, 3 h, 37 °C). EV subtypes were isolated from platelet poor plasma by immunomagnetic bead selection (**A**). PBMCs from healthy volunteer blood were co-incubated with HLMECs for 2 h. Purified EV subtypes were then incubated in co-cultures for 4 h and cell activation and cytokine release were assessed (**B)**.

4.4. Results

4.4.1. EV subtype production in LPS-stimulated whole blood

To develop antibody panels for detecting EV subtypes in plasma, I used platelet-poor plasmas obtained from LPS-stimulated whole blood at a single time point (3 h). A maximum of three antibodies were included in each combination based on the brightest fluorophores available (PE, PE-Cy7 and APC/ Alexa Fluor™ 647). Platelet-EVs were initially identified by expression of CD61 and CD42b, but subsequently, a combination of anti-CD31, anti-CD41, with anti-CD61 was used (**Figure 4.2**). CD45 was used as the pan leukocyte-EV marker, combined with anti-CD11b and anti-CD66b for neutrophil-EVs. With LPS stimulation, monocyte-EV levels were very low or undetectable using antibodies against CD11b, CD14, and HLA-DR. Furthermore, the majority of $CD11b^+$ events were $CD66b^+$, suggesting neutrophil origin rather than monocyte or natural killer (NK) cell, which also express CD11b but at lower levels than neutrophils and monocytes (422). Erythrocyte-derived EVs were detected as CD235α-positive and CD45-negative events. A $CD45^+$, $CD11b^-$ population was designated as lymphocyte-EVs. However, the identity of this population was not investigated further. In addition to specific antigen markers, EVs were stained with annexin V-FITC alone as a generic EV marker.

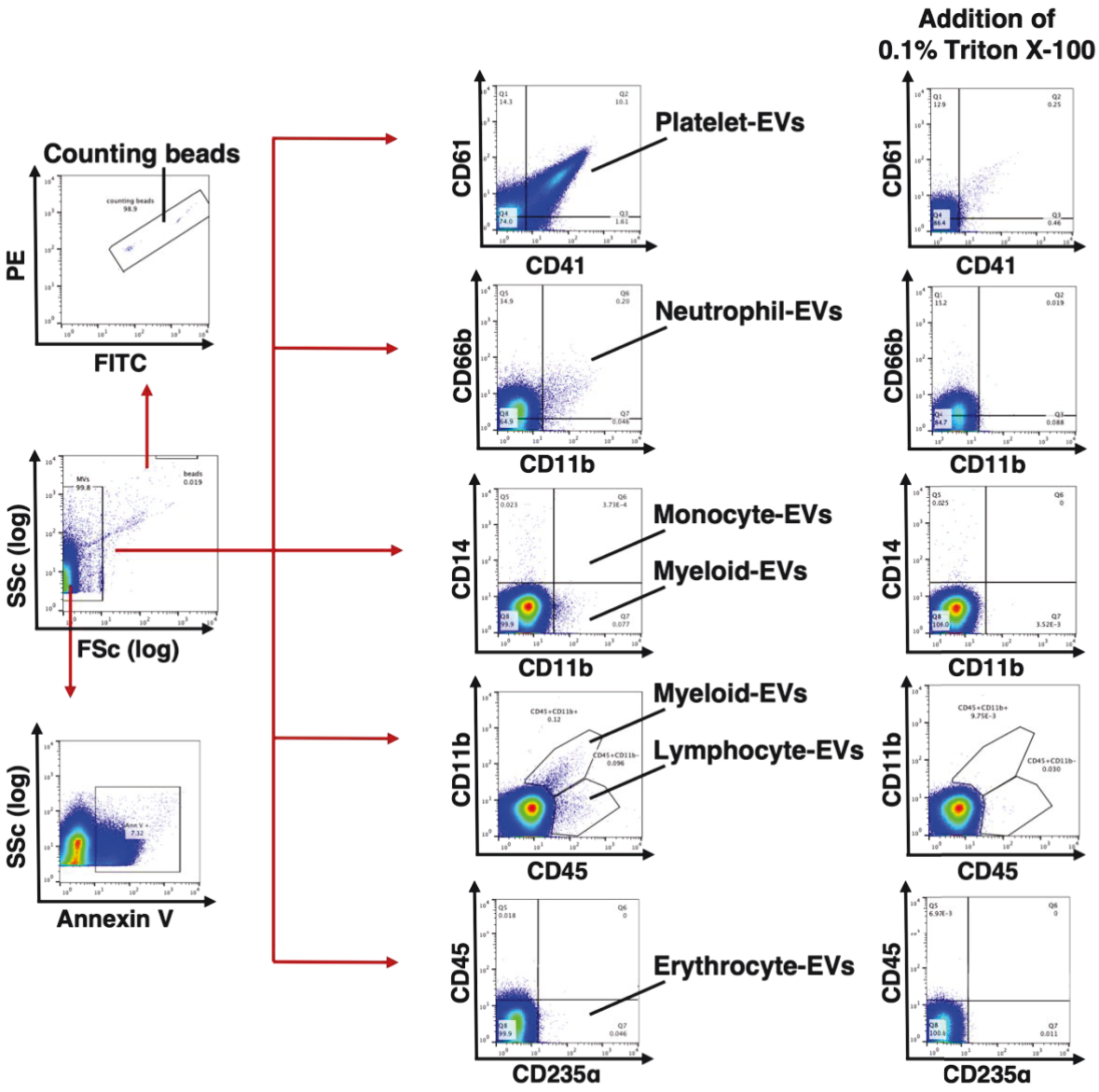

Figure 4.2. Flow cytometric identification of EV subtypes in LPS-stimulated blood.
Heparinised blood from healthy volunteers was stimulated with LPS (100 ng/mL, 3 h, 37 °C). Platelet poor plasma was obtained by centrifugation and stained with antibodies, followed by dilution and acquisition. Detectable levels of platelet-, neutrophil-, myeloid-, and lymphocyte- ($CD45^+$, $CD11b^-$) EVs were observed.

With EV detection methods established, I investigated the early kinetics of EV production in whole blood during stimulation with LPS. Annexin V staining demonstrated an overall increase in EV levels from 2 up to 4 h of LPS treatment compared to baseline levels (**Figure 4.3, A**). A marked elevation of platelet-EVs was apparent at 2 h, reaching statistical significance at 3 and

4 h (**Figure 4.3, B**). Neutrophil-EV levels were increased significantly at 3 h but appeared to decrease by 4 h (**Figure 4.3, C**). In contrast, no changes were observed in the numbers of monocyte-, lymphocyte-, and erythrocyte-EVs over the 4 h LPS treatment (**Figure 4.3, D-F**). Based on these observations, the 3 h time point was chosen for EV production in subsequent assays.

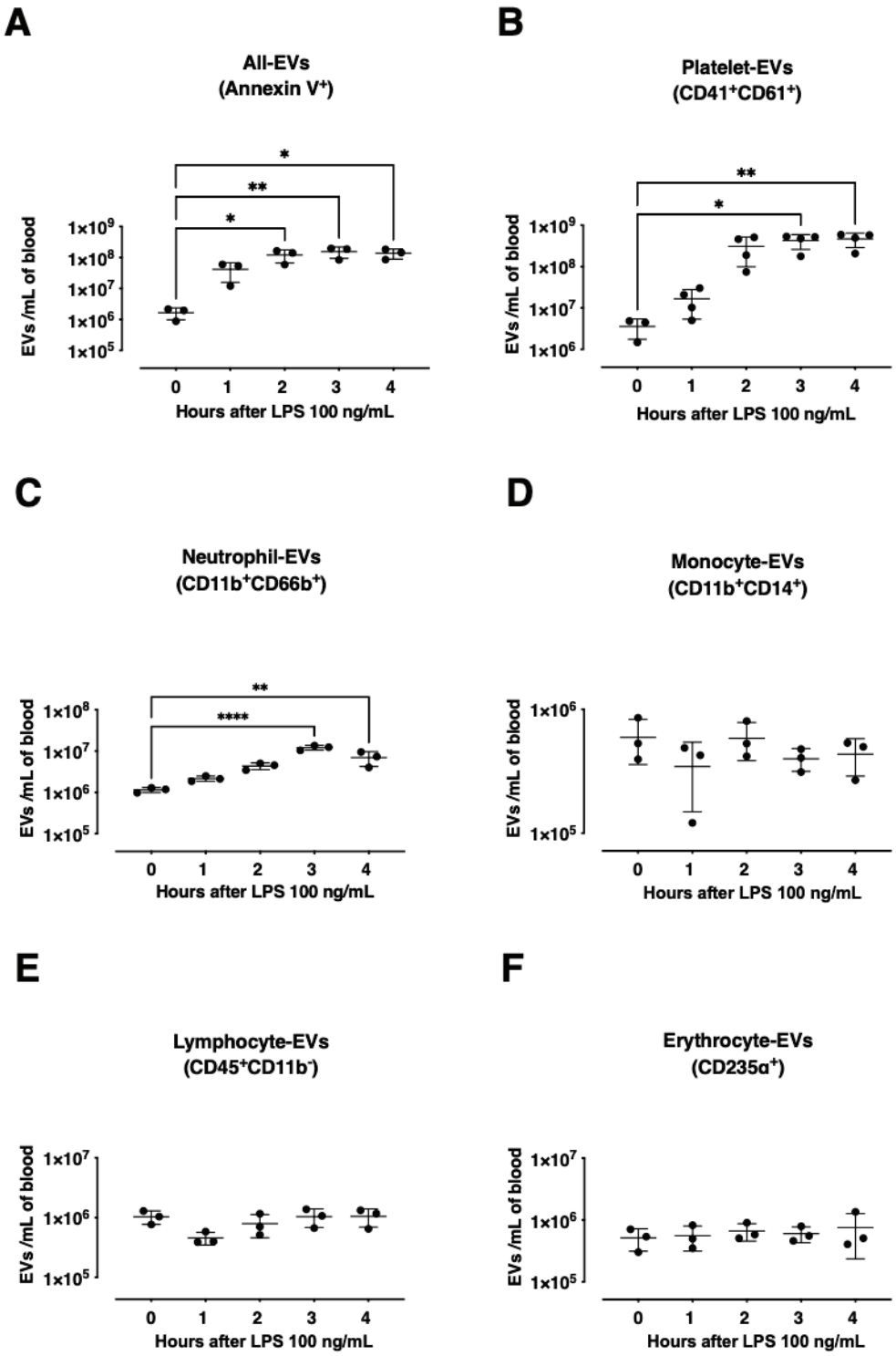

Figure 4.3. Kinetics of EV production in LPS-stimulated whole blood.
Heparinised blood from healthy volunteers was stimulated with LPS (100 ng/mL) over a 4 h period at 37 °C. EVs were stained in platelet poor plasma collected at 0, 1, 2, 3, and 4 h and quantified by flow cytometry. Levels of annexin V positive EVs significantly increased after 2 h LPS treatment (**A**). Platelet- and neutrophil-EVs were elevated significantly at 3 h whereas no significant change in monocyte-, lymphocyte-, and erythrocyte-EVs levels was detected (**B-F**). Data are log-transformed and analysed by one-way ANOVA with Bonferroni's multiple comparisons test (A-F; mean ± SD). n=3-4, *p<0.05, **p<0.01, ****p<0.0001.

4.4.2. Immunoaffinity isolation of myeloid- and platelet-EVs from LPS-stimulated blood

In our *in vivo* mouse adoptive transfer model, we used anti-CD11b MicroBeads (Miltenyi Biotec) to evaluate the role of myeloid-EVs in pulmonary vascular inflammation (357). Despite the very low levels of detectable monocyte-EVs in the human whole blood model, for the purpose of direct comparison with the mouse model data, we developed a method for isolation of human $CD11b^+$ EVs using the same mouse/human-specific anti-CD11b MicroBeads.

Myeloid-EV purity and yields were monitored during the isolation process using CD45, CD11b, and CD66b as markers, with similar EV numbers obtained using either $CD45^+$, $CD11b^+$ or $CD66b^+$, $CD11b^+$ gated events. However, in eluted material, detection using anti-CD11b staining was lost, suggesting blocking of available epitopes by CD11b MicroBeads, which is not surprising as the same monoclonal M1/70 antibody was used for both. EV counts were therefore determined using anti-CD45 and anti-CD66b staining. Most of these EVs appeared to be present in the eluted fraction and absent from the unbound flow-through (**Figure 4.4**).

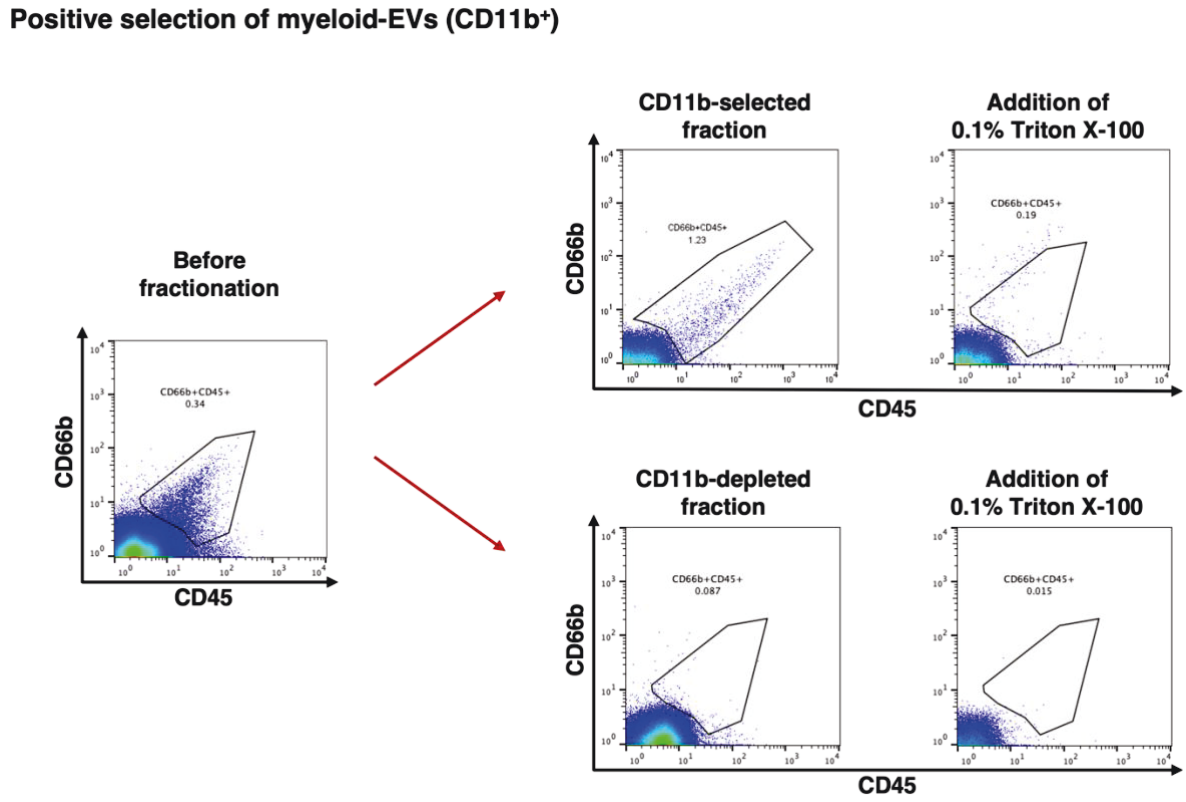

Figure 4.4. Isolation of myeloid-EVs by CD11b immunomagnetic bead separation.
EVs obtained from LPS-stimulated whole blood were incubated with CD11b MicroBeads and passed through a magnetised column. CD11b bead-bound EVs were retained on the column and eluted (CD11b-selected fraction), while unbound EVs were discarded in the flow through (CD11b-depleted fraction). Representative flow cytometry plots from n=6 repeats.

In an analysis of six experiments, a comparison of the pre-column and eluted material indicated a 65±28% recovery of myeloid-EVs. As an indication of purification efficiency, numbers of platelet-EVs were reduced by 99±1 % following CD11b bead separation (**Figure 4.6**).

Platelet-EVs were isolated using anti-CD61 MicroBeads. Platelet-EV numbers were quantified by CD61, CD41, and CD31, but as with CD11b bead separation, CD61 also appeared to be obscured post-isolation. Platelet-EVs were eluted with minimal loss of platelet-EVs ($CD41^+CD31^+$) in the unbound fraction (**Figure 4.5**). The recovery for platelet-EVs was 57±18 % and neutrophil-EV depletion was 98±2 % (**Figure 4.6**).

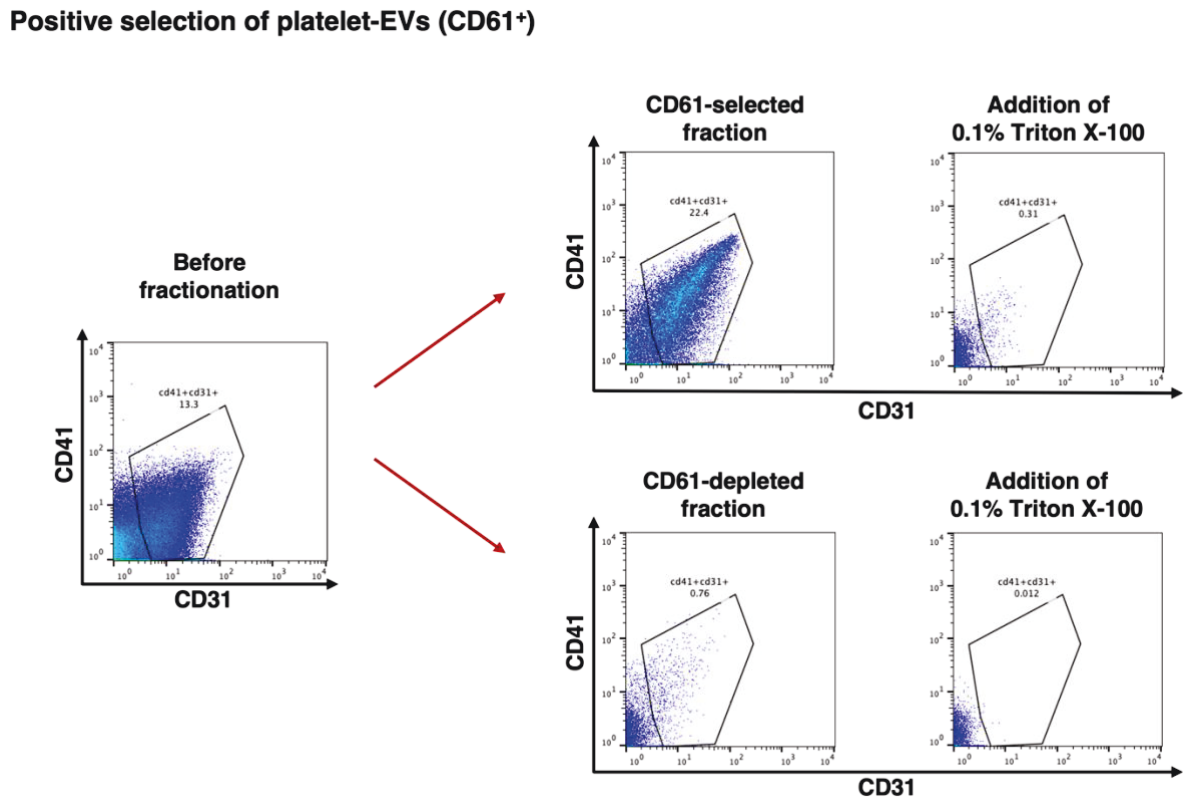

Figure 4.5. Isolation of platelet-EVs by CD61 immunomagnetic bead separation.
EVs obtained from LPS-stimulated whole blood were incubated with CD61 MicroBeads and passed through a magnetised column. CD61 bead-bound EVs were retained on the column and eluted (CD61-selected fraction), while unbound EVs were discarded in the flow through (CD61-depleted fraction). Representative flow cytometry plots from n=6 repeats.

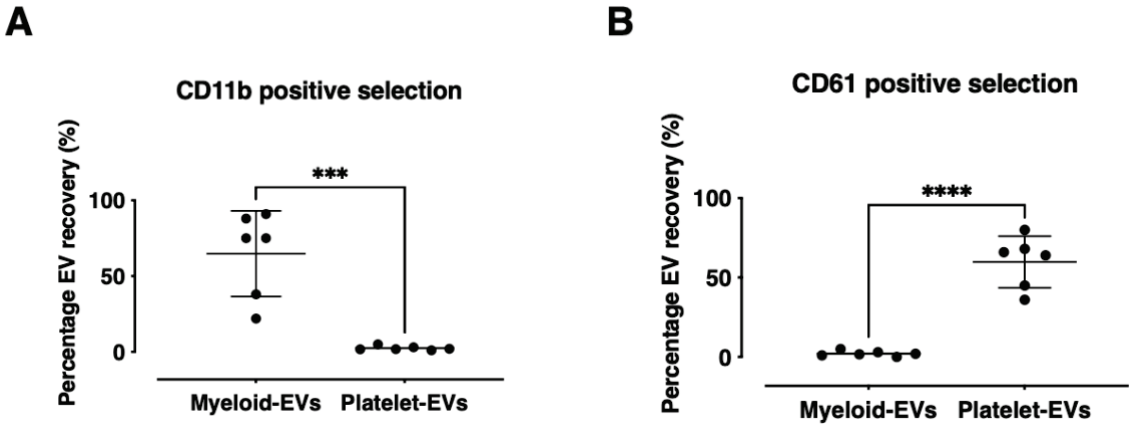

Figure 4.6. EV subtype recovery with CD11b and CD61 immunomagnetic bead positive selection.
Myeloid- and platelet-EVs were separated from a mixed EV population by immunomagnetic bead CD11b and CD61 positive selection respectively. Both CD11b and CD61 positive selection yielded sufficient numbers of myeloid- or platelet-EVs, with complete depletion of other EV subtypes (>98 %) (**A-B**). Data are analysed by two-tailed unpaired t-test (A-B; mean ± SD). n=6, ***p<0.001, ****p<0.0001.

4.4.3. Myeloid- but not platelet-EVs induce inflammatory activation of target cells

With the methods for myeloid- and platelet-EV isolation from LPS-treated whole blood established, my next aim was to determine their pro-inflammatory activity. For this, I developed a co-culture model consisting of confluent PBMCs and HLMECs based on the group's previously described mouse model for simulating monocyte-endothelial cell interactions within the pulmonary microvasculature (423).

To develop the method, I first evaluated responses to LPS, titrating concentrations from 0.001 to 100 ng/mL. The assay was performed in media containing FBS at 10 % to ensure LPS sensitivity (358). Inflammatory cell responses were determined by upregulation of cell adhesion molecules or activation markers on HLMEC (**Figure 4.7, A-C**), and monocyte surface (**Figure 4.7, D-E**).

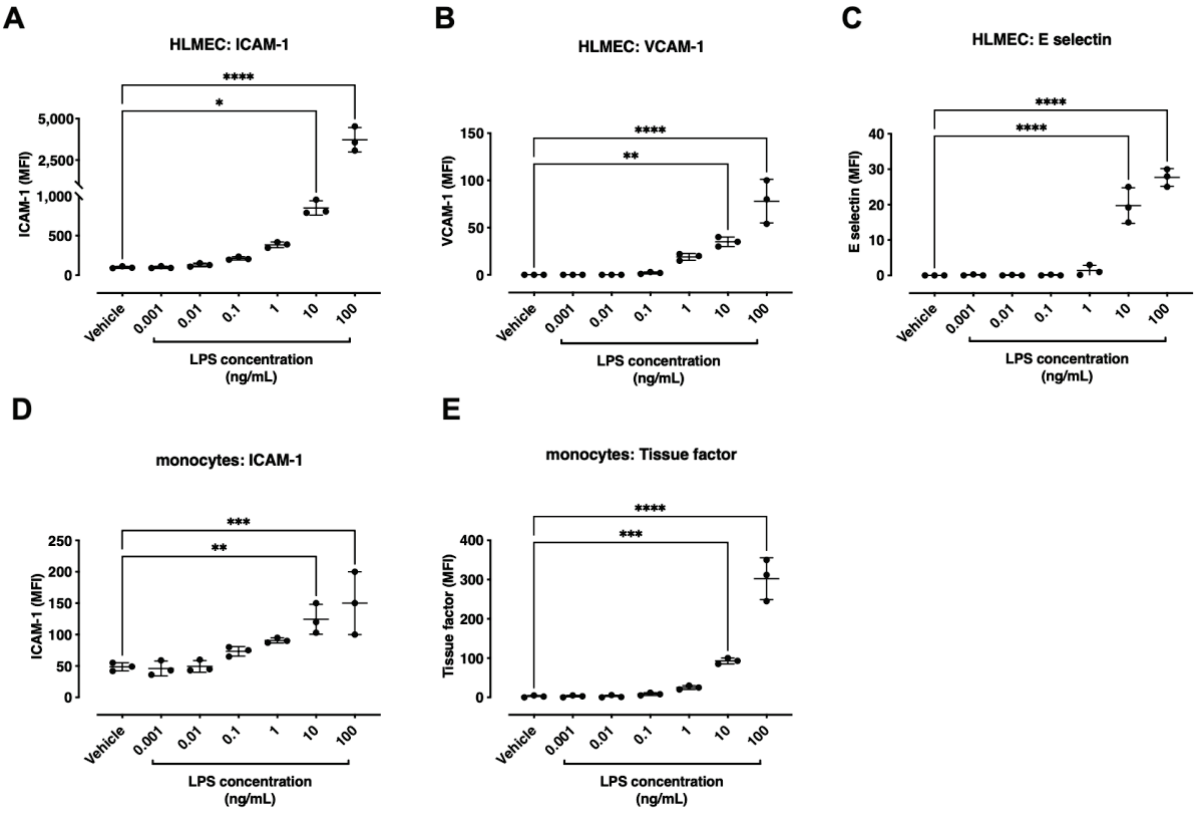

Figure 4.7. Titration of LPS in an *in vitro* co-culture model of pulmonary vascular inflammation. PBMCs and HLMECs were co-cultured for 2 h before treatment with serially diluted LPS (0.001-100 ng/mL, 4 h) in 10 % FBS-supplemented EBM. HLMEC and monocyte responses were analysed by flow cytometry. LPS concentrations ≥10 ng/mL significantly upregulated the expression of ICAM-1 (A), VCAM-1 (B), and E-selectin (C) on HLMECs and activation markers ICAM-1 (D) and tissue factor on monocytes (E). Data are analysed by one-way ANOVA with Bonferroni's multiple comparisons test compared to vehicle-treated cells (A-E; mean ± SD). n=3, *p<0.05, **p<0.01, ***p<0.001, ****p<0.0001.

For co-culture stimulation experiments, EV numbers were standardised to 6 x 10^6 EVs/well based on the maximum numbers of circulating neutrophil-EVs observed previously by our group in 1 mL of septic patient plasma (246). Addition of myeloid-EVs to co-cultures under plasma/serum-free conditions resulted in significant upregulation of the endothelial cell ICAM-1, VCAM-1, and E-selectin (**Figure 4.8, A-C**) and release of the pro-inflammatory cytokines TNF-α, IL-8, MCP-1, and IL-6 (**Figure 4.9, A-D**). Treatment with Miltenyi MicroBeads alone did not induce HLMEC activation or cytokine release. Platelet-EVs produced only a small increase in cell adhesion molecule expression compared to CD61 MicroBeads alone, which reached statistical significance only in the case of VCAM-1 expression. These findings

mirrored the observations in mice and suggested that myeloid-EVs might have a significant pro-inflammatory activity within the human pulmonary vasculature during sepsis.

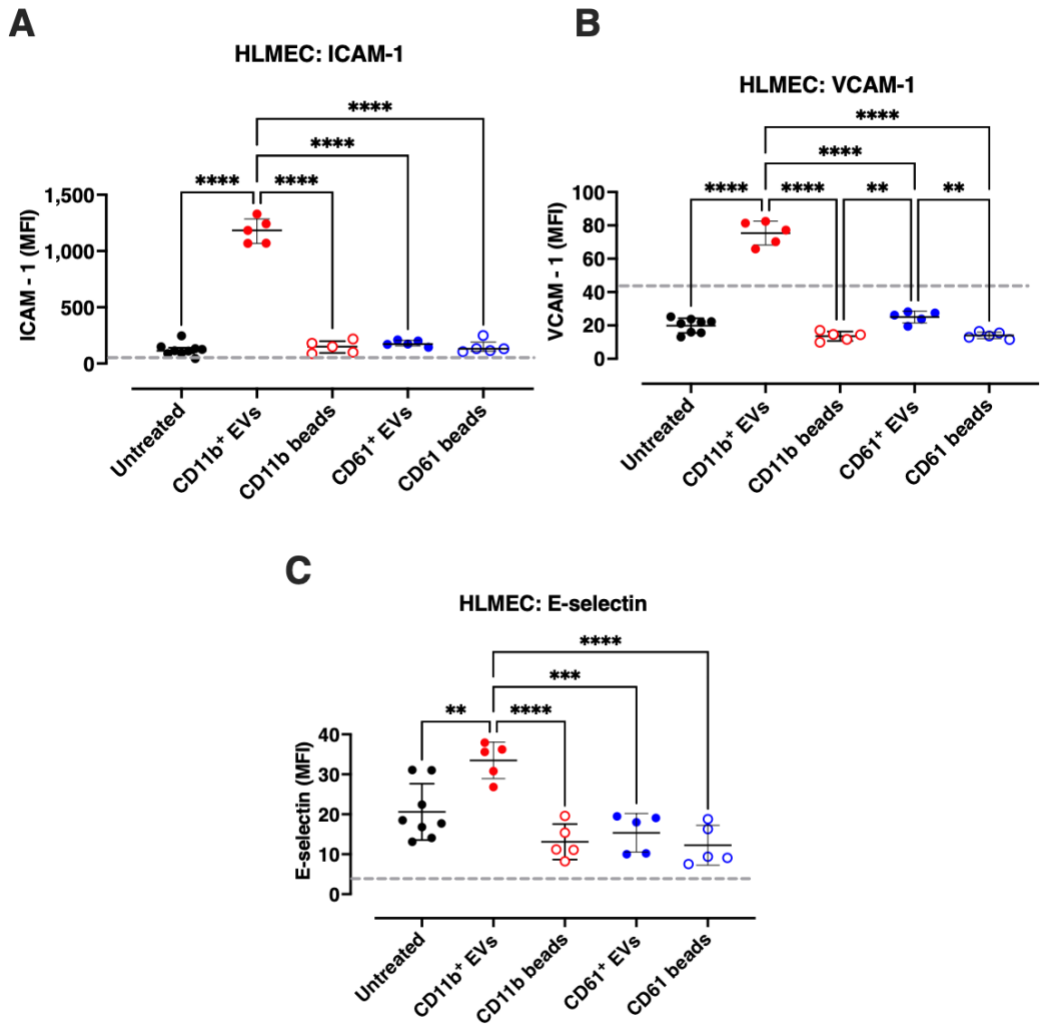

Figure 4.8. Myeloid-EV activation of HLMECs in co-culture with PBMCs.
PBMCs and HLMECs were co-cultured for 2 h before co-incubation with positively selected $CD11b^+$ myeloid- or $CD61^+$ platelet-EVs (6 x 10^6/well) for 4 h. Cell activation was measured by flow cytometry. Only treatment with myeloid-EVs induced significant upregulation in the expression of HLMEC adhesion molecules: ICAM-1 (**A**), VCAM-1 (**B**), and E-selectin (**C**). Dotted line indicates the expression level of adhesion molecules on untreated HLMECs in monoculture. Data are analysed by one-way ANOVA with Bonferroni's multiple comparisons test (A and B; mean ± SD); or Kruskal-Wallis with Dunn's multiple comparisons test (C; median ± interquartile range). n=5-8, **p<0.01, ***p<0.001, ****p<0.0001.

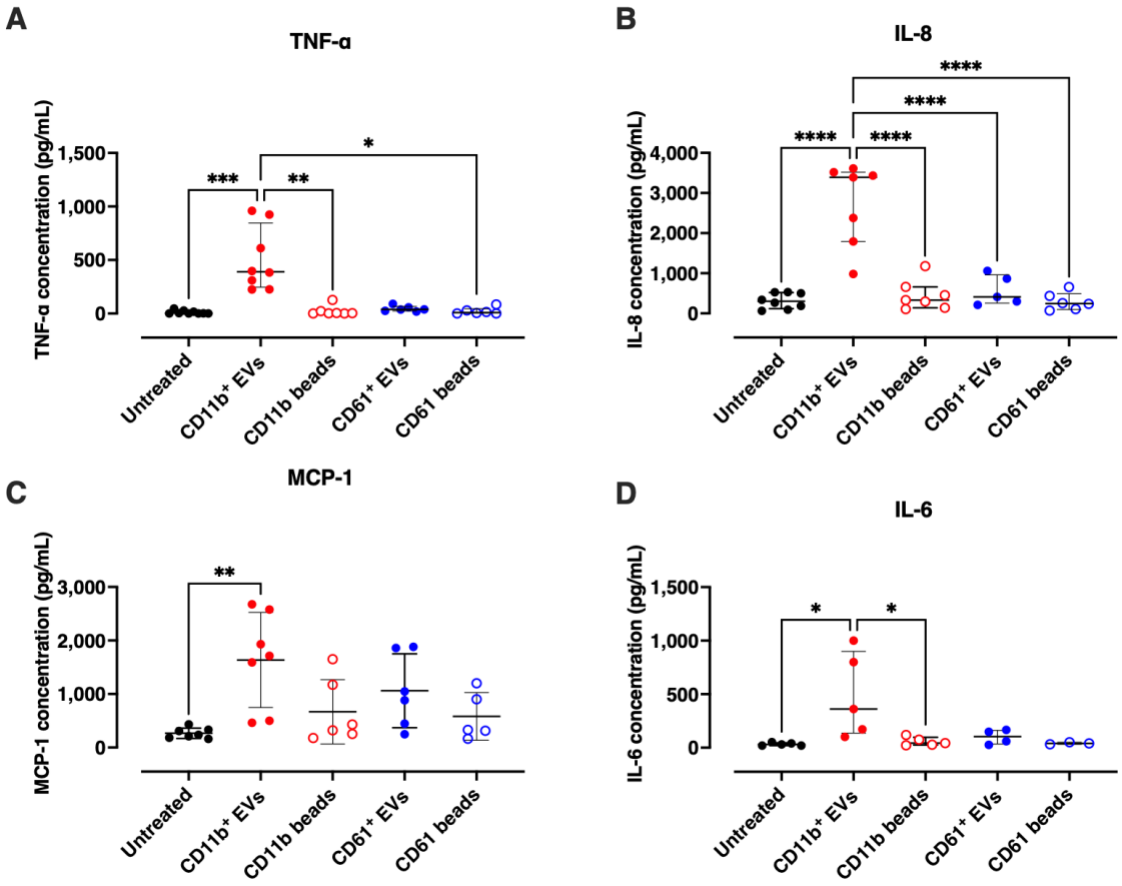

Figure 4.9. Myeloid-EVs induce pro-inflammatory cytokine release in the PBMC-HLMEC co-culture model.
PBMCs and HLMECs were co-cultured for 2 h before co-incubation with positively selected $CD11b^+$ myeloid- or $CD61^+$ platelet-EVs (6 x 10^6/well) for 4 h. Pro-inflammatory cytokine release was measured by ELISA. Only treatment with myeloid-EVs induced significant release of pro-inflammatory cytokines TNF-α (**A**), IL-8 (**B**), MCP-1 (**C**), and IL-6 (**D**). Data are analysed by Kruskal-Wallis with Dunn's multiple comparisons test (A, B, and D; median ± interquartile range); or one-way ANOVA with Bonferroni's multiple comparisons test (C; mean ± SD). n=5-8, **p<0.01, ***p<0.001, ****p<0.0001.

Having shown that myeloid-EVs are potent inducers of inflammatory cell activation and cytokine release in the co-culture model, I next investigated the PBMC dependency of these responses. Treatment of HLMECs with either myeloid- or platelet-EVs did not result in any upregulation in adhesion molecule surface expression or cytokine release in the absence of PBMCs. Untreated (control) alongside LPS-primed HLMECs were used to assess any potential synergistic effect of myeloid-EVs towards inflammatory endothelial cell activation, but no responses were observed, indicating that the myeloid-EV inflammatory activities in this

model were largely dependent on PBMCs (**Figure 4.10**). Again, these findings agree with our observations in mice, where intravascular monocyte depletion by clodronate liposome completely reversed the EV-induced lung injury (357).

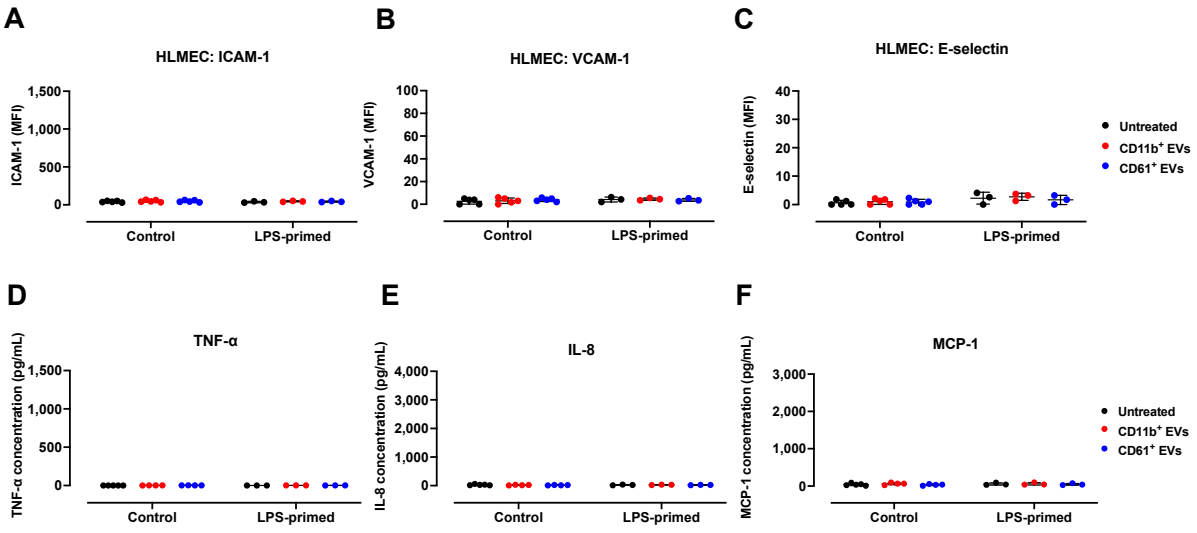

Figure 4.10. Myeloid-EVs do not induce inflammatory responses in HLMEC-only cultures. Positively selected CD11b$^+$ myeloid- or CD61$^+$ platelet-EVs (6 x 10^6/well) were incubated with untreated or LPS-primed (1 ng/mL, 2 h) HLMEC monocultures for 4 h. HLMEC activation and pro-inflammatory cytokine release were measured by flow cytometry and ELISA. Under both control or LPS-primed conditions no endothelial cell activation (**A-C**) or cytokine release (**D-G**) was observed. Data are analysed by two-way ANOVA with Sidak's multiple comparisons test (A-G; mean ± SD). n=3-4.

4.5. Discussion

Recent work in mouse models by our group demonstrated increased uptake of circulating EVs in the lungs by intravascular marginated monocytes during endotoxaemia and the potential for them to produce pulmonary vascular inflammation (281). In this investigation, I aimed to characterise human EV production in an *ex vivo* LPS-stimulated whole blood model of sepsis-induced inflammation and evaluate the pro-inflammatory activity of EVs in a human co-culture model of pulmonary vascular inflammation. I first investigated acute EV production in whole blood during LPS stimulation and demonstrated increases in platelet- and neutrophil-derived EVs but none of the other evaluated subtypes. On this basis, and findings in the mouse model (357), I developed an immunoaffinity-based positive selection method for $CD61^+$ platelet-EVs and $CD11b^+$ myeloid-EVs from plasma. The isolated myeloid- but not platelet-EVs elicited significant cell activation and pro-inflammatory cytokine release in a PBMC-HLMEC co-culture model of pulmonary vascular inflammation.

Incubation of healthy volunteer whole blood with LPS resulted in significant increases in platelet- and neutrophil-EVs, but no detectable changes in the monocyte-, erythrocyte- or $CD45^+$, $CD11b^-$ EV populations. This limited response differs from some observations of increases of multiple EV subtypes in septic patients (288, 294), but is more in line with the findings of Nieuwland et al., in meningococcal sepsis patients where statistically significant increases were limited to platelet and neutrophil-EVs (286). Studies describing EV production in whole blood *ex vivo* appear to be rare. Aras et al., investigated EV production in LPS whole blood as part of a study on EV-mediated coagulation which included LPS-challenged healthy volunteers (302). They found comparable results with non-platelet-EV tissue factor expression in volunteers and whole blood, and in contrast to our results, observed elevation of monocyte-EVs. This discrepancy may be explained by the much longer, 24 hour, LPS (10 ng/mL) stimulation period required to generate consistent increases between different individuals, compared to our incubation that did not exceed 4 hours. In our case, a larger sample size may

be necessary to conclude this investigation. More recently, Cointe et al., produced granulocyte-EVs in whole blood stimulated with LPS (1 µg/mL) for 12 hours, although details on EV levels were not presented (424). Similar to whole blood, details on EV subtype levels in healthy volunteers and animal models of LPS-induced endotoxaemia are also very limited, with most of these focusing on EV functions in coagulation, either via platelet-, monocyte-, or total-EVs (299, 301, 302, 418-421, 425, 426). In conclusion, LPS-stimulation of whole blood may be a suitable model for generation of platelet- and neutrophil-EVs under *in vitro* conditions and although key features of *in vivo* environment are not included (e.g., a source of endothelial-EVs) the response has some resemblance to the patterns of EV increases in sepsis patients.

Generation of EVs from isolated cell populations is a convenient method for studying EV subtype functions but may not be able to reproduce the *in vivo* conditions that affect EV functions. In isolated primary cells and cell lines, LPS has been used mainly to produce EVs from monocytes (302, 427-430). In our group, we found that LPS does not generate significant release of EVs from isolated neutrophils (**Chapter 3**, **Figure 3.4**), although it does appear to promote EV production following neutrophil adherence (386). An additional disadvantage of using isolated primary cells is the potential effects of the isolation procedure and removal from the blood environment, especially in the case of easily activated populations like platelets and neutrophils. Therefore, based on the significant increases in platelet- and neutrophil-EVs in LPS-stimulated whole blood, we considered immunoaffinity separation of these subtypes worthwhile for functional studies despite the technical challenges and additional costs.

Although binding of EVs to beads, particularly smaller exosomes, is routinely used to facilitate phenotypic and biochemical analysis (431-434), its use for functional studies is much more limited. Agouni et al., used CD61 positive selection or depletion to assess the involvement of platelet-EVs in endothelial dysfunction *in vitro* (435), and very recently granulocyte-EVs were isolated with CD15 beads from LPS-stimulated whole blood (424). We used Miltenyi MicroBeads based on their availability and small size, reported by the manufacturer as ~50

nm diameter (https://www.miltenyibiotec.com/GB-en/resources/macs-handbook/macs-technologies/cell-separation/magnetic-cell-separation.html#gref). For comparison to our mouse model work, anti-CD11b beads were used for neutrophil- and monocyte-EVs termed here as 'myeloid-EVs', despite low numbers of the latter were generated in LPS-stimulated human blood. Following guidelines from the manufacturer for cell separation, with certain adaptations such as the omission of the cell washing step prior to the EV-bead incubation, the method was straightforward, reproducibly generating high yield and purity of both EV populations. One notable advantage of the EV separation on affinity columns was the ease and efficiency of performing multiple washes (x3) as compared to an equivalent centrifugation protocol.

Surface expression of classic, parent cell specific, markers enabled us to isolate specific EV subpopulations for functional studies related to pulmonary vascular inflammation. Exploiting this property, I demonstrated that $CD11b^+$ myeloid- but not $CD61^+$ platelet-EVs induce potent pro-inflammatory responses in the PBMC-HLMEC co-culture model. Inflammatory effects of beads were ruled out when they were added directly to co-cultures without EVs. More importantly, the lack of activity in platelet-EV preparations indicated that carry over of inflammatory mediators such as LPS or cytokines from whole blood was negligible. Our findings mirror those of Mesri et al., where the leukocyte- but not platelet-EVs were implicated as the active component of fMLP-stimulated whole blood supernatants, responsible for the release of IL-6 and MCP-1 from HUVECs directly (326). However, further evaluation of the responses in our model demonstrated that they were absolutely PBMC-dependent, as no cytokine production or HLMEC activation was observed in HLMEC only cultures. Although there are some overlaps in the models used by us and by Mesri et al., there are also several key material and protocol differences that limit the conclusions that can be drawn.

The lack of activity in platelet-EVs may be considered surprising as apart from their potent pro-coagulant activity (286, 298), they have also been shown to possess pro-inflammatory, pro-adhesion, and aggregating properties (436-441). Barry et al., reported that thrombin-

generated platelet-EVs induced prostacyclin production and cyclooxygenase-2 expression, as well as increased monocyte adhesion and ICAM-1 upregulation in HUVECs, all of which were mediated by platelet-EV associated arachidonic acid (440, 441). In separate studies, LPS-induced platelet-EVs transferred IL-1β in HUVECs eliciting inflammatory activation and neutrophil adhesion, although such responses were not replicated in our co-culture or monoculture model (438, 439). In all of these studies, platelet-EVs were produced following stimulation of isolated platelets as opposed to our whole blood method, which might explain the functional heterogeneity observed. Measurement of IL-1β or arachidonic acid content of the platelet-EVs produced in this study might be necessary for future assays to better explain these differences. Moreover, as contradicting findings with anti-inflammatory effects of thrombin-generated (from isolated platelets) or sepsis patient-derived platelet-EVs have also been reported (442, 443), further exploration of their functional properties in physiologically relevant models or patient samples, presents an interesting area for future studies.

These preliminary findings demonstrated a specific and potent activity of human myeloid-EVs matching the results from the mouse *in vivo* EV subtype to *ex vivo* isolated perfused lung model of injury/inflammation. On this basis, we decided to pursue this strategy further, hypothesising that neutrophil-EVs represent the active pro-inflammatory EVs in LPS-stimulated whole blood.

5. Neutrophil-EV activity in an *in vitro* model of pulmonary vascular inflammation

5.1. Background

Despite the well-documented increases in levels of neutrophil-EVs in several inflammatory disease states, their role in modulating vascular inflammation is less clear with diverse and occasionally contradicting findings of pro- and anti-inflammatory properties. The common characteristic of studies describing the anti-inflammatory effects of neutrophil-EVs is the type of target cells used in *in vitro* functional assays, primarily leukocytes. Thus, treatment of macrophages, monocyte-derived dendritic cells, or natural killer cells with neutrophil-EVs triggered increased secretion of anti-inflammatory cytokines TGF-β and IL-10 by interfering with the NF-κB signalling (242, 382, 383, 444). In line with their anti-inflammatory functions, these and similar studies demonstrated reductions in the release of pro-inflammatory cytokines such as IL-1β, IL-6, IL-8, IL-12, and TNF-α following neutrophil-EV treatment (242, 329, 444, 445).

On the other hand, pro-inflammatory properties of neutrophil-EVs have also been reported, in specific target cell populations, including increased production of IL-6 and IL-8 by endothelial cells (325, 326), synthesis of LTB_4 by neutrophils (446), enhanced superoxide, IL-6 or TNF-α release from primary monocytes (293, 445), and increased CD80, CD86, and HLA-DR expression on THP-1 cells (monocyte-like cancer cell line) (324). More recently it was shown that fMLP-derived neutrophil-EVs activated the NF-κB pathway inducing pro-inflammatory gene transcription (NF-κB) and endothelial cell activation by delivering miR-155 to endothelial cells and monocytes during atherosclerosis (352). By using anti-neutrophilic cytoplasmic antibodies from vasculitis patients for neutrophil-EV release, Hong and colleagues not only found these EVs as capable of increasing ICAM-1 expression on endothelial cells, ROS production, and IL-6 and IL-8 release, but neutrophil-EV treatment of HUVECs resulted in elevated levels of thrombin secretion, supporting an indirect role in the coagulation cascade (319). Moreover, apart from cytokine secretion or cell activation, neutrophil-EVs have also been linked with prothrombotic processes and coagulation. Wang and colleagues reported

that neutrophil-EVs form complexes with neutrophil extracellular traps (NETs) following phorbol 12 myristate 13-acetate (PMA) treatment, which then increased thrombin formation via the intrinsic coagulation pathway in mice (447). Lastly, neutrophil-EVs have been found capable of promoting bacterial aggregation and killing (297, 327, 328).

A potentially significant limitation of these studies for understanding the biology and pathogenic roles of circulating neutrophil-EVs is that they are generated from isolated neutrophils *in vitro* or in an extravascular compartment *in vivo*. To understand the role of neutrophil-EVs in sepsis and ALI it may be necessary to study populations generated *in vivo* in blood or in *in vitro* models that better recreate the vascular environment. In **Chapter 4** I showed that positive immunomagnetic bead selection of myeloid- and platelet-EVs, produced in a physiological whole blood LPS model, allowed the meaningful and direct comparison of different EV subtypes released under identical conditions. Myeloid- but not platelet-EVs were found to be pro-inflammatory, activating cells and inducing cytokine release in a PBMC-HLMEC co-culture model of pulmonary vascular inflammation. Based on existing literature on the pro-inflammatory activities of neutrophil-EVs described above (293, 319, 324-326, 352), the lack of monocyte-derived EVs in the LPS-stimulated whole blood model, and preliminary findings within the team (448), we hypothesised that neutrophil-EVs generated in the LPS stimulated whole blood model were responsible for the observed *in vitro* and *ex vivo* responses. To test this hypothesis, I developed a methodology for the isolation of neutrophil-EVs from plasma and characterised their activity in the cell culture model of pulmonary vascular inflammation.

5.2. Aims

To evaluate the pro-inflammatory activity of human neutrophil-EVs produced in the LPS-stimulated whole blood model of systemic inflammation and their potential roles in indirect ALI, I aimed to:

1. Develop methods for isolation of neutrophil-EVs from plasma by immunomagnetic bead selection.
2. Evaluate the pro-inflammatory effects of neutrophil-EVs in the PBMC-HLMEC model.
3. Determine the role of monocytes in the neutrophil-EV-induced responses.
4. Identify the mechanisms of HLMEC activation by neutrophil-EVs.
5. Assess the neutrophil-EV activities under flow conditions in the adherent monocyte-HLMEC co-culture model (**Chapter 3**).

5.3. Protocols

5.3.1. Positive and negative selection of neutrophil-EVs

EVs were generated by LPS stimulation of heparinised whole blood (100 ng/mL, 3 h, 37 °C) and enriched by differential centrifugation as described in **Chapter 4**. Neutrophil-EVs were then isolated by immunoaffinity positive or negative selection.

For positive selection, the isolation kit StraightFrom® Whole Blood CD66b MicroBeads (Miltenyi Biotec) was adapted for the isolation of EVs. Ratios of 1 µL CD66b bead suspension per 1 x 10^6 neutrophil-EVs ($CD66b^+CD11b^+$) to EV sorting buffer of 1:100 (e.g., 10 µL microbeads for 1 x 10^7 $CD66b^+CD11b^+$ EVs in a final volume of 1 mL) were used. Samples were mixed with EVs and incubated for 15 min at 4 °C with mixing every 5 min and then passed through magnetised MS or LS columns (Miltenyi Biotec). Columns were washed three times and bead-bound EVs were eluted by removal from the magnetic field, washed twice by centrifugation and resuspended in EBM-HAS for subsequent use in functional assays.

To obtain 'untouched' neutrophil-EVs ($CD11b^+CD66b^+$) by negative selection the MACSxpress® Whole Blood Neutrophil Isolation Kit (Miltenyi Biotec) was adapted for EV isolation by an undergraduate student (Miss Claudia Peinador-Marin) as part of her Batchelor's thesis. In this method, all other cell types within the blood, except for neutrophils, were tagged with the antibody-conjugated MicroBeads. Instead of the manufacturer's recommended bead suspension volume ratio to blood volume, we estimated the amount of beads required based on the number of platelets normally present in 1 mL volume of human blood (1.5 x 10^8 - 4 x 10^8 platelets/mL) (449) and extrapolated the average of this number (2.75 x 10^8 platelets/mL) to an equivalent amount of platelet-EVs. Based on further evaluation of neutrophil-EV yield and platelet-EV contamination, a ratio of bead suspension to platelet-EVs of 1:4 (e.g., 250 µL beads to 2.75 x 10^8 platelet-EVs) was determined as the most appropriate. Beads and EVs were incubated in EV sorting buffer for 5 min at room temperature

in a rotating wheel to allow continuous mixing. EVs were then applied to a magnetised MS column and the flow through was collected, washed twice by centrifugation, and resuspended in EBM-HAS.

Neutrophils-EVs (positively or negatively selected) were kept overnight in ice before use in functional assays. The number of platelet- and neutrophil-EVs was determined in the isolated samples by flow cytometry for assessment of the isolation method efficacy.

5.3.2. Neutrophil-EV functional assays

The pro-inflammatory activities of isolated neutrophil-EVs were determined in the co-culture model of PBMCs and HLMECs under plasma/serum-free conditions as previously described (**Chapter 4**, **Section 4.4.3**). After initial titration assays, neutrophil-EVs' concentration was standardised to 2 x 10^7 neutrophil-EVs per well in 48-well plates in a final volume of 500 µL. Untreated and LPS-treated (10 ng/mL with 10 % FBS-containing media) wells were included in all assays as negative and positive controls, respectively. In some co-culture experiments, pure monocytes were isolated from PBMCs using the Pan Monocyte Isolation Kit (Miltenyi Biotec) as per the manufacturer's instructions. For assessing the role of secreted soluble TNF-α in co-culture responses, a neutralising anti-TNF-α antibody (clone: MAb1, Biolegend) or isotype control (clone: MOPC-21, Biolegend) was added at 10 µg/mL to co-cultures 30 min before the addition of neutrophil-EVs. Following experimental procedures, cell activation and cytokine release were assessed by flow cytometry and ELISA, respectively.

5.3.3. Neutrophil-EV activities under flow conditions

The ibidi® PFC system (see **Chapter 3**) was used to assess the effect of flow on EV activity in co-cultures, using the 0.4 mm µ-Slide I Luer slides (ibidi®) and the 1.6 mm perfusion set (ibidi®).

HLMECs (1.2 x 10^5) were seeded in channel slides, left to adhere overnight in static conditions, and adapted to flow for 24 h. HLMECs were then treated with TNF-α (100 ng/mL), for 2 h under static conditions, flushed out with media, and PBMCs (2.4 x 10^5) were added for a further 2 h under static conditions to allow cell adherence. Flow was then applied producing shear stress of 5 dyn/cm^2 for 1 h. Media was replaced and neutrophil-EVs were added to the circuit at 4 x 10^7 neutrophil-EVs/mL and re-circulated for 2 or 4 h under the same flow conditions. Cell activation was assessed by flow cytometry for expression of surface activation markers on HLMECs and monocytes and release of pro-inflammatory cytokines in the perfusate via ELISA.

5.3.4. Electron Microscopy

CD66b MicroBead-isolated neutrophil-EVs were imaged by transmission electron microscopy (TEM). For detailed methods, see **Chapter 2**.

5.4. Results

5.4.1. Neutrophil-EV isolation via immunoaffinity-based assays

Prior to CD66b bead selection, neutrophil-EV numbers were determined by staining for expression of CD66b, CD11b, and CD15. After incubation with CD66b MicroBeads and elution from columns, CD11b and CD15 were used to monitor yields and purity. The majority of bead-bound $CD11b^+$, $CD15^+$ neutrophil-EVs were eluted from the column with minimal amounts in the unbound flow-through fraction (**Figure 5.1**). Compared to neutrophil-EV numbers in mixed EVs from centrifuged platelet poor plasma, this isolation method yielded an 89±6 % neutrophil-EV recovery, with 99±1 % platelet-EV depletion (**Figure 5.2**).

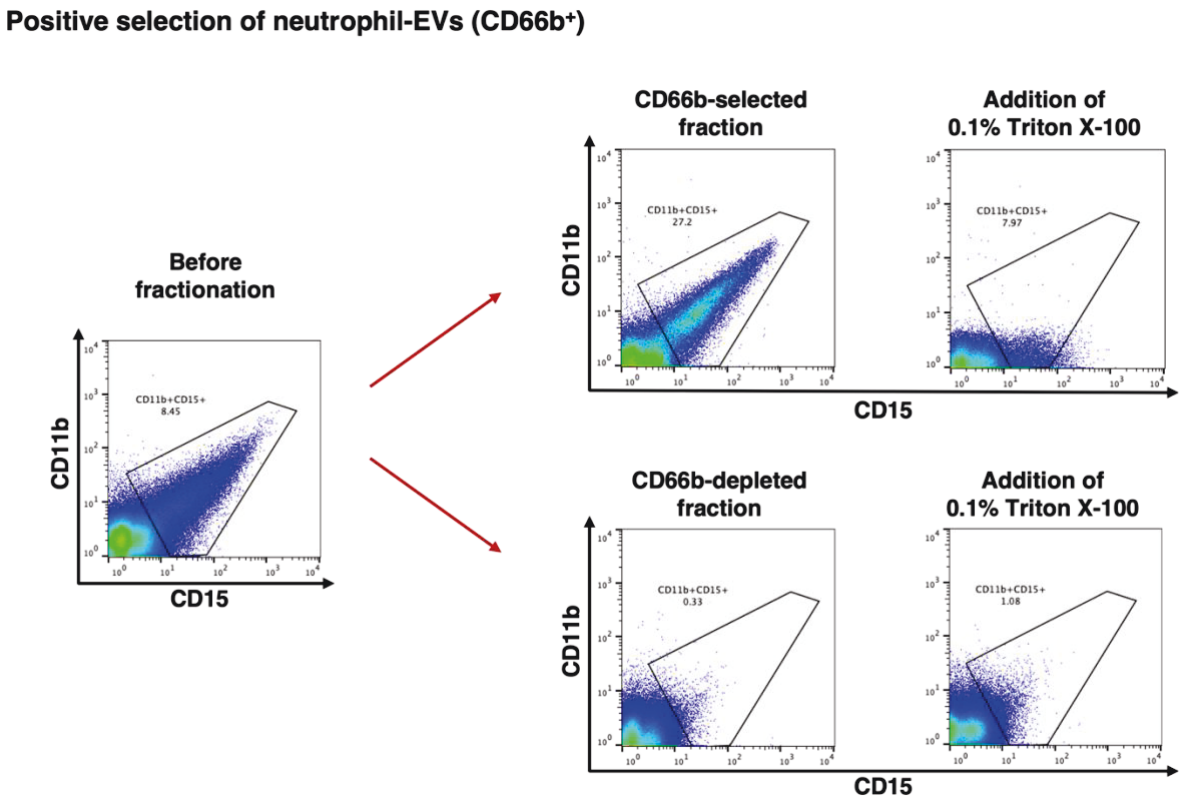

Figure 5.1. Isolation of neutrophil-EVs using CD66b immunomagnetic MicroBead separation. Mixed EVs were obtained from LPS-stimulated whole blood and incubated with CD66b MicroBeads (15 min, 4 °C). Following loading onto magnetised columns, the total flow through (CD66b-depleted fraction) was collected and bound material eluted by removal from the magnetic field (CD66b-selected fraction). Representative flow cytometry plots of n=6 repeats.

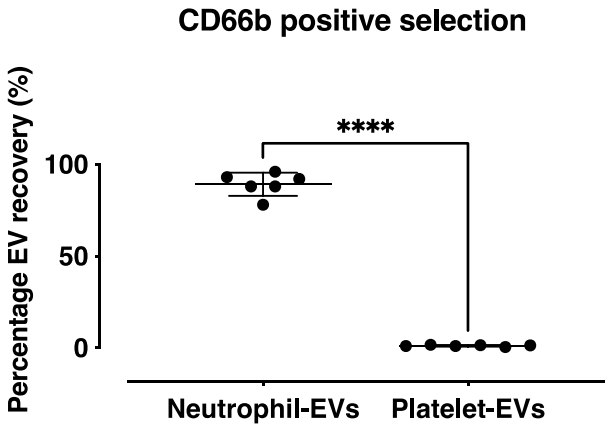

Figure 5.2. Neutrophil-EV recovery with CD66b immunomagnetic bead positive selection. Neutrophil-EVs were separated from a mixed EV population by CD66b immunomagnetic bead positive selection. This isolation method yielded sufficient numbers of neutrophil-EVs with complete depletion of platelet-EVs (~99 %), the major non-neutrophil-derived EV population present in the unfractionated sample. Data are analysed by two-tailed unpaired t-test (mean ± SD). n=6, ****p<0.0001.

5.4.2. Assessment of EV morphology after CD66b immunomagnetic bead selection

To determine the morphological effects of CD66b MicroBead binding to neutrophil-EVs the samples were run on a flow cytometer equipped with a violet 405 nm laser (Cytek® Northern Lights™) for higher resolution and sensitivity (263). ApogeeMix beads (Apogee Flow Systems) were used as an SSc size reference (**Figure 5.3**).

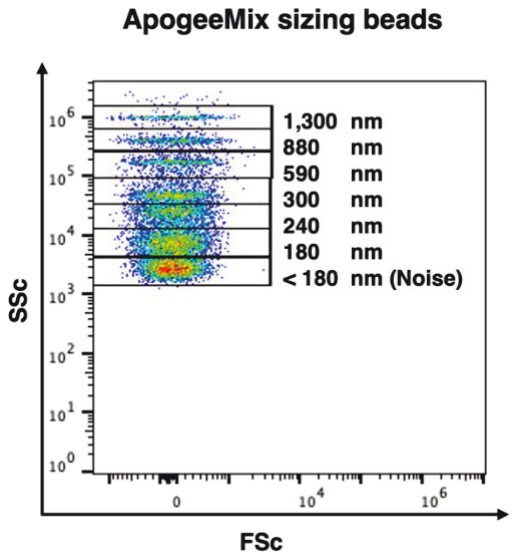

Figure 5.3. Flow cytometric pseudocolour density plot showing the ApogeeMix sizing bead gating.
The ApogeeMix sizing beads consist of a mixture of non-fluorescent silica beads of different sizes ranging from 1,300 to 180 nm. These beads can be detected by flow cytometry and offer a tool to separate particles of different sizes based on the forward and side scatter.

Neutrophil-EVs pre- and post-CD66b MicroBead sorting were stained for CD11b and CD15 expression, acquired and then back-gated to forward versus side scatter plots (**Figure 5.4**). CD66b MicroBead selected neutrophil-EVs showed a uniform increase in size distribution, although somewhat less than what was expected based on Miltenyi's reported MicroBead size of 50 nm.

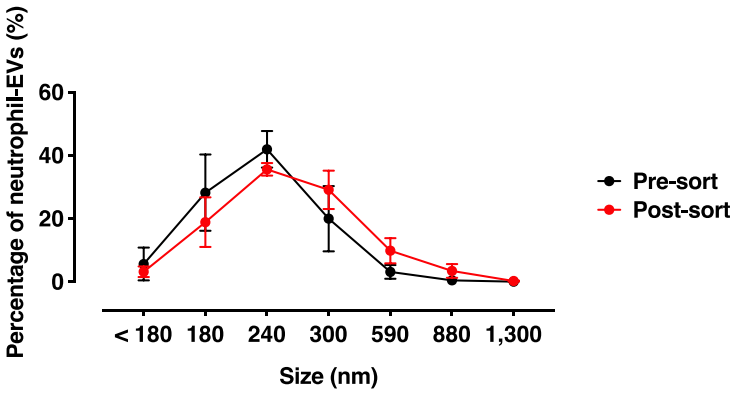

Figure 5.4. Size distribution of neutrophil-EVs before and after CD66b immunomagnetic bead isolation.

Neutrophil-EVs pre- and post-isolation were gated as $CD11b^+$, $CD15^+$ events (data not shown). ApogeeMix sizing beads were used to form sizing regions within the range of 1,300-180 nm and the EV numbers within each region were calculated as a percentage of the total. Before their incubation with CD66b MicroBeads, 4 %, 20 %, 42 %, and 28 % of neutrophil-EVs were within the 590, 300, 240, and 180 nm gates, respectively, while after the isolation, 10 %, 29 % 36 %, and 19 % were within the 590, 300, 240, and 180 nm gates, respectively. The remaining < 10 % of neutrophil-EVs were less than 180 nm in both pre- and post-sort samples. Data are analysed by two-way ANOVA with Sidak's multiple comparisons test (mean ± SD). n=3.

CD66b MicroBead isolated neutrophil-EVs were imaged by TEM. Neutrophil-EVs shown in **Figure 5.5,** were spherical and less than 0.2 µm. Interestingly, beads appear to be attached in clusters with large areas of the EV surfaces free of beads. Although beads might become detached despite the stringent fixation, it is also possible that all beads remain bound and the uneven distribution matches that of membrane CD66b, which is a lipid raft-embedded protein that has been shown to cluster when crosslinked by antibodies (389).

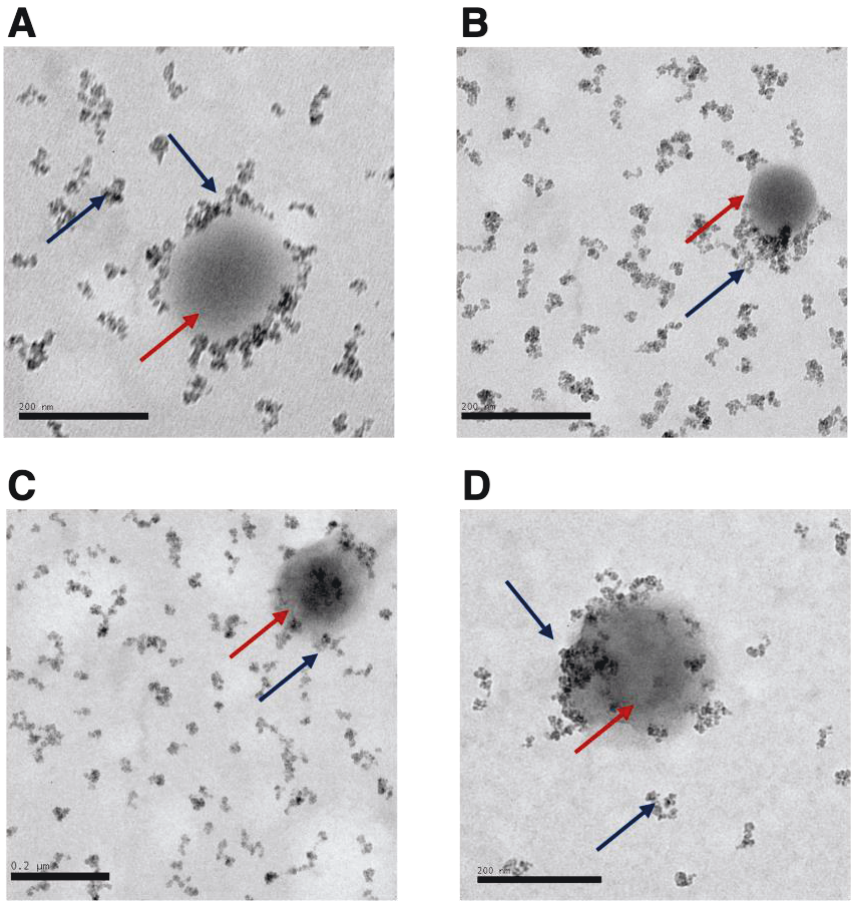

Figure 5.5. Transmission electron microscopy imaging of CD66b MicroBead-selected neutrophil-EVs.
Isolated neutrophil-EVs were fixed in 2.5 % glutaraldehyde for 1 h on ice and then prepared for TEM imaging. Representative images of neutrophil-EVs post CD66b positive selection (**A-D**). Red arrows depict the neutrophil-EVs and blue arrows indicate the CD66b microbeads (scale bar= 200 nm).

5.4.3. Neutrophil-EVs induce cell activation and pro-inflammatory cytokine release in PBMC-HLMEC co-culture

The pro-inflammatory activities of neutrophil-EVs were assessed in the co-culture model of PBMCs and HLMECs, established in **Chapter 4**. To evaluate neutrophil-EV activity, I first performed a titration experiment, using a concentration range based around 6 x 10^6 EVs/well that was used for myeloid- and platelet-EVs in **Chapter 4**. Neutrophil-EVs produced a concentration-dependent activation of HLMECs (ICAM-1 expression) and monocytes (tissue factor expression) and release the pro-inflammatory cytokines TNF-α and IL-8 (**Figure 5.6**).

Although responses did not reach a plateau at the highest concentration of 2 x 10^7 EVs/well, because of the requirement for healthy volunteer donor blood, I decided to use this concentration in all subsequent assays.

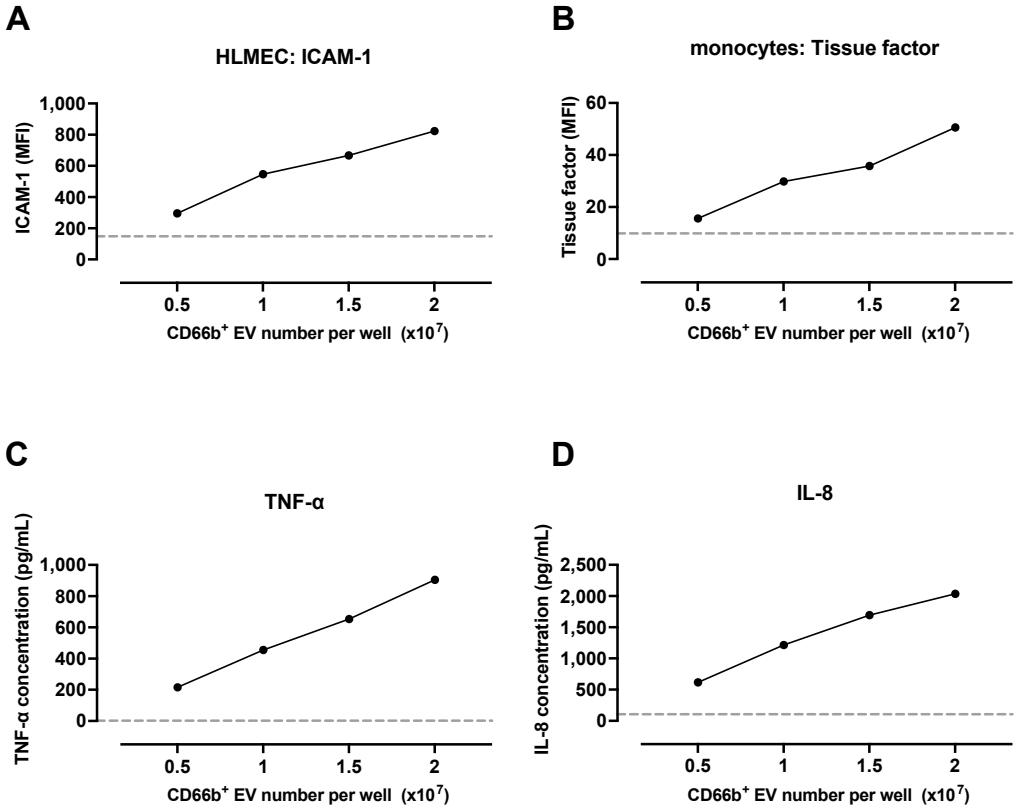

Figure 5.6. Titration of neutrophil-EVs in PBMC-HLMEC co-culture.
CD66b MicroBead-isolated neutrophil-EVs were added to co-cultures at 0.5, 1, 1.5, and 2 x 10^7 per well (in 500 µL) and incubated for 4 h. Cell activation was determined by flow cytometric analysis of ICAM-1 on HLMECs (**A**) and tissue factor expression on monocytes (**B**) and shown as MFI. TNF-α (**C**) and IL-8 (**D**) release into supernatants was measured via ELISA. The dotted line represents the levels in untreated cells. Pilot study (n=1).

Neutrophil-EVs induced significant upregulation of adhesion molecules ICAM-1, VCAM-1, and E-selectin on HLMEC surface (**Figure 5.7, A-C**). Similarly, monocyte activation markers ICAM-1, tissue factor, and CD86 were all increased by neutrophil-EV treatment (**Figure 5.7, D-F**), as was the release of pro-inflammatory cytokines TNF-α, IL-8, MCP-1, IL-6, and IL-1β

(**Figure 5.8**). In contrast, treatment with CD66b MicroBeads alone had no effect on these responses.

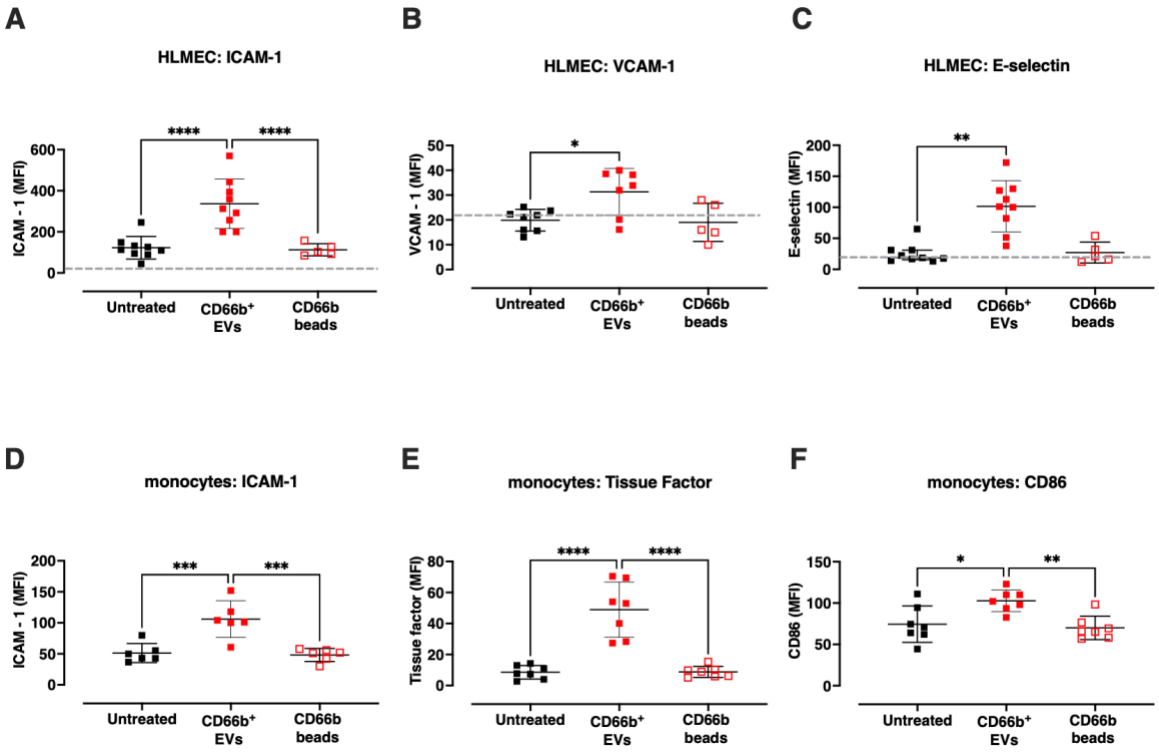

Figure 5.7. Neutrophil-EVs induce pro-inflammatory responses in PBMC-HLMEC co-cultures. Neutrophil-EVs (2 x 10^7/well) were added to PBMC-HLMEC co-cultures and incubated for 4 h. Neutrophil-EV treatment induced significant upregulation of HLMEC surface adhesion molecules ICAM-1 (**A**), VCAM-1 (**B**), E-selectin (**C**) (dotted line indicates the cell adhesion molecule expression in untreated HLMEC-only cultures) and monocyte activation markers ICAM-1 (**D**), tissue factor (**E**), and CD86 (**F**). Treatment with CD66b MicroBeads alone had no effect on these responses. Data are analysed by one-way ANOVA with Bonferroni's multiple comparisons test (A, B and D-F; mean ± SD); or Kruskal-Wallis with Dunn's multiple comparisons test (C; median ± interquartile range). n=5-9, *p<0.05, **p<0.01, ***p<0.001, ****p<0.0001.

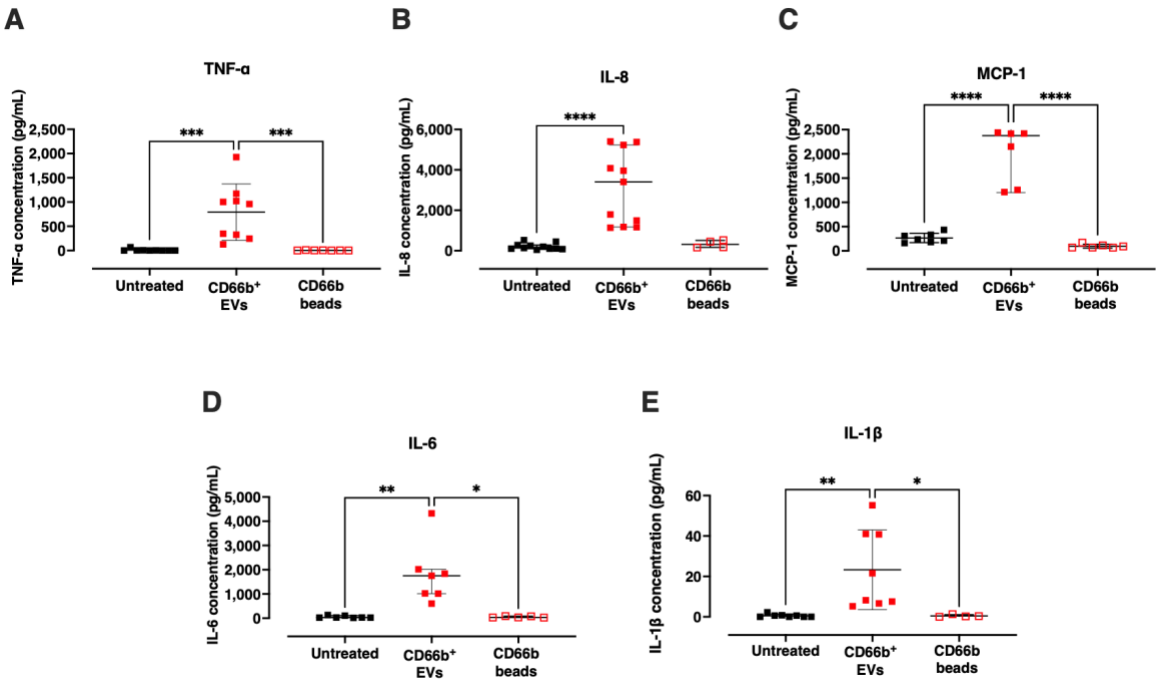

Figure 5.8. Neutrophil-EVs induce pro-inflammatory cytokine release in PBMC-HLMEC co-cultures.

Neutrophil-EVs (2 x 10^7/well) were added to PBMC-HLMEC co-cultures and incubated for 4 h. Cell- and EV-free supernatants were assessed by ELISA for cytokine release. Neutrophil-EV treatment induced significant secretion of the pro-inflammatory cytokines TNF-α (**A**), IL-8 (**B**), MCP-1 (**B**), IL-6 (**D**), and IL-1β (**E**), while MicroBeads alone had no effect on these responses. Data are analysed by one-way ANOVA with Bonferroni's multiple comparisons test (A, C and E; mean ± SD); or Kruskal-Wallis with Dunn's multiple comparisons test (B and D; median ± interquartile range). n=4-9, *p<0.05, **p<0.01, ***p<0.001, ****p<0.0001.

To determine whether neutrophil-EV mediated responses were dependent on bound CD66b MicroBeads, neutrophil-EV isolation by negative immunomagnetic bead selection was investigated. This work was carried out in collaboration with an undergraduate student (Miss Claudia Peinador-Marin) as part of her Batchelor's thesis project. For this negative immunomagnetic EV isolation, we adapted the MACSxpress® Whole Blood Neutrophil Isolation Kit (Miltenyi Biotec) for EV isolation. Neutrophil-EVs were detected within the flow-through sample, with low levels of platelet-EVs present in this fraction (**Figure 5.9**). By using the same markers as the CD66b MicroBead positive selection (CD11b, CD15, CD66b) for neutrophil-EV quantification, with this methodology, a 60±2 % neutrophil-EV recovery with

negligible platelet-EV contamination (99±1 % platelet-EV depletion) was observed (**Figure 5.10**).

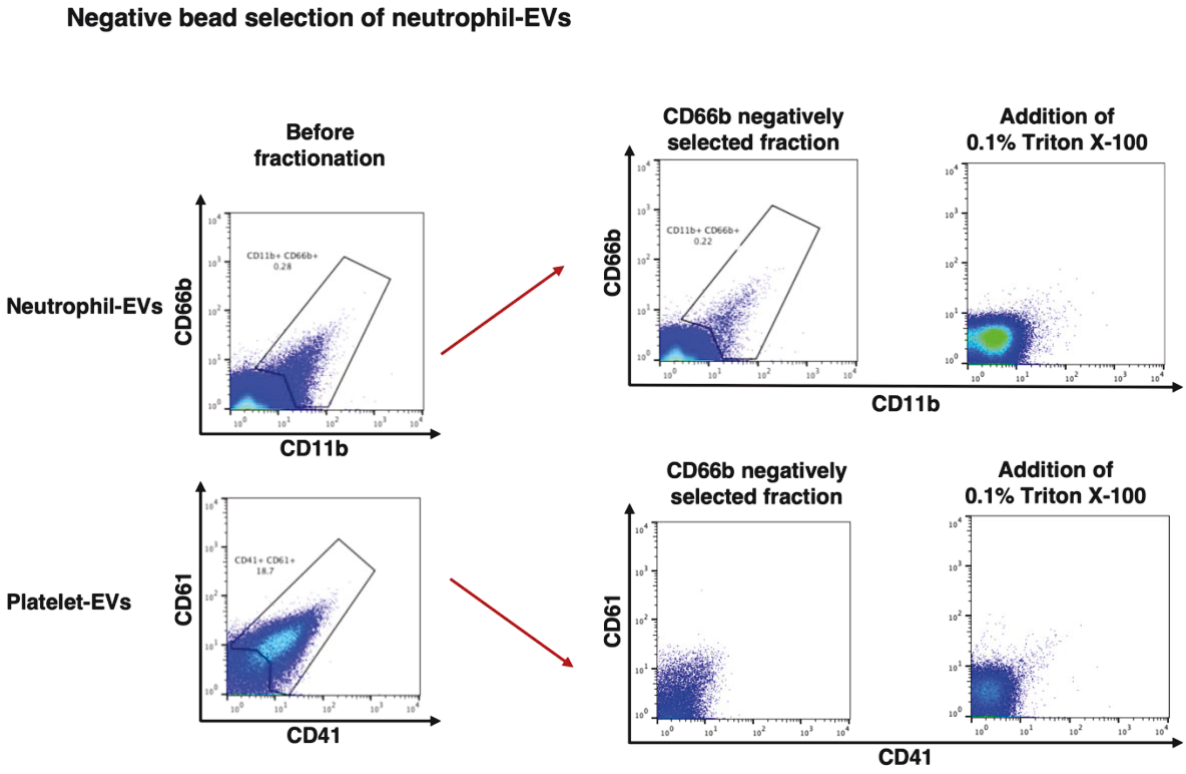

Figure 5.9. Isolation of neutrophil-EVs by negative immunomagnetic bead selection.
Mixed EVs were obtained from LPS-stimulated whole blood, incubated with MACSxpress® beads (5 min, room temperature), and loaded directly onto a magnetised column. Unbound neutrophil-EVs were collected in the flow-through, while small numbers of platelet-EVs ($CD61^{+}CD41^{+}$) were observed in this fraction. Representative flow cytometry plots of n=6 repeats.

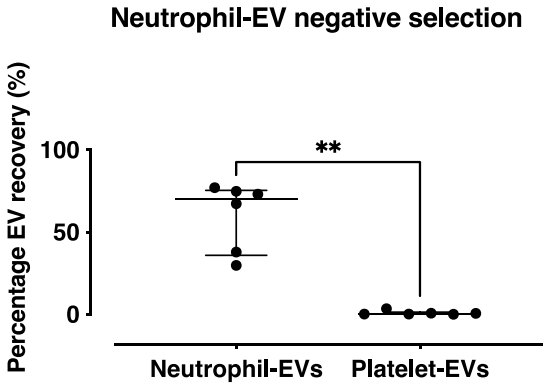

Figure 5.10. Neutrophil-EV recovery with negative immunomagnetic bead selection.
Neutrophil-EVs were separated from a mixed EV population by negative immunomagnetic bead selection. This isolation method yielded sufficient numbers of neutrophil-EVs with depletion of platelet-EVs (~99 %), the major non-neutrophil-derived EV population present in the unfractionated sample. Data are analysed by Mann Whitney test (median ± interquartile range). n=6, **p<0.01.

Incubation of the 'untouched' neutrophil-EV preparations in PBMC-HLMEC co-cultures induced similar responses to CD66b MicroBead-isolated neutrophil-EVs: upregulation of ICAM-1, VCAM-1, and E-selectin expression on HLMECs (**Figure 5.11, A-C**); upregulation of ICAM-1 and tissue factor on monocytes (**Figure 5.11, D-E**); and increased production of pro-inflammatory cytokines (**Figure 5.12**). By contrast, the platelet-EV-enriched/neutrophil-EV-depleted column-retentate was relatively inactive producing a statistically significant response only in the case of ICAM-1 upregulation. These data confirmed that the EV pro-inflammatory activity was largely present in the untouched neutrophil-EV fraction and therefore not dependent on beads.

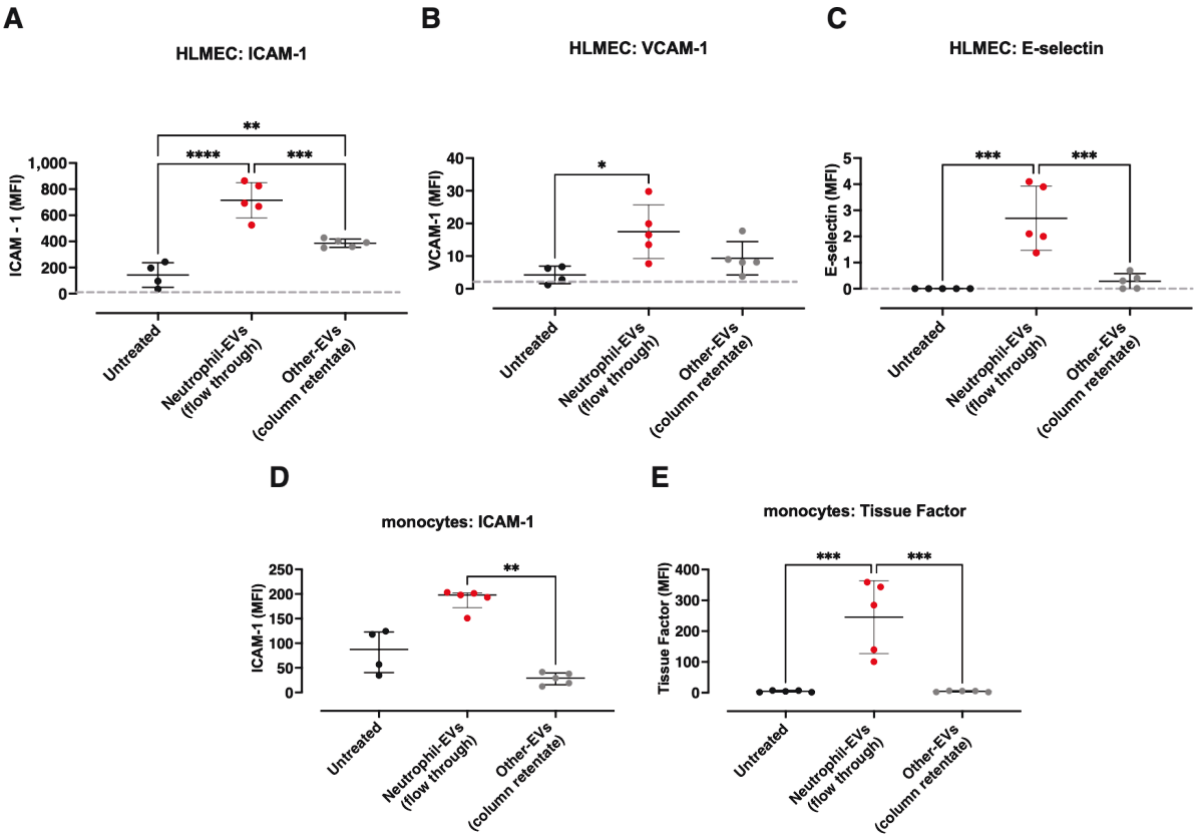

Figure 5.11. Negatively-selected neutrophil-EVs induce cell activation in PBMC-HLMEC co-culture.

Negatively selected neutrophil-EVs (2 x 10^7/well) were incubated in co-cultures of PBMCs and HLMECs for 4 h. Equal amounts of other-EVs (present in column-retentate (eluted) fraction) standardised by platelet-EVs, were used for comparison. Neutrophil-EV treatment induced increased expression of cell adhesion molecules ICAM-1 (**A**), VCAM-1 (**B**), E-selectin (**C**) on HLMECs and ICAM-1 (**D**) and tissue factor (**E**) on monocytes. A small increase in HLMEC-ICAM-1 was observed with the addition of the eluted EV fraction (column retentate fraction). Data are analysed by one-way ANOVA with Bonferroni's multiple comparisons test (A-C, and E; mean ± SD); or Kruskal-Wallis with Dunn's multiple comparisons test (D; median ± interquartile range). n=4-5, *p<0.05, **p<0.01, ***p<0.001, ****p<0.0001.

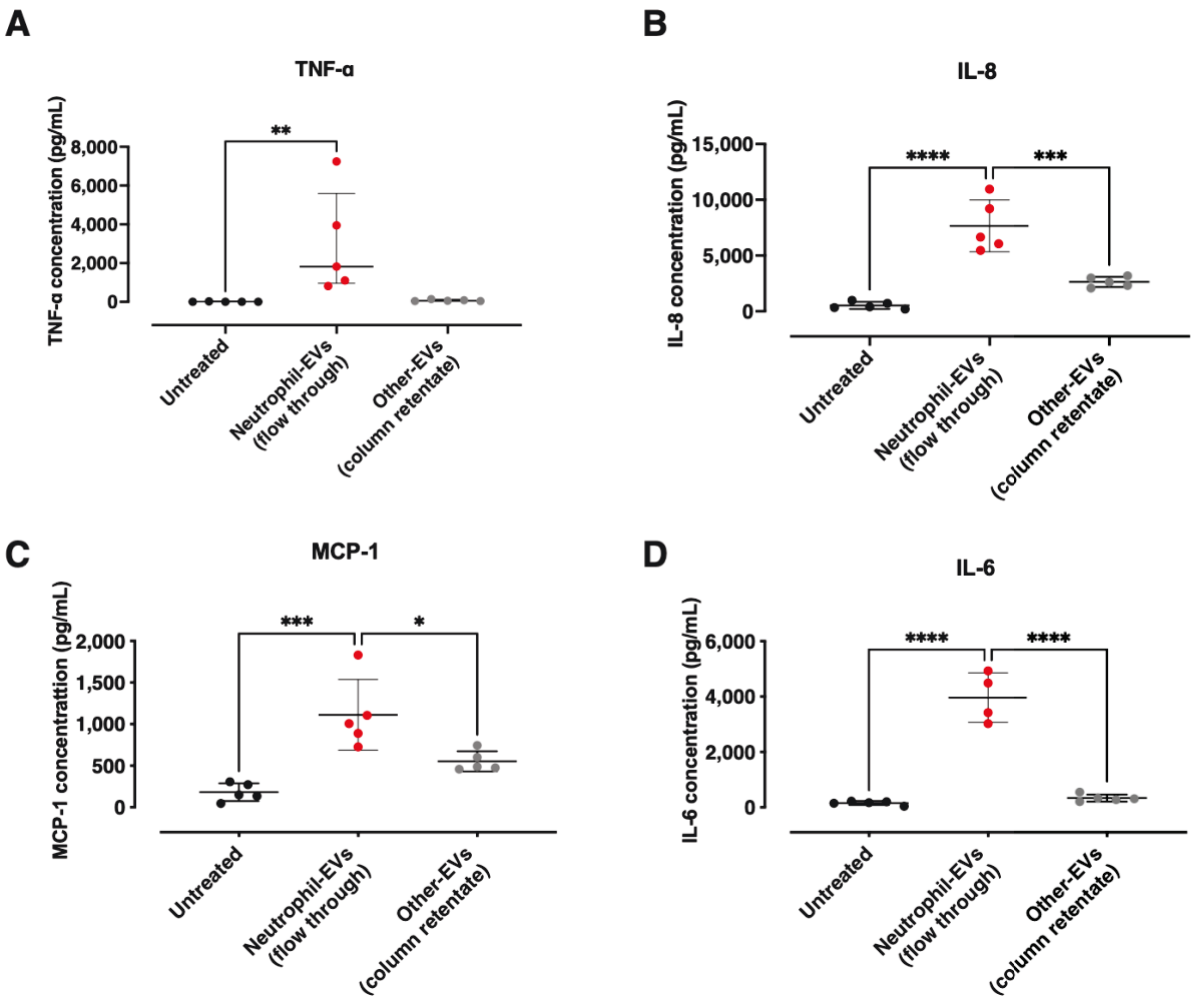

Figure 5.12. Negatively-selected neutrophil-EVs induce pro-inflammatory cytokine release in PBMC-HLMEC co-cultures.

Negatively selected neutrophil-EVs (2 x 10^7/well) were added to PBMC-HLMEC co-cultures and incubated for 4 h. Equal amounts of other-EVs (present in column-retentate (eluted) fraction) standardised by platelet-EVs, were used for comparison. Cell- and EV-free supernatants were assessed by ELISA for pro-inflammatory cytokine release. Neutrophil-EV treatment induced significant secretion of the pro-inflammatory cytokines TNF-α (**A**), IL-8 (**B**), MCP-1 (**C**), and IL-6 (**D**), while no responses were observed with the addition of the neutrophil-EV depleted fraction (column retentate). Data are analysed by one-way ANOVA with Bonferroni's multiple comparisons test (A, C and E; mean ± SD); or Kruskal-Wallis with Dunn's multiple comparisons test (B and D; median ± interquartile range). n=4-9, *p<0.05, **p<0.01, ***p<0.001, ****p<0.0001.

Although negative selection allowed the use of 'untouched' neutrophil-EVs in functional assays, it has the caveat that the isolated material cannot be as pure as the one resulting from the positive selection. In fact, data produced by an undergraduate student (Miss Claudia Peinador-Marin) revealed that negatively isolated neutrophil-EV samples included serum

lipoproteins that were not removed from the isolated neutrophil-EV subpopulation during the negative selection (data not shown). Moreover, there is the possibility that smaller EVs from any EV subtype might not be fully retained by the column (because of their small size) and flow through in the isolated neutrophil-EV samples. Having demonstrated that the neutrophil-EV activity was not dependent on bead-presence, it was decided that positive immunoaffinity selection did ensure that any observed responses could be attributed to the MicroBead-bound EV subtype and therefore it was chosen as the most appropriate neutrophil-EV isolation method for subsequent studies.

5.4.4. Neutrophil-EV activation of HLMECs is monocyte and TNF-α dependent

As our previous findings in the mouse isolated perfused lung model revealed a direct role of marginated monocytes for the myeloid-EV activity (357) combined with findings in **Chapter 4** of PBMC-dependent myeloid-EV responses *in vitro*, the monocyte dependency of the neutrophil-EV induced responses was investigated. Incubation of neutrophil-EVs with HLMECs cultured alone did not result in any upregulation of adhesion molecule expression (**Figure 5.13**). The neutrophil-EV activity was also assessed in HLMEC cultures that were pre-treated with LPS (1 ng/ml, without FBS, 2 h) to simulate a priming effect. However, no responses were observed, indicating that the neutrophil-EV inflammatory activities in this model were largely dependent upon PBMC presence.

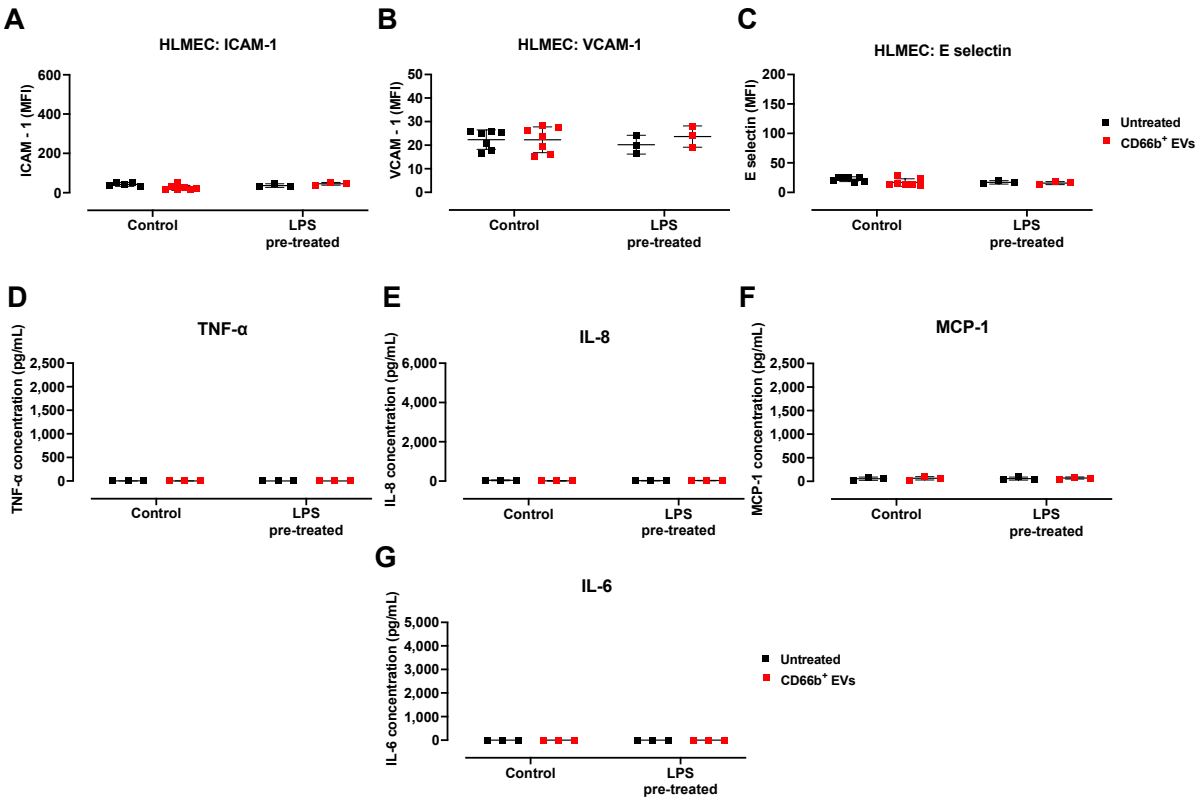

Figure 5.13. Neutrophil-EVs do not activate HLMECs in the absence of PBMCs.
Neutrophil-EVs (2 x 10^7/well) were incubated with untreated or LPS primed (1 ng/mL, 2 h) HLMEC-only cultures for 4 h. Under these conditions, no HLMEC activation (**A-C**) or pro-inflammatory cytokine release (**D-G**) was observed. Data are analysed by two-way ANOVA with Sidak's multiple comparisons test (A-G; mean ± SD). n=3.

To delineate the contribution of monocytes to neutrophil-EV-induced responses in PBMC-HLMEC co-cultures, I used monocytes isolated from PBMCs by negative immunomagnetic bead selection. Comparison of PBMC- and monocyte-HLMEC co-cultures revealed that monocytes produced the same level of cell activation and cytokine release as did the PBMCs, suggesting that monocytes are likely to be the primary responders to neutrophil-EVs and mediators of their activity in PBMC-HLMEC co-cultures (**Figure 5.14**).

For the sake of brevity, only data for ICAM-1 on HLMECs, tissue factor on monocytes, and the pro-inflammatory cytokines TNF-α and/or IL-8, are shown for the remainder of this thesis. In cases of outliers or differences in the observed responses, the relevant graphs will be included in the respective figures.

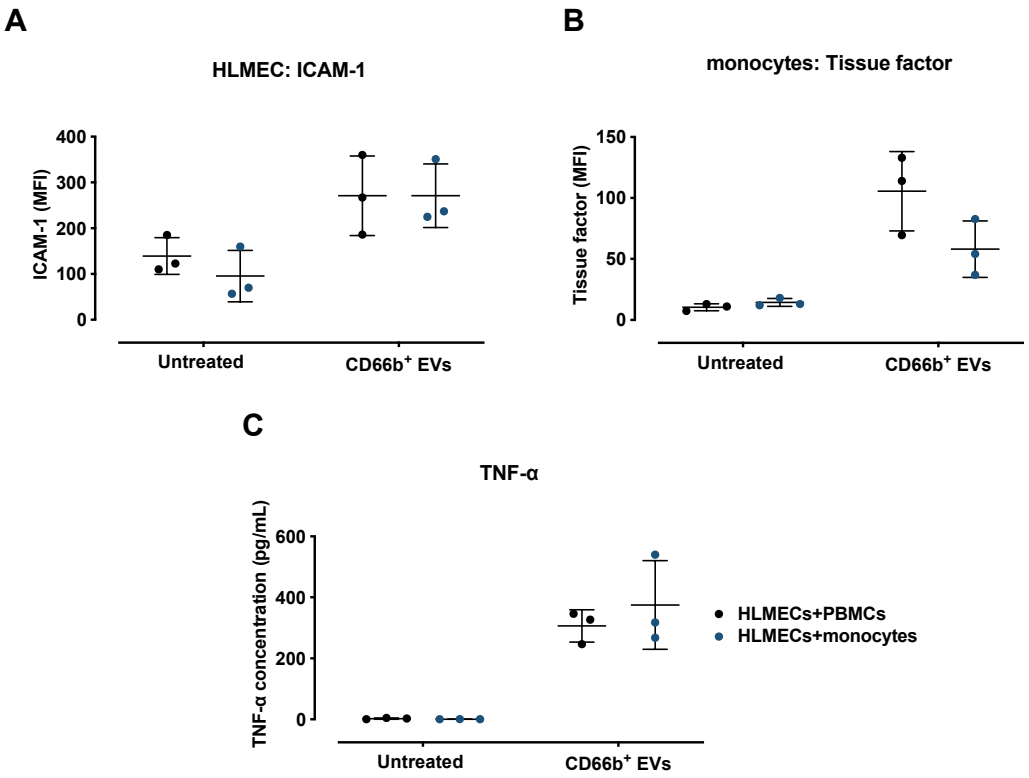

Figure 5.14. Monocytes are responsible for the neutrophil-EV-induced inflammation in co-culture with HLMECs.
Neutrophil-EVs (2 x 10^7/well) were incubated with PBMC-HLMEC or monocyte-HLMEC co-cultures for 4 h. No significant differences were observed in the activation level of HLMECs (**A**), monocytes (**B**), or release of pro-inflammatory cytokines (**C**) between PBMC- and monocyte-HLMEC co-culture models. Data are analysed by two-way ANOVA with Sidak's multiple comparisons test (A-C; mean ± SD). n=3.

As our group had previously shown that TNF-α plays a central role in monocyte-mediated pulmonary endothelial cell activation (355), I decided to investigate its contribution to HLMEC activation in PBMC-HLMEC co-culture. I found that in the presence of an anti-TNF-α neutralising antibody, HLMEC activation was completely reversed, with adhesion molecule expression reaching similar levels as the untreated or isotype-treated cells (**Figure 5.15**).

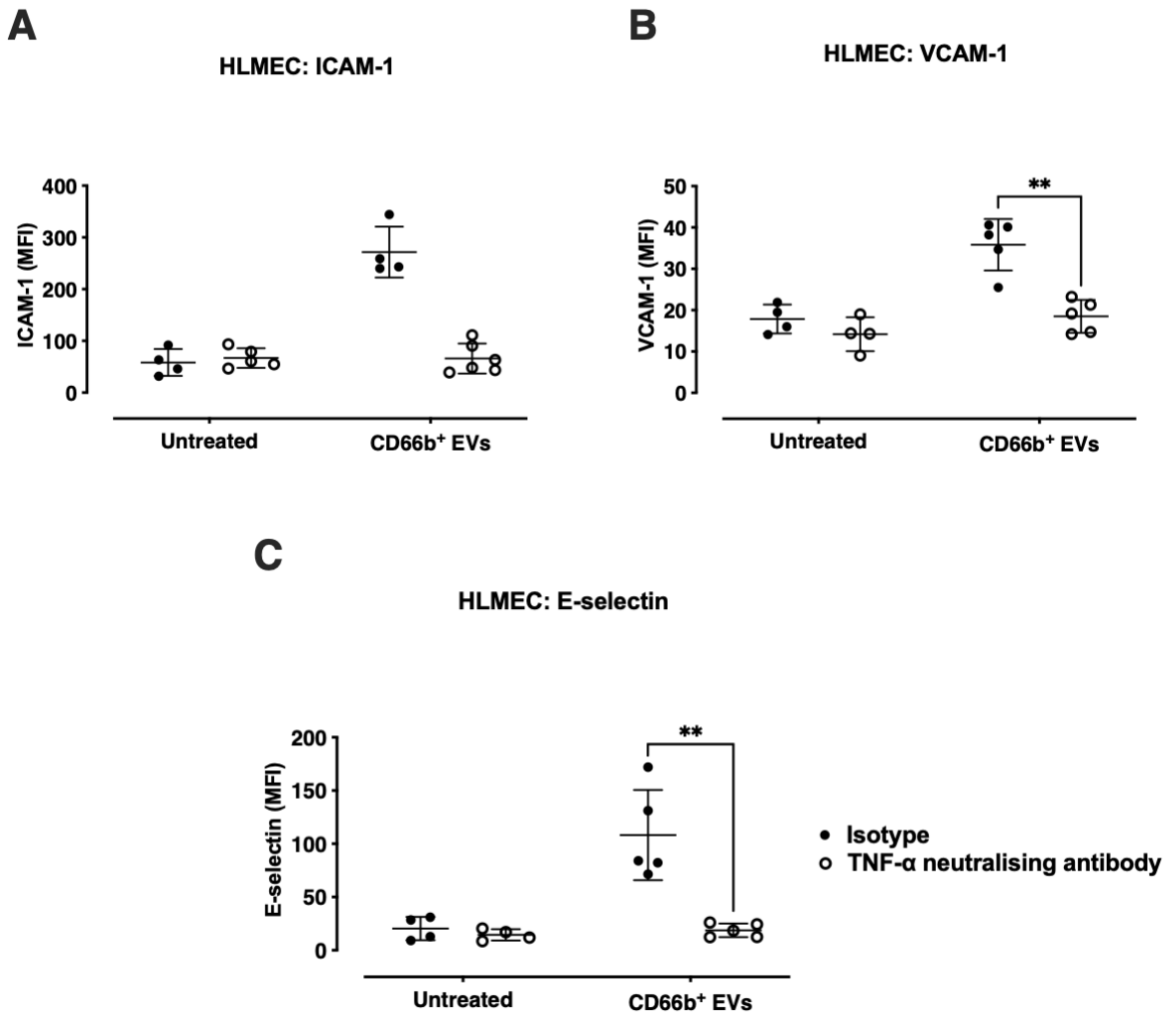

Figure 5.15. Neutrophil-EV mediated HLMEC activation is TNF-α dependent.
Neutrophil-EVs (2 x 10^7/well) were incubated with co-cultures of PBMCs and HLMECs in the presence of an anti-TNF-α neutralising antibody (10 µg/mL) or isotype control (10 µg/mL). Antibody or isotype control was added to cells 30 min prior to neutrophil-EV addition and not removed throughout the 4 h EV incubation period. TNF-α neutralisation completely reversed the neutrophil-EV-induced endothelial cell activation (**A-C**). Data are analysed by two-way ANOVA with Sidak's multiple comparisons test (A-C; mean ± SD). n=4-6, **p<0.01, ***p<0.001.

5.4.5. Assessment of neutrophil-EV activity under physiological flow conditions

Previously several-fold increased neutrophil-EV uptake by monocytes was found under flow conditions (**Chapter 3**, **Section 3.4.7**). It was therefore hypothesised that increased neutrophil-EV interactions with monocytes under flow would lead to enhancement of their pro-inflammatory effects. In our established protocols for PBMC-HLMEC co-culture under flow, HLMECs were pre-activated with TNF-α (100 ng/ml) to promote monocyte adherence. Here,

I first assessed whether TNF-α HLMEC pre-activation might enhance the neutrophil-EV activity. In these experiments, HLMEC cell adhesion molecule expression was already upregulated by the TNF-α pre-treatment, and no further increase was produced by neutrophil-EVs (**Figure 5.16, A**). In the case of monocyte activation or TNF-α and IL-8 release, HLMEC pre-activation did not affect these responses, with or without neutrophil-EV treatment (**Figure 5.15, B-D**).

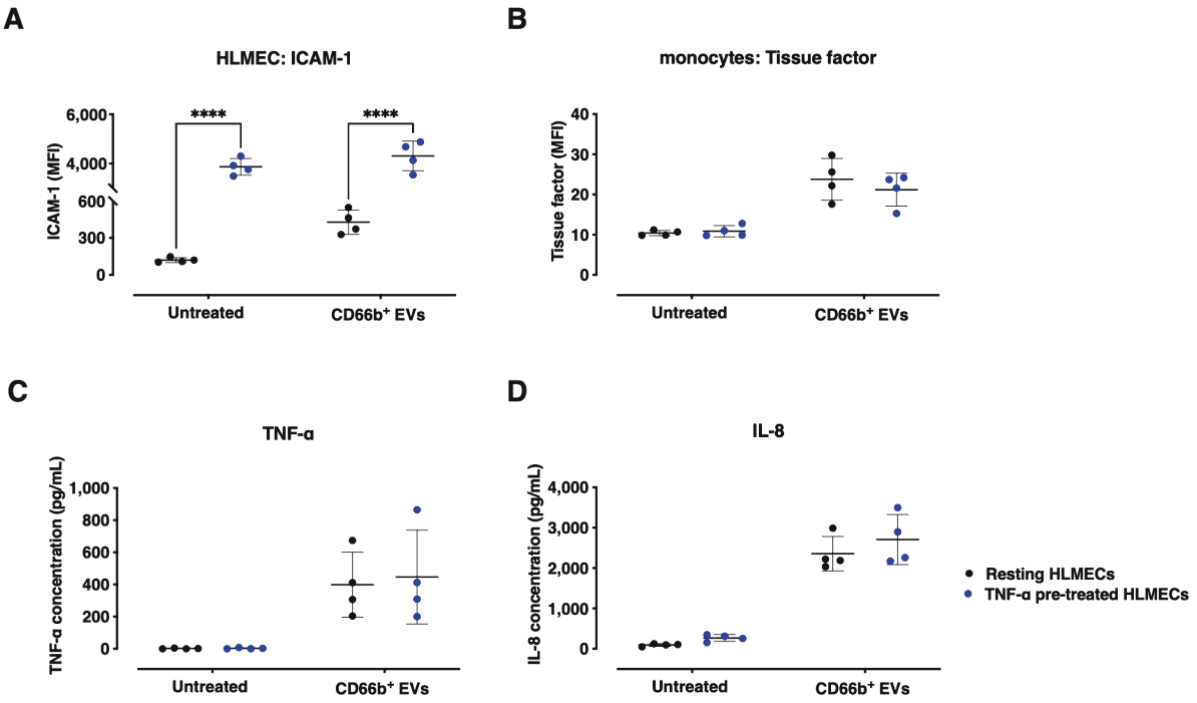

Figure 5.16. HLMEC pre-activation with TNF-α does not affect the neutrophil-EV-induced monocyte activation and cytokine release.
HLMECs were pre-treated with TNF-α (100 ng/mL, 2 h) followed by co-culture with PBMCs for 2 h and then incubated with neutrophil-EVs (2 x 10^7/well) for a further 4 h. TNF-α pre-activation induced significant upregulation on HLMEC ICAM-1 (**A**) but had no effect on the monocyte tissue factor expression (**B**), TNF-α (**C**) or IL-8 release (**D**). The measurable neutrophil-EV-induced responses were not modified by TNF-α pre-activation of HLMECs (**B-D**). Data are analysed by two-way ANOVA with Sidak's multiple comparisons test (A-D; mean ± SD). n=4, ****p<0.0001.

For the evaluation of neutrophil-EV activity under flow, a physiological shear stress value of 5 dyn/cm^2 estimated for capillaries (348, 349) was used. Our established model of neutrophil-

EV uptake by PBMC-HLMEC co-cultures under flow conditions was optimised for 1 h incubation of co-cultures with neutrophil-EVs, preceded by 1 h adaptation of co-cultures to flow (**Chapter 3**). However, here to allow sufficient time for neutrophil-EVs to release their activities on target cells, the co-incubation of cells and EVs under flow conditions had to be increased to 4 h. Pilot assays revealed that although about 2/3rd of monocytes adhere after 1 h flow adaptation period, numbers were drastically reduced after 4 h co-incubation under flow conditions (**Figure 5.17**), with the majority detached from HLMEC monolayers. In separate experiments, a protocol of a 2 h co-incubation period of cells and EVs, slightly increased the number of adherent monocytes at the end of the assay, but still, monocyte numbers were significantly lower compared to static culture.

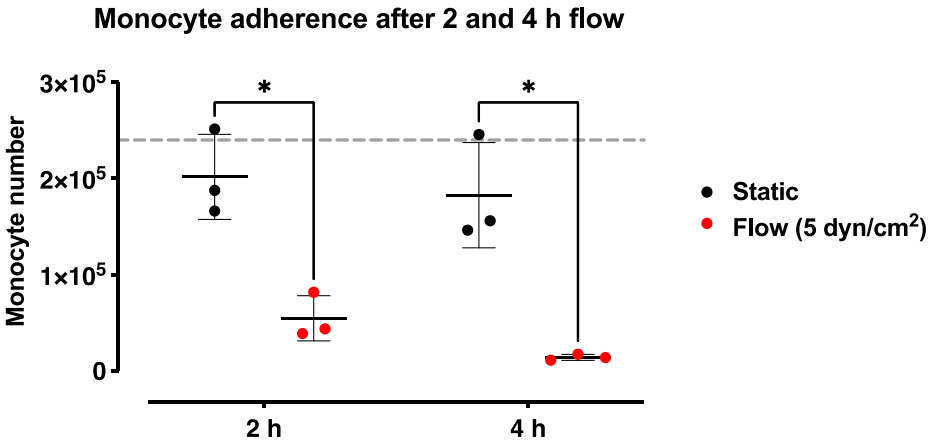

Figure 5.17. Effect of prolonged flow treatment in monocyte adherence.
PBMCs were added to TNF-α (100 ng/mL, 2 h) pre-activated, flow-adapted (24 h, 5 dyn/cm^2) HLMEC monolayers for 2 h under static conditions, followed by 1 h flow adaptation (5 dyn/cm^2). Media was replaced, non-adherent cells were discarded, and co-cultures were incubated for another 2 or 4 h with or without flow. Numbers of adherent monocytes were determined at the end of the assay by flow cytometry. The 2 h incubation period slightly increased adherent monocyte numbers, albeit both 2 and 4 h incubation periods markedly decreased the number of adherent monocytes compared to static culture. Dotted line represents the number of monocytes originally added to slides. Data are analysed by two-way ANOVA with Sidak's multiple comparisons test (mean ± SD). n=3, *p<0.05.

Due to project time constraints, it was decided to assess neutrophil-EV activities under flow with both 2 and 4 h EV-target cell co-incubation periods rather than modifying the protocol

further to enhance monocyte adherence and retention. LPS treatment (10 ng/mL, in the presence of 10 % EV-depleted FBS) of co-cultures under static and flow conditions was used for comparison. It was found that flow conditions alone (without EVs or LPS) induced TNF-α, and IL-8 release (TNF-α concentration: untreated 2 h: static: 1.0±0.2 vs. flow: 179.4±163.9, untreated 4 h static: 37.1±7.5 vs. flow: 114.7±43.9), (IL-8 concentration: untreated 2 h: static: 315.4±51.5 vs. flow: 578.3±433.5, untreated 4 h: static: 2,479±8 vs. flow: 4,534.0±3,384.3). The subsequent challenge with neutrophil-EVs under flow conditions in the 2 h protocol, resulted in increased TNF-α release compared to static conditions (neutrophil-EV treatment: static: 28.2±33.7 vs. flow: 328.6±33.3) but was not significantly higher than TNF-α release from flow alone treatment (without neutrophil-EVs) (flow: untreated:179.4±163.9 vs. neutrophil-EVs: 328.5±33.3). IL-8 release was not increased with 2 h treatment (**Figure 5.18, A, B**). With the 4 h co-incubation protocol, no differences were observed between static or flow neutrophil-EV treatment in both TNF-α and IL-8 levels (**Figure 5.18, C, D**). Likewise, the LPS response, in both 2 and 4 h protocols, was not modified by the presence of flow (**Figure 5.18, A-D**).

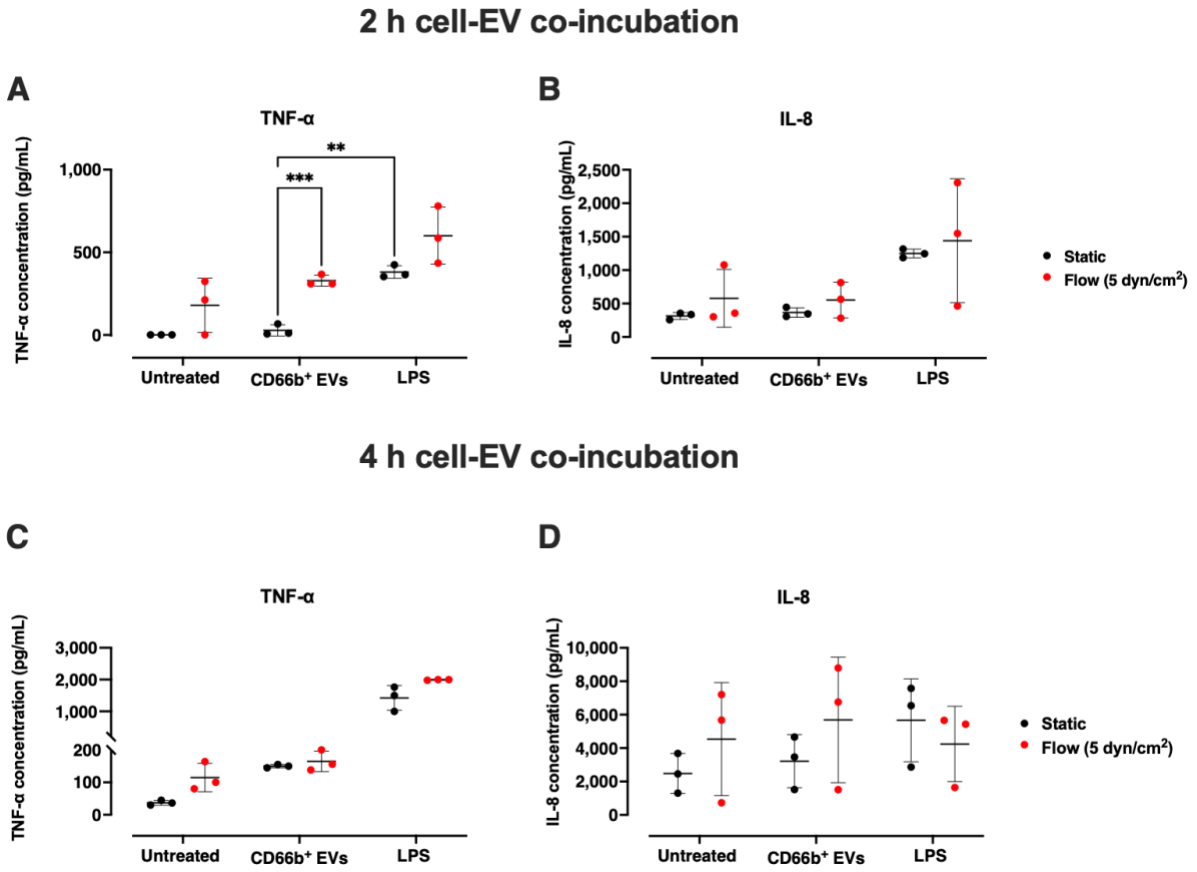

Figure 5.18. Flow culture does not affect the neutrophil-EV-mediated cytokine release in PBMC-HLMEC co-cultures.

PBMCs were added to TNF-α (100 ng/mL, 2 h) pre-activated, flow-adapted (24 h, 5 dyn/cm^2) HLMEC monolayers for 2 h under static conditions, followed by 1 h flow adaptation (5 dyn/cm^2). Media was replaced and non-adherent cells were discarded. Neutrophil-EVs (4 x 10^7/mL) or LPS (10 ng/mL) were added to co-cultures for 2 or 4 h with or without flow. At 2 h, neutrophil-EV induced TNF-α release was significantly higher compared to static (**A**) while IL-8 was not significantly different (**B**). At 4 h, both TNF-α (**C**) and IL-8 levels (**D**) following EV treatment were similar between static and flow culture. No detectable differences were observed in LPS-mediated cytokine release between flow and static conditions at both 2 and 4 h protocols. Data are analysed by two-way ANOVA with Bonferroni's multiple comparisons test (A-D; mean ± SD). n=3, *p<0.05.

5.5. Discussion

Previous work has demonstrated that neutrophil-EVs are inducers of pro- or anti-inflammatory cell activation, but the determinants of these opposite effects have not been fully defined yet. In this study, my aim was to evaluate the pro-inflammatory properties of neutrophil-EVs produced during LPS stimulation of whole blood, as an *in vitro* model with higher relevance to sepsis. Moreover, instead of focussing on a single target cell population, I evaluated the neutrophil-EV activities in a PBMC-HLMEC co-culture model of pulmonary vascular inflammation (previously developed in **Chapter 4**). Neutrophil-EVs were successfully isolated from LPS-stimulated whole blood by both positive and negative immunoaffinity-based selection methods. Their functional assessment revealed that neutrophil-EVs induced significant release of cytokines and upregulation of cell adhesion molecules on HLMECs. Furthermore, monocytes were identified as the primary responder cells inducing activation of HLMECs via their release of TNF-α. A proposed model of neutrophil-EV-induced pulmonary vascular inflammation is summarised in **Figure 5.19**.

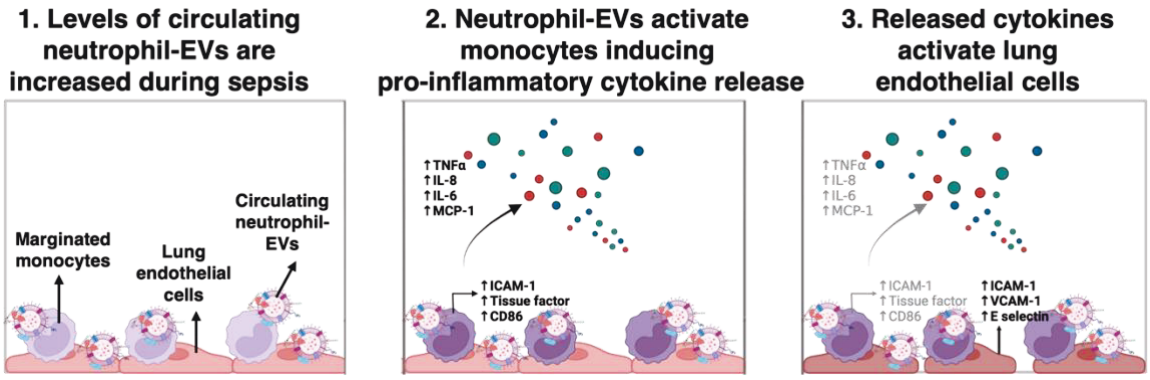

Figure 5.19. Summary of the proposed mechanisms involved in neutrophil-EV-induced cell activation and pro-inflammatory cytokine release.
During systemic inflammation, neutrophil-EVs are significantly increased in numbers and interact with lung-marginated monocytes, inducing upregulation of surface activation markers and release of pro-inflammatory cytokines such as TNF-α, which in turn activate lung endothelial cells resulting in upregulation of adhesion molecules on their surface. Figure designed with Biorender.

Isolation of neutrophil-EVs was based on anti-CD66b immunoaffinity separation. CD66b is a granulocyte marker expressed on neutrophils and eosinophils (389, 450), widely used as a neutrophil-EV marker (242, 292, 322, 352, 384). Eosinophils account for a very small proportion of circulating leukocytes (1-5 % of peripheral leukocytes) (451), whereas neutrophils are the most abundant granulocytes within the bloodstream (50-70 % of all leukocytes) (452). Although not evaluated, the presence of significant numbers of eosinophil-EVs in the isolated samples was considered unlikely and therefore for the sake of clarity we decided to refer to the CD66b isolated EVs as 'neutrophil-EVs'.

Addition of neutrophil-EVs to PBMC-HLMEC co-cultures upregulated the expression of surface activation markers on HLMECs and monocytes (ICAM-1, VCAM-1, E-selection on HLMECs and ICAM-1, tissue factor, CD86 on monocytes) and increased the release of pro-inflammatory cytokines TNF-α, IL-8, IL-6, IL-1β, and MCP-1. Incubations of cells with beads alone did not induce any of these responses. Although these findings mirror those of Danesh et al., where among other EV subtypes, only granulocyte-derived EVs activated monocytes towards the release of pro-inflammatory cytokines such as TNF-α, IL-6, IL-1β, MIP-1α, and GM-CSF (293), the responses observed in our study were of higher magnitude and occurred much faster (within 4 h as opposed to 24 h). A possible explanation of this phenomenon could be the fact that Danesh et al., used spontaneously released granulocyte-EVs (produced from prolonged 24 h incubation of isolated granulocytes), and therefore the inflammatory cargo of these might be less potent compared to the LPS-induced neutrophil-EVs produced in our whole blood model.

Having demonstrated that positively selected neutrophil-EVs induce pro-inflammatory responses, the potential modification of responses by binding of the anti-CD66b MicroBeads to EVs was considered. According to the manufacturer, the CD66b MicroBeads used for positive selection were of 50 nm size (same as the CD11b and CD61 MicroBeads used in **Chapter 4**). Flow cytometry assessment of the neutrophil-EV size before and after the isolation, with the use of the ApogeeMix sizing beads as a reference, revealed that the majority

of EVs produced and isolated in our assay were between 600 and 180 nm size range, about 3-12 times larger than the beads and that their size (determined by side-scatter 405 nm laser profiles) did not appear to be substantially increased by bead binding. Interestingly electron microscopy observations indicated that the CD66b MicroBeads appeared somewhat smaller than 50 nm and did not cover the whole EV surface. Therefore, we believe that EV activities and interactions with target cells occur without significant impedance by bound beads. Indeed, negative isolation of neutrophil-EVs, resulting in 'untouched' EV preparations, induced similar pro-inflammatory responses in PBMC-HLMEC co-cultures and in the same experiments the neutrophil-EV depleted fraction (column-retained and eluted EVs) did not cause any significant cell activation or cytokine release apart from a small ICAM-1 increase on HLMECs. These findings confirmed the neutrophil-EV specificity of the reported responses and suggested that the beads were inert in our assays.

Of note, it was observed that negatively isolated EVs produced slightly higher responses compared to the positively selected (bead-bound) neutrophil-EVs. This was attributed to either potential co-isolation of smaller EVs of other subpopulations that could not be fully retained on the magnetic column and were below threshold detection level on the used flow cytometer, or the co-isolated lipoproteins that were detected on the negatively isolated samples (data not shown). Indeed, low-density lipoproteins and EVs have overlapping densities of 1.019-1.063 g/mL and 1.06-1.21 g/mL respectively, allowing for the co-isolation of both during the differential centrifugation (255). This was considered a major caveat for the purposes of this study, as lipoprotein presence could enable LPS carryover as previously suggested (453-455). We acknowledge that additional purification assays such as size-exclusion chromatography would help eliminate plasma lipoproteins (456, 457) to improve the negative selection method for neutrophil-EV isolation but due to time constraints, this was not further investigated. It was therefore decided that positive selection would be the most appropriate isolation method to use for subsequent functional assays.

The early cytokine release and lack of responses in HLMEC only cultures suggested that monocytes played a significant role in neutrophil-EV-induced responses in the PBMC-HLMEC co-culture model. This interpretation was confirmed by the lack of significant differences in the levels of neutrophil-EV induced cytokine release and cell activation marker expression between isolated monocyte-HLMEC and PBMC-HLMEC co-cultures. Similarly, Lok and colleagues reported a monocyte-dependent cell activation after treatment of HUVECs and monocyte-like cells (THP-1) with EVs isolated from preeclamptic patients (458). However, in contrast to our findings, direct endothelial cell activation and injury have been previously reported by neutrophil-EV treatment. Mesri et al., observed endothelial cell activation, presented with upregulation of adhesion molecule expression and IL-6 and IL-8 secretion after treatment with fMLP-derived neutrophil-EVs in HUVECs (325, 326). Apart from the different protocol used in these studies and ours (fMLP stimulation of isolated neutrophils (325) or whole blood (326) vs. LPS treatment of whole blood), the responses observed by Mesri and colleagues were of much lower magnitude (3-fold difference in IL-6 levels) and detected after extended EV incubation period (10-12 h), as opposed to our acute cytokine release at 4 h. Kolonics et al., also observed endothelial activation induced by neutrophil-EVs produced via zymosan opsonisation, with IL-8 release and VCAM-1 upregulation, but again with a prolonged EV treatment period of 24 h (371). Likewise, 24 h incubation of HUVECs with neutrophil-EVs isolated by vasculitis patients resulted in increases in ICAM-1, IL-6, and IL-8 (319). Apart from release of pro-inflammatory cytokines, injurious effects of neutrophil-EVs (cellular cytotoxicity, loss of membrane integrity, increased permeability, and monocyte transendothelial migration) have also been observed after prolonged neutrophil-EV treatment of endothelial cells monolayers (322, 352, 384). Based on these findings, we attributed the lack of responses in our HLMEC only model to either a limited incubation period (‘acute’ vs. ‘chronic’ neutrophil-EV effects) or different cargo of neutrophil-EVs because of the known heterogeneity of neutrophil-EVs that results from different production conditions (292, 371, 459). As we only studied the direct and acute effects of neutrophil-EVs on target cells, we

cannot rule out their potential in causing monocyte-independent endothelial cell activation or injury with prolonged co-incubation.

Contrasting with the current findings, neutrophil-EVs have been linked to anti-inflammatory processes mainly against macrophages and neutrophils as target cells. A Mer tyrosine kinase (MerTK) receptor-dependent downregulation of pro-inflammatory cytokine release from macrophages after neutrophil-EV treatment (330), alongside TGF-β secretion by both macrophages and macrophage-derived-dendritic cells was previously reported by the Schifferli's group (242, 329). MerTK is not present or expressed at low levels in undifferentiated monocytes (460), hence we believe that this might be a key factor for the lack of anti-inflammatory responses in our model. In a separate study, neutrophil-EVs induced by fMLP stimulation of isolated neutrophils were shown to be rich in the anti-inflammatory protein annexin A1, and inhibited neutrophil migration and interactions with HUVECs under flow conditions and produced anti-inflammatory effects towards neutrophils (331). Data produced by a colleague in the group (Miss Eirini Sachouli) suggested that neutrophil-EVs produced from isolated neutrophils stimulated by LPS followed by fMLP were inactive in mixed leukocyte-HLMEC cultures, whereas neutrophil-EVs produced within whole blood by using the same stimuli, induced cytokine release and pro-inflammatory cell activation (461). Additionally, others have compared the properties of neutrophil-EVs produced under different environments or stimulatory agents and observed distinct functional properties even upon the same target cells (292, 371). Collectively these findings suggest that differences in the neutrophil-EV properties could be explained by the specific stimulation protocol used and key variables it affects (e.g., the status of the parent cell: primed or resting; stimulus type; the environment: isolated cells adherent or in suspension or whole blood) and the type of responder target cells.

In **Chapter 3**, I presented evidence of differential EV uptake between resting/inflammatory and static/flow cultures of target cells, suggesting that static culture may not incorporate important features of the *in vivo* target cell-EV interactions. Here, an attempt was made to

assess the impact that the increased neutrophil-EV uptake by monocytes under flow had on inflammatory responses, but this was only partly successful due to the detachment of monocytes during stimulation. Nonetheless, these experiments revealed that flow could have a significant effect on inflammatory responses and that this, in turn, might modify the response of monocyte to neutrophil-EVs. Therefore, further exploration and development of this model is warranted.

Overall, the findings presented in this chapter revealed the pro-inflammatory properties of *ex vivo* generated neutrophil-EVs during systemic inflammation and pointed to the key role of marginated monocytes in orchestration of microvascular inflammation.

6. Evaluation of mechanisms responsible for neutrophil-EV pro-inflammatory activity

Parts of the data produced for this chapter have been published as a conference abstract

Tsiridou DM, Sachouli E, Takata M, O'Dea KP. Neutrophil-Derived Microvesicles Enhance Pulmonary Vascular Inflammation via a Toll-like Receptor 4 Signaling-Dependent Mechanism. The FASEB Journal. 2022 May;36. (462)

6.1. Background

In the previous chapter (**Chapter 5**) I demonstrated that neutrophil-EVs isolated from LPS-stimulated whole blood induce activation of monocytes leading to pro-inflammatory cytokine release and activation of pulmonary endothelial cells *in vitro*. My next aim was to evaluate the signalling mechanisms(s) responsible for the pro-inflammatory activities of neutrophil-EVs.

Despite extensive research into neutrophil-EVs over several decades, the biological roles in inflammation and the molecular mechanisms underlying them, remain incompletely understood. This is partly due to the considerable heterogeneity of neutrophil-EVs and the fact that most studies mainly have focused on their anti-inflammatory activities to date (459, 463). Since EVs derive from activated neutrophils, they will likely replicate their parental cell effects on target cells such as monocytes (459). Therefore, it is possible that similar molecular activities are responsible for neutrophil and neutrophil-EV activation of monocytes, or conversely, the activity is unique to neutrophil-EVs.

Neutrophils are typically the first responders to injury or infection, recruited to local sites by chemoattractants released mainly from tissue resident macrophages and mast cells (464). Once recruited, a feedback loop is initiated that involves the secretion of pro-inflammatory factors, which attract monocytes that amplify local responses and modulate neutrophil functions. Examples of neutrophil mediators that can enhance monocyte functions include (but are not limited to) ROS (319, 326, 465), α-defensins (466-468), cathepsin G (469), and granule products such as cationic peptides (azurocidin also known as CAP37 or heparin binding protein and cathelicidin also known as LL37) (107, 470, 471).

Neutrophil-EVs carry a multitude of inflammatory molecules or biosynthetic machinery as part of their molecular cargo. Examples include NADPH oxidase for ROS generation (292, 445, 472), histones (473, 474), myeloid-related protein 8/14 (MRP8/14) (also known as calgranulin A/B, calprotectin, S100A8/A9) (292, 475-479), cationic peptides (azurocidin and cathelicidin)

(297), and heat shock protein 70 (HSP70) (292, 480). Moreover, neutrophil-EVs carry pro-inflammatory cytokines such as IL-1β (318) and therefore may be able to activate target cells via this signalling pathway. Besides bioactive proteins, eicosanoids such as prostaglandins D2, E2, and leukotriene B4 have also been found in neutrophil-EVs (296, 446). Additionally, transcellular transfer of precursor lipid, arachidonic acid, from neutrophil-EVs has been shown to enable platelet production of thromboxane A2 which subsequently induced pro-inflammatory endothelial cell activation (481). Of more direct relevance to this study is the demonstration that LPS-activated neutrophils release platelet activating receptor (PAF)-bearing vesicles subsequent to neutrophil adhesion (386). Lastly, neutrophil-EVs have been found to be enriched in small noncoding microRNAs (miRNAs), such as miR-30d-5p (482), miR-155 (352), transfer of which led to activation of the NF-κB pathway in target cells (macrophages and endothelial cells) *in vitro*.

To identify neutrophil-EV cargo responsible for early monocyte responses, our strategy was to evaluate major pathways that neutrophil-EVs are likely to activate in monocytes, focussing on ROS-mediated signalling, G-protein-coupled receptor (GPCR) signalling, or Toll-like receptor (TLR) signalling. As the *in vitro* models used in this study relied on primary cells, I focused on pharmacologic- and antibody-based blocking strategies, with inhibitors targeting receptors and key signalling pathways mentioned above. This approach was adaptive and therefore as the role of dominant pathways was revealed, I switched focus entirely to these.

6.2. Aims

To characterise the nature of neutrophil-EV pro-inflammatory mediators that lead to monocyte activation, I aimed to:

1. Evaluate the role of intracellular kinase signalling in neutrophil-EV-induced responses.
2. Assess the contribution of ROS, TLR, and GPCR signalling to neutrophil-EV-induced responses.
3. Identify the molecular mediator(s) responsible for neutrophil-EV induced responses.

6.3. Protocols

6.3.1. Neutrophil-EV production and purification

Neutrophil-EVs were produced from LPS-stimulated whole blood and isolated via CD66b positive immunomagnetic bead selection as described in the previous chapter (**Chapter 5**).

6.3.2. Neutrophil-EV functional assays

For increased efficiency, the PBMC-HLMEC co-culture model was adapted for smaller scale high throughput assays and instead of 48-well plates (as used in **Chapters 4 and 5)**, 96-well plates were used. For this scaling down, HLMECs were seeded at 3 x 10^4 cells/well, PBMCs at 6 x 10^4 monocytes/well, and neutrophil-EVs were added at 1 x 10^7/well in a final volume of 250 µL.

Table 6.1 summarises all the inhibitors, blocking antibodies, and chemicals used in intervention assays in this study, alongside the treatment concentrations and incubation conditions. In each case, treatment of cells or EVs with inhibitors was carried out for the stated time prior to co-incubation of cells and EVs and continued for the full 4 h stimulation period unless otherwise stated. In assays where serum presence was required, FBS was centrifuged at 20,800 x g for 1 h to remove larger EVs.

EV counts by flow cytometry were normally determined before addition to co-cultures, but in experiments where EVs were lysed prior to incubation with cells, EV counts and dilutions were performed before lysis. EVs were lysed by two consecutive freeze-thaw cycles of -80 °C and 37 °C in a water bath, followed by sonication at 50 Hz, for 2 min.

Inhibitor/ blocking antibody	Target	Concentration	Incubation conditions	Application
anti-HSP70 monoclonal antibody (clone 4G4) (Invitrogen)	EVs	1:100 antibody dilution	30 min, 37 °C	Heat shock protein 70 blocking
Ultra-LEAF™ anti-S100A8/A9 heterodimer blocking antibody (clone A15105B) (Biolegend)	EVs	1 µg/mL, 10 µg/mL	30 min, 37 °C	MRP8/14 blocking
Ultra-LEAF™ anti-TLR4 antibody (CD284) (clone HTA125) (Biolegend)	cells	10 µg/mL	30 min, 37 °C	TLR4 blocking
Diphenyleneiodonium (DPI) (Sigma-Aldrich)	cells	20 µM	30 min, 37 °C	ROS inhibition
DNase I (New England Biolabs)	EVs	200 U/mL	1 h, 37 °C	free DNA/ NETs degradation
Heat-labile proteinase K (New England Biolabs)	EVs	2.5 U/mL	45 min, 37 °C +15 min, 55 °C	protein degradation
LY294002 (Peprotech)	cells	50 µM	30 min, 37 °C	PI3K inhibition
Ultra-LEAF™ mouse IgG2a, κ isotype (clone MOPC-173) (Biolegend)	cells	10 µg/mL	30 min, 37 °C	isotype control
Ultra-LEAF™ mouse IgG2b, κ isotype (clone MG2b-57) (Biolegend)	EVs	10 µg/mL	30 min, 37 °C	isotype control
N-acetyl-l-cysteine (NAC) (Sigma-Aldrich)	cells	1 mM, 5mM	30 min, 37 °C	ROS inhibition
Paquinimod (Sigma-Aldrich)	EVs	10 µM, 50 µM	1 h, ice	MRP14 inhibition
Polymyxin B (Sigma-Aldrich)	EVs	10 µg/mL	1 h, ice	LPS neutralisation

SB203580 (Tocris Bioscience)	cells	10 µM	30 min, 37 °C	p38 kinase inhibition
Superoxide dismutase (SOD) (Sigma-Aldrich)	cells	100 U/mL, 1000 U/mL	30 min, 37 °C	ROS inhibition
TAK-242 (Calbiochem)	cells	10 µM	30 min, 37 °C	TLR4 inhibition
U0126 (Sigma-Aldrich)	cells	10 µM	30 min, 37 °C	MEK1/2 inhibition

Table 6.1. List of inhibitors, antibodies, and chemicals used in functional assays to determine neutrophil-EV signalling mechanisms.

6.3.3. LPS association with blood cells and EVs

To assess LPS binding and/or uptake by different cell populations within the blood, a fluorescent conjugate of LPS was used. Heparinised whole blood from healthy volunteers was incubated with either unlabelled LPS (100 ng/mL) or Alexa Fluor™ 488-conjugated LPS (Invitrogen) (1 µg/mL) for 3 h, at 37 °C. Following stimulation, whole blood and platelet poor plasma were stained with cell/EV marker antibodies. Following antibody staining, blood was incubated with 1 x Lyse/Fix buffer (BD Biosciences) for 10 min at room temperature for red blood cell lysis and cell fixation. LPS binding to cells and EVs was assessed by flow cytometry and quantified as cell- or EV-associated Alexa Fluor™ 488 fluorescence.

6.3.4. LPS ELISA

LPS levels in EV preparations were assessed using an LPS ELISA kit (Aviva systems biology). Prior to the ELISA, neutrophil- and platelet-EVs were isolated by positive immunomagnetic bead selection, washed twice, and lysed by freeze-thawing and sonication as described above.

6.4. Results

6.4.1. Neutrophil-EV activity involves p38, ERK1/2, and PI3K signalling pathways

As we had found that neutrophil-EV-induced release of TNF-α was responsible for HLMEC activation in the co-culture, we decided to evaluate MAPK signalling by pharmacological inhibition of p38 and ERK1/2 (483). To obtain a more complete picture, we also assessed the inhibition of phosphoinositide 3-kinase (PI3K) and c-Jun N-terminal kinase (JNK) pathways, which have been linked to neutrophil-EV uptake and induction of endothelial cell activation and cytokine release (326, 329). Neutrophil-EV induced TNF-α and IL-8 release in PBMC-HLMEC co-cultures was completely inhibited in the presence of SB203580, a selective p38 inhibitor, U0126, a MEK1/2 inhibitor (a downstream target of the ERK1/2 pathway), or LY294002, a PI3K inhibitor. By contrast, JNK-1 blocking by SP600125 treatment did not affect the neutrophil-EV mediated cytokine release (**Figure 6.1, A and B**). LPS was used as a comparator stimulus. As expected, blocking of p38 and ERK1/2 pathways was effective overall in reducing TNF-α and IL-8 release. However, contrasting with neutrophil-EVs PI3K inhibition had little effect, as was the case of JNK-1 inhibition (**Figure 6.1, C and D**).

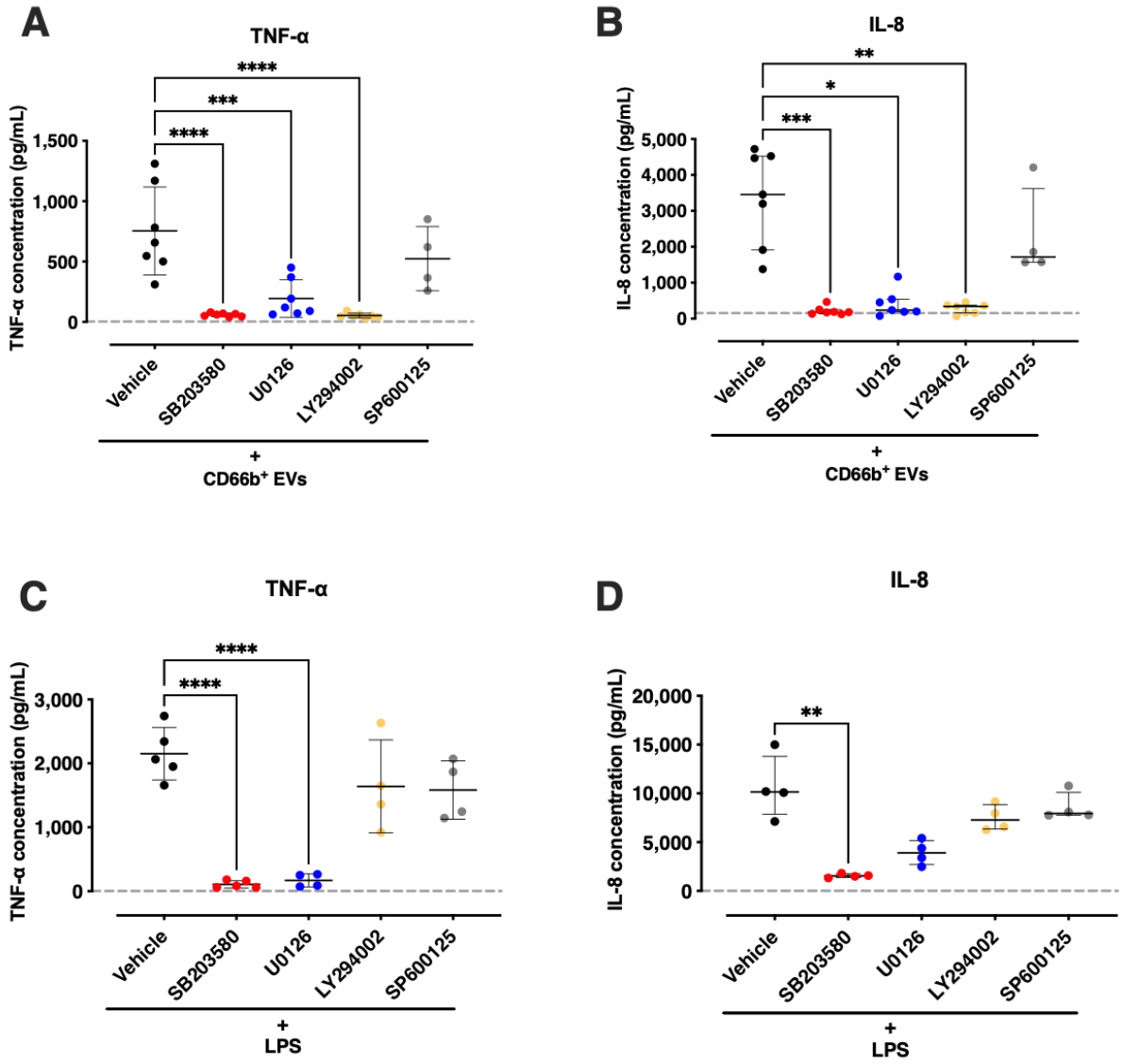

Figure 6.1. Neutrophil-EV induced cytokine production in PBMC-HLMEC co-culture is p38, ERK1/2, and PI3K dependent.

Neutrophil-EVs (1 x 10^7/well) or LPS (10 ng/mL with 10 % FBS) were incubated with co-cultures of PBMCs and HLMECs (4 h) in the presence of SB203580 (10 μM), U0126 (10 μM), LY294002 (50 μM), SP600125 (10 μM), or vehicle control (DMSO, 0.1 %). p38, MEK1/2, and PI3K inhibition significantly reduced the neutrophil-EV mediated TNF-α and IL-8 release, while JNK-1 blockade did not (**A-B**). LPS-induced TNF-α and IL-8 release was sensitive to p38 and MEK1/2 inhibition, while PI3K and JNK-1 blockade did not significantly modify these responses (**C-D**). Dotted line represents untreated co-cultures. Data are analysed by one-way ANOVA with Bonferroni's multiple comparisons test (A and C; mean ± SD); or Kruskal-Wallis with Dunn's multiple comparisons test (B and D; median ± interquartile range). n=4-7, *p<0.05, **p<0.01, ***p<0.001, ****p<0.0001.

6.4.2. Neutrophil-EVs do not induce cell activation through ROS

ROS are potent microbicidal and pro-inflammatory mediator released from neutrophils and have been linked to activation of the above MAPK kinase pathways (484). Neutrophil-EVs have also been found to produce ROS following their stimulation with PMA (292). Based on this evidence, we hypothesised that the neutrophil-EV-induced pro-inflammatory cytokine release is mediated by ROS. Co-cultures of PBMCs and HLMECs were stimulated with neutrophil-EVs in the presence of three known ROS inhibitors. LPS was used as a comparator treatment to assess ROS-dependent signalling as well as potential off-target effects occurring due to inhibitor toxicity. The broad spectrum free radical scavenger N-acetyl-l-cysteine (NAC) (485) was tested in two different concentrations (1 mM and 5 mM) without having any significant effect in TNF-α, and IL-8 secretion induced by either neutrophil-EVs or LPS (**Figure 6.2, A and B**).

The effect of superoxide dismutase (SOD) a membrane impermeant enzyme that catalyses the dismutation of superoxide ($\cdot O_2^-$) into molecular oxygen and hydrogen peroxide (H_2O_2) was tested (486). In the presence of SOD (100 or 1000 U/mL), neither neutrophil-EV nor LPS responses were affected (**Figure 6.2, C and D**).

Lastly, the flavoprotein oxidoreductase diphenyleneiodonium (DPI) was used to inhibit NADPH oxidase mediated production of $\cdot O_2^-$. Interestingly, DPI treatment of co-cultures significantly decreased the neutrophil-EV and LPS induced TNF-α and IL-8 release suggesting similar activation mechanisms (**Figure 6.2, E and F**).

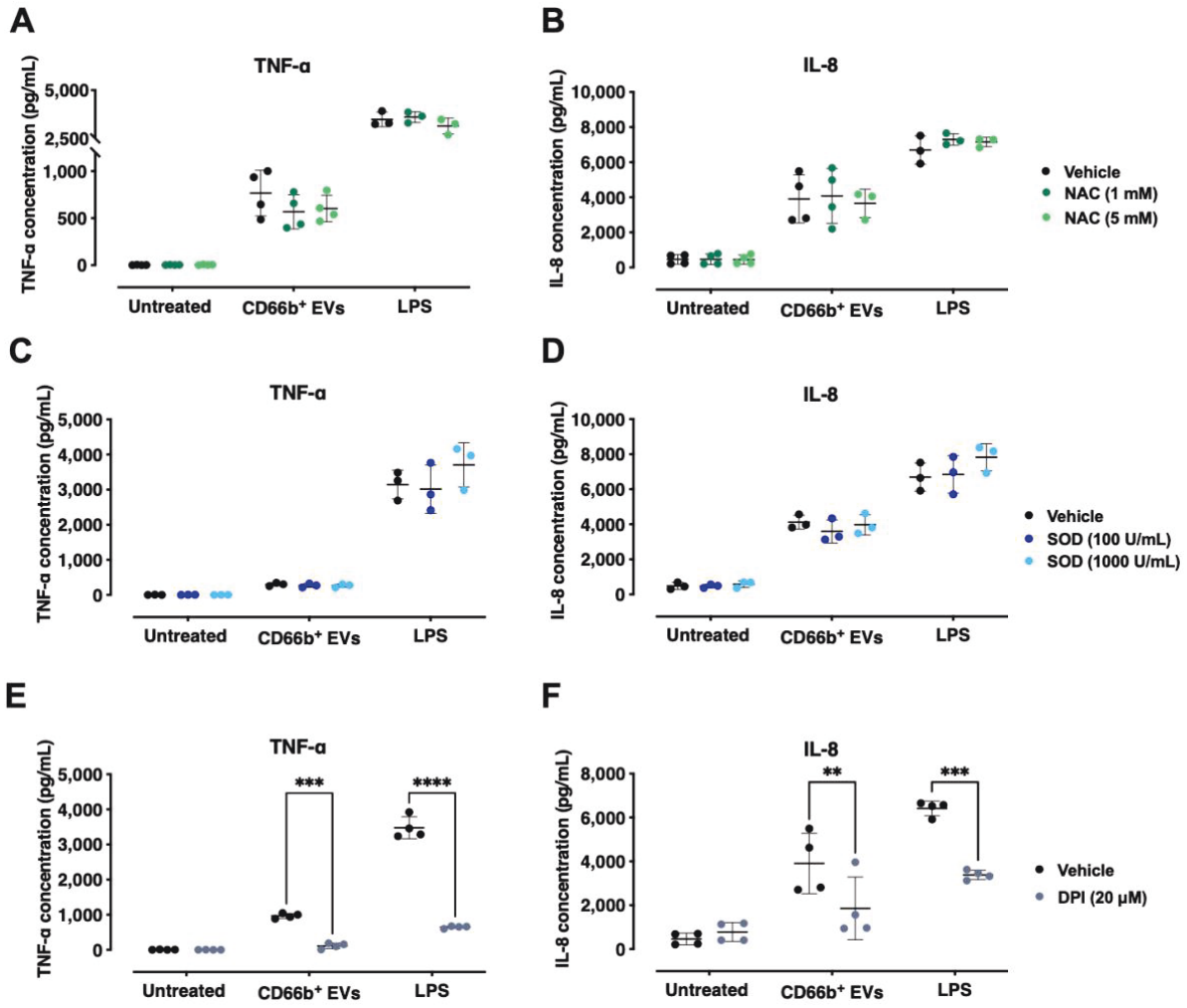

Figure 6.2. Neutrophil-EV-induced pro-inflammatory cytokine release is not ROS-dependent. Neutrophil-EVs (1 x 10^7/well) or LPS (10 ng/mL with 10 % FBS) were incubated with co-cultures of PBMCs and HLMECs in the presence of NAC (1 mM, 5 mM) (**A, B**), SOD (100 U/mL, 1000 U/mL) (**C, D**), DPI (20 µM) (**E, F**) or vehicle control (DMSO, 0.1 %) for 4 h. Neither NAC nor SOD treatment had any significant effect on neutrophil-EV and LPS-induced TNF-α and IL-8 release compared to vehicle control. DPI significantly reduced TNF-α and IL-8 release in both neutrophil-EV and LPS-treated co-cultures. Data are analysed by two-way ANOVA with Sidak's multiple comparisons test (A-F; mean ± SD). n=3-4, **p<0.01, ***p<0.001, ****p<0.0001.

6.4.3. Neutrophil-EVs induce pro-inflammatory cell activation and cytokine release in a TLR4-dependent mechanism

Given the observed similarities in kinase and ROS inhibition profiles between neutrophil-EVs and LPS, we decided to investigate whether neutrophil-EV-induced cytokine production was TLR4 dependent. Initially, an anti-TLR4 blocking antibody was used to block surface TLR4 on target cells prior to EV addition. By using LPS treatment as control, the antibody efficacy was confirmed. Interestingly, TLR4 blocking significantly attenuated the neutrophil-EV-induced cell activation and cytokine release (**Figure 6.3**).

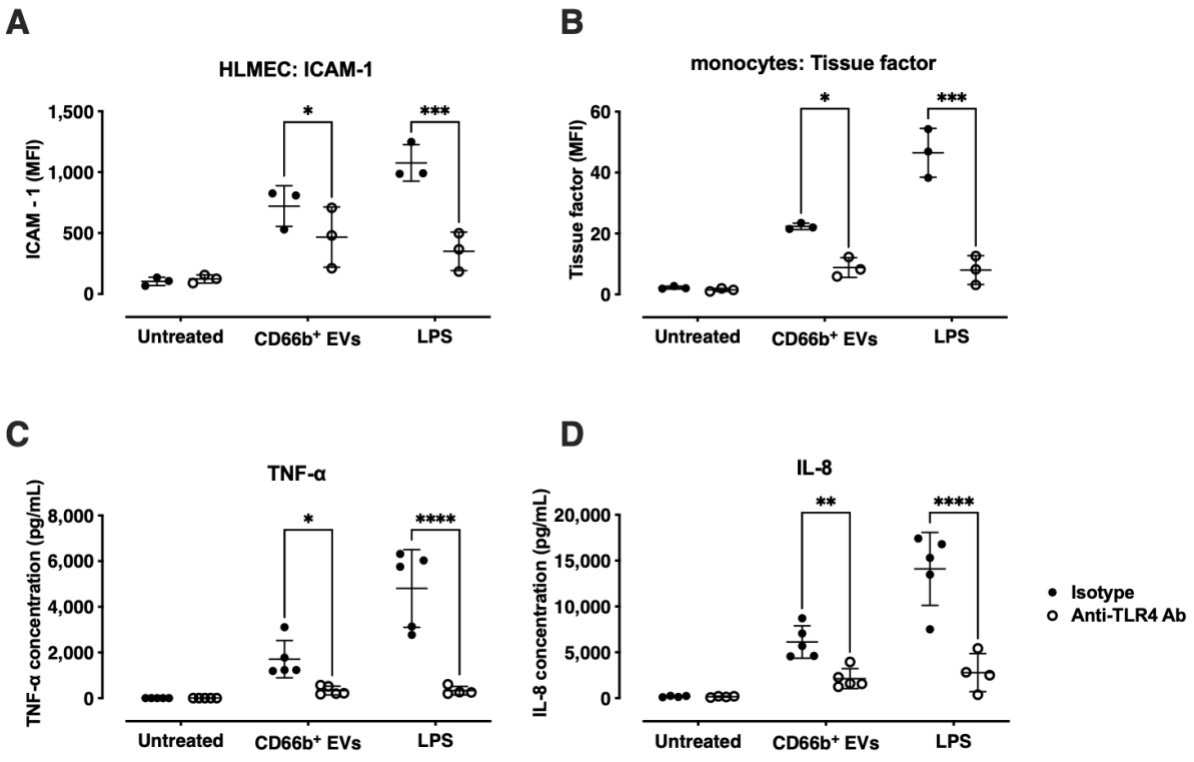

Figure 6.3. Neutrophil-EV-induced pro-inflammatory responses are inhibited by an anti-TLR4 blocking antibody.
Neutrophil-EVs (1 x 10^7/well) or LPS (10 ng/mL with 10 % FBS) were incubated with co-cultures of PBMCs and HLMECs in the presence of an anti-TLR4 blocking antibody (10 µg/mL) or isotype control (10 µg/mL) for 4 h. Anti-TLR4 treatment significantly reduced neutrophil-EV and LPS-induced upregulation of ICAM-1 on HLMECs (**A**), tissue factor on monocytes (**B**), and release of TNF-α (**C**), and IL-8 (**D**). Data are analysed by two-way ANOVA with Sidak's multiple comparisons test (A-D; mean ± SD). n=3-5, *p<0.05, **p<0.01, ***p<0.001, ****p<0.0001.

To confirm the above observations of TLR4 involvement in neutrophil-EV signalling, a cell-permeable TLR4 inhibitor, TAK-242, was used. Measuring inhibition of LPS-induced TNF-α release, an optimal concentration of TAK-242 for TLR4 blockade was determined (data not shown). Treatment of co-cultures with TAK-242 completely inhibited neutrophil-EV-induced upregulation of ICAM-1 on HLMECs, tissue factor on monocytes, and TNF-α and IL-8 release (**Figure 6.4**).

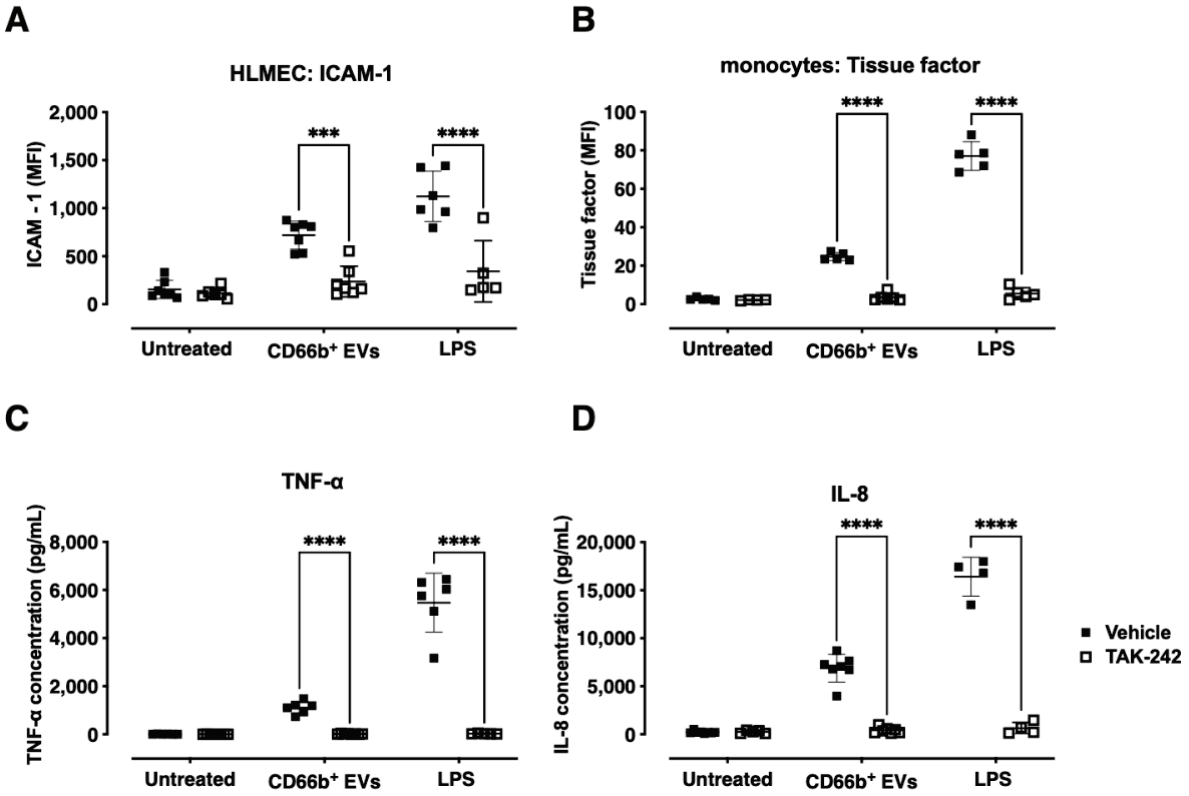

Figure 6.4. Blockade of TLR4 in PBMC-HLMEC co-cultures abolishes the neutrophil-EV pro-inflammatory activities.
Neutrophil-EVs (1 x 10^7/well) or LPS (10 ng/mL with 10 % FBS) were incubated with co-cultures of PBMCs and HLMECs in the presence of TAK-242 (10 μM) or vehicle control (DMSO, 0.1 %) for 4 h. TLR4 blockade completely reversed upregulation of ICAM-1 on HLMECs (**A**), tissue factor on monocytes (**B**), and inhibited TNF-α (**C**), and IL-8 (**D**) release after neutrophil-EV or LPS treatment. Data are analysed by two-way ANOVA with Sidak's multiple comparisons test (A-D; mean ± SD). n=5-8, ****p<0.0001.

6.4.4. Assessment of LPS involvement in neutrophil-EV activity

Although various DAMPs have been shown to signal through TLR4, production of EVs in LPS-stimulated blood suggested that monocyte activation by neutrophil-EVs could be due to LPS carryover. We considered this possibility in the previous study on myeloid-EVs (**Chapter 4**), but the extensive washing of column-bound EVs and the absence of cytokine-inducing activity in platelet-EVs isolated in parallel argued strongly against LPS contamination. To revisit this possibility in this study, we decided to use more orthogonal approaches to comprehensively evaluate the LPS involvement in the neutrophil-EV responses produced here.

We first assessed the potential for preferential or specific binding of LPS to neutrophil-EVs, which could explain the lack of activity in isolated platelet-EVs. We used a fluorescently-labelled LPS to stimulate whole blood and then assessed levels associated with released EVs. Although both non-conjugated LPS and Alexa Fluor™ 488-conjugated LPS were E. coli derived, we observed that a higher dose of the fluorescent LPS conjugate (1 µg/mL) was necessary to produce similar amounts of neutrophil-EVs to the non-conjugated LPS (100 ng/mL). Comparison of fluorescence levels associated with monocytes, platelets, and neutrophils, revealed that monocytes had relatively high amounts of LPS, with levels of ~50-fold lower on neutrophils and about half of that on platelets (**Figure 6.5**).

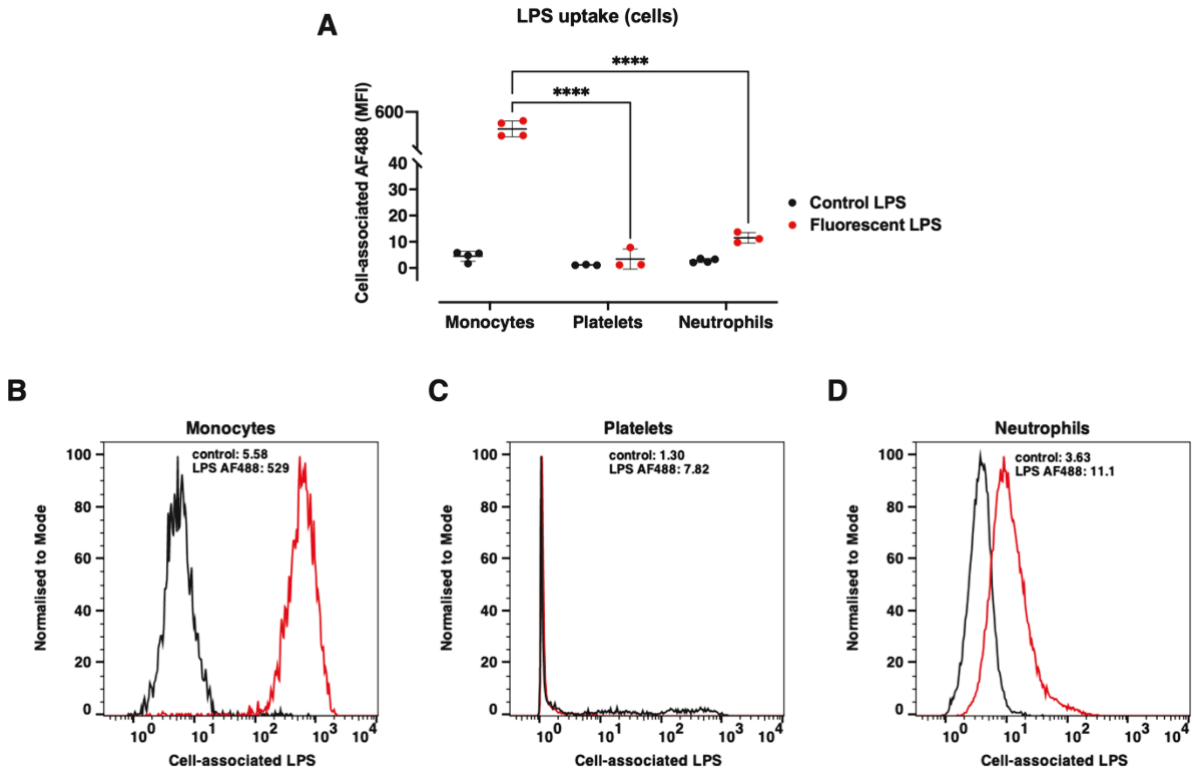

Figure 6.5. Preferential uptake of fluorescence-conjugated LPS in monocytes in whole blood. Heparinised whole blood was stimulated with unlabelled LPS (100 ng/mL, 3 h, 37 °C) or Alexa Fluor™ 488-conjugated-LPS (1 µg/mL, 3 h, 37 °C) in rotation. Monocyte-, platelet-, and neutrophil-associated LPS was quantified by flow cytometric analysis and presented as cell-associated AF488 fluorescence. Monocytes had the maximum LPS-uptake capacity compared to the two other cell populations (**A**). Data are analysed by two-way ANOVA with Sidak's multiple comparisons test (A; mean ± SD). n=3-4, ****p<0.0001. Histograms representative of n=4 experiments indicating cell-associated AF488 fluorescence on monocytes, platelets, and neutrophils (**B-D**).

LPS-associated with EV subtypes was also evaluated in the same assays. Following LPS stimulation of whole blood with non-conjugated or Alexa Fluor™ 488-conjugated LPS, monocyte-, neutrophil-, and platelet-EVs were determined in platelet poor plasma by flow cytometry. Alexa Fluor™ 488 fluorescence was detectable in all EVs, but levels were very similar between subtypes (**Figure 6.6**), suggesting that LPS does not preferentially associate with neutrophil-EVs, and this cannot explain the difference in activity between neutrophil- and platelet-EVs.

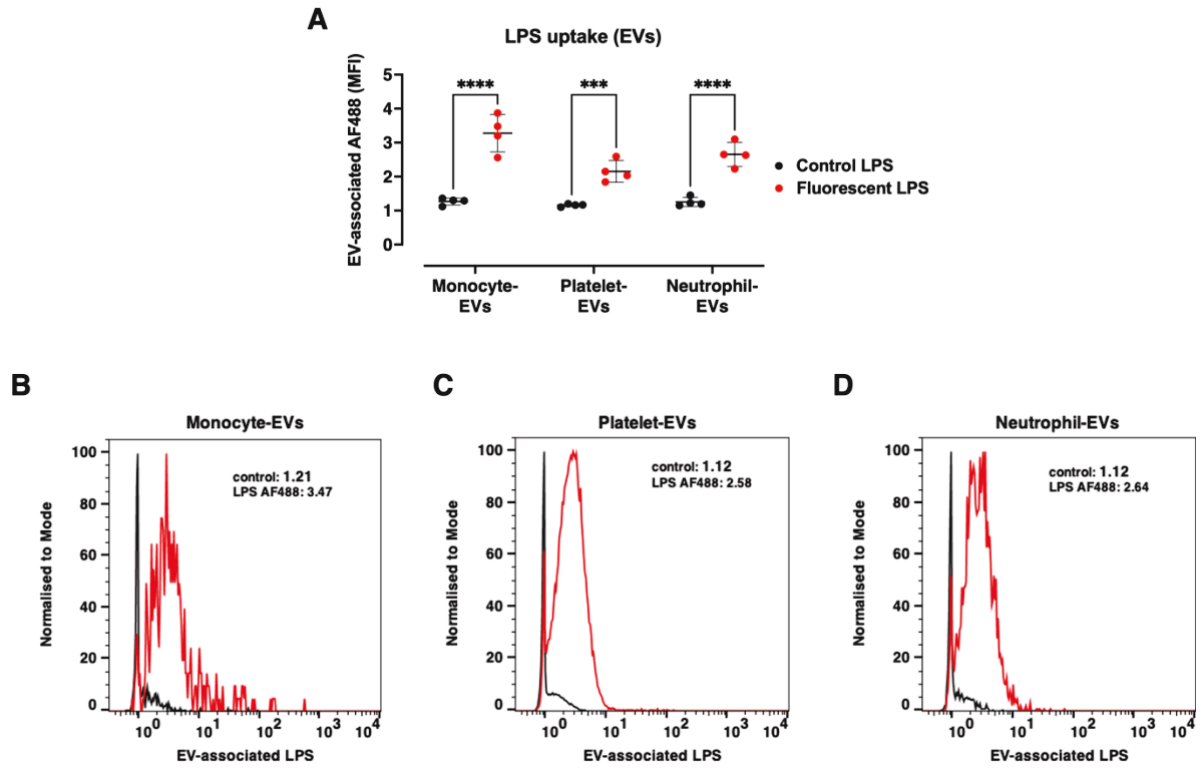

Figure 6.6. Similar levels of fluorescence-conjugated LPS are present in monocyte-, platelet-, and neutrophil-EVs.

Heparinised whole blood was stimulated with non-fluorescent LPS (100 ng/mL, 3 h, 37 °C) or Alexa Fluor™ 488 conjugated-LPS (1 µg/mL, 3 h, 37 °C) in rotation. Monocyte-, platelet-, and neutrophil-EVs were analysed in platelet poor plasma by flow cytometry for EV-associated AF488 fluorescence. Levels of LPS were similar in all three EV subtypes (**A**). Data are analysed by two-way ANOVA with Sidak's multiple comparisons test (A; mean ± SD). n=4, *p<0.05, **p<0.01, ***p<0.001. Histograms representative of n=4 experiments indicating EV-associated AF488 fluorescence on monocyte-, platelet-, and neutrophil-EVs (**B-D**).

Next, the LPS content of lysed neutrophil-EVs (1 x 10^7) was quantified using a commercially supplied LPS ELISA kit. An equal amount of platelet-EVs immunoaffinity isolated from LPS-stimulated whole blood was analysed as a comparator non-active EV preparation. A concentration of less than 30 pg/mL was found per 1 x 10^7 neutrophil-EVs (**Figure 6.7**). As the volume of the EV suspensions assayed was 50 µL, the total amount of LPS added to co-culture assays was <1.5 pg. Similar amounts of LPS levels were detected in the neutrophil- and platelet-EVs, confirming the results found with fluorescent LPS-exposed EVs (**Figure 6.6**).

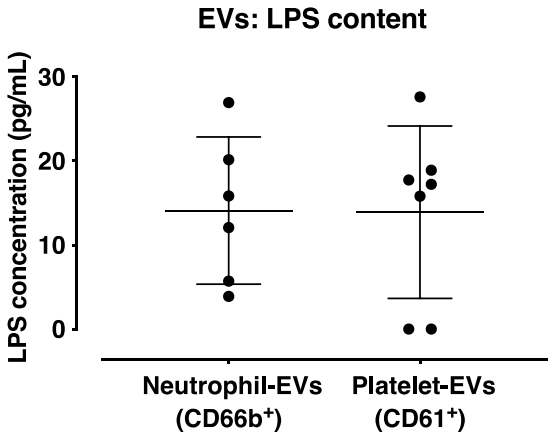

Figure 6.7. Quantification of LPS in isolated neutrophil- and platelet-EVs.
LPS levels were determined in neutrophil- and platelet- EVs by ELISA. EVs were lysed by two repeated freeze-thaw cycles (-80 °C to 37 °C), followed by a 2 min sonication at 50 Hz. Both EV subtypes carried similar levels of LPS ranging from 0-30 pg/mL. Data are analysed by two-tailed unpaired t-test (mean ± SD). n=6-7.

As a standard method for assessing LPS contamination in functional assays, we investigated the effect of polymyxin B treatment on neutrophil-EV-induced responses in PBMC-HLMEC co-cultures. Polymyxin B is a neutralising LPS antibiotic that binds to lipid A and blocks its activity. Pre-treatment of neutrophil-EVs with polymyxin B did not lead to significant reduction in cell activation and cytokine release, whereas it completely blocked the LPS-induced cell activation, carried out in parallel as a positive control (**Figure 6.8**).

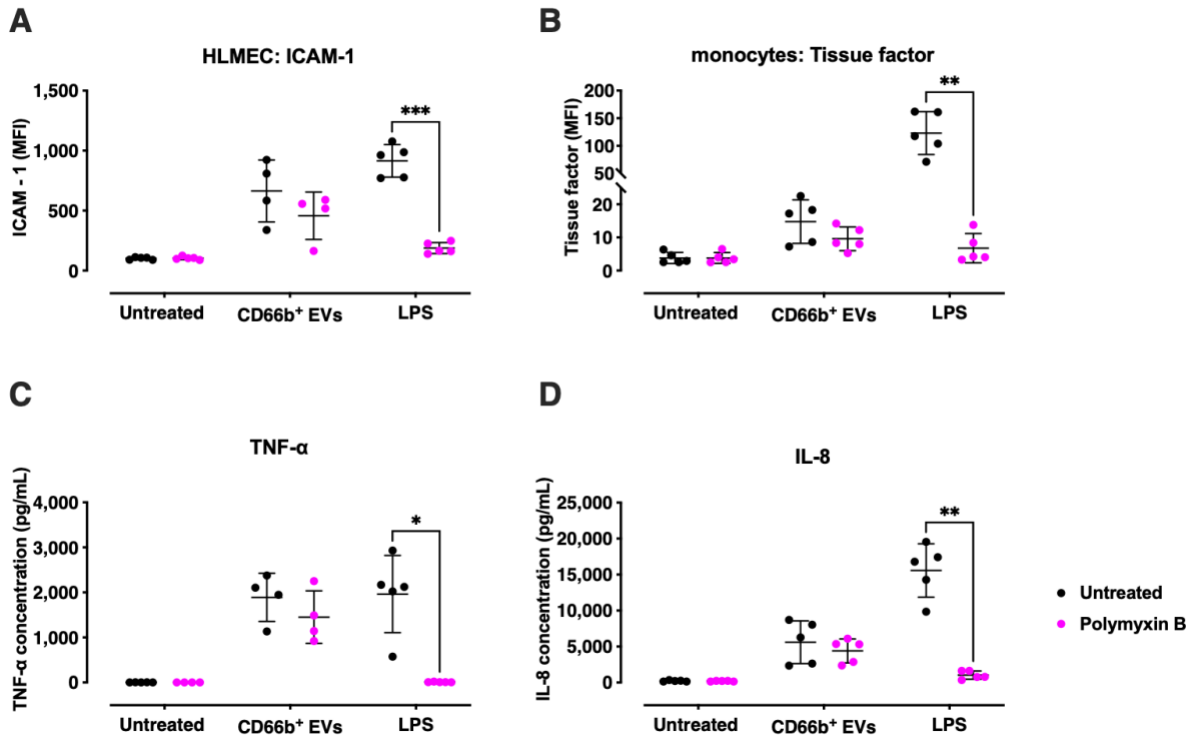

Figure 6.8. Neutrophil-EV activities are not inhibited by polymyxin B treatment.
Neutrophil-EVs (1 x 10^7/well) or LPS (10 ng/mL with 10 % FBS) were treated with polymyxin B (10 µg/mL, 1 h, in ice) prior to incubation with co-cultures of PBMCs and HLMECs for 4 h. Polymyxin B treatment did not significantly alter neutrophil-EV induced upregulation of ICAM-1 on HLMECs (**A**), tissue factor on monocytes (**B**), and release of TNF-α (**C**) or IL-8 (**D**), whereas it completely inhibited LPS-induced responses. Data are analysed by two-way ANOVA with Sidak's multiple comparisons test (A-D; mean ± SD). n=4-5, *p<0.05, **p<0.001, ***p<0.001.

LPS signalling requires the formation of a complex with CD14, MD-2, and LPS binding protein (LBP), which is normally present in serum, to induce inflammatory signalling in monocytes and endothelial cells (487, 488). Of note, the neutrophil-EV functional assays were conducted under serum-free conditions throughout this investigation. We, therefore, speculated that if the neutrophil-EV activity was dependent on trace amounts of LPS, serum would be critical to generate measurable responses (**Figure 6.9**). I compared neutrophil-EV treatment of PBMC-HLMEC co-cultures with or without (EV-depleted) FBS but its presence did not affect the responses. In sharp contrast, FBS was essential for the generation of detectable response to LPS at 1 ng/mL and significantly enhanced the responses to LPS at 10 ng/mL LPS. As it was

unlikely for neutrophil-EVs to include higher concentration of LPS than 1 ng/mL, these findings suggest that neutrophil-EV activity is most possibly not mediated by residual LPS content.

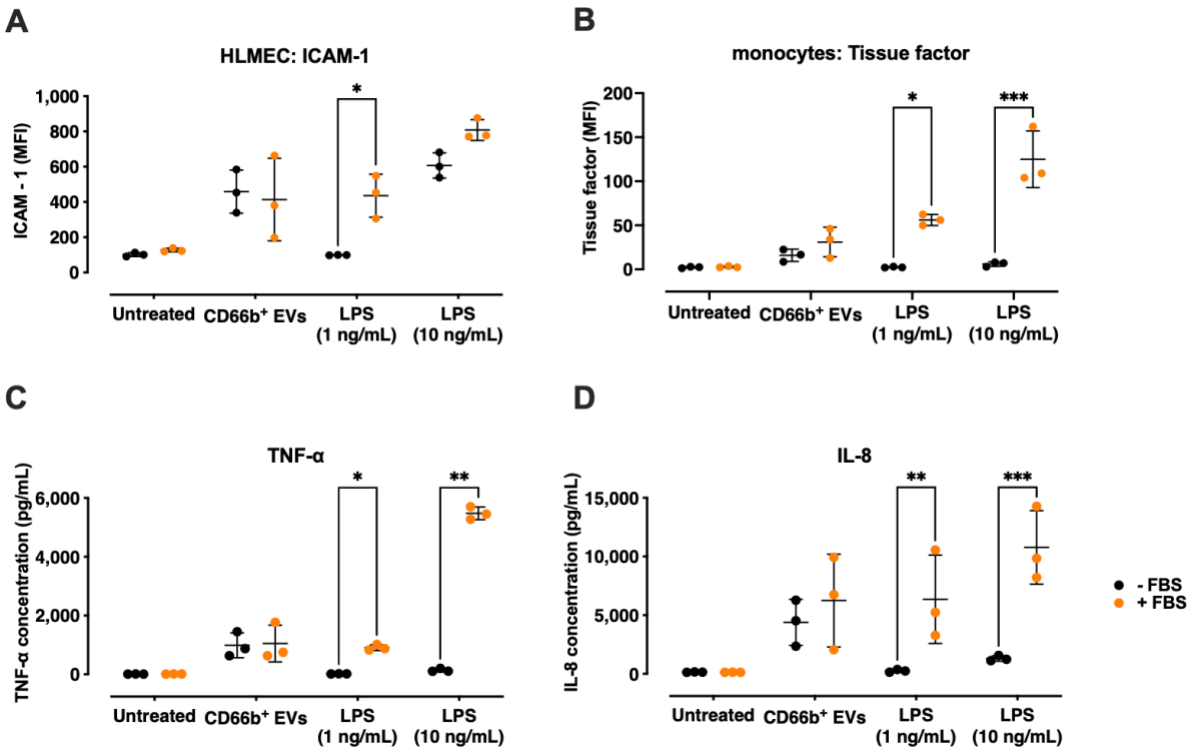

Figure 6.9. Neutrophil-EV-mediated cell activation is not affected by serum.
Neutrophil-EVs (1 x 10^7/well) or LPS (1 or 10 ng/mL) were incubated with co-cultures of PBMCs and HLMECs with or without 10 % FBS for 4 h. The presence of FBS was necessary for lower LPS concentration (1 ng/mL) to induce upregulation of ICAM-1 on HLMECs (**A**), tissue factor on monocytes (**B**), and release of TNF-α (**C**) or IL-8 (**D**), while it significantly enhanced the response elicited by higher LPS concentration (10 ng/mL). By contrast, neutrophil-EV responses were independent of FBS. Data are analysed by two-way ANOVA with Sidak's multiple comparisons test (A-D; mean ± SD). n=3, *p<0.05, **p<0.01, ***p<0.001.

We then wondered whether neutrophil-EVs internalise and carry LPS as 'hidden' cargo that is not accessible to polymyxin B neutralisation. To investigate this possibility, neutrophil-EVs were lysed by two freeze-thaw cycles and sonication to expose any hidden LPS. I then assessed their activity and any modification by treatments with polymyxin B and/or FBS treatment (**Figure 6.10**). Neutrophil-EVs remained active despite the lysis treatment and neither polymyxin B nor FBS treatment alone or in combination appeared to significantly

modify the responses. These findings provide further evidence that any neutrophil-EV cargo of LPS is not bioactive.

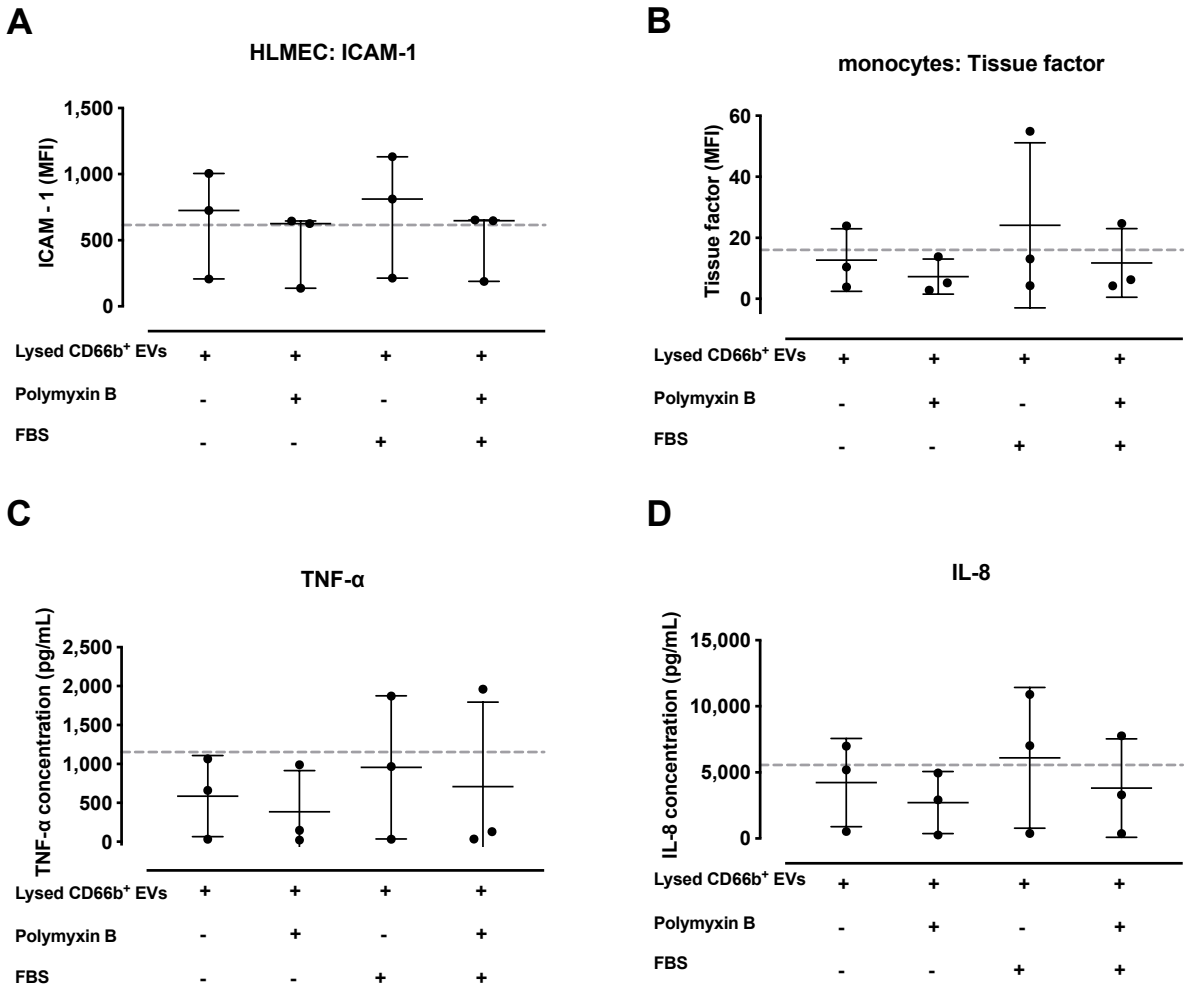

Figure 6.10. Effect of polymyxin B and FBS treatment on lysed neutrophil-EV activity.
Neutrophil-EVs were lysed by two repeated freeze-thaw cycles (-80 °C to 37 °C), followed by sonication for 2 min at 50 Hz. Lysed EVs were treated with polymyxin B (10 µg/mL, 1 h, in ice) or left untreated and added to co-cultures of PBMCs and HLMECs at 1 x 10^7/well for 4 h with or without 10 % FBS. Polymyxin B and FBS treatment, alone or in combination, did not modify the upregulation of ICAM-1 on HLMECs (**A**), tissue factor on monocytes (**B**), and release of TNF-α (**C**) or IL-8 (**D**). Dotted line represents the response elicited by intact neutrophil-EVs. Data are analysed by Kruskal-Wallis with Dunn's multiple comparisons test (A; median ± interquartile range); or one-way ANOVA with Bonferroni's multiple comparisons test (B-D; mean ± SD). n=3.

6.4.5. Neutrophil-EV activity is mediated by surface proteins

As our data pointed to neutrophil-EV activation of TLR4 signalling independently of LPS, we hypothesised that the activity was a neutrophil-derived endogenous protein or modified lipid. To assess the contribution of protein, I used proteinase K treatment to digest all proteins on the neutrophil-EV surface. To avoid additional centrifugation steps for post-treatment EV washing, I used a heat-labile proteinase K that could be inactivated by brief incubation at 55 °C. Incubation with proteinase K and heat treatment completely attenuated neutrophil-EV-induced responses (**Figure 6.11**). A 'sham' control of heat-treated-only neutrophil-EVs produced a partial reduction of activity that was significant in the case of TNF-α (**Figure 6.11, C**). Although complicating the analysis of the proteinase K effect, the sensitivity to heat treatment also supported a role for proteins which can be denatured and inactivated with relatively mild heat treatment protocols as used here (e.g., complement). By contrast, neither proteinase K nor heat treatment had any effect on LPS-induced responses, providing further evidence the neutrophil-EV activity was LPS-independent.

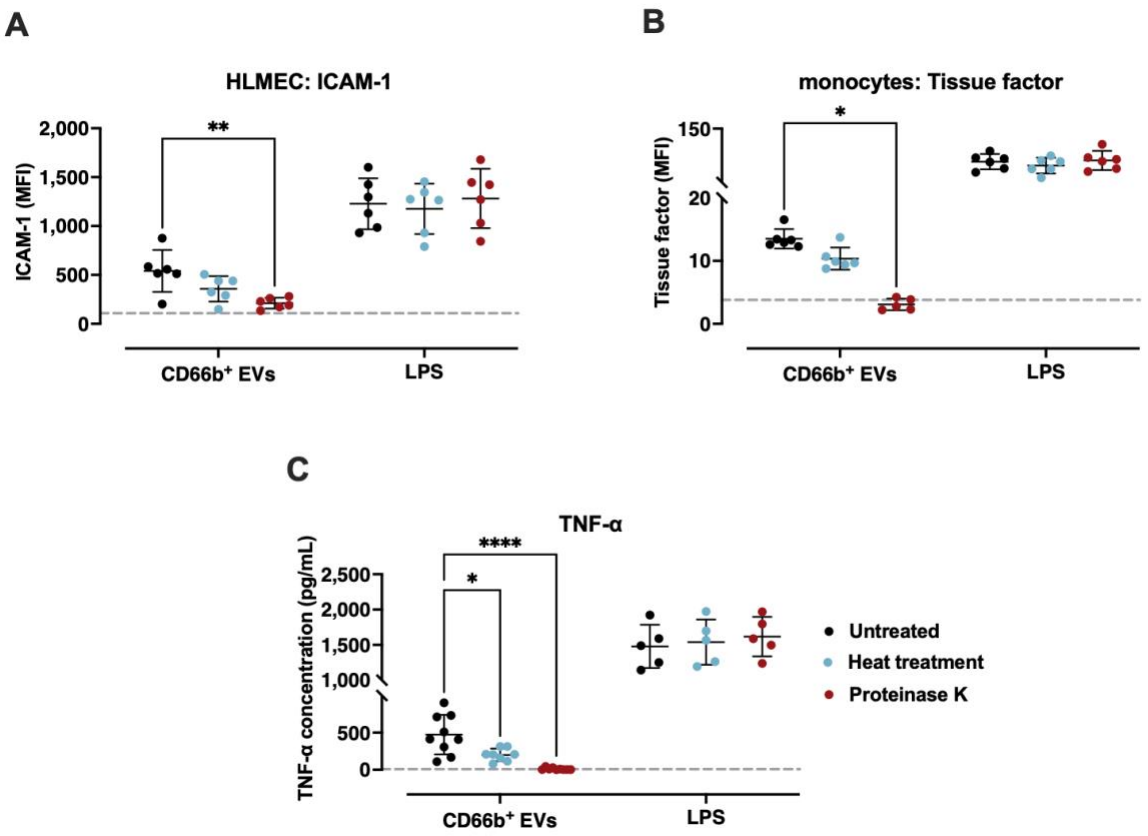

Figure 6.11. Neutrophil-EV activity depends on surface proteins.
Neutrophil-EVs (1 x 10^7/well) or LPS (10 ng/mL) were treated with proteinase K (2.5 U/mL, 45 min, 37 °C) followed by enzyme inactivation by heat treatment (15 min, 55 °C) and then incubated with co-cultures of PBMCs and HLMECs for 4 h. In LPS-treated wells, 10 % FBS was supplemented after the proteinase K treatment. Untreated or heat-treated only (45 min at 37 °C followed by 15 min at 55 °C) EVs were used as controls. Proteinase K treatment of neutrophil-EVs inhibited the upregulation of ICAM-1 on HLMECs (**A**), tissue factor on monocytes (**B**), and release of TNF-α (**C**). Heat treatment alone partially reduced the observed responses, reaching statistical significance only in the case of TNF-α release. Neither proteinase K nor heat treatment had any effect on the LPS-induced responses. Dotted line indicates the baseline levels of untreated co-cultures. Data are analysed by two-way ANOVA with Sidak's multiple comparisons test (A-C; mean ± SD). n=5-9, *p<0.05, **p<0.01, ****p<0.0001.

We then considered the possibility that LPS is bound to EV surface proteins in an active form and loses activity once released by protein digestion in a serum-free medium. I repeated the above proteinase K treatments with the addition of FBS to PBMC-HLMEC co-cultures to support signalling by any unbound LPS. However, FBS addition had no effect on the activity of the proteinase K-treated neutrophil-EVs (**Figure 6.12**). These findings further supported the

notion that neutrophil-EV activity is not driven by neutrophil-EV bound LPS and that the neutrophil-EV stimulatory component is found in their surface protein fraction.

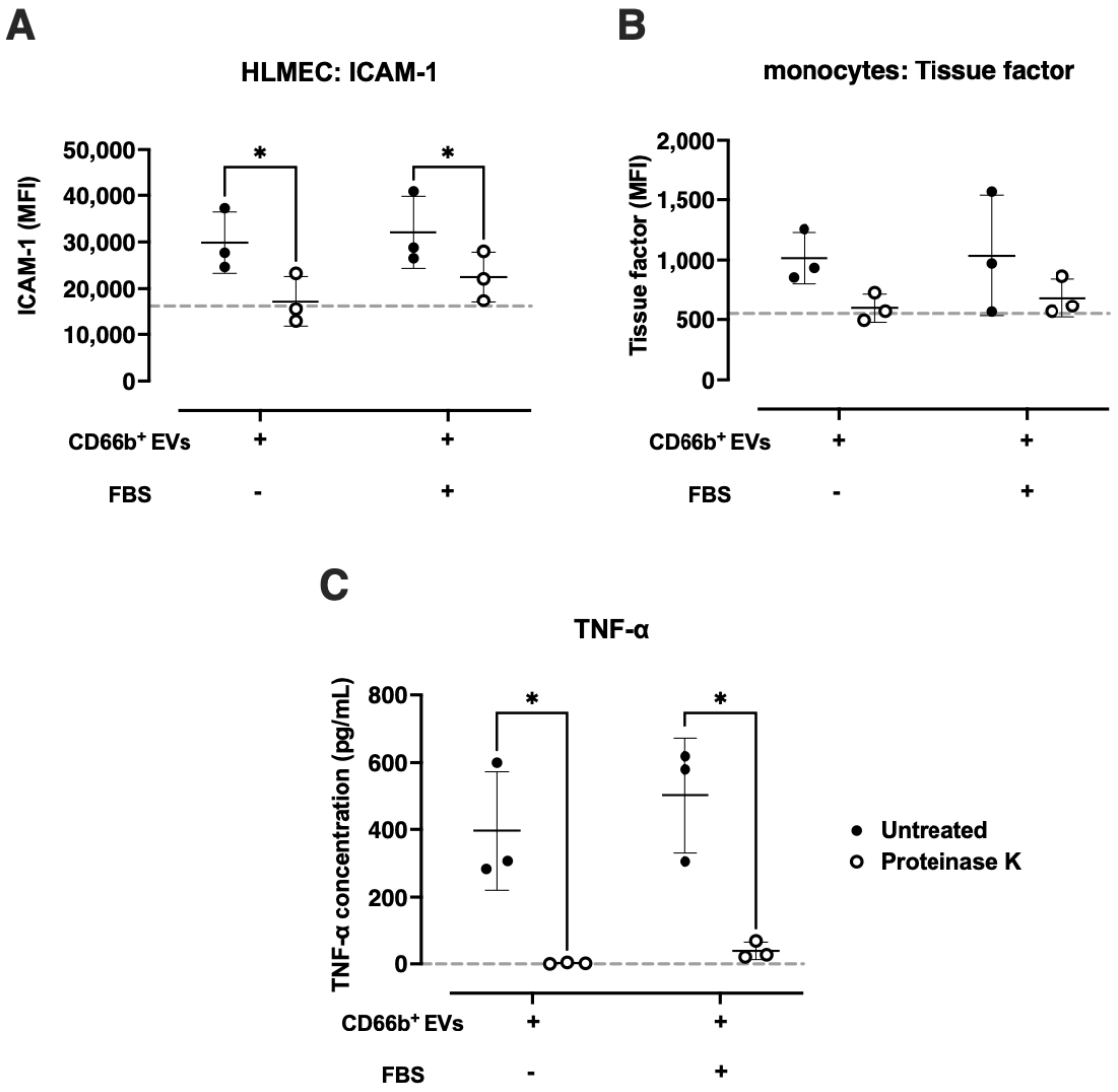

Figure 6.12. The proteinase K-mediated inhibition of neutrophil-EV activity is not reversed by FBS.

Neutrophil-EVs (1 x 10^7/well) were treated with proteinase K (2.5 U/mL, 45 min, 37 °C) followed by enzyme inactivation (15 min, 55 °C) and added to PBMC-HLMEC co-cultures for 4 h with or without 10 % FBS. The presence of FBS did not enhance the upregulation of ICAM-1 on HLMECs (**A**), tissue factor on monocytes (**B**), and release of TNF-α (**C**) by proteinase K-treated neutrophil-EVs. Dotted line indicates the cell activation and cytokine release levels in untreated co-cultures. Data are analysed by two-way ANOVA with Sidak's multiple comparisons test (A-C; mean ± SD). n=3, *p<0.05. Note: for these experiments, the Cytek® Northern Lights™ flow cytometer was used.

6.4.6. Preliminary investigation of specific TLR4 agonists on neutrophil-EVs

LPS is a known stimulus for neutrophil extracellular trap (NET) formation in blood (489, 490), while NETs themselves may be capable of activity with TLR4 signalling via associated DAMPs (potentially proteins, e.g., MRP8/14) and DNA (491, 492). Since cell-free NETs have the potential to carry neutrophil markers such as CD16 (493), we could not exclude the possibility of CD66b presence on NETs and therefore NET co-isolation from blood with neutrophil-EVs. Using a DNA stain (SYTOX Green) and an anti-myeloperoxidase (MPO) antibody, NETs could not be detected in neutrophil-EV preparations by flow cytometry (data not shown). As an alternative strategy, I carried out DNase I treatment to solubilise potential NET structures and release bound proteins. In these experiments, LPS was used as a positive control to determine any non-specific effect of DNase I treatment. No obvious differences were observed with DNase I treatment in the neutrophil-EV-induced cell activation and cytokine release (**Figure 6.13**).

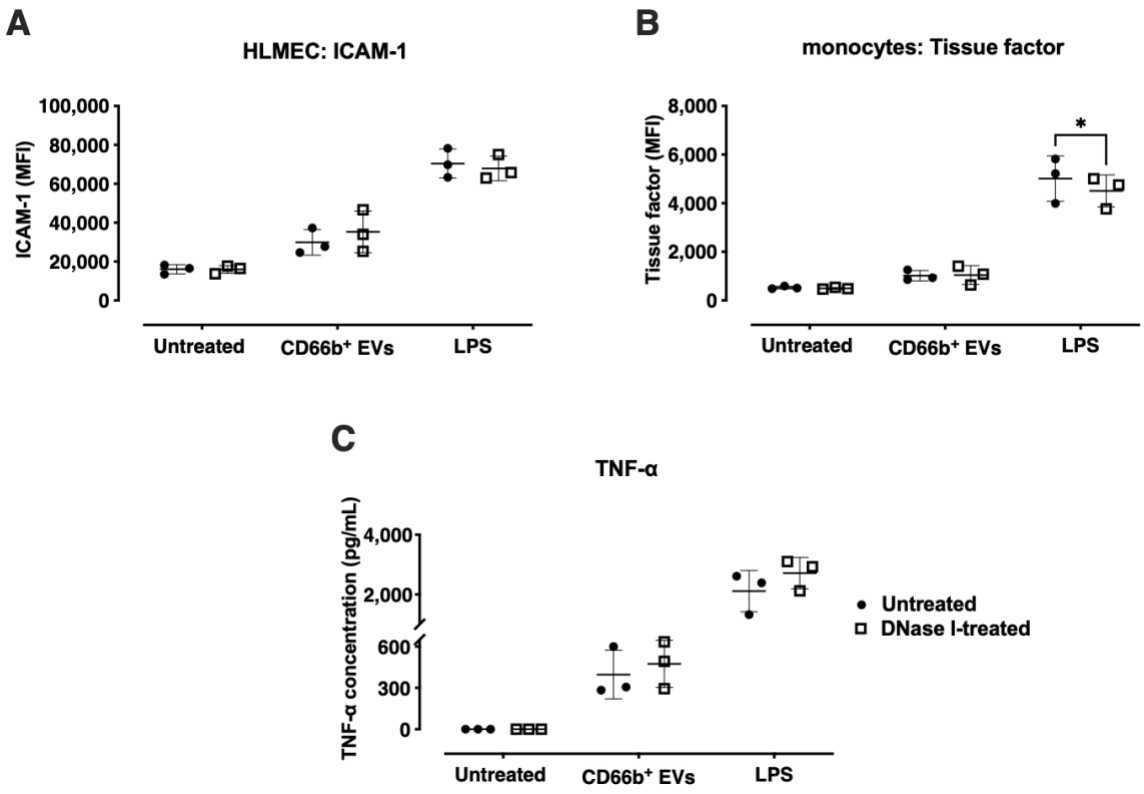

Figure 6.13. Neutrophil-EV pro-inflammatory activity is not sensitive to DNase I treatment. Neutrophil-EVs (1 x 10^7/well) or LPS (10 ng/mL with 10 % FBS) were treated with DNase I (200 U/mL, 15 min, 37 °C) and added to PBMC-HLMEC co-cultures (4 h). DNase I treatment did not significantly modify the LPS or neutrophil-EV activity in terms of ICAM-1 upregulation on HLMECs (**A**), or TNF-α release (**C**), although it did produce a small decrease in the LPS-induced upregulation of tissue factor on monocytes, without affecting that induced by neutrophil-EVs (**B**). Data are analysed by two-way ANOVA with Sidak's multiple comparisons test (A-C; mean ± SD). n=3, *p<0.05. Note, for these experiments the Cytek® Northern Lights™ flow cytometer was used.

Previous proteomic analyses have demonstrated that neutrophil-EVs contain a vast number of parent cell proteins including DAMP-like molecules that signal through the TLR4 pathway (292, 297, 476). I chose two candidate proteins to investigate based on their reported expression in neutrophils or their EVs, TLR4 signalling, and commercial availability of blocking agents. The first of these was the MRP8/14 complex which has recently been shown to be expressed on a special type of neutrophil-EVs released during rolling (475). Blocking of MRP8/14 with a neutralising antibody (**Figure 6.14**) or an MRP14 small molecule inhibitor, Paquinimod (**Figure 6.15**), did not affect the neutrophil-EV mediated responses.

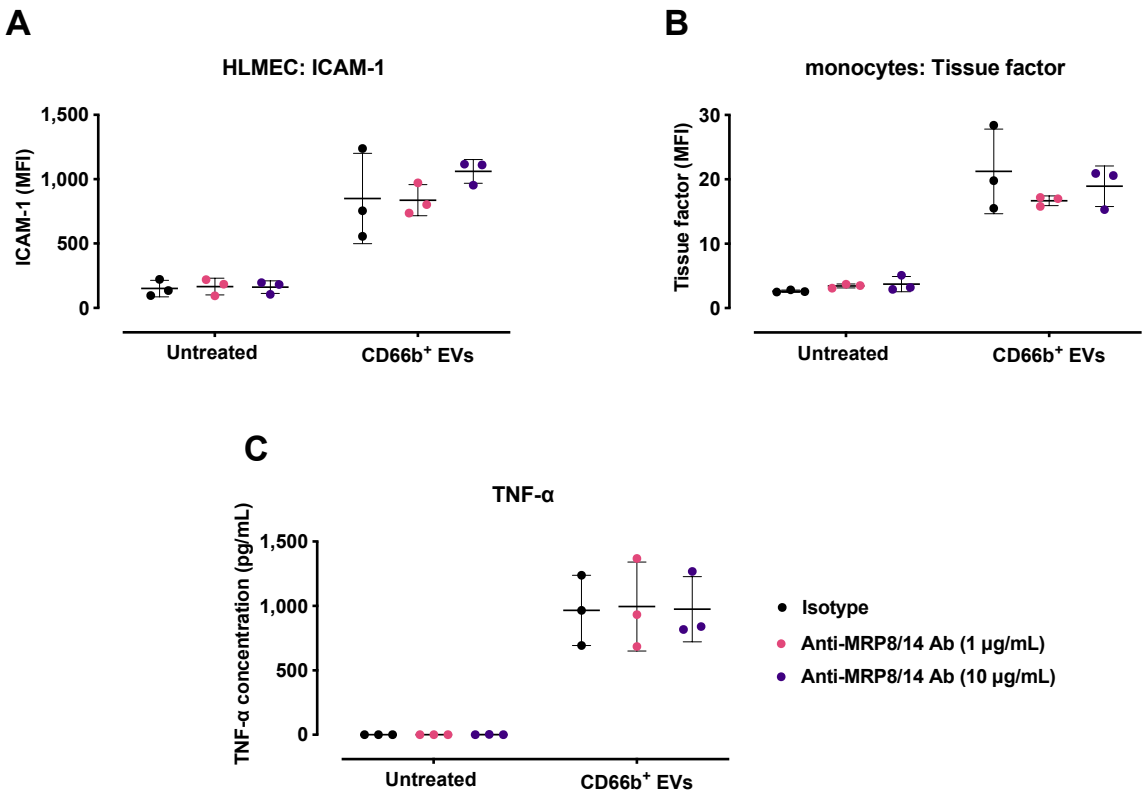

Figure 6.14. Neutrophil-EV-induced pro-inflammatory responses are not inhibited by an anti-MRP8/14 blocking antibody.
Co-cultures of PBMCs and HLMECs were co-incubated with neutrophil-EVs (1 x 10^7/well, 4 h) pre-treated with an anti-MRP8/14 blocking antibody (1 µg/mL or 10 µg/mL) or isotype control (10 µg/mL). Anti-MRP8/14 treatment did not affect the neutrophil-EV-induced upregulation of ICAM-1 on HLMECs (**A**), tissue factor on monocytes (**B**) or TNF-α release (**C**). Data are analysed by two-way ANOVA with Sidak's multiple comparisons test (A-C; mean ± SD). n=3.

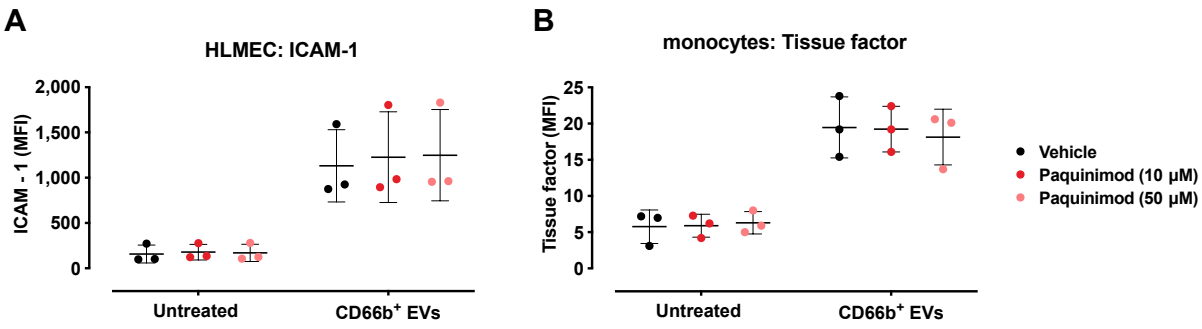

Figure 6.15. Neutrophil-EV-induced pro-inflammatory responses are not affected by treatment with Paquinimod, an MRP14 small molecule inhibitor.
Co-cultures of PBMCs and HLMECs were co-incubated with neutrophil-EVs (1 x 10^7/well, 4 h) pre-treated with Paquinimod (10 µM or 50 µM, 1 h, ice) or vehicle control (DMSO, 0.1 %). Inhibition of MRP14 on neutrophil-EVs did not affect the neutrophil-EV-induced upregulation of ICAM-1 on HLMECs (**A**) and tissue factor on monocytes (**B**). Data are analysed by two-way ANOVA with Sidak's multiple comparisons test (A-B; mean ± SD). n=3.

I also investigated HSP70, but blockade with a neutralising antibody did not result in any differences in neutrophil-EV-induced cell activation (**Figure 6.16**). The results presented in **Figure 6.16** represent 3 technical replicates from the same experiment and therefore further repeats are required to obtain definite answers on the direct role and existence of HSP70 on neutrophil-EVs.

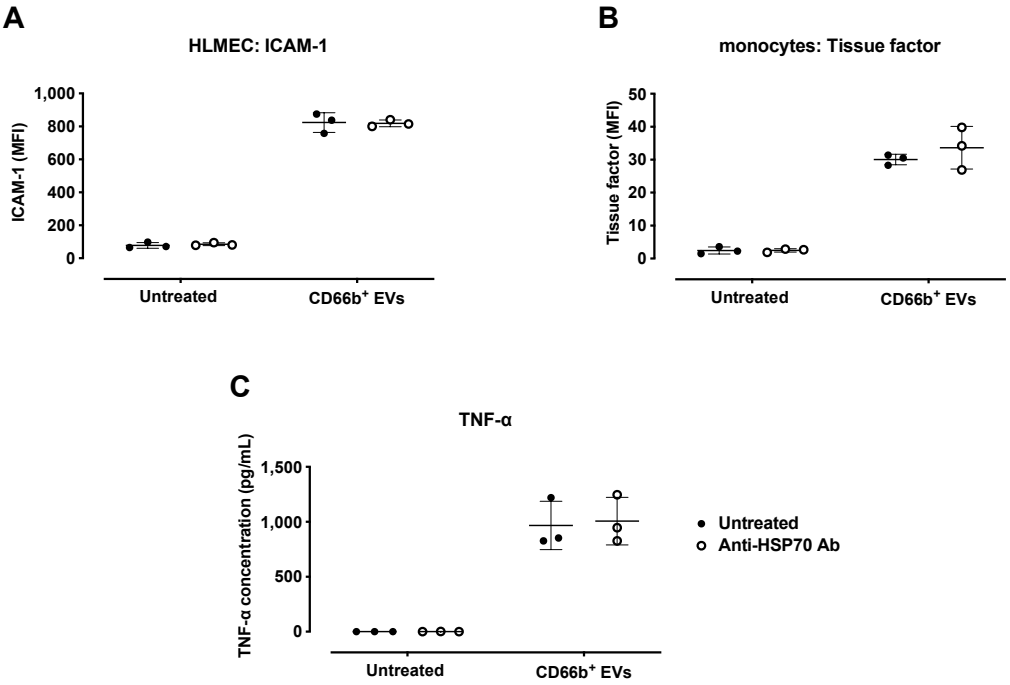

Figure 6.16. HSP70 blockade by neutralising antibody treatment does not influence the neutrophil-EV pro-inflammatory responses.
Co-cultures of PBMCs and HLMECs were co-incubated with neutrophil-EVs (1 x 10^7/well, 4 h) pre-treated with a blocking anti-HSP70 antibody (1:100 antibody dilution, 30 min, 37 °C). HSP70 blocking on neutrophil-EVs did not affect the neutrophil-EV-induced upregulation of ICAM-1 on HLMECs (**A**), tissue factor on monocytes (**B**), and TNF-α release (**C**). (A-C; mean ± SD). n=3 technical replicates (statistical analysis not performed).

6.5. Discussion

In this chapter, I investigated the mechanisms underlying neutrophil-EV pro-inflammatory signalling, with a particular focus on TNF-α release. I found that the neutrophil-EV-induced responses were mediated by surface proteins that interacted with TLR4 on target cells activating downstream MAPK p38, ERK1/2 as well as PI3K pathways. Despite similarities between neutrophil-EV and LPS responses and signalling pathways involved (TLR4 and MAPK pathways), a series of investigations revealed that the neutrophil-EV activity is not a result of LPS carry-over from the whole blood assay. Instead, I found that the activity may reside in protein(s) on the surface of neutrophil-EVs suggesting a neutrophil-derived endogenous DAMP capable of signalling via monocyte TLR4. Collectively, these findings support the initial hypothesis that neutrophil-EVs are potent long-range mediators, acting as vehicles for DAMPs, minimising a loss of activity within the circulation before acting on target sites such as the pulmonary vasculature. The proposed model of neutrophil-EV signalling in monocytes is shown in **Figure 6.17**.

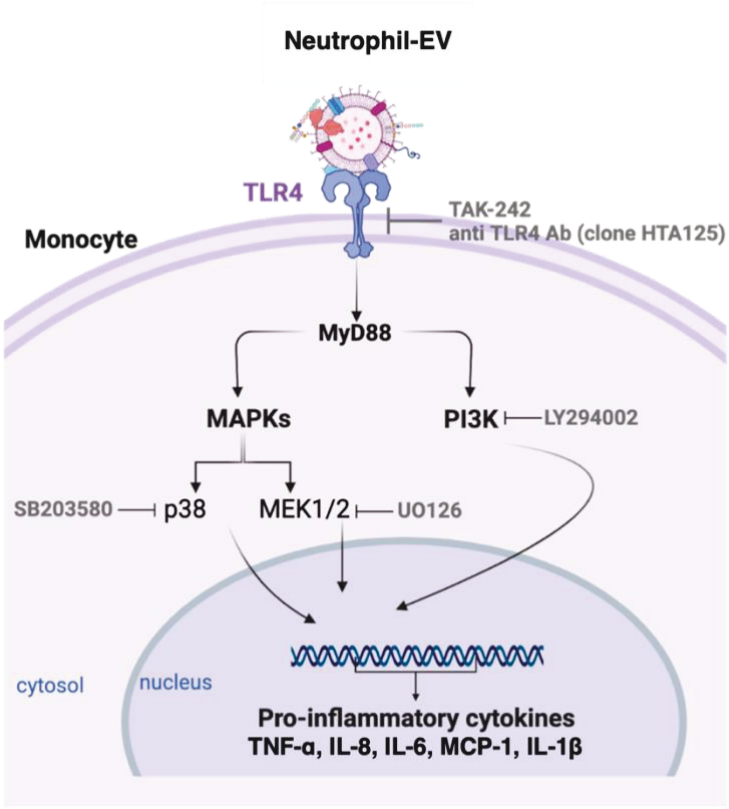

Figure 6.17. Schematic presentation of the proposed model for neutrophil-EV signalling on monocytes towards pro-inflammatory cytokine release.
Neutrophil-EVs carry DAMP-like surface proteins interacting with TLR4 on monocytes. Upon ligation, TLR4 activates downstream kinase pathways such as p38, ERK1/2, and PI3K inducing subsequent pro-inflammatory cytokine release (TNF-α, IL-8, IL-6, MCP-1, and IL-1β). Figure designed with Biorender.

Inflammatory activation of leukocyte populations within the lung microvasculature is a critical event that leads to excessive lung inflammation. Having observed increased levels of pro-inflammatory cytokines, including TNF-α, in co-culture supernatants following neutrophil-EV treatment, upstream kinase pathways known to be involved in such monocyte responses were explored. By using specific kinase inhibitors, I found that blockade of p38 and MEK1/2 (upstream regulator of ERK1/2), significantly decreased neutrophil-EV-induced pro-inflammatory cytokine release. However, JNK-1 inhibition did not result in similar inhibition, having no effect on the neutrophil-EV pro-inflammatory phenotype. Contrasting with this finding, Mesri et al., previously described pro-inflammatory activation of HUVECs following neutrophil-EV treatment, leading to IL-8 and IL-6 secretion which was reversible by JNK-1

blockade (326). As neutrophil-EV activity in the present study was driven by monocytes, the lack of JNK-1 blocking effect here may not be surprising and indicates that different signalling pathways could be involved in neutrophil-EV-induced endothelial cell and monocyte activation.

Apart from MAPKs the role of PI3K, a kinase that belongs to a different kinase family mainly involved in the AKT/mTOR pathway, was also investigated in neutrophil-EV signalling. PI3K has been previously linked to endocytosis as a regulator of the actin cytoskeleton and its inhibition in macrophages by wortmannin or LY294002 treatment ablated neutrophil-EV or tumour cell exosome uptake (473, 494). Despite its well-defined role in endocytosis processes, its involvement in LPS-induced responses in monocytes has been somewhat controversial. Some studies reported that PI3K acts as a negative regulator of LPS-induced cytokines, as its inhibition increased TNF-α and tissue factor expression in LPS-treated monocytes (495, 496), while others demonstrated that PI3K has a central role in enhancing downstream TLR4 signalling and cytokine release, mainly IL-1β (497). Here, PI3K blockade by LY294002 treatment significantly decreased the inflammatory activation of HLMECs and monocytes and abolished cytokine release following neutrophil-EV treatment, while it did not affect the LPS-induced responses. Although these findings provide the basis for further exploration of PI3K's role in neutrophil-EV signalling, further research is needed to first determine whether decreased neutrophil-EV activity after PI3K inhibition is a result of decreased EV uptake. Nevertheless, the observed differences between neutrophil-EVs and LPS activity with PI3K blockade, support the notion that although produced following LPS stimulation of whole blood, neutrophil-EVs may have a distinct mechanism of action.

Apart from their microbicidal activities in neutrophils, ROS are involved in MAPK activation in endothelial cells, monocytes, and macrophages (484, 498, 499). Neutrophil-EVs can produce ROS via NADPH oxidase, which in turn can trigger pro-inflammatory signalling in these target cells (292, 445, 472). These findings prompted us to address whether ROS are involved in the pro-inflammatory neutrophil-EV phenotype in the PBMC-HLMEC co-culture model. Despite the supporting evidence of ROS-mediated neutrophil-EV activity, stimulation of co-cultures

with neutrophil-EVs in the presence of ROS inhibitors NAC and SOD, did not have any effect on the pro-inflammatory responses. Of note, SOD is a membrane-impermeable inhibitor that converts $\cdot O_2^-$ into H_2O_2 and the addition of catalase, which decomposes H_2O_2, would be required to prevent any extracellular ROS activities. Although catalase was tested in this study, the commercially available product used, produced background cell activation and cytokine release in our assays (data not shown). Therefore, additional experiments with a higher-grade catalase would be needed to complete this line of investigation. In the same experiments DPI, a NAPDH oxidase inhibitor, was tested which interestingly resulted in a significant decrease in cell activation and cytokine release in both neutrophil-EV and LPS-treated co-cultures. Park et al., demonstrated that NADPH oxidase is involved in LPS-induced ROS production and NF-κB activation mediated by TLR4 signalling (500). These findings combined with our observations on the sensitivity of neutrophil-EV and LPS activity to DPI inhibition, suggest that they may have a similar mechanism of action and therefore we decided to investigate it further by assessing the role of the TLR4 pathway.

TLR4-mediated EV signalling was previously reported by others. EVs, obtained from erythrocytes, mesenteric lymph nodes, or tumour cells induced increased pro-inflammatory cytokine release, which was reversible by TLR4 inhibition (501-503). In addition, several TLR4 ligands such as HMGB-1 (504), HSP70 (292, 480), MRP8/14 (292, 475-478), and citrullinated histones (317, 473, 474) have been found present in neutrophil-EVs either as cargo or surface molecules. Here, we demonstrated that neutrophil-EV activity could be partially inhibited by an anti-TLR4 antibody and completely inhibited by a cell-permeable TLR4 inhibitor, TAK-242. These findings supported the notion that neutrophil-EVs might be carrying TLR4 activating proteins responsible for their pro-inflammatory properties. However, because of the prolonged exposure of neutrophils and neutrophil-EVs to LPS in the whole blood assay, and the absence of pro-inflammatory activity in the fMLP-generated neutrophil-EVs found by my colleagues (461), we decided to perform an in-depth investigation into whether LPS association with neutrophil-EVs was responsible for their pro-inflammatory activity.

Using a fluorescent LPS conjugate, I found that monocytes had several-fold higher LPS binding/uptake capacity compared to neutrophils and platelets in agreement with previous findings from Schlichting et al., (505). Interestingly, I found that although LPS binding/uptake was detected in EVs, the levels were consistent between monocyte-, neutrophil-, and platelet-EVs. However, as monocyte-EV numbers did not increase during LPS stimulation, the $CD11b^+$ $CD14^+$ EVs analysed may have been present in plasma already and not derived from LPS-loaded parent monocytes. The LPS content of 1×10^7 neutrophil- or platelet-EVs (EV number added per well in PBMC-HLMEC co-culture) was measured by ELISA and found similar in both subtypes and of much lower level (0-30 pg/mL, 1.5 pg total), much lower than the minimum LPS concentration (≥1 ng/mL) needed to produce a detectable pro-inflammatory cell activation (**Figure 4.7**). Nevertheless, we explored the potential for signalling by neutrophil-EV bound LPS by pre-incubating and assaying in the presence of the LPS-neutralising antibiotic, polymyxin B, but found that responses were not significantly reduced. Lastly, neutrophil-EV responses were not enhanced in the presence of FBS, in contrast to its very substantial enhancement of responses to LPS. Therefore, despite their prolonged exposure to LPS in whole blood, the evidence obtained suggested that neutrophil-EV-induced TLR4-dependent effects were not LPS-dependent. It should be noted that the biological activity of several DAMPs (e.g., high-mobility group protein 1 (HMGB-1), heat shock protein 60 (HSP60), Calreticulin) has been partly attributed to their affinity for, and binding to, LPS (506-508), hence there was a need for the stringent assessment of this phenomenon as a potential mechanism of EV pro-inflammatory activity.

Then, we sought to further characterise the endogenous neutrophil-EV-associated TLR4 activating molecule(s). As described above, there are various protein molecules candidates that fit the definition of DAMPs. Alternatively, TLR4 signalling by EV lipids has been demonstrated, via phospholipids extracted from ATP-stimulated macrophages (mouse J774.1 cell line) (509) and oxidised lipids in EVs from rheumatoid arthritis patients or released from HUVECs and HEK293 cells following oxidative stress (510). To determine the molecular

nature of the neutrophil-EV activity, we decided that protease treatment without EV destruction (as opposed to complete solubilisation required for lipid functional assays) might be the most effective strategy. We predicted that activity loss would indicate membrane lipid dependence or intra-vesicle cargo activity. We followed a similar protocol to Luong et al., who used proteinase K treatment to distinguish between intrinsic TLR4-stimulating activity of recombinant HSP70 protein and that derived from endotoxin contamination (511). We demonstrated that heat labile proteinase K followed by inactivation by heat-treatment ablated neutrophil-EV activity, with heat treatment alone producing a partial reduction in activity. Furthermore, the addition of FBS to co-culture assays did not restore responses, arguing against the release of EV-bound LPS following the digestion of surface proteins. Therefore, we concluded that the TLR4 agonist on neutrophil-EVs is surface protein-dependent and independent of membrane lipids or DAMP-bound LPS.

We investigated a potential inflammatory role for NETs produced in the whole blood assay and co-isolated with neutrophil-EVs. As previous research has indicated, LPS treatment of neutrophils in the presence of platelets induces NET release (489, 490). In a recent study, Tsourouktsoglou et al., demonstrated that NET-associated histones and DNA signal through a TLR4-dependent mechanism to induce IL-1β release from monocytes (492). Moreover, Wang et al., showed that PMA stimulation of neutrophils induced the formation of NET-EV complexes that were rich in HMGB-1, and mediated leukocyte recruitment via TLR2 and TLR4 signalling (504). Based on this evidence, we decided to assess if the TLR4-mediated neutrophil-EV activity in our model involved NETs. Flow cytometric staining for externalised MPO and DNA (SYTOX Green) did not reveal the presence of NETs in the isolated neutrophil-EV preparations. Furthermore, DNase I, used as a means to solubilise any NET material did not modify the neutrophil-EV induced activity, suggesting that NET-associated DNA is not the activating mediator on the neutrophil-EV preparations. Taken together, these findings suggest that NETs are unlikely to play a significant role in neutrophil-EV responses observed in this study. However, DNase-treated samples were not centrifuged prior to their addition to co-

cultures and therefore theoretically proteins released from digested NETs could be present. To completely rule out a contribution of NET-associated proteins to the inflammatory activity of neutrophil-EV preparations additional experiments may be necessary.

Finally based on the evidence that neutrophil-EV activity is mediated by TLR4-activating proteins, I performed a preliminary investigation to identify the responsible molecule(s). Although appropriate methodologies for this aim would include proteomic analysis (including active and non-active neutrophil-EVs) or immunoprecipitation assays with TLR4 and neutrophil-EVs and western blot analysis, these were not attempted due to time constraints. Instead, based on published data showing the abundance of two TLR4-activating ligands, MRP8/14, and HSP70 on neutrophil-EVs (292, 475), I investigated these two candidates. Blocking treatments with neutralising antibodies or an MRP14 small molecule inhibitor did not affect the neutrophil-EV-induced responses. I also performed a preliminary investigation of neutrophil-derived cationic peptides cathelicidin and azurocidin, which can activate inflammatory responses (470, 471, 512-516). However, neither peptide elicited detectable responses in co-culture assays. Clearly, more systematic approaches are needed as indicated above, with potential expansion of the work to *in vivo* mouse models where generic modification of primary cells is feasible.

Overall, even though we were not able to identify the specific active molecule(s) on neutrophil-EVs, the findings in this chapter provide strong evidence that neutrophil-EVs are DAMP-carriers causing TLR4-dependent pro-inflammatory activation and potential injury of resident cells in vascular beds such as the lung vasculature.

7. Conclusions and future directions

7.1. Summary of findings

Since the recognition of EVs as functional entities, many studies have highlighted their importance in intercellular communication describing them as emerging mediators in several pathophysiological conditions. In sepsis observational studies, circulating EVs have been largely used as biomarkers, assessing their relationship with disease mechanisms and severity. However, the exact mechanisms responsible for their biological activity in sepsis and ALI have not been explored in detail.

In this project, I investigated the role of neutrophil-derived EVs, as mediators inducing pro-inflammatory activation of target cells residing within the lung microvasculature and made several advances and novel findings. Firstly, by studying the neutrophil-EV uptake under resting and inflammatory conditions, I discovered an interaction between flow and inflammation that differentially affects the uptake of neutrophil-EVs by HLMECs and adherent monocytes. Secondly, I developed an *ex vivo* LPS-stimulated whole blood model of EV production that allowed the direct evaluation of different EV subtypes produced in the same environment under sepsis-like conditions. Using this more clinically relevant model, I demonstrated the potent pro-inflammatory properties of neutrophil-EVs and the key role of monocytes in promoting vascular endothelial inflammation. Lastly, further exploration of EV signalling mechanisms, with a focus on the pro-inflammatory neutrophil-EVs, revealed that they appear to carry TLR4-activating proteins through which they induce pro-inflammatory and pro-coagulant functionality in monocytes. This chapter will discuss the major findings observed in this study, alongside their implications and future opportunities.

7.1.1. Neutrophil-EV uptake by vascular target cells populations is regulated by flow and inflammation

In **Chapter 3**, I demonstrated that flow has an important role in neutrophil-EV uptake by both pulmonary endothelial cells (HLMECs) and monocytes. The project was initially developed to address the discrepancy our group had observed in the uptake of EVs by HLMECs *in vitro* and the relative lack of EV uptake by mouse lung endothelial cells *in vivo* (281). Contrary to our hypothesis, neutrophil-EVs were taken up by HLMECs under flow conditions, demonstrated previously with coronary arterial or umbilical vein endothelial cells with synthetic nanoparticles, neutrophil-EVs, and macromolecules (350-354). As EV binding will be promoted by convective transport under flow conditions, negative regulation by shear stress forces is not the only factor to consider when compared to static conditions. Moreover, HLMEC activation by TNF-α pre-treatment revealed a significant increase in neutrophil-EV uptake that was promoted by increasing shear stress. This finding suggests that interactions between EVs and target cells may be increased during local or systemic vascular inflammation, and therefore, could play a key role in facilitating EV functions in regulating normal inflammatory reactions as well as contributing to dysfunctional processes during sepsis. The opposing effects of reduced and increased EV uptake with increasing shear stress in resting and activated HLMECs suggested that different molecular mechanisms might be regulating the neutrophil-EV binding and/or internalisation under these conditions. For example, distinct receptor-ligand pairs might be involved in the recognition and capture under resting and inflammatory conditions and could be explored, especially in syndromes that involve dysregulation of blood flow such as sepsis/septic shock and hypoxic vasoconstriction. Indeed, although existing studies have reported that EV uptake might be a result of non-specific recognition with generic surface molecules such as phosphatidylserine (271, 273, 517) or scavenger receptors (277, 281, 518, 519), there are others that support receptor-specific recognition and EV uptake such as ICAM-1 (352, 520, 521)

As monocytes have a major role in the development of indirect ALI (355, 356) and dominate EV uptake within the lung microvasculature under resting and inflammatory conditions in mice (281), I developed a co-culture model of PBMCs and HLMECs under both static and flow conditions. The importance of convection transport of particles was demonstrated by a dramatic increase (~10-fold) in neutrophil-EV uptake by monocytes under flow conditions. This finding supports our contention that *in vitro* static culture may not accurately model EV effects on target cell populations, in this case underestimate their interactions with monocytes. This notion should be taken into consideration when attempting to extrapolate evidence obtained by *in vitro* static systems. It is therefore recommended that *in vitro* findings on EV interactions with target cells, should be confirmed by *in vivo*, *ex vivo*, or *in vitro* models with the presence of flow forces before definitive conclusions are made. Here, such an attempt has been made with pilot experiments to assess monocyte activation by neutrophil-EVs under flow conditions (**Chapter 5**) that will be further investigated in future assays.

7.1.2. Neutrophil-EV activity in an *in vitro* model of pulmonary vascular inflammation

In **Chapter 4**, I investigated the kinetics of EV subtype release in an *ex vivo* model of LPS whole blood stimulation and assessed their pro-inflammatory activity in a PBMC-HLMEC co-culture model of pulmonary vascular inflammation. EVs are released by several cell populations within the circulation, with the potential to interact with and affect the function of specific target cell vascular populations. Using this model, EV subtypes were produced in a more physiological setting than that of the standard isolated cell stimulation models, but to achieve this benefit, it was necessary to perform EV subtype immunoaffinity isolation. In agreement with some previous reports in sepsis patients, platelet and neutrophil-EVs were the two main populations acutely increased in the whole blood assay (246, 286). As a continuation of our previous mouse work, CD11b and CD61 immunomagnetic beads were used for the isolation of myeloid-EVs (neutrophil- and monocyte-derived) and platelet-EVs

respectively. When PBMC-HLMEC co-cultures were treated with these, a sharp contrast between their activities was observed, with only $CD11b^+$ myeloid-EVs inducing potent pro-inflammatory responses with PBMC-dependent upregulation of HLMEC adhesion molecule expression accompanied by pro-inflammatory cytokine release. The lack of platelet-EV-induced responses is somewhat surprising as their role in inflammation has been described before with both pro- (438-441) and anti-inflammatory properties (442, 443). Therefore, further research is needed to explore their features in relevant models of EV production (i.e., whole blood) and functional assessment (i.e., models including several target cells of interest).

In **Chapter 5**, I moved the focus onto neutrophil-EVs based on the relatively small numbers of monocyte-EVs produced during whole blood stimulation and their previously reported pro-inflammatory phenotype (292, 293, 319, 324-326, 352, 384, 448, 522). Preliminary studies indicated that anti-CD66b immunomagnetic bead-isolated neutrophil-EVs showed similar activity to the myeloid-EV preparations. A dominant role for monocytes in the generation of responses in co-cultures was observed in these assays. Lung-marginated monocytes have been studied by our group in the past, in EV-independent direct (523-525) and indirect ALI (355, 356), as well as myeloid-EV-induced oedema formation in a mouse isolated perfused lung model (357). TNF-α was found to be the principal mediator of the HLMEC responses measured. Other cytokines were produced in the assay, and it is possible that neutrophil-EVs could produce other direct (i.e., monocyte- and TNF-α-independent) responses or effects on HLMECs or other types of endothelial cells such as ROS release (526), myeloperoxidase-induced endothelial cell permeability (322), or neutrophil-elastase mediated effects (380, 527). Nonetheless, these results suggest that EV-induced TNF-α released locally from monocytes within the pulmonary microvasculature would have a greater potency than that derived from remote sites and transported to the lungs via the circulation. These findings together, highlight that neutrophil-EVs produced during sepsis could serve as endogenous inflammatory mediators inducing pro-inflammatory signalling and subsequent responses in vascular beds such as the lung microvasculature. However, this effect may not be as significant in the

presence of high systemic endotoxin concentrations which can occur in sepsis and therefore the role of neutrophil-EVs might be more prevalent when they are released into the circulation from local compartmentalised sites of infection and not during acute bacteraemia.

7.1.3. Neutrophil-EV signalling through TLR4 pathway

Finally, in **Chapter 6**, I carried out mechanistic studies into the neutrophil-EV-induced monocyte activation. I first demonstrated essential roles for p38 MAPK, ERK1/2, and PI3K signalling pathways in TNF-α release in monocytes. The role of ROS was then investigated, as they have been involved in MAPK signalling in monocytes, macrophages, and endothelial cells (484, 498, 499) but findings were inconclusive. However, similarities in the neutrophil-EV and LPS-induced responses (i.e., sensitivity to MAPK and NADPH oxidase inhibitors), prompted us to investigate the role of TLR4 signalling, as a central receptor in downstream LPS signalling. In agreement with previous reports of TLR4 involvement in EV signalling (501-503, 509), the neutrophil-EV responses observed in this study were fully dependent on TLR4 and based on several lines of evidence, not due to EV-associated LPS. On the contrary to LPS, neutrophil-EV pro-inflammatory activities were fully abolished following protease digestion by proteinase K or heat treatment, supporting the idea that neutrophil-EV activity is protein dependent. Although NETs have been previously involved in TLR4 signalling (492, 504), it is unlikely for them to be involved in the observed neutrophil-EV signalling as DNase I treatment did not affect their activity, as opposed to NETs sensitivity to such digestion (528). Lastly, preliminary experiments were performed to block known TLR4 ligands that have been found in abundant levels on neutrophil-EVs, namely the myeloid-protein 8/14 (MRP8/14) and heat shock protein 70 (HSP70). Despite supporting evidence in the literature for their existence in neutrophil-EVs and their TLR4 signalling dependency, I did not observe any reduction in responses as a result of specific blocking treatments.

Overall, these findings suggest that neutrophil-EVs produced during systemic inflammation, such as gram-negative bacterial sepsis, could act as endogenous inflammatory vehicles participating in intercellular communication via TLR4 signalling. Although DAMPs might not be as potent inflammatory mediators as LPS in local responses, neutrophil-EVs carrying DAMPs have a much stronger long-range signalling capacity compared to LPS or other soluble mediators that could be diluted or neutralised within the circulation. Through their interactions with target effector cells such as marginated monocytes and/or neutrophils in isolated sites such as the lung microvasculature, they might represent a novel, alternative paradigm for the systemic propagation of inflammation, playing a critical role in the development of sepsis/SIRS induced indirect ALI. Although further research is needed to characterise the neutrophil-EV cargoes and fully understand their biological implications, this hypothesis if correct, might lead to the development of novel strategies targeting EVs instead of soluble circulating inflammatory mediators to attenuate or reverse organ dysfunction during sepsis.

7.2. Remaining questions and future work

This study's findings increased our understanding of how neutrophil-EVs interact with tissue resident target cells, specifically monocytes. However, our observations raised important questions that warrant further investigation in future studies.

1. **Are there specific receptor-ligand pairs mediating neutrophil-EV uptake by target cells under resting and inflammatory conditions?**

Although we demonstrated that increasing flow forces modify neutrophil-EV uptake differently in healthy and inflammatory conditions, further exploration of the specific uptake mechanisms could provide crucial insights into the specific receptor-ligand pairs mediating neutrophil-EV uptake in health and disease. Blocking EV uptake by targeting individual receptors that are activated only under inflammatory states and allow interactions between specific EV subtypes and target cell populations leading to excessive inflammation and tissue damage, is a therapeutic option for the development of EV-based therapies to combat indirect ALI, without losing any homeostatic and potentially protective effects of other non-injurious EVs.

2. **How do neutrophil-EVs induce endothelial cell injury?**

Apart from inflammatory phenotypes, neutrophil-EVs have been shown to be directly pro-injurious (321-323, 384, 527) and therefore the next step would be to determine their capacity in inducing pulmonary endothelial cell injury and barrier dysfunction, key processes leading to oedema formation, and subsequently assess the TNF-α and TLR4 involvement in these processes. For this work, initially, a more complex *in vitro* model including additional cell populations, found within the pulmonary vasculature under inflammatory conditions, such as neutrophils, would be more suitable. Following *in vitro* experimentation, transfer of these assays to *in vivo* or *ex vivo* mouse models including the previously established isolated perfused lung model (357) would be necessary to substantiate and develop the findings. Thus, neutrophil-EV signalling assessed within the lung microvasculature will incorporate other

important anatomical (systemic or local) factors and cellular sources that cannot be fully modelled in an *in vitro* situation.

3. What are the physical interactions necessary for neutrophil-EV signalling in monocytes?

From our findings, it is not clear whether neutrophil-EV uptake by monocytes is a pre-requisite for them to elicit their pro-inflammatory responses. We observed a neutrophil-EV PI3K dependency, which based on previous findings of PI3K involvement in endocytosis pathways (473, 494), could be linked to inhibition of EV uptake rather than PI3K signalling *per se*. Additionally, the sensitivity of neutrophil-EV activity to proteinase K was attributed to activating proteins on the neutrophil-EV surface, however, we cannot exclude the possibility that surface proteins might be acting as binding receptors or internalisation triggers that are essential for TLR4 (surface or endosomal) engagement and signalling. Uptake assays with proteinase K-treated neutrophil-EVs is the first step in addressing this question. Functional assays in the presence of endocytosis inhibitors in future studies will provide clearer answers to these speculations and determine the role of EV uptake on their functional properties.

4. How are pro-inflammatory neutrophil-EVs generated?

EV properties and molecular cargoes are affected by multiple parameters such as the status of the parent cell, the stimulus the parent cell was exposed to, and the environment in that the EVs were produced (214, 371, 459). A parallel study in our group compared the inflammatory activity of neutrophil-EVs generated in whole blood or isolated neutrophils using the same stimuli ('2-hit' LPS followed by fMLP stimulation) and found that only the neutrophil-EVs produced in whole blood were pro-inflammatory (461). This could explain the majority of studies reporting anti-inflammatory or anti-bacterial effects of neutrophil-EVs as they mainly use isolated neutrophils for EV production in *in vitro* models (241, 242, 297, 329-331, 380, 444). Determining the exact mechanisms that lead to pro-inflammatory neutrophil-EV

generation and subsequently targeting these pathways is likely to be critical in understanding their roles in indirect ALI.

5. Which is the molecular cargo of neutrophil-EVs?

In the last chapter of this thesis, I obtained substantial evidence that the neutrophil-EV activity is mediated by TLR4-activating surface proteins. Simple LPS carryover was ruled out and a literature search for known DAMP molecules that could be present in neutrophil-EVs was performed. However, inhibition of our two top candidates MRP8/14 and HSP70 did not dampen the pro-inflammatory responses. Further evaluation of the inhibitors used in our preliminary assays is needed before their final dismissal from the candidate list. Proteomic analysis comparing differences between these pro-inflammatory neutrophil-EVs and non/anti-inflammatory EVs from isolated neutrophils stimulated in monoculture (461), as well as pull-down assays with recombinant TLR4 or the TLR4-MD2 complex followed by probing for neutrophil-EV ligands, are alternative strategies to be pursued. Subsequent genetic manipulation of neutrophil-like cell lines such as the PLB-985 or HL60 cells can be used as a tool to knock out the identified molecules and confirm their involvement in the neutrophil-EV-induced cell activation and potentially injury. We appreciate though that neutrophil-EVs might also be carrying other types of pro-inflammatory mediators apart from proteins, such as miRNA molecules and eicosanoids, and their existence and role in neutrophil-EV mediated pro-inflammatory responses within the lung microvasculature should also be studied in detail in future studies.

7.3. Concluding remarks

In this study, I investigated the neutrophil-EVs as mediators for the propagation of inflammation from the systemic circulation to the lung during acute systemic inflammation and demonstrated their pro-inflammatory capabilities. My findings highlighted the central role of marginated monocytes in neutrophil-EV-induced responses and described a novel role of neutrophil-EVs as vehicles for DAMP activity via TLR4 activating proteins. Further research on the characterisation of their proteomic profile will provide tools for their targeting in therapeutic strategies towards sepsis-induced indirect ALI.

8. References

1. Wheeler AP, Bernard GR. Acute lung injury and the acute respiratory distress syndrome: a clinical review. Lancet. 2007;369(9572):1553-64.
2. Phua J, Badia JR, Adhikari NK, Friedrich JO, Fowler RA, Singh JM, et al. Has mortality from acute respiratory distress syndrome decreased over time?: A systematic review. Am J Respir Crit Care Med. 2009;179(3):220-7.
3. Pham T, Rubenfeld GD. Fifty Years of Research in ARDS. The Epidemiology of Acute Respiratory Distress Syndrome. A 50th Birthday Review. Am J Respir Crit Care Med. 2017;195(7):860-70.
4. Ashbaugh D, Boyd Bigelow D, Petty T, Levine B. ACUTE RESPIRATORY DISTRESS IN ADULTS. The Lancet. 1967;290(7511):319-23.
5. Ashbaugh D. David Ashbaugh reminisces. The Lancet Respiratory Medicine. 2017;5(6):474.
6. Bernard GR, Artigas A, Brigham KL, Carlet J, Falke K, Hudson L, et al. The American-European Consensus Conference on ARDS. Definitions, mechanisms, relevant outcomes, and clinical trial coordination. Am J Respir Crit Care Med. 1994;149(3 Pt 1):818-24.
7. Ranieri VM, Rubenfeld GD, Thompson BT, Ferguson ND, Caldwell E, Fan E, et al. Acute respiratory distress syndrome: the Berlin Definition. JAMA. 2012;307(23):2526-33.
8. Quartin AA, Campos MA, Maldonado DA, Ashkin D, Cely CM, Schein RMH. Acute lung injury outside of the ICU: incidence in respiratory isolation on a general ward. Chest. 2009;135(2):261-8.
9. Sweatt AJ, Levitt JE. Evolving epidemiology and definitions of the acute respiratory distress syndrome and early acute lung injury. Clin Chest Med. 2014;35(4):609-24.
10. Thompson BT, Chambers RC, Liu KD. Acute Respiratory Distress Syndrome. New England Journal of Medicine. 2017;377(6):562-72.
11. Bellani G, Laffey JG, Pham T, Fan E, Brochard L, Esteban A, et al. Epidemiology, Patterns of Care, and Mortality for Patients With Acute Respiratory Distress Syndrome in Intensive Care Units in 50 Countries. JAMA. 2016;315(8):788-800.
12. Summers C, Singh NR, Worpole L, Simmonds R, Babar J, Condliffe AM, et al. Incidence and recognition of acute respiratory distress syndrome in a UK intensive care unit. Thorax. 2016;71(11):1050-1.
13. Johnson ER, Matthay MA. Acute lung injury: epidemiology, pathogenesis, and treatment. J Aerosol Med Pulm Drug Deliv. 2010;23(4):243-52.
14. Ware LB, Matthay MA. The acute respiratory distress syndrome. N Engl J Med. 2000;342(18):1334-49.
15. Matthay MA, Zimmerman GA. Acute lung injury and the acute respiratory distress syndrome: four decades of inquiry into pathogenesis and rational management. Am J Respir Cell Mol Biol. 2005;33(4):319-27.
16. Matthay MA, Zemans RL. The acute respiratory distress syndrome: pathogenesis and treatment. Annu Rev Pathol. 2011;6:147-63.
17. Mackay A, Al-Haddad M. Acute lung injury and acute respiratory distress syndrome. Continuing Education in Anaesthesia Critical Care & Pain. 2009;9(5):152-6.
18. Hughes KT, Beasley MB. Pulmonary Manifestations of Acute Lung Injury: More Than Just Diffuse Alveolar Damage. Arch Pathol Lab Med. 2017;141(7):916-22.
19. Tomashefski JF, Jr. Pulmonary pathology of the adult respiratory distress syndrome. Clin Chest Med. 1990;11(4):593-619.
20. Yang SC, Tsai YF, Pan YL, Hwang TL. Understanding the role of neutrophils in acute respiratory distress syndrome. Biomed J. 2021;44(4):439-46.
21. Matthay MA, Zemans RL, Zimmerman GA, Arabi YM, Beitler JR, Mercat A, et al. Acute respiratory distress syndrome. Nature reviews Disease primers. 2019;5(1):18-.
22. Katzenstein AL, Myers JL, Mazur MT. Acute interstitial pneumonia. A clinicopathologic, ultrastructural, and cell kinetic study. Am J Surg Pathol. 1986;10(4):256-67.
23. Ichikado K, Muranaka H, Gushima Y, Kotani T, Nader HM, Fujimoto K, et al. Fibroproliferative changes on high-resolution CT in the acute respiratory distress syndrome predict mortality and ventilator dependency: a prospective observational cohort study. BMJ Open. 2012;2(2):e000545.

24. Papazian L, Doddoli C, Chetaille B, Gernez Y, Thirion X, Roch A, et al. A contributive result of open-lung biopsy improves survival in acute respiratory distress syndrome patients. Crit Care Med. 2007;35(3):755-62.
25. Martin C, Papazian L, Payan MJ, Saux P, Gouin F. Pulmonary fibrosis correlates with outcome in adult respiratory distress syndrome. A study in mechanically ventilated patients. Chest. 1995;107(1):196-200.
26. Shaver CM, Bastarache JA. Clinical and biological heterogeneity in acute respiratory distress syndrome: direct versus indirect lung injury. Clin Chest Med. 2014;35(4):639-53.
27. Rocco PR, Zin WA. Pulmonary and extrapulmonary acute respiratory distress syndrome: are they different? Curr Opin Crit Care. 2005;11(1):10-7.
28. Pelosi P, D'Onofrio D, Chiumello D, Paolo S, Chiara G, Capelozzi VL, et al. Pulmonary and extrapulmonary acute respiratory distress syndrome are different. Eur Respir J Suppl. 2003;42:48s-56s.
29. GATTINONI L, PELOSI P, SUTER PM, PEDOTO A, VERCESI P, LISSONI A. Acute Respiratory Distress Syndrome Caused by Pulmonary and Extrapulmonary Disease. American Journal of Respiratory and Critical Care Medicine. 1998;158(1):3-11.
30. Schutte H, Lohmeyer J, Rosseau S, Ziegler S, Siebert C, Kielisch H, et al. Bronchoalveolar and systemic cytokine profiles in patients with ARDS, severe pneumonia and cardiogenic pulmonary oedema. European Respiratory Journal. 1996;9(9):1858-67.
31. Menezes SL, Bozza PT, Neto HC, Laranjeira AP, Negri EM, Capelozzi VL, et al. Pulmonary and extrapulmonary acute lung injury: inflammatory and ultrastructural analyses. J Appl Physiol (1985). 2005;98(5):1777-83.
32. Bauer TT, Montón C, Torres A, Cabello H, Fillela X, Maldonado A, et al. Comparison of systemic cytokine levels in patients with acute respiratory distress syndrome, severe pneumonia, and controls. Thorax. 2000;55(1):46-52.
33. Doyle RL, Szaflarski N, Modin GW, Wiener-Kronish JP, Matthay MA. Identification of patients with acute lung injury. Predictors of mortality. Am J Respir Crit Care Med. 1995;152(6 Pt 1):1818-24.
34. Sloane PJ, Gee MH, Gottlieb JE, Albertine KH, Peters SP, Burns JR, et al. A multicenter registry of patients with acute respiratory distress syndrome. Physiology and outcome. Am Rev Respir Dis. 1992;146(2):419-26.
35. Calfee CS, Janz DR, Bernard GR, May AK, Kangelaris KN, Matthay MA, et al. Distinct molecular phenotypes of direct vs indirect ARDS in single-center and multicenter studies. Chest. 2015;147(6):1539-48.
36. Luo L, Shaver CM, Zhao Z, Koyama T, Calfee CS, Bastarache JA, et al. Clinical Predictors of Hospital Mortality Differ Between Direct and Indirect ARDS. Chest. 2017;151(4):755-63.
37. Zhu N, Zhang D, Wang W, Li X, Yang B, Song J, et al. A Novel Coronavirus from Patients with Pneumonia in China, 2019. N Engl J Med. 2020;382(8):727-33.
38. Dong E, Du H, Gardner L. An interactive web-based dashboard to track COVID-19 in real time. Lancet Infect Dis. 2020;20(5):533-4.
39. Gattinoni L, Coppola S, Cressoni M, Busana M, Rossi S, Chiumello D. COVID-19 Does Not Lead to a "Typical" Acute Respiratory Distress Syndrome. Am J Respir Crit Care Med. 2020;201(10):1299-300.
40. Aslan A, Aslan C, Zolbanin NM, Jafari R. Acute respiratory distress syndrome in COVID-19: possible mechanisms and therapeutic management. Pneumonia. 2021;13(1):14.
41. Gibson PG, Qin L, Puah SH. COVID-19 acute respiratory distress syndrome (ARDS): clinical features and differences from typical pre-COVID-19 ARDS. Med J Aust. 2020;213(2):54-6.e1.
42. Marini JJ, Gattinoni L. Management of COVID-19 Respiratory Distress. JAMA. 2020;323(22):2329-30.
43. Tzotzos SJ, Fischer B, Fischer H, Zeitlinger M. Incidence of ARDS and outcomes in hospitalized patients with COVID-19: a global literature survey. Critical Care. 2020;24(1):516.
44. Attaway AH, Scheraga RG, Bhimraj A, Biehl M, Hatipoğlu U. Severe covid-19 pneumonia: pathogenesis and clinical management. Bmj. 2021;372:n436.

45. Fan E, Beitler JR, Brochard L, Calfee CS, Ferguson ND, Slutsky AS, et al. COVID-19-associated acute respiratory distress syndrome: is a different approach to management warranted? Lancet Respir Med. 2020;8(8):816-21.
46. Patel BV, Arachchillage DJ, Ridge CA, Bianchi P, Doyle JF, Garfield B, et al. Pulmonary Angiopathy in Severe COVID-19: Physiologic, Imaging, and Hematologic Observations. American Journal of Respiratory and Critical Care Medicine. 2020;202(5):690-9.
47. Ackermann M, Verleden SE, Kuehnel M, Haverich A, Welte T, Laenger F, et al. Pulmonary Vascular Endothelialitis, Thrombosis, and Angiogenesis in Covid-19. New England Journal of Medicine. 2020;383(2):120-8.
48. Welker C, Huang J, Gil IJN, Ramakrishna H. 2021 Acute Respiratory Distress Syndrome Update, With Coronavirus Disease 2019 Focus. Journal of Cardiothoracic and Vascular Anesthesia. 2022;36(4):1188-95.
49. Slutsky AS, Ranieri VM. Ventilator-induced lung injury. New England Journal of Medicine. 2013;369(22):2126-36.
50. Griffiths MJD, McAuley DF, Perkins GD, Barrett N, Blackwood B, Boyle A, et al. Guidelines on the management of acute respiratory distress syndrome. BMJ Open Respiratory Research. 2019;6(1):e000420.
51. Wiedemann HP, Wheeler AP, Bernard GR, Thompson BT, Hayden D, deBoisblanc B, et al. Comparison of two fluid-management strategies in acute lung injury. N Engl J Med. 2006;354(24):2564-75.
52. Dreyfuss D, Saumon G. Role of tidal volume, FRC, and end-inspiratory volume in the development of pulmonary edema following mechanical ventilation. Am Rev Respir Dis. 1993;148(5):1194-203.
53. Bajwa EK, Malhotra CK, Thompson BT, Christiani DC, Gong MN. Statin therapy as prevention against development of acute respiratory distress syndrome: an observational study. Critical care medicine. 2012;40(5):1470-7.
54. McAuley DF, Laffey JG, O'Kane CM, Perkins GD, Mullan B, Trinder TJ, et al. Simvastatin in the acute respiratory distress syndrome. N Engl J Med. 2014;371(18):1695-703.
55. Wang Y, Zhong M, Wang Z, Song J, Wu W, Zhu D. The preventive effect of antiplatelet therapy in acute respiratory distress syndrome: a meta-analysis. Critical Care. 2018;22(1):60.
56. Bernard GR, Wheeler AP, Arons MM, Morris PE, Paz HL, Russell JA, et al. A trial of antioxidants N-acetylcysteine and procysteine in ARDS. The Antioxidant in ARDS Study Group. Chest. 1997;112(1):164-72.
57. Bernard GR, Luce JM, Sprung CL, Rinaldo JE, Tate RM, Sibbald WJ, et al. High-dose corticosteroids in patients with the adult respiratory distress syndrome. N Engl J Med. 1987;317(25):1565-70.
58. Duggal A, Ganapathy A, Ratnapalan M, Adhikari NK. Pharmacological treatments for acute respiratory distress syndrome: systematic review. Minerva Anestesiol. 2015;81(5):567-88.
59. Calfee CS, Matthay MA. Nonventilatory treatments for acute lung injury and ARDS. Chest. 2007;131(3):913-20.
60. Sweeney RM, Griffiths M, McAuley D. Treatment of acute lung injury: current and emerging pharmacological therapies. Semin Respir Crit Care Med. 2013;34(4):487-98.
61. Kor DJ, Erlich J, Gong MN, Malinchoc M, Carter RE, Gajic O, et al. Association of prehospitalization aspirin therapy and acute lung injury: results of a multicenter international observational study of at-risk patients. Crit Care Med. 2011;39(11):2393-400.
62. Walkey AJ, Wiener RS. Macrolide antibiotics and survival in patients with acute lung injury. Chest. 2012;141(5):1153-9.
63. Simonis FD, de Iudicibus G, Cremer OL, Ong DSY, van der Poll T, Bos LD, et al. Macrolide therapy is associated with reduced mortality in acute respiratory distress syndrome (ARDS) patients. Annals of Translational Medicine. 2018;6(2):3.

64. Zeiher BG, Artigas A, Vincent JL, Dmitrienko A, Jackson K, Thompson BT, et al. Neutrophil elastase inhibition in acute lung injury: results of the STRIVE study. Crit Care Med. 2004;32(8):1695-702.
65. Matthay MA, Brower RG, Carson S, Douglas IS, Eisner M, Hite D, et al. Randomized, placebo-controlled clinical trial of an aerosolized β_2-agonist for treatment of acute lung injury. Am J Respir Crit Care Med. 2011;184(5):561-8.
66. Gates S, Perkins GD, Lamb SE, Kelly C, Thickett DR, Young JD, et al. Beta-Agonist Lung injury TrIal-2 (BALTI-2): a multicentre, randomised, double-blind, placebo-controlled trial and economic evaluation of intravenous infusion of salbutamol versus placebo in patients with acute respiratory distress syndrome. Health Technol Assess. 2013;17(38):v-vi, 1-87.
67. Anzueto A, Baughman RP, Guntupalli KK, Weg JG, Wiedemann HP, Raventós AA, et al. Aerosolized surfactant in adults with sepsis-induced acute respiratory distress syndrome. Exosurf Acute Respiratory Distress Syndrome Sepsis Study Group. N Engl J Med. 1996;334(22):1417-21.
68. McAuley DF, Cross LM, Hamid U, Gardner E, Elborn JS, Cullen KM, et al. Keratinocyte growth factor for the treatment of the acute respiratory distress syndrome (KARE): a randomised, double-blind, placebo-controlled phase 2 trial. Lancet Respir Med. 2017;5(6):484-91.
69. Paine R, 3rd, Standiford TJ, Dechert RE, Moss M, Martin GS, Rosenberg AL, et al. A randomized trial of recombinant human granulocyte-macrophage colony stimulating factor for patients with acute lung injury. Crit Care Med. 2012;40(1):90-7.
70. Matthay MA, Calfee CS, Zhuo H, Thompson BT, Wilson JG, Levitt JE, et al. Treatment with allogeneic mesenchymal stromal cells for moderate to severe acute respiratory distress syndrome (START study): a randomised phase 2a safety trial. Lancet Respir Med. 2019;7(2):154-62.
71. Mac Sweeney R, McAuley DF. Mesenchymal stem cell therapy in acute lung injury: is it time for a clinical trial? Thorax. 2012;67(6):475-6.
72. Prasanna P, Rathee S, Upadhyay A, Sulakshana S. Nanotherapeutics in the treatment of acute respiratory distress syndrome. Life Sci. 2021;276:119428.
73. Bone RC, Balk RA, Cerra FB, Dellinger RP, Fein AM, Knaus WA, et al. Definitions for sepsis and organ failure and guidelines for the use of innovative therapies in sepsis. The ACCP/SCCM Consensus Conference Committee. American College of Chest Physicians/Society of Critical Care Medicine. Chest. 1992;101(6):1644-55.
74. Angus DC, Linde-Zwirble WT, Lidicker J, Clermont G, Carcillo J, Pinsky MR. Epidemiology of severe sepsis in the United States: analysis of incidence, outcome, and associated costs of care. Crit Care Med. 2001;29(7):1303-10.
75. Brun-Buisson C. The epidemiology of the systemic inflammatory response. Intensive Care Med. 2000;26 Suppl 1(Suppl 1):S64-74.
76. Schrijver IT, Kemperman H, Roest M, Kesecioglu J, de Lange DW. Myeloperoxidase can differentiate between sepsis and non-infectious SIRS and predicts mortality in intensive care patients with SIRS. Intensive Care Medicine Experimental. 2017;5(1):43.
77. Rello J, Valenzuela-Sánchez F, Ruiz-Rodriguez M, Moyano S. Sepsis: A Review of Advances in Management. Adv Ther. 2017;34(11):2393-411.
78. Singer M, Deutschman CS, Seymour CW, Shankar-Hari M, Annane D, Bauer M, et al. The Third International Consensus Definitions for Sepsis and Septic Shock (Sepsis-3). JAMA. 2016;315(8):801-10.
79. Vincent JL, Opal SM, Marshall JC, Tracey KJ. Sepsis definitions: time for change. Lancet. 2013;381(9868):774-5.
80. Levy MM, Fink MP, Marshall JC, Abraham E, Angus D, Cook D, et al. 2001 sccm/esicm/accp/ats/sis international sepsis definitions conference. Intensive care medicine. 2003;29(4):530-8.
81. Kim HI, Park S. Sepsis: Early Recognition and Optimized Treatment. Tuberc Respir Dis (Seoul). 2019;82(1):6-14.
82. Gaieski DF, Mikkelsen ME, Band RA, Pines JM, Massone R, Furia FF, et al. Impact of time to antibiotics on survival in patients with severe sepsis or septic shock in whom early

goal-directed therapy was initiated in the emergency department. Crit Care Med. 2010;38(4):1045-53.
83. Vincent J-L, Moreno R, Takala J, Willatts S, De Mendonça A, Bruining H, et al. The SOFA (Sepsis-related Organ Failure Assessment) score to describe organ dysfunction/failure. Springer-Verlag; 1996.
84. Vincent J-L, Jones G, David S, Olariu E, Cadwell KK. Frequency and mortality of septic shock in Europe and North America: a systematic review and meta-analysis. Crit Care [Internet]. 2019 2019/05//; 23(1):[196 p.].
85. Kumar G, Kumar N, Taneja A, Kaleekal T, Tarima S, McGinley E, et al. Nationwide trends of severe sepsis in the 21st century (2000-2007). Chest. 2011;140(5):1223-31.
86. Burki TK. Sharp rise in sepsis deaths in the UK. The Lancet Respiratory Medicine. 2018;6(11):826.
87. Nutbeam T.; Daniels R. The Sepsis Manual 5th edition Birmingham: United Kingdom Sepsis Trust2019 [5th:[Available from: https://sepsistrust.org/wp-content/uploads/2020/01/5th-Edition-manual-080120.pdf.
88. Hudson LD, Milberg JA, Anardi D, Maunder RJ. Clinical risks for development of the acute respiratory distress syndrome. Am J Respir Crit Care Med. 1995;151(2 Pt 1):293-301.
89. Vincent JL, Sakr Y, Sprung CL, Ranieri VM, Reinhart K, Gerlach H, et al. Sepsis in European intensive care units: results of the SOAP study. Crit Care Med. 2006;34(2):344-53.
90. Rubenfeld GD, Caldwell E, Peabody E, Weaver J, Martin DP, Neff M, et al. Incidence and outcomes of acute lung injury. N Engl J Med. 2005;353(16):1685-93.
91. Stapleton RD, Wang BM, Hudson LD, Rubenfeld GD, Caldwell ES, Steinberg KP. Causes and timing of death in patients with ARDS. Chest. 2005;128(2):525-32.
92. Englert JA, Bobba C, Baron RM. Integrating molecular pathogenesis and clinical translation in sepsis-induced acute respiratory distress syndrome. JCI Insight. 2019;4(2).
93. Bone RC. Sir Isaac Newton, sepsis, SIRS, and CARS. Crit Care Med. 1996;24(7):1125-8.
94. Gomez HG, Gonzalez SM, Londoño JM, Hoyos NA, Niño CD, Leon AL, et al. Immunological characterization of compensatory anti-inflammatory response syndrome in patients with severe sepsis: a longitudinal study*. Crit Care Med. 2014;42(4):771-80.
95. Vergadi E, Vaporidi K, Tsatsanis C. Regulation of Endotoxin Tolerance and Compensatory Anti-inflammatory Response Syndrome by Non-coding RNAs. Frontiers in Immunology. 2018;9.
96. Jaffer U, Wade RG, Gourlay T. Cytokines in the systemic inflammatory response syndrome: a review. HSR Proc Intensive Care Cardiovasc Anesth. 2010;2(3):161-75.
97. Adib-Conquy M, Cavaillon JM. Compensatory anti-inflammatory response syndrome. Thromb Haemost. 2009;101(1):36-47.
98. Ward NS, Casserly B, Ayala A. The compensatory anti-inflammatory response syndrome (CARS) in critically ill patients. Clin Chest Med. 2008;29(4):617-25, viii.
99. Hotchkiss RS, Coopersmith CM, McDunn JE, Ferguson TA. The sepsis seesaw: tilting toward immunosuppression. Nat Med. 2009;15(5):496-7.
100. Remick DG. Pathophysiology of sepsis. Am J Pathol. 2007;170(5):1435-44.
101. Cavaillon J-M, Adib-Conquy M, Cloëz-Tayarani I, Fitting C. Immunodepression in sepsis and SIRS assessed by ex vivo cytokine production is not a generalized phenomenon: a review. Journal of endotoxin research. 2001;7(2):85-93.
102. Cavaillon JM, Adrie C, Fitting C, Adib-Conquy M. Reprogramming of circulatory cells in sepsis and SIRS. J Endotoxin Res. 2005;11(5):311-20.
103. Deutschman CS, Tracey KJ. Sepsis: current dogma and new perspectives. Immunity. 2014;40(4):463-75.
104. Chiu S, Bharat A. Role of monocytes and macrophages in regulating immune response following lung transplantation. Curr Opin Organ Transplant. 2016;21(3):239-45.
105. Zimmerman GA, Prescott SM, McIntyre TM. Endothelial cell interactions with granulocytes: tethering and signaling molecules. Immunol Today. 1992;13(3):93-100.

106. Chertov O, Ueda H, Xu LL, Tani K, Murphy WJ, Wang JM, et al. Identification of human neutrophil-derived cathepsin G and azurocidin/CAP37 as chemoattractants for mononuclear cells and neutrophils. J Exp Med. 1997;186(5):739-47.
107. Soehnlein O, Zernecke A, Eriksson EE, Rothfuchs AG, Pham CT, Herwald H, et al. Neutrophil secretion products pave the way for inflammatory monocytes. Blood. 2008;112(4):1461-71.
108. Selders GS, Fetz AE, Radic MZ, Bowlin GL. An overview of the role of neutrophils in innate immunity, inflammation and host-biomaterial integration. Regen Biomater. 2017;4(1):55-68.
109. Häger M, Cowland JB, Borregaard N. Neutrophil granules in health and disease. J Intern Med. 2010;268(1):25-34.
110. Amarante-Mendes GP, Adjemian S, Branco LM, Zanetti LC, Weinlich R, Bortoluci KR. Pattern Recognition Receptors and the Host Cell Death Molecular Machinery. Frontiers in Immunology. 2018;9.
111. Takeuchi O, Akira S. Pattern recognition receptors and inflammation. Cell. 2010;140(6):805-20.
112. Gentile LF, Moldawer LL. DAMPs, PAMPs, and the origins of SIRS in bacterial sepsis. Shock (Augusta, Ga). 2013;39(1):113-4.
113. Fein AM, Lippmann M, Holtzman H, Eliraz A, Goldberg SK. The risk factors, incidence, and prognosis of ARDS following septicemia. Chest. 1983;83(1):40-2.
114. Bertani B, Ruiz N. Function and Biogenesis of Lipopolysaccharides. EcoSal Plus. 2018;8(1):10.1128/ecosalplus.ESP-0001-2018.
115. Kawasaki T, Kawai T. Toll-Like Receptor Signaling Pathways. Frontiers in Immunology. 2014;5.
116. Takeda K, Akira S. Toll-like receptors. Curr Protoc Immunol. 2015;109:14.2.1-.2.0.
117. Goldblum SE, Brann TW, Ding X, Pugin J, Tobias PS. Lipopolysaccharide (LPS)-binding protein and soluble CD14 function as accessory molecules for LPS-induced changes in endothelial barrier function, in vitro. J Clin Invest. 1994;93(2):692-702.
118. Pålsson-McDermott EM, O'Neill LA. Signal transduction by the lipopolysaccharide receptor, Toll-like receptor-4. Immunology. 2004;113(2):153-62.
119. El-Zayat SR, Sibaii H, Mannaa FA. Toll-like receptors activation, signaling, and targeting: an overview. Bulletin of the National Research Centre. 2019;43(1):187.
120. Chen Z, Shao Z, Mei S, Yan Z, Ding X, Billiar T, et al. Sepsis Upregulates CD14 Expression in a MyD88-Dependent and Trif-Independent Pathway. Shock. 2018;49(1):82-9.
121. Cuenda A, Rousseau S. p38 MAP-kinases pathway regulation, function and role in human diseases. Biochim Biophys Acta. 2007;1773(8):1358-75.
122. Hoffmann A, Levchenko A, Scott ML, Baltimore D. The IkappaB-NF-kappaB signaling module: temporal control and selective gene activation. Science. 2002;298(5596):1241-5.
123. Matzinger P. The danger model: a renewed sense of self. Science. 2002;296(5566):301-5.
124. Seong S-Y, Matzinger P. Hydrophobicity: an ancient damage-associated molecular pattern that initiates innate immune responses. Nature Reviews Immunology. 2004;4(6):469-78.
125. Degryse B, Bonaldi T, Scaffidi P, Müller S, Resnati M, Sanvito F, et al. The high mobility group (HMG) boxes of the nuclear protein HMG1 induce chemotaxis and cytoskeleton reorganization in rat smooth muscle cells. J Cell Biol. 2001;152(6):1197-206.
126. Fitrolaki MD, Dimitriou H, Venihaki M, Katrinaki M, Ilia S, Briassoulis G. Increased extracellular heat shock protein 90α in severe sepsis and SIRS associated with multiple organ failure and related to acute inflammatory-metabolic stress response in children. Medicine (Baltimore). 2016;95(35):e4651.
127. Zhang Q, Raoof M, Chen Y, Sumi Y, Sursal T, Junger W, et al. Circulating mitochondrial DAMPs cause inflammatory responses to injury. Nature. 2010;464(7285):104-7.
128. Chen GY, Nuñez G. Sterile inflammation: sensing and reacting to damage. Nat Rev Immunol. 2010;10(12):826-37.

129. Ahmed AI, Soliman RA, Samir S. Cell Free DNA and Procalcitonin as Early Markers of Complications in ICU Patients with Multiple Trauma and Major Surgery. Clin Lab. 2016;62(12):2395-404.
130. Andersson U, Tracey KJ. HMGB1 is a therapeutic target for sterile inflammation and infection. Annu Rev Immunol. 2011;29:139-62.
131. Chaudhry H, Zhou J, Zhong Y, Ali MM, McGuire F, Nagarkatti PS, et al. Role of cytokines as a double-edged sword in sepsis. In Vivo. 2013;27(6):669-84.
132. Bozza FA, Salluh JI, Japiassu AM, Soares M, Assis EF, Gomes RN, et al. Cytokine profiles as markers of disease severity in sepsis: a multiplex analysis. Critical Care. 2007;11(2):R49.
133. Zanotti S, Kumar A, Kumar A. Cytokine modulation in sepsis and septic shock. Expert Opin Investig Drugs. 2002;11(8):1061-75.
134. Mera S, Tatulescu D, Cismaru C, Bondor C, Slavcovici A, Zanc V, et al. Multiplex cytokine profiling in patients with sepsis. Apmis. 2011;119(2):155-63.
135. Gogos CA, Drosou E, Bassaris HP, Skoutelis A. Pro- versus anti-inflammatory cytokine profile in patients with severe sepsis: a marker for prognosis and future therapeutic options. J Infect Dis. 2000;181(1):176-80.
136. Anderson GD, Hauser SD, McGarity KL, Bremer ME, Isakson PC, Gregory SA. Selective inhibition of cyclooxygenase (COX)-2 reverses inflammation and expression of COX-2 and interleukin 6 in rat adjuvant arthritis. The Journal of clinical investigation. 1996;97(11):2672-9.
137. Ejima K, Layne MD, Carvajal IM, Kritek PA, Baron RM, Chen YH, et al. Cyclooxygenase-2-deficient mice are resistant to endotoxin-induced inflammation and death. Faseb j. 2003;17(10):1325-7.
138. Funk CD. Prostaglandins and leukotrienes: advances in eicosanoid biology. Science. 2001;294(5548):1871-5.
139. Durán WN, Milazzo VJ, Sabido F, Hobson RW, 2nd. Platelet-activating factor modulates leukocyte adhesion to endothelium in ischemia-reperfusion. Microvasc Res. 1996;51(1):108-15.
140. Dalli J, Colas RA, Quintana C, Barragan-Bradford D, Hurwitz S, Levy BD, et al. Human Sepsis Eicosanoid and Proresolving Lipid Mediator Temporal Profiles: Correlations With Survival and Clinical Outcomes. Crit Care Med. 2017;45(1):58-68.
141. Mariano F, Guida G, Donati D, Tetta C, Cavalli PL, Verzetti G, et al. Production of platelet-activating factor in patients with sepsis-associated acute renal failure. Nephrol Dial Transplant. 1999;14(5):1150-7.
142. Suputtamongkol Y, Intaranongpai S, Smith MD, Angus B, Chaowagul W, Permpikul C, et al. A double-blind placebo-controlled study of an infusion of lexipafant (Platelet-activating factor receptor antagonist) in patients with severe sepsis. Antimicrob Agents Chemother. 2000;44(3):693-6.
143. Memiş D, Karamanlioğlu B, Turan A, Koyuncu O, Pamukçu Z. Effects of lornoxicam on the physiology of severe sepsis. Crit Care. 2004;8(6):R474-82.
144. Haupt MT, Jastremski MS, Clemmer TP, Metz CA, Goris GB. Effect of ibuprofen in patients with severe sepsis: a randomized, double-blind, multicenter study. The Ibuprofen Study Group. Crit Care Med. 1991;19(11):1339-47.
145. Bernard GR, Wheeler AP, Russell JA, Schein R, Summer WR, Steinberg KP, et al. The effects of ibuprofen on the physiology and survival of patients with sepsis. The Ibuprofen in Sepsis Study Group. N Engl J Med. 1997;336(13):912-8.
146. Luster AD. Chemokines--chemotactic cytokines that mediate inflammation. N Engl J Med. 1998;338(7):436-45.
147. Vermont CL, Hazelzet JA, de Kleijn ED, van den Dobbelsteen GP, de Groot R. CC and CXC chemokine levels in children with meningococcal sepsis accurately predict mortality and disease severity. Crit Care. 2006;10(1):R33.
148. Kunkel SL, Standiford T, Kasahara K, Strieter RM. Interleukin-8 (IL-8): The Major Neutrophil Chemotactic Factor in the Lung. Experimental Lung Research. 1991;17(1):17-23.

149. Türler A, Schwarz NT, Türler E, Kalff JC, Bauer AJ. MCP-1 causes leukocyte recruitment and subsequently endotoxemic ileus in rat. American Journal of Physiology-Gastrointestinal and Liver Physiology. 2002;282(1):G145-G55.
150. Gerszten RE, Garcia-Zepeda EA, Lim YC, Yoshida M, Ding HA, Gimbrone MA, Jr., et al. MCP-1 and IL-8 trigger firm adhesion of monocytes to vascular endothelium under flow conditions. Nature. 1999;398(6729):718-23.
151. Turner MD, Nedjai B, Hurst T, Pennington DJ. Cytokines and chemokines: At the crossroads of cell signalling and inflammatory disease. Biochimica et Biophysica Acta (BBA) - Molecular Cell Research. 2014;1843(11):2563-82.
152. Chousterman BG, Swirski FK, Weber GF. Cytokine storm and sepsis disease pathogenesis. Semin Immunopathol. 2017;39(5):517-28.
153. Leser HG, Gross V, Scheibenbogen C, Heinisch A, Salm R, Lausen M, et al. Elevation of serum interleukin-6 concentration precedes acute-phase response and reflects severity in acute pancreatitis. Gastroenterology. 1991;101(3):782-5.
154. Schouten M, Wiersinga WJ, Levi M, van der Poll T. Inflammation, endothelium, and coagulation in sepsis. J Leukoc Biol. 2008;83(3):536-45.
155. van der Poll T, de Waal Malefyt R, Coyle SM, Lowry SF. Antiinflammatory cytokine responses during clinical sepsis and experimental endotoxemia: sequential measurements of plasma soluble interleukin (IL)-1 receptor type II, IL-10, and IL-13. J Infect Dis. 1997;175(1):118-22.
156. Munford RS, Pugin J. Normal responses to injury prevent systemic inflammation and can be immunosuppressive. Am J Respir Crit Care Med. 2001;163(2):316-21.
157. Bogdan C, Nathan C. Modulation of macrophage function by transforming growth factor beta, interleukin-4, and interleukin-10. Ann N Y Acad Sci. 1993;685:713-39.
158. van der Poll T, de Boer JD, Levi M. The effect of inflammation on coagulation and vice versa. Curr Opin Infect Dis. 2011;24(3):273-8.
159. Aird WC. The role of the endothelium in severe sepsis and multiple organ dysfunction syndrome. Blood. 2003;101(10):3765-77.
160. Bateman RM, Sharpe MD, Jagger JE, Ellis CG. Sepsis impairs microvascular autoregulation and delays capillary response within hypoxic capillaries. Critical Care. 2015;19(1):389.
161. De Backer D, Donadello K, Sakr Y, Ospina-Tascon G, Salgado D, Scolletta S, et al. Microcirculatory alterations in patients with severe sepsis: impact of time of assessment and relationship with outcome. Critical care medicine. 2013;41(3):791-9.
162. Sakr Y, Dubois M-J, De Backer D, Creteur J, Vincent J-L. Persistent microcirculatory alterations are associated with organ failure and death in patients with septic shock. Critical care medicine. 2004;32(9):1825-31.
163. Miranda M, Balarini M, Caixeta D, Bouskela E. Microcirculatory dysfunction in sepsis: pathophysiology, clinical monitoring, and potential therapies. American Journal of Physiology-Heart and Circulatory Physiology. 2016;311(1):H24-H35.
164. Barichello T, Generoso JS, Singer M, Dal-Pizzol F. Biomarkers for sepsis: more than just fever and leukocytosis—a narrative review. Critical Care. 2022;26(1):14.
165. Faix JD. Biomarkers of sepsis. Crit Rev Clin Lab Sci. 2013;50(1):23-36.
166. Livaditi O, Kotanidou A, Psarra A, Dimopoulou I, Sotiropoulou C, Augustatou K, et al. Neutrophil CD64 expression and serum IL-8: sensitive early markers of severity and outcome in sepsis. Cytokine. 2006;36(5-6):283-90.
167. Cardelli P, Ferraironi M, Amodeo R, Tabacco F, De Blasi R, Nicoletti M, et al. Evaluation of neutrophil CD64 expression and procalcitonin as useful markers in early diagnosis of sepsis. International journal of immunopathology and pharmacology. 2008;21(1):43-9.
168. Streimish I, Bizzarro M, Northrup V, Wang C, Renna S, Koval N, et al. Neutrophil CD64 as a diagnostic marker in neonatal sepsis. The Pediatric infectious disease journal. 2012;31(7):777.

169. Genel F, Atlihan F, Gulez N, Kazanci E, Vergin C, Terek DT, et al. Evaluation of adhesion molecules CD64, CD11b and CD62L in neutrophils and monocytes of peripheral blood for early diagnosis of neonatal infection. World J Pediatr. 2012;8(1):72-5.
170. Juskewitch JE, Abraham RS, League SC, Jenkins SM, Smith CY, Enders FT, et al. Monocyte HLA-DR expression and neutrophil CD64 expression as biomarkers of infection in critically ill neonates and infants. Pediatr Res. 2015;78(6):683-90.
171. Landelle C, Lepape A, Voirin N, Tognet E, Venet F, Bohé J, et al. Low monocyte human leukocyte antigen-DR is independently associated with nosocomial infections after septic shock. Intensive Care Med. 2010;36(11):1859-66.
172. Monneret G, Lepape A, Voirin N, Bohé J, Venet F, Debard AL, et al. Persisting low monocyte human leukocyte antigen-DR expression predicts mortality in septic shock. Intensive Care Med. 2006;32(8):1175-83.
173. Narvaez-Rivera RM, Rendon A, Salinas-Carmona MC, Rosas-Taraco AG. Soluble RAGE as a severity marker in community acquired pneumonia associated sepsis. BMC Infect Dis. 2012;12:15.
174. Bopp C, Hofer S, Weitz J, Bierhaus A, Nawroth PP, Martin E, et al. sRAGE is Elevated in Septic Patients and Associated With Patients Outcome. Journal of Surgical Research. 2008;147(1):79-83.
175. Endo S, Suzuki Y, Takahashi G, Shozushima T, Ishikura H, Murai A, et al. Usefulness of presepsin in the diagnosis of sepsis in a multicenter prospective study. J Infect Chemother. 2012;18(6):891-7.
176. Bergquist M, Samuelsson L, Larsson A, Tydén J, Johansson J, Lipcsey M. TNFR1, TNFR2, neutrophil gelatinase-associated lipocalin and heparin binding protein in identifying sepsis and predicting outcome in an intensive care cohort. Sci Rep. 2020;10(1):15350.
177. de Pablo R, Monserrat J, Reyes E, Díaz D, Rodríguez-Zapata M, de la Hera A, et al. Sepsis-induced acute respiratory distress syndrome with fatal outcome is associated to increased serum transforming growth factor beta-1 levels. European journal of internal medicine. 2012;23(4):358-62.
178. Liu Z, Meng Z, Li Y, Zhao J, Wu S, Gou S, et al. Prognostic accuracy of the serum lactate level, the SOFA score and the qSOFA score for mortality among adults with Sepsis. Scandinavian Journal of Trauma, Resuscitation and Emergency Medicine. 2019;27(1):51.
179. Gomez H, Kellum JA. Lactate in sepsis. JAMA. 2015;313(2):194-5.
180. Singer AJ, Taylor M, Domingo A, Ghazipura S, Khorasonchi A, Thode Jr HC, et al. Diagnostic characteristics of a clinical screening tool in combination with measuring bedside lactate level in emergency department patients with suspected sepsis. Academic Emergency Medicine. 2014;21(8):853-7.
181. Nichol AD, Egi M, Pettila V, Bellomo R, French C, Hart G, et al. Relative hyperlactatemia and hospital mortality in critically ill patients: a retrospective multi-centre study. Critical care. 2010;14(1):1-9.
182. Pierrakos C, Velissaris D, Bisdorff M, Marshall JC, Vincent J-L. Biomarkers of sepsis: time for a reappraisal. Critical Care. 2020;24(1):287.
183. McFadyen JD, Zeller J, Potempa LA, Pietersz GA, Eisenhardt SU, Peter K. C-reactive protein and its structural isoforms: an evolutionary conserved marker and central player in inflammatory diseases and beyond. Vertebrate and Invertebrate Respiratory Proteins, Lipoproteins and other Body Fluid Proteins. 2020:499-520.
184. Simon L, Gauvin F, Amre DK, Saint-Louis P, Lacroix J. Serum Procalcitonin and C-Reactive Protein Levels as Markers of Bacterial Infection: A Systematic Review and Meta-analysis. Clinical Infectious Diseases. 2004;39(2):206-17.
185. Marshall JC. Why have clinical trials in sepsis failed? Trends Mol Med. 2014;20(4):195-203.
186. Dellinger RP. The Surviving Sepsis Campaign: Where have we been and where are we going? Cleve Clin J Med. 2015;82(4):237-44.
187. Rivers E, Nguyen B, Havstad S, Ressler J, Muzzin A, Knoblich B, et al. Early goal-directed therapy in the treatment of severe sepsis and septic shock. N Engl J Med. 2001;345(19):1368-77.

188. Boonen E, Vervenne H, Meersseman P, Andrew R, Mortier L, Declercq PE, et al. Reduced cortisol metabolism during critical illness. N Engl J Med. 2013;368(16):1477-88.
189. Fisher CJ, Jr., Agosti JM, Opal SM, Lowry SF, Balk RA, Sadoff JC, et al. Treatment of septic shock with the tumor necrosis factor receptor:Fc fusion protein. The Soluble TNF Receptor Sepsis Study Group. N Engl J Med. 1996;334(26):1697-702.
190. Opal SM, Fisher CJ, Jr., Dhainaut JF, Vincent JL, Brase R, Lowry SF, et al. Confirmatory interleukin-1 receptor antagonist trial in severe sepsis: a phase III, randomized, double-blind, placebo-controlled, multicenter trial. The Interleukin-1 Receptor Antagonist Sepsis Investigator Group. Crit Care Med. 1997;25(7):1115-24.
191. Skrupky Lee P, Kerby Paul W, Hotchkiss Richard S. Advances in the Management of Sepsis and the Understanding of Key Immunologic Defects. Anesthesiology. 2011;115(6):1349-62.
192. Wiedermann CJ, Kaneider NC. A meta-analysis of controlled trials of recombinant human activated protein C therapy in patients with sepsis. BMC Emerg Med. 2005;5:7.
193. Nadel S, Goldstein B, Williams MD, Dalton H, Peters M, Macias WL, et al. Drotrecogin alfa (activated) in children with severe sepsis: a multicentre phase III randomised controlled trial. Lancet. 2007;369(9564):836-43.
194. Scarlatescu E, Tomescu D, Arama SS. Anticoagulant Therapy in Sepsis. The Importance of Timing. J Crit Care Med (Targu Mures). 2017;3(2):63-9.
195. Bernard GR, Vincent J-L, Laterre P-F, LaRosa SP, Dhainaut J-F, Lopez-Rodriguez A, et al. Efficacy and Safety of Recombinant Human Activated Protein C for Severe Sepsis. New England Journal of Medicine. 2001;344(10):699-709.
196. Angus DC. Drotrecogin alfa (activated) ... a sad final fizzle to a roller-coaster party. Critical Care. 2012;16(1):107.
197. Sprung CL, Annane D, Keh D, Moreno R, Singer M, Freivogel K, et al. Hydrocortisone therapy for patients with septic shock. N Engl J Med. 2008;358(2):111-24.
198. Group H-ASS. Ziegler EJ, Fisher CJJr, Sprung CL, Starube RC, Sadoff JC, Foulke GE et al. Treatment of Gram negative bacteremia and septic shock with HA-1A human monoclonal antibody against endotoxin. A randomized, doubleblind, placebocontrolled trial. N Engl J Med. 1991;324:429-36.
199. Dellinger RP, Bagshaw SM, Antonelli M, Foster DM, Klein DJ, Marshall JC, et al. Effect of Targeted Polymyxin B Hemoperfusion on 28-Day Mortality in Patients With Septic Shock and Elevated Endotoxin Level: The EUPHRATES Randomized Clinical Trial. JAMA. 2018;320(14):1455-63.
200. Levin M, Quint PA, Goldstein B, Barton P, Bradley JS, Shemie SD, et al. Recombinant bactericidal/permeability-increasing protein (rBPI21) as adjunctive treatment for children with severe meningococcal sepsis: a randomised trial. The Lancet. 2000;356(9234):961-7.
201. Opal SM, Laterre PF, Francois B, LaRosa SP, Angus DC, Mira JP, et al. Effect of eritoran, an antagonist of MD2-TLR4, on mortality in patients with severe sepsis: the ACCESS randomized trial. JAMA. 2013;309(11):1154-62.
202. Davies R, O'Dea K, Gordon A. Immune therapy in sepsis: Are we ready to try again? Journal of the Intensive Care Society. 2018;19(4):326-44.
203. Yáñez-Mó M, Siljander PR, Andreu Z, Zavec AB, Borràs FE, Buzas EI, et al. Biological properties of extracellular vesicles and their physiological functions. J Extracell Vesicles. 2015;4:27066.
204. Wolf P. The nature and significance of platelet products in human plasma. British journal of haematology. 1967;13(3):269-88.
205. Tetta C, Ghigo E, Silengo L, Deregibus MC, Camussi G. Extracellular vesicles as an emerging mechanism of cell-to-cell communication. Endocrine. 2013;44(1):11-9.
206. Inal JM, Ansa-Addo EA, Stratton D, Kholia S, Antwi-Baffour SS, Jorfi S, et al. Microvesicles in health and disease. Arch Immunol Ther Exp (Warsz). 2012;60(2):107-21.
207. Colombo M, Raposo G, Théry C. Biogenesis, secretion, and intercellular interactions of exosomes and other extracellular vesicles. Annu Rev Cell Dev Biol. 2014;30:255-89.

208. Morello M, Minciacchi VR, de Candia P, Yang J, Posadas E, Kim H, et al. Large oncosomes mediate intercellular transfer of functional microRNA. Cell Cycle. 2013;12(22):3526-36.
209. Bobrie A, Colombo M, Krumeich S, Raposo G, Théry C. Diverse subpopulations of vesicles secreted by different intracellular mechanisms are present in exosome preparations obtained by differential ultracentrifugation. J Extracell Vesicles. 2012;1.
210. Théry C, Witwer KW, Aikawa E, Alcaraz MJ, Anderson JD, Andriantsitohaina R, et al. Minimal information for studies of extracellular vesicles 2018 (MISEV2018): a position statement of the International Society for Extracellular Vesicles and update of the MISEV2014 guidelines. J Extracell Vesicles. 2018;7(1):1535750.
211. Gustafson D, Veitch S, Fish JE. Extracellular Vesicles as Protagonists of Diabetic Cardiovascular Pathology. Frontiers in Cardiovascular Medicine. 2017;4.
212. Elmore S. Apoptosis: a review of programmed cell death. Toxicologic pathology. 2007;35(4):495-516.
213. Jing W, Wang H, Zhan L, Yan W. Extracellular Vesicles, New Players in Sepsis and Acute Respiratory Distress Syndrome. Frontiers in Cellular and Infection Microbiology. 2022;12.
214. Lőrincz Á M, Schütte M, Timár CI, Veres DS, Kittel Á, McLeish KR, et al. Functionally and morphologically distinct populations of extracellular vesicles produced by human neutrophilic granulocytes. J Leukoc Biol. 2015;98(4):583-9.
215. Xu X, Lai Y, Hua Z-C. Apoptosis and apoptotic body: disease message and therapeutic target potentials. Bioscience reports. 2019;39(1).
216. Brinton LT, Sloane HS, Kester M, Kelly KA. Formation and role of exosomes in cancer. Cell Mol Life Sci. 2015;72(4):659-71.
217. Wu M, Wang G, Hu W, Yao Y, Yu X-F. Emerging roles and therapeutic value of exosomes in cancer metastasis. Molecular Cancer. 2019;18(1):53.
218. Syn NL, Wang L, Chow EK, Lim CT, Goh BC. Exosomes in Cancer Nanomedicine and Immunotherapy: Prospects and Challenges. Trends Biotechnol. 2017;35(7):665-76.
219. Jella KK, Nasti TH, Li Z, Malla SR, Buchwald ZS, Khan MK. Exosomes, Their Biogenesis and Role in Inter-Cellular Communication, Tumor Microenvironment and Cancer Immunotherapy. Vaccines (Basel). 2018;6(4):69.
220. Costa-Silva B, Aiello NM, Ocean AJ, Singh S, Zhang H, Thakur BK, et al. Pancreatic cancer exosomes initiate pre-metastatic niche formation in the liver. Nat Cell Biol. 2015;17(6):816-26.
221. Wendler F, Stamp GW, Giamas G. Tumor-Stromal Cell Communication: Small Vesicles Signal Big Changes. Trends Cancer. 2016;2(7):326-9.
222. Devhare PB, Ray RB. Extracellular vesicles: Novel mediator for cell to cell communications in liver pathogenesis. Mol Aspects Med. 2018;60:115-22.
223. Doyle LM, Wang MZ. Overview of Extracellular Vesicles, Their Origin, Composition, Purpose, and Methods for Exosome Isolation and Analysis. Cells. 2019;8(7):727.
224. Crescitelli R, Lässer C, Szabó TG, Kittel A, Eldh M, Dianzani I, et al. Distinct RNA profiles in subpopulations of extracellular vesicles: apoptotic bodies, microvesicles and exosomes. J Extracell Vesicles. 2013;2:10.3402/jev.v2i0.20677.
225. Gireud-Goss M, Reyes S, Wilson M, Farley M, Memarzadeh K, Srinivasan S, et al. Distinct mechanisms enable inward or outward budding from late endosomes/multivesicular bodies. Exp Cell Res. 2018;372(1):1-15.
226. Kunder CA, St John AL, Li G, Leong KW, Berwin B, Staats HF, et al. Mast cell-derived particles deliver peripheral signals to remote lymph nodes. J Exp Med. 2009;206(11):2455-67.
227. Tricarico C, Clancy J, D'Souza-Schorey C. Biology and biogenesis of shed microvesicles. Small GTPases. 2017;8(4):220-32.
228. Loyer X, Vion AC, Tedgui A, Boulanger CM. Microvesicles as cell-cell messengers in cardiovascular diseases. Circ Res. 2014;114(2):345-53.
229. Raposo G, Stoorvogel W. Extracellular vesicles: exosomes, microvesicles, and friends. J Cell Biol. 2013;200(4):373-83.

230. Cocucci E, Meldolesi J. Ectosomes and exosomes: shedding the confusion between extracellular vesicles. Trends Cell Biol. 2015;25(6):364-72.
231. Muralidharan-Chari V, Clancy JW, Sedgwick A, D'Souza-Schorey C. Microvesicles: mediators of extracellular communication during cancer progression. J Cell Sci. 2010;123(Pt 10):1603-11.
232. McVey M, Tabuchi A, Kuebler WM. Microparticles and acute lung injury. American Journal of Physiology-Lung Cellular and Molecular Physiology. 2012;303(5):L364-L81.
233. Bevers EM, Williamson PL. Getting to the Outer Leaflet: Physiology of Phosphatidylserine Exposure at the Plasma Membrane. Physiol Rev. 2016;96(2):605-45.
234. Morel O, Jesel L, Freyssinet JM, Toti F. Cellular mechanisms underlying the formation of circulating microparticles. Arterioscler Thromb Vasc Biol. 2011;31(1):15-26.
235. van der Pol E, Böing AN, Harrison P, Sturk A, Nieuwland R. Classification, functions, and clinical relevance of extracellular vesicles. Pharmacol Rev. 2012;64(3):676-705.
236. Connor DE, Exner T, Ma DD, Joseph JE. The majority of circulating platelet-derived microparticles fail to bind annexin V, lack phospholipid-dependent procoagulant activity and demonstrate greater expression of glycoprotein Ib. Thromb Haemost. 2010;103(5):1044-52.
237. Jeanneteau J, Hibert P, Martinez MC, Tual-Chalot S, Tamareille S, Furber A, et al. Microparticle release in remote ischemic conditioning mechanism. Am J Physiol Heart Circ Physiol. 2012;303(7):H871-7.
238. Ma F, Liu H, Shen Y, Zhang Y, Pan S. Platelet-derived microvesicles are involved in cardio-protective effects of remote preconditioning. Int J Clin Exp Pathol. 2015;8(9):10832-9.
239. Fink K, Feldbrügge L, Schwarz M, Bourgeois N, Helbing T, Bode C, et al. Circulating annexin V positive microparticles in patients after successful cardiopulmonary resuscitation. Crit Care. 2011;15(5):R251-R.
240. Thiagarajan P, Tait JF. Collagen-induced exposure of anionic phospholipid in platelets and platelet-derived microparticles. J Biol Chem. 1991;266(36):24302-7.
241. Rhys HI, Dell'Accio F, Pitzalis C, Moore A, Norling LV, Perretti M. Neutrophil Microvesicles from Healthy Control and Rheumatoid Arthritis Patients Prevent the Inflammatory Activation of Macrophages. EBioMedicine. 2018;29:60-9.
242. Gasser O, Schifferli JA. Activated polymorphonuclear neutrophils disseminate anti-inflammatory microparticles by ectocytosis. Blood. 2004;104(8):2543-8.
243. Zakharova L, Svetlova M, Fomina AF. T cell exosomes induce cholesterol accumulation in human monocytes via phosphatidylserine receptor. J Cell Physiol. 2007;212(1):174-81.
244. Keller S, Ridinger J, Rupp A-K, Janssen JW, Altevogt P. Body fluid derived exosomes as a novel template for clinical diagnostics. Journal of translational medicine. 2011;9(1):1-9.
245. Au - Lässer C, Au - Eldh M, Au - Lötvall J. Isolation and Characterization of RNA-Containing Exosomes. JoVE. 2012(59):e3037.
246. O'Dea KP, Porter JR, Tirlapur N, Katbeh U, Singh S, Handy JM, et al. Circulating Microvesicles Are Elevated Acutely following Major Burns Injury and Associated with Clinical Severity. PLOS ONE. 2016;11(12):e0167801.
247. Caby M-P, Lankar D, Vincendeau-Scherrer C, Raposo G, Bonnerot C. Exosomal-like vesicles are present in human blood plasma. International immunology. 2005;17(7):879-87.
248. Pisitkun T, Shen R-F, Knepper MA. Identification and proteomic profiling of exosomes in human urine. Proceedings of the National Academy of Sciences. 2004;101(36):13368-73.
249. Poliakov A, Spilman M, Dokland T, Amling CL, Mobley JA. Structural heterogeneity and protein composition of exosome-like vesicles (prostasomes) in human semen. The Prostate. 2009;69(2):159-67.
250. Berckmans RJ, Sturk A, van Tienen LM, Schaap MC, Nieuwland R. Cell-derived vesicles exposing coagulant tissue factor in saliva. Blood, The Journal of the American Society of Hematology. 2011;117(11):3172-80.
251. Admyre C, Johansson SM, Qazi KR, Filén JJ, Lahesmaa R, Norman M, et al. Exosomes with immune modulatory features are present in human breast milk. J Immunol. 2007;179(3):1969-78.

252. Street JM, Barran PE, Mackay CL, Weidt S, Balmforth C, Walsh TS, et al. Identification and proteomic profiling of exosomes in human cerebrospinal fluid. Journal of translational medicine. 2012;10(1):1-7.
253. Levänen B, Bhakta NR, Paredes PT, Barbeau R, Hiltbrunner S, Pollack JL, et al. Altered microRNA profiles in bronchoalveolar lavage fluid exosomes in asthmatic patients. Journal of Allergy and Clinical Immunology. 2013;131(3):894-903. e8.
254. Soni S, Garner JL, O'Dea KP, Koh M, Finney L, Tirlapur N, et al. Intra-alveolar neutrophil-derived microvesicles are associated with disease severity in COPD. Am J Physiol Lung Cell Mol Physiol. 2021;320(1):L73-l83.
255. Brennan K, Martin K, FitzGerald SP, O'Sullivan J, Wu Y, Blanco A, et al. A comparison of methods for the isolation and separation of extracellular vesicles from protein and lipid particles in human serum. Scientific Reports. 2020;10(1):1039.
256. Furi I, Momen-Heravi F, Szabo G. Extracellular vesicle isolation: present and future. Annals of translational medicine. 2017;5(12):263-.
257. Konoshenko MY, Lekchnov EA, Vlassov AV, Laktionov PP. Isolation of Extracellular Vesicles: General Methodologies and Latest Trends. BioMed Research International. 2018;2018:8545347.
258. Dinkla S, Brock R, Joosten I, Bosman GJ. Gateway to understanding microparticles: standardized isolation and identification of plasma membrane-derived vesicles. Nanomedicine. 2013;8(10):1657-68.
259. Lobb RJ, Becker M, Wen Wen S, Wong CSF, Wiegmans AP, Leimgruber A, et al. Optimized exosome isolation protocol for cell culture supernatant and human plasma. J Extracell Vesicles. 2015;4(1):27031.
260. Livshits MA, Khomyakova E, Evtushenko EG, Lazarev VN, Kulemin NA, Semina SE, et al. Isolation of exosomes by differential centrifugation: Theoretical analysis of a commonly used protocol. Scientific reports. 2015;5(1):1-14.
261. Hartjes TA, Mytnyk S, Jenster GW, van Steijn V, van Royen ME. Extracellular Vesicle Quantification and Characterization: Common Methods and Emerging Approaches. Bioengineering (Basel). 2019;6(1):7.
262. Chandler WL. Measurement of microvesicle levels in human blood using flow cytometry. Cytometry B Clin Cytom. 2016;90(4):326-36.
263. McVey MJ, Spring CM, Kuebler WM. Improved resolution in extracellular vesicle populations using 405 instead of 488 nm side scatter. J Extracell Vesicles. 2018;7(1):1454776.
264. Nolte-'t Hoen EN, van der Vlist EJ, Aalberts M, Mertens HC, Bosch BJ, Bartelink W, et al. Quantitative and qualitative flow cytometric analysis of nanosized cell-derived membrane vesicles. Nanomedicine. 2012;8(5):712-20.
265. van der Vlist EJ, Nolte-'t Hoen EN, Stoorvogel W, Arkesteijn GJ, Wauben MH. Fluorescent labeling of nano-sized vesicles released by cells and subsequent quantitative and qualitative analysis by high-resolution flow cytometry. Nat Protoc. 2012;7(7):1311-26.
266. Morales-Kastresana A, Jones JC. Flow Cytometric Analysis of Extracellular Vesicles. In: Hill AF, editor. Exosomes and Microvesicles: Methods and Protocols. New York, NY: Springer New York; 2017. p. 215-25.
267. Koliha N, Wiencek Y, Heider U, Jüngst C, Kladt N, Krauthäuser S, et al. A novel multiplex bead-based platform highlights the diversity of extracellular vesicles. J Extracell Vesicles. 2016;5(1):29975.
268. Buzás EI, Tóth EÁ, Sódar BW, Szabó-Taylor KÉ. Molecular interactions at the surface of extracellular vesicles. Seminars in Immunopathology. 2018;40(5):453-64.
269. Fitzgerald W, Freeman ML, Lederman MM, Vasilieva E, Romero R, Margolis L. A System of Cytokines Encapsulated in ExtraCellular Vesicles. Scientific Reports. 2018;8(1):8973.
270. Boilard E. Extracellular vesicles and their content in bioactive lipid mediators: more than a sack of microRNA. J Lipid Res. 2018;59(11):2037-46.

271. Dasgupta SK, Le A, Chavakis T, Rumbaut RE, Thiagarajan P. Developmental endothelial locus-1 (Del-1) mediates clearance of platelet microparticles by the endothelium. Circulation. 2012;125(13):1664-72.
272. French KC, Antonyak MA, Cerione RA. Extracellular vesicle docking at the cellular port: Extracellular vesicle binding and uptake. Semin Cell Dev Biol. 2017;67:48-55.
273. Dasgupta SK, Abdel-Monem H, Niravath P, Le A, Bellera RV, Langlois K, et al. Lactadherin and clearance of platelet-derived microvesicles. Blood. 2009;113(6):1332-9.
274. Faille D, El-Assaad F, Mitchell AJ, Alessi MC, Chimini G, Fusai T, et al. Endocytosis and intracellular processing of platelet microparticles by brain endothelial cells. J Cell Mol Med. 2012;16(8):1731-8.
275. Huang-Doran I, Zhang CY, Vidal-Puig A. Extracellular Vesicles: Novel Mediators of Cell Communication In Metabolic Disease. Trends Endocrinol Metab. 2017;28(1):3-18.
276. Mulcahy LA, Pink RC, Carter DR. Routes and mechanisms of extracellular vesicle uptake. J Extracell Vesicles. 2014;3.
277. Willekens FL, Werre JM, Kruijt JK, Roerdinkholder-Stoelwinder B, Groenen-Döpp YA, van den Bos AG, et al. Liver Kupffer cells rapidly remove red blood cell-derived vesicles from the circulation by scavenger receptors. Blood. 2005;105(5):2141-5.
278. Matsumoto A, Takahashi Y, Chang HY, Wu YW, Yamamoto A, Ishihama Y, et al. Blood concentrations of small extracellular vesicles are determined by a balance between abundant secretion and rapid clearance. J Extracell Vesicles. 2020;9(1):1696517.
279. Rand ML, Wang H, Bang KW, Packham MA, Freedman J. Rapid clearance of procoagulant platelet-derived microparticles from the circulation of rabbits. J Thromb Haemost. 2006;4(7):1621-3.
280. Al Faraj A, Gazeau F, Wilhelm C, Devue C, Guérin CL, Péchoux C, et al. Endothelial cell-derived microparticles loaded with iron oxide nanoparticles: feasibility of MR imaging monitoring in mice. Radiology. 2012;263(1):169-78.
281. O'Dea KP, Tan YY, Shah S, V Patel B, C Tatham K, Wilson MR, et al. Monocytes mediate homing of circulating microvesicles to the pulmonary vasculature during low-grade systemic inflammation. J Extracell Vesicles. 2020;9(1):1706708.
282. Raeven P, Zipperle J, Drechsler S. Extracellular Vesicles as Markers and Mediators in Sepsis. Theranostics. 2018;8(12):3348-65.
283. Kunz N, Xia BT, Kalies KU, Klinger M, Gemoll T, Habermann JK, et al. Cell-Derived Nanoparticles are Endogenous Modulators of Sepsis With Therapeutic Potential. Shock. 2017;48(3):346-54.
284. Burgelman M, Vandendriessche C, Vandenbroucke RE. Extracellular Vesicles: A Double-Edged Sword in Sepsis. Pharmaceuticals. 2021;14(8):829.
285. Berckmans RJ, Nieuwland R, Böing AN, Romijn FP, Hack CE, Sturk A. Cell-derived microparticles circulate in healthy humans and support low grade thrombin generation. Thrombosis and haemostasis. 2001;85(04):639-49.
286. Nieuwland R, Berckmans RJ, McGregor S, Böing AN, Romijn FP, Westendorp RG, et al. Cellular origin and procoagulant properties of microparticles in meningococcal sepsis. Blood. 2000;95(3):930-5.
287. Matsumoto H, Yamakawa K, Ogura H, Koh T, Matsumoto N, Shimazu T. Enhanced expression of cell-specific surface antigens on endothelial microparticles in sepsis-induced disseminated intravascular coagulation. Shock. 2015;43(5):443-9.
288. Lashin HMS, Nadkarni S, Oggero S, Jones HR, Knight JC, Hinds CJ, et al. Microvesicle Subsets in Sepsis Due to Community Acquired Pneumonia Compared to Faecal Peritonitis. Shock. 2018;49(4):393-401.
289. Mostefai HA, Meziani F, Mastronardi ML, Agouni A, Heymes C, Sargentini C, et al. Circulating microparticles from patients with septic shock exert protective role in vascular function. Am J Respir Crit Care Med. 2008;178(11):1148-55.
290. Lehner GF, Harler U, Haller VM, Feistritzer C, Hasslacher J, Dunzendorfer S, et al. Characterization of microvesicles in septic shock using high-sensitivity flow cytometry. Shock: Injury, Inflammation, and Sepsis: Laboratory and Clinical Approaches. 2016;46(4):373-81.

291. Zhang Y, Meng H, Ma R, He Z, Wu X, Cao M, et al. CIRCULATING MICROPARTICLES, BLOOD CELLS, AND ENDOTHELIUM INDUCE PROCOAGULANT ACTIVITY IN SEPSIS THROUGH PHOSPHATIDYLSERINE EXPOSURE. Shock. 2016;45(3):299-307.
292. Dalli J, Montero-Melendez T, Norling LV, Yin X, Hinds C, Haskard D, et al. Heterogeneity in neutrophil microparticles reveals distinct proteome and functional properties. Mol Cell Proteomics. 2013;12(8):2205-19.
293. Danesh A, Inglis HC, Abdel-Mohsen M, Deng X, Adelman A, Schechtman KB, et al. Granulocyte-Derived Extracellular Vesicles Activate Monocytes and Are Associated With Mortality in Intensive Care Unit Patients. Frontiers in immunology. 2018;9:956-.
294. Joop K, Berckmans RJ, Nieuwland R, Berkhout J, Romijn FP, Hack CE, et al. Microparticles from patients with multiple organ dysfunction syndrome and sepsis support coagulation through multiple mechanisms. Thromb Haemost. 2001;85(5):810-20.
295. Matsumoto H, Yamakawa K, Ogura H, Koh T, Matsumoto N, Shimazu T. Clinical significance of tissue factor and CD13 double-positive microparticles in Sirs patients with trauma and severe sepsis. Shock: Injury, Inflammation, and Sepsis: Laboratory and Clinical Approaches. 2017;47(4):409-15.
296. Dalli J, Norling LV, Montero-Melendez T, Canova DF, Lashin H, Pavlov AM, et al. Microparticle alpha-2-macroglobulin enhances pro-resolving responses and promotes survival in sepsis. EMBO molecular medicine. 2014;6(1):27-42.
297. Timár CI, Lorincz AM, Csépányi-Kömi R, Vályi-Nagy A, Nagy G, Buzás EI, et al. Antibacterial effect of microvesicles released from human neutrophilic granulocytes. Blood. 2013;121(3):510-8.
298. Ogura H, Kawasaki T, Tanaka H, Koh T, Tanaka R, Ozeki Y, et al. Activated platelets enhance microparticle formation and platelet-leukocyte interaction in severe trauma and sepsis. J Trauma. 2001;50(5):801-9.
299. Larsson A, Lundahl T, Eriksson M, Lundkvist K, Lindahl T. Endotoxin induced platelet microvesicle formation measured by flow cytometry. Platelets. 1996;7(3):153-8.
300. Curry N, Raja A, Beavis J, Stanworth S, Harrison P. Levels of procoagulant microvesicles are elevated after traumatic injury and platelet microvesicles are negatively correlated with mortality. J Extracell Vesicles. 2014;3:25625-.
301. Mooberry MJ, Bradford R, Hobl EL, Lin FC, Jilma B, Key NS. Procoagulant microparticles promote coagulation in a factor XI-dependent manner in human endotoxemia. Journal of thrombosis and haemostasis : JTH. 2016;14(5):1031-42.
302. Aras O, Shet A, Bach RR, Hysjulien JL, Slungaard A, Hebbel RP, et al. Induction of microparticle- and cell-associated intravascular tissue factor in human endotoxemia. Blood. 2004;103(12):4545-53.
303. Shaver CM, Woods J, Clune JK, Grove BS, Wickersham NE, McNeil JB, et al. Circulating microparticle levels are reduced in patients with ARDS. Crit Care. 2017;21(1):120.
304. Puhm F, Boilard E, Machlus KR. Platelet Extracellular Vesicles. Arteriosclerosis, Thrombosis, and Vascular Biology. 2021;41(1):87-96.
305. Eustes AS, Dayal S. The Role of Platelet-Derived Extracellular Vesicles in Immune-Mediated Thrombosis. Int J Mol Sci. 2022;23(14).
306. Morel O, Toti F, Hugel B, Bakouboula B, Camoin-Jau L, Dignat-George F, et al. Procoagulant Microparticles. Arteriosclerosis, Thrombosis, and Vascular Biology. 2006;26(12):2594-604.
307. Müller I, Klocke A, Alex M, Kotzsch M, Luther T, Morgenstern E, et al. Intravascular tissue factor initiates coagulation via circulating microvesicles and platelets. The FASEB Journal. 2003;17(3):1-20.
308. Falati S, Liu Q, Gross P, Merrill-Skoloff G, Chou J, Vandendries E, et al. Accumulation of tissue factor into developing thrombi in vivo is dependent upon microparticle P-selectin glycoprotein ligand 1 and platelet P-selectin. J Exp Med. 2003;197(11):1585-98.
309. Sinauridze EI, Kireev DA, Popenko NY, Pichugin AV, Panteleev MA, Krymskaya OV, et al. Platelet microparticle membranes have 50- to 100-fold higher specific procoagulant activity than activated platelets. Thromb Haemost. 2007;97(3):425-34.

310. Jimenez JJ, Jy W, Mauro LM, Horstman LL, Soderland C, Ahn YS. Endothelial microparticles released in thrombotic thrombocytopenic purpura express von Willebrand factor and markers of endothelial activation. Br J Haematol. 2003;123(5):896-902.
311. Delabranche X, Boisramé-Helms J, Asfar P, Berger A, Mootien Y, Lavigne T, et al. Microparticles are new biomarkers of septic shock-induced disseminated intravascular coagulopathy. Intensive Care Medicine. 2013;39(10):1695-703.
312. Zecher D, Cumpelik A, Schifferli JA. Erythrocyte-derived microvesicles amplify systemic inflammation by thrombin-dependent activation of complement. Arterioscler Thromb Vasc Biol. 2014;34(2):313-20.
313. Hashemi Tayer A, Amirizadeh N, Ahmadinejad M, Nikougoftar M, Deyhim MR, Zolfaghari S. Procoagulant Activity of Red Blood Cell-Derived Microvesicles during Red Cell Storage. Transfusion Medicine and Hemotherapy. 2019;46(4):224-30.
314. Murao A, Brenner M, Aziz M, Wang P. Exosomes in Sepsis. Frontiers in Immunology. 2020;11.
315. Essandoh K, Yang L, Wang X, Huang W, Qin D, Hao J, et al. Blockade of exosome generation with GW4869 dampens the sepsis-induced inflammation and cardiac dysfunction. Biochimica et Biophysica Acta (BBA) - Molecular Basis of Disease. 2015;1852(11):2362-71.
316. Gao K, Jin J, Huang C, Li J, Luo H, Li L, et al. Exosomes Derived From Septic Mouse Serum Modulate Immune Responses via Exosome-Associated Cytokines. Frontiers in Immunology. 2019;10.
317. Nair RR, Mazza D, Brambilla F, Gorzanelli A, Agresti A, Bianchi ME. LPS-Challenged Macrophages Release Microvesicles Coated With Histones. Front Immunol. 2018;9:1463.
318. Coleman LG, Jr., Maile R, Jones SW, Cairns BA, Crews FT. HMGB1/IL-1β complexes in plasma microvesicles modulate immune responses to burn injury. PLOS ONE. 2018;13(3):e0195335.
319. Hong Y, Eleftheriou D, Hussain AA, Price-Kuehne FE, Savage CO, Jayne D, et al. Anti-neutrophil cytoplasmic antibodies stimulate release of neutrophil microparticles. J Am Soc Nephrol. 2012;23(1):49-62.
320. Majumdar R, Tavakoli Tameh A, Parent CA. Exosomes Mediate LTB4 Release during Neutrophil Chemotaxis. PLoS Biol. 2016;14(1):e1002336.
321. Butin-Israeli V, Houser MC, Feng M, Thorp EB, Nusrat A, Parkos CA, et al. Deposition of microparticles by neutrophils onto inflamed epithelium: a new mechanism to disrupt epithelial intercellular adhesions and promote transepithelial migration. Faseb j. 2016;30(12):4007-20.
322. Pitanga TN, de Aragão França L, Rocha VCJ, Meirelles T, Matos Borges V, Gonçalves MS, et al. Neutrophil-derived microparticles induce myeloperoxidase-mediated damage of vascular endothelial cells. BMC Cell Biology. 2014;15(1):21.
323. Slater TW, Finkielsztein A, Mascarenhas LA, Mehl LC, Butin-Israeli V, Sumagin R. Neutrophil microparticles deliver active myeloperoxidase to injured mucosa to inhibit epithelial wound healing. The Journal of immunology. 2017;198(7):2886-97.
324. Prakash PS, Caldwell CC, Lentsch AB, Pritts TA, Robinson BR. Human microparticles generated during sepsis in patients with critical illness are neutrophil-derived and modulate the immune response. J Trauma Acute Care Surg. 2012;73(2):401-6; discussion 6-7.
325. Mesri M, Altieri DC. Endothelial cell activation by leukocyte microparticles. J Immunol. 1998;161(8):4382-7.
326. Mesri M, Altieri DC. Leukocyte microparticles stimulate endothelial cell cytokine release and tissue factor induction in a JNK1 signaling pathway. J Biol Chem. 1999;274(33):23111-8.
327. Herrmann IK, Bertazzo S, O'Callaghan DJ, Schlegel AA, Kallepitis C, Antcliffe DB, et al. Differentiating sepsis from non-infectious systemic inflammation based on microvesicle-bacteria aggregation. Nanoscale. 2015;7(32):13511-20.
328. Kumagai Y, Murakami T, Kuwahara A, Iba T, Reich J, Nagaoka I. Antimicrobial peptide LL-37 ameliorates a murine sepsis model via the induction of microvesicle release from neutrophils. Innate Immun. 2020;26(7):565-79.

329. Eken C, Martin PJ, Sadallah S, Treves S, Schaller M, Schifferli JA. Ectosomes released by polymorphonuclear neutrophils induce a MerTK-dependent anti-inflammatory pathway in macrophages. J Biol Chem. 2010;285(51):39914-21.
330. Eken C, Sadallah S, Martin PJ, Treves S, Schifferli JA. Ectosomes of polymorphonuclear neutrophils activate multiple signaling pathways in macrophages. Immunobiology. 2013;218(3):382-92.
331. Dalli J, Norling LV, Renshaw D, Cooper D, Leung K-Y, Perretti M. Annexin 1 mediates the rapid anti-inflammatory effects of neutrophil-derived microparticles. Blood. 2008;112(6):2512-9.
332. Soni S, Wilson MR, O'Dea KP, Yoshida M, Katbeh U, Woods SJ, et al. Alveolar macrophage-derived microvesicles mediate acute lung injury. Thorax. 2016;71(11):1020-9.
333. Soni S, O'Dea KP, Tan YY, Cho K, Abe E, Romano R, et al. ATP redirects cytokine trafficking and promotes novel membrane TNF signaling via microvesicles. Faseb j. 2019;33(5):6442-55.
334. Cerri C, Chimenti D, Conti I, Neri T, Paggiaro P, Celi A. Monocyte/macrophage-derived microparticles up-regulate inflammatory mediator synthesis by human airway epithelial cells. J Immunol. 2006;177(3):1975-80.
335. Eyre J, Burton JO, Saleem MA, Mathieson PW, Topham PS, Brunskill NJ. Monocyte- and endothelial-derived microparticles induce an inflammatory phenotype in human podocytes. Nephron Exp Nephrol. 2011;119(3):e58-66.
336. Bardelli C, Amoruso A, Federici Canova D, Fresu L, Balbo P, Neri T, et al. Autocrine activation of human monocyte/macrophages by monocyte-derived microparticles and modulation by PPARγ ligands. Br J Pharmacol. 2012;165(3):716-28.
337. Zheng D, Zhang J, Zhang Z, Kuang L, Zhu Y, Wu Y, et al. Endothelial Microvesicles Induce Pulmonary Vascular Leakage and Lung Injury During Sepsis. Frontiers in Cell and Developmental Biology. 2020;8.
338. Densmore JC, Signorino PR, Ou J, Hatoum OA, Rowe JJ, Shi Y, et al. Endothelium-derived microparticles induce endothelial dysfunction and acute lung injury. Shock. 2006;26(5):464-71.
339. Kerris EWJ, Hoptay C, Calderon T, Freishtat RJ. Platelets and platelet extracellular vesicles in hemostasis and sepsis. Journal of Investigative Medicine. 2020;68(4):813-20.
340. Levesque MJ, Nerem RM. The elongation and orientation of cultured endothelial cells in response to shear stress. J Biomech Eng. 1985;107(4):341-7.
341. Ostrowski MA, Huang NF, Walker TW, Verwijlen T, Poplawski C, Khoo AS, et al. Microvascular endothelial cells migrate upstream and align against the shear stress field created by impinging flow. Biophysical journal. 2014;106(2):366-74.
342. De Backer D, Creteur J, Preiser JC, Dubois MJ, Vincent JL. Microvascular blood flow is altered in patients with sepsis. Am J Respir Crit Care Med. 2002;166(1):98-104.
343. De Backer D, Orbegozo Cortes D, Donadello K, Vincent JL. Pathophysiology of microcirculatory dysfunction and the pathogenesis of septic shock. Virulence. 2014;5(1):73-9.
344. Edul VS, Enrico C, Laviolle B, Vazquez AR, Ince C, Dubin A. Quantitative assessment of the microcirculation in healthy volunteers and in patients with septic shock. Crit Care Med. 2012;40(5):1443-8.
345. Shih CC, Liu CM, Chao A, Lee CT, Hsu YC, Yeh YC. Matched Comparison of Microcirculation Between Healthy Volunteers and Patients with Sepsis. Asian J Anesthesiol. 2018;56(1):14-22.
346. Colbert JF, Schmidt EP. Endothelial and Microcirculatory Function and Dysfunction in Sepsis. Clin Chest Med. 2016;37(2):263-75.
347. Frame MD, Sarelius IH. Endothelial cell dilatory pathways link flow and wall shear stress in an intact arteriolar network. J Appl Physiol (1985). 1996;81(5):2105-14.
348. Kuebler WM, Kuhnle GE, Groh J, Goetz AE. Leukocyte kinetics in pulmonary microcirculation: intravital fluorescence microscopic study. J Appl Physiol (1985). 1994;76(1):65-71.

349. Kuebler W, Kuhnle G, Groh J, Goetz A. Contribution of selectins to leucocyte sequestration in pulmonary microvessels by intravital microscopy in rabbits. The Journal of Physiology. 1997;501(Pt 2):375.
350. Lin A, Sabnis A, Kona S, Nattama S, Patel H, Dong JF, et al. Shear-regulated uptake of nanoparticles by endothelial cells and development of endothelial-targeting nanoparticles. J Biomed Mater Res A. 2010;93(3):833-42.
351. Dickerson JB, Blackwell JE, Ou JJ, Shinde Patil VR, Goetz DJ. Limited adhesion of biodegradable microspheres to E- and P-selectin under flow. Biotechnology and Bioengineering. 2001;73(6):500-9.
352. Gomez I, Ward B, Souilhol C, Recarti C, Ariaans M, Johnston J, et al. Neutrophil microvesicles drive atherosclerosis by delivering miR-155 to atheroprone endothelium. Nature Communications. 2020;11(1):214.
353. Mairey E, Genovesio A, Donnadieu E, Bernard C, Jaubert F, Pinard E, et al. Cerebral microcirculation shear stress levels determine Neisseria meningitidis attachment sites along the blood-brain barrier. J Exp Med. 2006;203(8):1939-50.
354. Barkefors I, Aidun CK, Ulrika Egertsdotter E. Effect of fluid shear stress on endocytosis of heparan sulfate and low-density lipoproteins. Journal of biomedicine and biotechnology. 2007;2007.
355. O'Dea KP, Young AJ, Yamamoto H, Robotham JL, Brennan FM, Takata M. Lung-marginated monocytes modulate pulmonary microvascular injury during early endotoxemia. American journal of respiratory and critical care medicine. 2005;172(9):1119-27.
356. O'Dea KP, Wilson MR, Dokpesi JO, Wakabayashi K, Tatton L, van Rooijen N, et al. Mobilization and margination of bone marrow Gr-1high monocytes during subclinical endotoxemia predisposes the lungs toward acute injury. The Journal of Immunology. 2009;182(2):1155-66.
357. Tan YY, O'Dea KP, Tsiridou DM, Pac Soo A, Koh MW, Beckett F, et al. Circulating Myeloid Cell-derived Extracellular Vesicles as Mediators of Indirect Acute Lung Injury. Am J Respir Cell Mol Biol. 2023;68(2):140-9.
358. Heumann D, Gallay P, Barras C, Zaech P, Ulevitch RJ, Tobias PS, et al. Control of lipopolysaccharide (LPS) binding and LPS-induced tumor necrosis factor secretion in human peripheral blood monocytes. J Immunol. 1992;148(11):3505-12.
359. Tsiridou DM, O'Dea KP, Tan YY, Takata M. Neutrophil-Derived Microvesicle Uptake under Flow Conditions in an In Vitro Model of Pulmonary Vascular Inflammation. The FASEB Journal. 2020;34(S1):1-.
360. Karasu E, Eisenhardt SU, Harant J, Huber-Lang M. Extracellular Vesicles: Packages Sent With Complement. Frontiers in Immunology. 2018;9.
361. Ginini L, Billan S, Fridman E, Gil Z. Insight into Extracellular Vesicle-Cell Communication: From Cell Recognition to Intracellular Fate. Cells. 2022;11(9).
362. Ohno S, Takanashi M, Sudo K, Ueda S, Ishikawa A, Matsuyama N, et al. Systemically injected exosomes targeted to EGFR deliver antitumor microRNA to breast cancer cells. Mol Ther. 2013;21(1):185-91.
363. Tian Y, Li S, Song J, Ji T, Zhu M, Anderson GJ, et al. A doxorubicin delivery platform using engineered natural membrane vesicle exosomes for targeted tumor therapy. Biomaterials. 2014;35(7):2383-90.
364. Grange C, Tapparo M, Bruno S, Chatterjee D, Quesenberry PJ, Tetta C, et al. Biodistribution of mesenchymal stem cell-derived extracellular vesicles in a model of acute kidney injury monitored by optical imaging. Int J Mol Med. 2014;33(5):1055-63.
365. Camussi G, Deregibus MC, Cantaluppi V. Role of stem-cell-derived microvesicles in the paracrine action of stem cells. Biochem Soc Trans. 2013;41(1):283-7.
366. Gatti S, Bruno S, Deregibus MC, Sordi A, Cantaluppi V, Tetta C, et al. Microvesicles derived from human adult mesenchymal stem cells protect against ischaemia-reperfusion-induced acute and chronic kidney injury. Nephrol Dial Transplant. 2011;26(5):1474-83.
367. Fisher AB, Al-Mehdi AB, Manevich Y. Shear stress and endothelial cell activation. Critical Care Medicine. 2002;30(5):S192-S7.

368. Fisher AB, Chien S, Barakat AI, Nerem RM. Endothelial cellular response to altered shear stress. Am J Physiol Lung Cell Mol Physiol. 2001;281(3):L529-33.
369. Amabile N, Renard J-M, Caussin C, Boulanger CM. Circulating immune complexes do not affect microparticle flow cytometry analysis in acute coronary syndrome. Blood. 2012;119(9):2174-5.
370. McCracken JM, Allen LA. Regulation of human neutrophil apoptosis and lifespan in health and disease. J Cell Death. 2014;7:15-23.
371. Kolonics F, Kajdácsi E, Farkas VJ, Veres DS, Khamari D, Kittel Á, et al. Neutrophils produce proinflammatory or anti-inflammatory extracellular vesicles depending on the environmental conditions. Journal of Leukocyte Biology. 2021;109(4):793-806.
372. Byrne A, Reen DJ. Lipopolysaccharide induces rapid production of IL-10 by monocytes in the presence of apoptotic neutrophils. J Immunol. 2002;168(4):1968-77.
373. Ren Y, Stuart L, Lindberg FP, Rosenkranz AR, Chen Y, Mayadas TN, et al. Nonphlogistic clearance of late apoptotic neutrophils by macrophages: efficient phagocytosis independent of beta 2 integrins. J Immunol. 2001;166(7):4743-50.
374. Shen G, Krienke S, Schiller P, Nießen A, Neu S, Eckstein V, et al. Microvesicles released by apoptotic human neutrophils suppress proliferation and IL-2/IL-2 receptor expression of resting T helper cells. European journal of immunology. 2017;47(5):900-10.
375. Wittmann S, Fröhlich D, Daniels S. Characterization of the human fMLP receptor in neutrophils and in Xenopus oocytes. Br J Pharmacol. 2002;135(6):1375-82.
376. Dorward DA, Lucas CD, Chapman GB, Haslett C, Dhaliwal K, Rossi AG. The role of formylated peptides and formyl peptide receptor 1 in governing neutrophil function during acute inflammation. Am J Pathol. 2015;185(5):1172-84.
377. Chen BP, Li YS, Zhao Y, Chen KD, Li S, Lao J, et al. DNA microarray analysis of gene expression in endothelial cells in response to 24-h shear stress. Physiol Genomics. 2001;7(1):55-63.
378. Ebong EE, Lopez-Quintero SV, Rizzo V, Spray DC, Tarbell JM. Shear-induced endothelial NOS activation and remodeling via heparan sulfate, glypican-1, and syndecan-1. Integr Biol (Camb). 2014;6(3):338-47.
379. Ayers L, Nieuwland R, Kohler M, Kraenkel N, Ferry B, Leeson P. Dynamic microvesicle release and clearance within the cardiovascular system: triggers and mechanisms. Clinical science. 2015;129(11):915-31.
380. Gasser O, Hess C, Miot S, Deon C, Sanchez JC, Schifferli JA. Characterisation and properties of ectosomes released by human polymorphonuclear neutrophils. Exp Cell Res. 2003;285(2):243-57.
381. Surmiak M, Gielicz A, Stojkov D, Szatanek R, Wawrzycka-Adamczyk K, Yousefi S, et al. LTB(4) and 5-oxo-ETE from extracellular vesicles stimulate neutrophils in granulomatosis with polyangiitis. J Lipid Res. 2020;61(1):1-9.
382. Johnson BL, 3rd, Midura EF, Prakash PS, Rice TC, Kunz N, Kalies K, et al. Neutrophil derived microparticles increase mortality and the counter-inflammatory response in a murine model of sepsis. Biochim Biophys Acta Mol Basis Dis. 2017;1863(10 Pt B):2554-63.
383. Pliyev BK, Kalintseva MV, Abdulaeva SV, Yarygin KN, Savchenko VG. Neutrophil microparticles modulate cytokine production by natural killer cells. Cytokine. 2014;65(2):126-9.
384. Ajikumar A, Long MB, Heath PR, Wharton SB, Ince PG, Ridger VC, et al. Neutrophil-Derived Microvesicle Induced Dysfunction of Brain Microvascular Endothelial Cells In Vitro. Int J Mol Sci. 2019;20(20).
385. El Habhab A, Altamimy R, Abbas M, Kassem M, Amoura L, Qureshi AW, et al. Significance of neutrophil microparticles in ischaemia-reperfusion: Pro-inflammatory effectors of endothelial senescence and vascular dysfunction. J Cell Mol Med. 2020;24(13):7266-81.
386. Watanabe J, Marathe GK, Neilsen PO, Weyrich AS, Harrison KA, Murphy RC, et al. Endotoxins stimulate neutrophil adhesion followed by synthesis and release of platelet-activating factor in microparticles. J Biol Chem. 2003;278(35):33161-8.

387. Pluskota E, Woody NM, Szpak D, Ballantyne CM, Soloviev DA, Simon DI, et al. Expression, activation, and function of integrin alphaMbeta2 (Mac-1) on neutrophil-derived microparticles. Blood. 2008;112(6):2327-35.
388. Lacy P. Mechanisms of degranulation in neutrophils. Allergy, Asthma & Clinical Immunology. 2006;2(3):1-11.
389. Yoon J, Terada A, Kita H. CD66b Regulates Adhesion and Activation of Human Eosinophils. The Journal of Immunology. 2007;179(12):8454-62.
390. Orr Y, Taylor JM, Cartland S, Bannon PG, Geczy C, Kritharides L. Conformational activation of CD11b without shedding of L-selectin on circulating human neutrophils. J Leukoc Biol. 2007;82(5):1115-25.
391. Pužar Dominkuš P, Stenovec M, Sitar S, Lasič E, Zorec R, Plemenitaš A, et al. PKH26 labeling of extracellular vesicles: Characterization and cellular internalization of contaminating PKH26 nanoparticles. Biochim Biophys Acta Biomembr. 2018;1860(6):1350-61.
392. Corso G, Heusermann W, Trojer D, Görgens A, Steib E, Voshol J, et al. Systematic characterization of extracellular vesicle sorting domains and quantification at the single molecule - single vesicle level by fluorescence correlation spectroscopy and single particle imaging. J Extracell Vesicles. 2019;8(1):1663043.
393. Pearce MJ, McIntyre TM, Prescott SM, Zimmerman GA, Whatley RE. Shear stress activates cytosolic phospholipase A2 (cPLA2) and MAP kinase in human endothelial cells. Biochem Biophys Res Commun. 1996;218(2):500-4.
394. Uhlig S, Yang Y, Waade J, Wittenberg C, Babendreyer A, Kuebler WM. Differential Regulation of Lung Endothelial Permeability in Vitro and in Situ. Cellular Physiology and Biochemistry. 2014;34(1):1-19.
395. Michel CC, Curry FE. Microvascular permeability. Physiol Rev. 1999;79(3):703-61.
396. Yang Y, Schmidt EP. The endothelial glycocalyx: an important regulator of the pulmonary vascular barrier. Tissue Barriers. 2013;1(1).
397. Durr E, Yu J, Krasinska KM, Carver LA, Yates JR, Testa JE, et al. Direct proteomic mapping of the lung microvascular endothelial cell surface in vivo and in cell culture. Nat Biotechnol. 2004;22(8):985-92.
398. Chatterjee S, Nieman GF, Christie JD, Fisher AB. Shear stress-related mechanosignaling with lung ischemia: lessons from basic research can inform lung transplantation. Am J Physiol Lung Cell Mol Physiol. 2014;307(9):L668-80.
399. Chatterjee S, Fisher AB. Mechanotransduction in the endothelium: role of membrane proteins and reactive oxygen species in sensing, transduction, and transmission of the signal with altered blood flow. Antioxid Redox Signal. 2014;20(6):899-913.
400. Yago T, Wu J, Wey CD, Klopocki AG, Zhu C, McEver RP. Catch bonds govern adhesion through L-selectin at threshold shear. J Cell Biol. 2004;166(6):913-23.
401. Finger EB, Puri KD, Alon R, Lawrence MB, von Andrian UH, Springer TA. Adhesion through L-selectin requires a threshold hydrodynamic shear. Nature. 1996;379(6562):266-9.
402. Yago T, Zarnitsyna VI, Klopocki AG, McEver RP, Zhu C. Transport governs flow-enhanced cell tethering through L-selectin at threshold shear. Biophys J. 2007;92(1):330-42.
403. da Costa Martins P, García-Vallejo JJ, van Thienen JV, Fernandez-Borja M, van Gils JM, Beckers C, et al. P-selectin glycoprotein ligand-1 is expressed on endothelial cells and mediates monocyte adhesion to activated endothelium. Arterioscler Thromb Vasc Biol. 2007;27(5):1023-9.
404. Macia E, Ehrlich M, Massol R, Boucrot E, Brunner C, Kirchhausen T. Dynasore, a cell-permeable inhibitor of dynamin. Dev Cell. 2006;10(6):839-50.
405. Patiño T, Soriano J, Barrios L, Ibáñez E, Nogués C. Surface modification of microparticles causes differential uptake responses in normal and tumoral human breast epithelial cells. Scientific Reports. 2015;5(1):11371.
406. Lesniak A, Fenaroli F, Monopoli MP, Åberg C, Dawson KA, Salvati A. Effects of the Presence or Absence of a Protein Corona on Silica Nanoparticle Uptake and Impact on Cells. ACS Nano. 2012;6(7):5845-57.

407. Lunov O, Syrovets T, Loos C, Beil J, Delacher M, Tron K, et al. Differential Uptake of Functionalized Polystyrene Nanoparticles by Human Macrophages and a Monocytic Cell Line. ACS Nano. 2011;5(3):1657-69.
408. Kamps JA, Morselt HW, Scherphof GL. Uptake of Liposomes Containing Phosphatidylserine by Liver Cellsin Vivoand by Sinusoidal Liver Cells in Primary Culture: In Vivo–in VitroDifferences. Biochemical and biophysical research communications. 1999;256(1):57-62.
409. Rothkopf C, Fahr A, Fricker G, Scherphof G, Kamps J. Uptake of phosphatidylserine-containing liposomes by liver sinusoidal endothelial cells in the serum-free perfused rat liver. Biochimica et Biophysica Acta (BBA)-Biomembranes. 2005;1668(1):10-6.
410. Tsiridou DM, O'Dea KP, Tan YY, Takata M. Late Breaking Abstract - Myeloid-derived microvesicles as acute mediators of sepsis-induced lung vascular inflammation. European Respiratory Journal. 2020;56(suppl 64):4468.
411. Exline MC, Justiniano S, Hollyfield JL, Berhe F, Besecker BY, Das S, et al. Microvesicular caspase-1 mediates lymphocyte apoptosis in sepsis. PLoS One. 2014;9(3):e90968.
412. Cavaillon JM, Munoz C, Fitting C, Misset B, Carlet J. Circulating cytokines: the tip of the iceberg? Circ Shock. 1992;38(2):145-52.
413. Poll Tvd, Jansen J, Endert E, Sauerwein HP, Deventer SJv. Noradrenaline inhibits lipopolysaccharide-induced tumor necrosis factor and interleukin 6 production in human whole blood. Infection and Immunity. 1994;62(5):2046-50.
414. Messerer DAC, Vidoni L, Erber M, Stratmann AEP, Bauer JM, Braun CK, et al. Animal-Free Human Whole Blood Sepsis Model to Study Changes in Innate Immunity. Frontiers in Immunology. 2020;11.
415. DeForge LE, Remick DG. Kinetics of TNF, IL-6, and IL-8 gene expression in LPS-stimulated human whole blood. Biochemical and Biophysical Research Communications. 1991;174(1):18-24.
416. Jemmett K, Macagno A, Molteni M, Heckels JE, Rossetti C, Christodoulides M. A Cyanobacterial Lipopolysaccharide Antagonist Inhibits Cytokine Production Induced by Neisseria meningitidis in a Human Whole-Blood Model of Septicemia. Infection and Immunity. 2008;76(7):3156-63.
417. Bernhard S, Hug S, Stratmann AEP, Erber M, Vidoni L, Knapp CL, et al. Interleukin 8 elicits rapid physiological changes in neutrophils that are altered by inflammatory conditions. Journal of Innate Immunity. 2021;13(4):225-41.
418. WOEI-A-JIN FJSH, DE KRUIF MD, GARCIA RODRIGUEZ P, OSANTO S, BERTINA RM. Microparticles expressing tissue factor are concurrently released with markers of inflammation and coagulation during human endotoxemia. Journal of Thrombosis and Haemostasis. 2012;10(6):1185-8.
419. Zubairova LD, Zubairov DM, Andrushko IA, Svintenok GY, Mustafin IG. Cell microvesicles during experimental endotoxemia. Bulletin of Experimental Biology and Medicine. 2006;142(5):573-6.
420. Eriksson M, Nelson D, Nordgren A, Larsson A. Increased platelet microvesicle formation is associated with mortality in a porcine model of endotoxemia. Acta Anaesthesiol Scand. 1998;42(5):551-7.
421. Lundahl TH, Lindahl TL, Fagerberg IH, Egberg N, Bunescu A, Larsson A. Activated platelets and impaired platelet function in intensive care patients analyzed by flow cytometry. Blood Coagul Fibrinolysis. 1996;7(2):218-20.
422. Cros J, Cagnard N, Woollard K, Patey N, Zhang SY, Senechal B, et al. Human CD14dim monocytes patrol and sense nucleic acids and viruses via TLR7 and TLR8 receptors. Immunity. 2010;33(3):375-86.
423. O'Dea KP, Dokpesi JO, Tatham KC, Wilson MR, Takata M. Regulation of monocyte subset proinflammatory responses within the lung microvasculature by the p38 MAPK/MK2 pathway. Am J Physiol Lung Cell Mol Physiol. 2011;301(5):L812-21.

424. Cointe S, Vallier L, Esnault P, Dacos M, Bonifay A, Macagno N, et al. Granulocyte microvesicles with a high plasmin generation capacity promote clot lysis and improve outcome in septic shock. Blood. 2022;139(15):2377-91.
425. Wang JG, Manly D, Kirchhofer D, Pawlinski R, Mackman N. Levels of microparticle tissue factor activity correlate with coagulation activation in endotoxemic mice. J Thromb Haemost. 2009;7(7):1092-8.
426. Wang Y, Zhang S, Luo L, Norström E, Braun O, Mörgelin M, et al. Platelet-derived microparticles regulates thrombin generation via phophatidylserine in abdominal sepsis. J Cell Physiol. 2018;233(2):1051-60.
427. Bernimoulin M, Waters EK, Foy M, Steele BM, Sullivan M, Falet H, et al. Differential stimulation of monocytic cells results in distinct populations of microparticles. J Thromb Haemost. 2009;7(6):1019-28.
428. Satta N, Toti F, Feugeas O, Bohbot A, Dachary-Prigent J, Eschwège V, et al. Monocyte vesiculation is a possible mechanism for dissemination of membrane-associated procoagulant activities and adhesion molecules after stimulation by lipopolysaccharide. J Immunol. 1994;153(7):3245-55.
429. Wen B, Combes V, Bonhoure A, Weksler BB, Couraud PO, Grau GE. Endotoxin-induced monocytic microparticles have contrasting effects on endothelial inflammatory responses. PLoS One. 2014;9(3):e91597.
430. Sarkar A, Mitra S, Mehta S, Raices R, Wewers MD. Monocyte derived microvesicles deliver a cell death message via encapsulated caspase-1. PLoS One. 2009;4(9):e7140.
431. Brahmer A, Neuberger E, Esch-Heisser L, Haller N, Jorgensen MM, Baek R, et al. Platelets, endothelial cells and leukocytes contribute to the exercise-triggered release of extracellular vesicles into the circulation. J Extracell Vesicles. 2019;8(1):1615820.
432. Clayton A, Court J, Navabi H, Adams M, Mason MD, Hobot JA, et al. Analysis of antigen presenting cell derived exosomes, based on immuno-magnetic isolation and flow cytometry. J Immunol Methods. 2001;247(1-2):163-74.
433. Greening DW, Xu R, Ji H, Tauro BJ, Simpson RJ. A protocol for exosome isolation and characterization: evaluation of ultracentrifugation, density-gradient separation, and immunoaffinity capture methods. Methods Mol Biol. 2015;1295:179-209.
434. Sharma P, Ludwig S, Muller L, Hong CS, Kirkwood JM, Ferrone S, et al. Immunoaffinity-based isolation of melanoma cell-derived exosomes from plasma of patients with melanoma. J Extracell Vesicles. 2018;7(1):1435138.
435. Agouni A, Lagrue-Lak-Hal AH, Ducluzeau PH, Mostefai HA, Draunet-Busson C, Leftheriotis G, et al. Endothelial dysfunction caused by circulating microparticles from patients with metabolic syndrome. Am J Pathol. 2008;173(4):1210-9.
436. Azevedo LC, Janiszewski M, Pontieri V, Pedro Mde A, Bassi E, Tucci PJ, et al. Platelet-derived exosomes from septic shock patients induce myocardial dysfunction. Crit Care. 2007;11(6):R120.
437. Boilard E, Nigrovic PA, Larabee K, Watts GFM, Coblyn JS, Weinblatt ME, et al. Platelets Amplify Inflammation in Arthritis via Collagen-Dependent Microparticle Production. Science. 2010;327(5965):580-3.
438. Lindemann S, Tolley ND, Dixon DA, McIntyre TM, Prescott SM, Zimmerman GA, et al. Activated platelets mediate inflammatory signaling by regulated interleukin 1beta synthesis. J Cell Biol. 2001;154(3):485-90.
439. Brown GT, McIntyre TM. Lipopolysaccharide signaling without a nucleus: kinase cascades stimulate platelet shedding of proinflammatory IL-1β-rich microparticles. J Immunol. 2011;186(9):5489-96.
440. Barry OP, Praticò D, Savani RC, FitzGerald GA. Modulation of monocyte-endothelial cell interactions by platelet microparticles. The Journal of Clinical Investigation. 1998;102(1):136-44.
441. Barry OP, Pratico D, Lawson JA, FitzGerald GA. Transcellular activation of platelets and endothelial cells by bioactive lipids in platelet microparticles. The Journal of clinical investigation. 1997;99(9):2118-27.

442. Szilágyi B, Fejes Z, Rusznyák Á, Fenyvesi F, Pócsi M, Halmi S, et al. Platelet Microparticles Enriched in miR-223 Reduce ICAM-1-Dependent Vascular Inflammation in Septic Conditions. Front Physiol. 2021;12:658524.
443. Laffont B, Corduan A, Rousseau M, Duchez AC, Lee CH, Boilard E, et al. Platelet microparticles reprogram macrophage gene expression and function. Thromb Haemost. 2016;115(2):311-23.
444. Eken C, Gasser O, Zenhaeusern G, Oehri I, Hess C, Schifferli JA. Polymorphonuclear neutrophil-derived ectosomes interfere with the maturation of monocyte-derived dendritic cells. J Immunol. 2008;180(2):817-24.
445. Alvarez-Jiménez VD, Leyva-Paredes K, García-Martínez M, Vázquez-Flores L, García-Paredes VG, Campillo-Navarro M, et al. Extracellular Vesicles Released from Mycobacterium tuberculosis-Infected Neutrophils Promote Macrophage Autophagy and Decrease Intracellular Mycobacterial Survival. Front Immunol. 2018;9:272.
446. Majumdar R, Tavakoli Tameh A, Arya SB, Parent CA. Exosomes mediate LTB4 release during neutrophil chemotaxis. PLoS Biol. 2021;19(7):e3001271.
447. Wang Y, Luo L, Braun OÖ, Westman J, Madhi R, Herwald H, et al. Neutrophil extracellular trap-microparticle complexes enhance thrombin generation via the intrinsic pathway of coagulation in mice. Scientific Reports. 2018;8(1):4020.
448. O'Dea KP, Takata M. Human Neutrophil-derived Microvesicles Activate Pulmonary Endothelial Cells In an In Vitro Model of Pulmonary Microvascular Inflammation. C105 RESPIRATORY FAILURE: MECHANISTIC INSIGHTS FROM LUNG INJURY MODELS. p. A6290-A.
449. Daly ME. Determinants of platelet count in humans. Haematologica. 2011;96(1):10-3.
450. Skubitz KM, Campbell KD, Ahmed K, Skubitz AP. CD66 family members are associated with tyrosine kinase activity in human neutrophils. The Journal of Immunology. 1995;155(11):5382-90.
451. Jung Y, Rothenberg ME. Roles and regulation of gastrointestinal eosinophils in immunity and disease. J Immunol. 2014;193(3):999-1005.
452. Kolaczkowska E, Kubes P. Neutrophil recruitment and function in health and inflammation. Nature Reviews Immunology. 2013;13(3):159-75.
453. Topchiy E, Cirstea M, Kong HJ, Boyd JH, Wang Y, Russell JA, et al. Lipopolysaccharide Is Cleared from the Circulation by Hepatocytes via the Low Density Lipoprotein Receptor. PLoS One. 2016;11(5):e0155030.
454. Walley KR, Francis GA, Opal SM, Stein EA, Russell JA, Boyd JH. The Central Role of Proprotein Convertase Subtilisin/Kexin Type 9 in Septic Pathogen Lipid Transport and Clearance. Am J Respir Crit Care Med. 2015;192(11):1275-86.
455. Levels JH, Marquart JA, Abraham PR, van den Ende AE, Molhuizen HO, van Deventer SJ, et al. Lipopolysaccharide is transferred from high-density to low-density lipoproteins by lipopolysaccharide-binding protein and phospholipid transfer protein. Infect Immun. 2005;73(4):2321-6.
456. Böing AN, van der Pol E, Grootemaat AE, Coumans FA, Sturk A, Nieuwland R. Single-step isolation of extracellular vesicles by size-exclusion chromatography. J Extracell Vesicles. 2014;3.
457. Welton JL, Webber JP, Botos LA, Jones M, Clayton A. Ready-made chromatography columns for extracellular vesicle isolation from plasma. J Extracell Vesicles. 2015;4:27269.
458. Lok CAR, Snijder KS, Nieuwland R, Van Der Post JAM, de Vos P, Faas MM. Microparticles of Pregnant Women and Preeclamptic Patients Activate Endothelial Cells in the Presence of Monocytes. American Journal of Reproductive Immunology. 2012;67(3):206-15.
459. Kolonics F, Szeifert V, Timár CI, Ligeti E, Lőrincz Á M. The Functional Heterogeneity of Neutrophil-Derived Extracellular Vesicles Reflects the Status of the Parent Cell. Cells. 2020;9(12).
460. Zizzo G, Hilliard BA, Monestier M, Cohen PL. Efficient clearance of early apoptotic cells by human macrophages requires M2c polarization and MerTK induction. J Immunol. 2012;189(7):3508-20.

461. Sachouli E, Tsiridou DM, Takata M, Gordon A, O'Dea KP. Stimulation of Neutrophils in Whole Blood Enhances the Pro-inflammatory Activity of Neutrophil-Derived Microvesicles. The FASEB Journal. 2022;36(S1).
462. Tsiridou DM, Sachouli E, Takata M, O'Dea KP. Neutrophil-Derived Microvesicles Enhance Pulmonary Vascular Inflammation via a Toll-like Receptor 4 Signaling-Dependent Mechanism. The FASEB Journal. 2022;36(S1).
463. Hong CW. Extracellular Vesicles of Neutrophils. Immune Netw. 2018;18(6):e43.
464. De Filippo K, Henderson RB, Laschinger M, Hogg N. Neutrophil chemokines KC and macrophage-inflammatory protein-2 are newly synthesized by tissue macrophages using distinct TLR signaling pathways. The Journal of Immunology. 2008;180(6):4308-15.
465. Soehnlein O, Kenne E, Rotzius P, Eriksson E, Lindbom L. Neutrophil secretion products regulate anti-bacterial activity in monocytes and macrophages. Clinical & Experimental Immunology. 2008;151(1):139-45.
466. Soehnlein O, Kai-Larsen Y, Frithiof R, Sorensen OE, Kenne E, Scharffetter-Kochanek K, et al. Neutrophil primary granule proteins HBP and HNP1–3 boost bacterial phagocytosis by human and murine macrophages. The Journal of clinical investigation. 2008;118(10):3491-502.
467. Territo MC, Ganz T, Selsted M, Lehrer R. Monocyte-chemotactic activity of defensins from human neutrophils. The Journal of clinical investigation. 1989;84(6):2017-20.
468. Chaly YV, Paleolog E, Kolesnikova T, Tikhonov I, Petratchenko E, Voitenok N. Neutrophil a-defensin human neutrophil peptide modulates cytoline production in human monocytes and adhesion molecule expression in endothelial cells. European cytokine network. 2000;11(2):257-66.
469. Sun R, Iribarren P, Zhang N, Zhou Y, Gong W, Cho EH, et al. Identification of neutrophil granule protein cathepsin G as a novel chemotactic agonist for the G protein-coupled formyl peptide receptor. The Journal of Immunology. 2004;173(1):428-36.
470. Soehnlein O, Xie X, Ulbrich H, Kenne E, Rotzius P, Flodgaard H, et al. Neutrophil-derived heparin-binding protein (HBP/CAP37) deposited on endothelium enhances monocyte arrest under flow conditions. J Immunol. 2005;174(10):6399-405.
471. Bowdish DME, Davidson DJ, Speert DP, Hancock REW. The Human Cationic Peptide LL-37 Induces Activation of the Extracellular Signal-Regulated Kinase and p38 Kinase Pathways in Primary Human Monocytes. The Journal of Immunology. 2004;172(6):3758-65.
472. Moraes JA, Frony AC, Barcellos-de-Souza P, Menezes da Cunha M, Brasil Barbosa Calcia T, Benjamim CF, et al. Downregulation of Microparticle Release and Pro-Inflammatory Properties of Activated Human Polymorphonuclear Neutrophils by LMW Fucoidan. J Innate Immun. 2019;11(4):330-46.
473. Allen ER, Whitefoot-Keliin KM, Palmatier EM, Mahon AR, Greenlee-Wacker MC. Extracellular vesicles from A23187-treated neutrophils cause cGAS-STING-dependent IL-6 production by macrophages. Frontiers in Immunology. 2022;13.
474. Paues Göranson S, Thålin C, Lundström A, Hållström L, Lasselin J, Wallén H, et al. Circulating H3Cit is elevated in a human model of endotoxemia and can be detected bound to microvesicles. Scientific Reports. 2018;8(1):12641.
475. Marki A, Buscher K, Lorenzini C, Meyer M, Saigusa R, Fan Z, et al. Elongated neutrophil-derived structures are blood-borne microparticles formed by rolling neutrophils during sepsis. Journal of Experimental Medicine. 2021;218(3).
476. Li L, Zuo X, Xiao Y, Liu D, Luo H, Zhu H. Neutrophil-derived exosome from systemic sclerosis inhibits the proliferation and migration of endothelial cells. Biochemical and Biophysical Research Communications. 2020;526(2):334-40.
477. Vargas A, Roux-Dalvai F, Droit A, Lavoie J-P. Neutrophil-derived exosomes: a new mechanism contributing to airway smooth muscle remodeling. American Journal of Respiratory Cell and Molecular Biology. 2016;55(3):450-61.
478. Headland SE, Jones HR, Norling LV, Kim A, Souza PR, Corsiero E, et al. Neutrophil-derived microvesicles enter cartilage and protect the joint in inflammatory arthritis. Sci Transl Med. 2015;7(315):315ra190.

479. Gresnigt MS, Joosten LAB, Verschueren I, van der Meer JWM, Netea MG, Dinarello CA, et al. Neutrophil-Mediated Inhibition of Proinflammatory Cytokine Responses. The Journal of Immunology. 2012;189(10):4806-15.
480. Shao S, Fang H, Zhang J, Jiang M, Xue K, Ma J, et al. Neutrophil exosomes enhance the skin autoinflammation in generalized pustular psoriasis via activating keratinocytes. The FASEB Journal. 2019;33(6):6813-28.
481. Rossaint J, Kühne K, Skupski J, Van Aken H, Looney MR, Hidalgo A, et al. Directed transport of neutrophil-derived extracellular vesicles enables platelet-mediated innate immune response. Nature communications. 2016;7(1):1-14.
482. Jiao Y, Zhang T, Zhang C, Ji H, Tong X, Xia R, et al. Exosomal miR-30d-5p of neutrophils induces M1 macrophage polarization and primes macrophage pyroptosis in sepsis-related acute lung injury. Critical Care. 2021;25(1):1-15.
483. Sweet MJ, Hume DA. Endotoxin signal transduction in macrophages. J Leukoc Biol. 1996;60(1):8-26.
484. McCubrey JA, LaHair MM, Franklin RA. Reactive oxygen species-induced activation of the MAP kinase signaling pathways. Antioxidants & redox signaling. 2006;8(9-10):1775-89.
485. Sun S-Y. N-acetylcysteine, reactive oxygen species and beyond. Cancer biology & therapy. 2010;9(2):109-10.
486. Yasui K, Baba A. Therapeutic potential of superoxide dismutase (SOD) for resolution of inflammation. Inflammation Research. 2006;55(9):359-63.
487. Guha M, Mackman N. LPS induction of gene expression in human monocytes. Cellular signalling. 2001;13(2):85-94.
488. Camussi G, Mariano F, Biancone L, De Martino A, Bussolati B, Montrucchio G, et al. Lipopolysaccharide binding protein and CD14 modulate the synthesis of platelet-activating factor by human monocytes and mesangial and endothelial cells stimulated with lipopolysaccharide. The Journal of Immunology. 1995;155(1):316-24.
489. Clark SR, Ma AC, Tavener SA, McDonald B, Goodarzi Z, Kelly MM, et al. Platelet TLR4 activates neutrophil extracellular traps to ensnare bacteria in septic blood. Nature Medicine. 2007;13(4):463-9.
490. Pieterse E, Rother N, Yanginlar C, Hilbrands LB, van der Vlag J. Neutrophils Discriminate between Lipopolysaccharides of Different Bacterial Sources and Selectively Release Neutrophil Extracellular Traps. Frontiers in Immunology. 2016;7.
491. Urban CF, Ermert D, Schmid M, Abu-Abed U, Goosmann C, Nacken W, et al. Neutrophil Extracellular Traps Contain Calprotectin, a Cytosolic Protein Complex Involved in Host Defense against Candida albicans. PLOS Pathogens. 2009;5(10):e1000639.
492. Tsourouktsoglou T-D, Warnatsch A, Ioannou M, Hoving D, Wang Q, Papayannopoulos V. Histones, DNA, and citrullination promote neutrophil extracellular trap inflammation by regulating the localization and activation of TLR4. Cell reports. 2020;31(5):107602.
493. Lelliott PM, Momota M, Lee MSJ, Kuroda E, Iijima N, Ishii KJ, et al. Rapid Quantification of NETs In Vitro and in Whole Blood Samples by Imaging Flow Cytometry. Cytometry A. 2019;95(5):565-78.
494. Feng D, Zhao WL, Ye YY, Bai XC, Liu RQ, Chang LF, et al. Cellular internalization of exosomes occurs through phagocytosis. Traffic. 2010;11(5):675-87.
495. Guha M, Mackman N. The phosphatidylinositol 3-kinase-Akt pathway limits lipopolysaccharide activation of signaling pathways and expression of inflammatory mediators in human monocytic cells. J Biol Chem. 2002;277(35):32124-32.
496. Schabbauer G, Tencati M, Pedersen B, Pawlinski R, Mackman N. PI3K-Akt pathway suppresses coagulation and inflammation in endotoxemic mice. Arterioscler Thromb Vasc Biol. 2004;24(10):1963-9.
497. Ojaniemi M, Glumoff V, Harju K, Liljeroos M, Vuori K, Hallman M. Phosphatidylinositol 3-kinase is involved in Toll-like receptor 4-mediated cytokine expression in mouse macrophages. Eur J Immunol. 2003;33(3):597-605.
498. Usatyuk PV, Vepa S, Watkins T, He D, Parinandi NL, Natarajan V. Redox regulation of reactive oxygen species-induced p38 MAP kinase activation and barrier dysfunction in lung microvascular endothelial cells. Antioxid Redox Signal. 2003;5(6):723-30.

499. Pober JS, Min W, Bradley JR. Mechanisms of endothelial dysfunction, injury, and death. Annu Rev Pathol. 2009;4:71-95.
500. Park HS, Jung HY, Park EY, Kim J, Lee WJ, Bae YS. Cutting Edge: Direct Interaction of TLR4 with NAD(P)H Oxidase 4 Isozyme Is Essential for Lipopolysaccharide-Induced Production of Reactive Oxygen Species and Activation of NF-κB1. The Journal of Immunology. 2004;173(6):3589-93.
501. Gao Y, Jin H, Tan H, Cai X, Sun Y. Erythrocyte-derived extracellular vesicles aggravate inflammation by promoting the proinflammatory macrophage phenotype through TLR4–MyD88–NF-κB–MAPK pathway. Journal of Leukocyte Biology. 2022;112(4):693-706.
502. Shen Y, Guo D, Weng L, Wang S, Ma Z, Yang Y, et al. Tumor-derived exosomes educate dendritic cells to promote tumor metastasis via HSP72/HSP105-TLR2/TLR4 pathway. OncoImmunology. 2017;6(12):e1362527.
503. Kojima M, Gimenes-Junior JA, Chan TW, Eliceiri BP, Baird A, Costantini TW, et al. Exosomes in postshock mesenteric lymph are key mediators of acute lung injury triggering the macrophage activation via Toll-like receptor 4. The FASEB Journal. 2018;32(1):97-110.
504. Wang Y, Du F, Hawez A, Mörgelin M, Thorlacius H. Neutrophil extracellular trap-microparticle complexes trigger neutrophil recruitment via high-mobility group protein 1 (HMGB1)-toll-like receptors(TLR2)/TLR4 signalling. Br J Pharmacol. 2019;176(17):3350-63.
505. Schlichting E, Aspelin T, Lyberg T. Interactions of endotoxin with human blood cells and serum proteins. Scand J Clin Lab Invest. 1996;56(2):167-76.
506. Erridge C. Endogenous ligands of TLR2 and TLR4: agonists or assistants? J Leukoc Biol. 2010;87(6):989-99.
507. Habich C, Kempe K, van der Zee R, Rümenapf R, Akiyama H, Kolb H, et al. Heat shock protein 60: specific binding of lipopolysaccharide. J Immunol. 2005;174(3):1298-305.
508. Deng M, Tang Y, Li W, Wang X, Zhang R, Zhang X, et al. The Endotoxin Delivery Protein HMGB1 Mediates Caspase-11-Dependent Lethality in Sepsis. Immunity. 2018;49(4):740-53.e7.
509. Thomas LM, Salter RD. Activation of macrophages by P2X7-induced microvesicles from myeloid cells is mediated by phospholipids and is partially dependent on TLR4. J Immunol. 2010;185(6):3740-9.
510. Manček-Keber M, Frank-Bertoncelj M, Hafner-Bratkovič I, Smole A, Zorko M, Pirher N, et al. Toll-like receptor 4 senses oxidative stress mediated by the oxidation of phospholipids in extracellular vesicles. Sci Signal. 2015;8(381):ra60.
511. Luong M, Zhang Y, Chamberlain T, Zhou T, Wright JF, Dower K, et al. Stimulation of TLR4 by recombinant HSP70 requires structural integrity of the HSP70 protein itself. Journal of Inflammation. 2012;9(1):11.
512. Wantha S, Alard JE, Megens RT, van der Does AM, Döring Y, Drechsler M, et al. Neutrophil-derived cathelicidin promotes adhesion of classical monocytes. Circ Res. 2013;112(5):792-801.
513. Mookherjee N, Brown KL, Bowdish DM, Doria S, Falsafi R, Hokamp K, et al. Modulation of the TLR-mediated inflammatory response by the endogenous human host defense peptide LL-37. J Immunol. 2006;176(4):2455-64.
514. Lee TD, Gonzalez ML, Kumar P, Grammas P, Pereira HA. CAP37, a neutrophil-derived inflammatory mediator, augments leukocyte adhesion to endothelial monolayers. Microvasc Res. 2003;66(1):38-48.
515. Rasmussen PB, Bjørn S, Hastrup S, Nielsen PF, Norris K, Thim L, et al. Characterization of recombinant human HBP/CAP37/azurocidin, a pleiotropic mediator of inflammation-enhancing LPS-induced cytokine release from monocytes. FEBS Lett. 1996;390(1):109-12.
516. Heinzelmann M, Mercer-Jones MA, Flodgaard H, Miller FN. Heparin-binding protein (CAP37) is internalized in monocytes and increases LPS-induced monocyte activation. J Immunol. 1998;160(11):5530-6.
517. Köppler B, Cohen C, Schlöndorff D, Mack M. Differential mechanisms of microparticle transfer toB cells and monocytes: anti-inflammatory propertiesof microparticles. Eur J Immunol. 2006;36(3):648-60.

518. Ghosh A, Li W, Febbraio M, Espinola RG, McCrae KR, Cockrell E, et al. Platelet CD36 mediates interactions with endothelial cell-derived microparticles and contributes to thrombosis in mice. J Clin Invest. 2008;118(5):1934-43.
519. Getts DR, Terry RL, Getts MT, Deffrasnes C, Müller M, van Vreden C, et al. Therapeutic inflammatory monocyte modulation using immune-modifying microparticles. Sci Transl Med. 2014;6(219):219ra7.
520. Rana S, Yue S, Stadel D, Zöller M. Toward tailored exosomes: the exosomal tetraspanin web contributes to target cell selection. Int J Biochem Cell Biol. 2012;44(9):1574-84.
521. Morelli AE, Larregina AT, Shufesky WJ, Sullivan ML, Stolz DB, Papworth GD, et al. Endocytosis, intracellular sorting, and processing of exosomes by dendritic cells. Blood. 2004;104(10):3257-66.
522. Youn Y-J, Shrestha S, Lee Y-B, Kim J-K, Lee JH, Hur K, et al. Neutrophil-derived trail is a proinflammatory subtype of neutrophil-derived extracellular vesicles. Theranostics. 2021;11(6):2770-87.
523. Tatham KC, O'Dea KP, Romano R, Donaldson HE, Wakabayashi K, Patel BV, et al. Intravascular donor monocytes play a central role in lung transplant ischaemia-reperfusion injury. Thorax. 2018;73(4):350-60.
524. Wakabayashi K, Wilson MR, Tatham KC, O'Dea KP, Takata M. Volutrauma, but not atelectrauma, induces systemic cytokine production by lung-marginated monocytes. Crit Care Med. 2014;42(1):e49-57.
525. Wilson MR, O'Dea KP, Zhang D, Shearman AD, van Rooijen N, Takata M. Role of lung-marginated monocytes in an in vivo mouse model of ventilator-induced lung injury. Am J Respir Crit Care Med. 2009;179(10):914-22.
526. Terrisse AD, Puech N, Allart S, Gourdy P, Xuereb JM, Payrastre B, et al. Internalization of microparticles by endothelial cells promotes platelet/endothelial cell interaction under flow. J Thromb Haemost. 2010;8(12):2810-9.
527. Genschmer KR, Russell DW, Lal C, Szul T, Bratcher PE, Noerager BD, et al. Activated PMN Exosomes: Pathogenic Entities Causing Matrix Destruction and Disease in the Lung. Cell. 2019;176(1):113-26.e15.
528. Mohanty T, Fisher J, Bakochi A, Neumann A, Cardoso JFP, Karlsson CAQ, et al. Neutrophil extracellular traps in the central nervous system hinder bacterial clearance during pneumococcal meningitis. Nature Communications. 2019;10(1):1667.